TIME TOPIC ACENDA: Sont 24, 2025 from 10:00nm, 4:00nm (ET) PRESENTER				
TOPIC AGENDA: Sept 24, 2025 from 10:00pm - 4:00pm (ET)	PRESENTER			
WELCOME	Evan Nef			
FSP Team Introductions	DOE/INL Project Manager			
Project Overview	Sebastian Corbisiero			
Introduction for DOE Laboratory Initiated Efforts	DOE Space Reactor Program			
	National Technical Director			
FSP Government Reference Design Review	Lee Mason			
	NASA FSP Tech. Lead			
	& Venkateswara Rao Dasari (DV)			
	DOE Space/Defense Reactors Chief Scientis			
FSP DOE/National Laboratory Moderator Efforts	DV & Caitlin Kohnert			
	DOE/LANL FSP Moderator Leads			
10 Minute Break				
FSP DOE/National Laboratory Shielding Efforts	DV & Alex Levinsky			
	DOE/LANL FSP Shielding Leads			
FSP DOE/National Laboratory Instrumentation and Control Efforts	DV & Dianne Ezell			
	DOE/ORNL FSP I&C Lead			
FSP DOE/National Laboratory Efforts—Question and Answers	Evan Nef			
	DOE/INL Project Manager			
1/2 Hour Break	1			
	WELCOME FSP Team Introductions Project Overview Introduction for DOE Laboratory Initiated Efforts  FSP Government Reference Design Review  FSP DOE/National Laboratory Moderator Efforts  10 Minute Break FSP DOE/National Laboratory Shielding Efforts  FSP DOE/National Laboratory Instrumentation and Control Efforts  FSP DOE/National Laboratory Efforts—Question and Answers			





Continued on the next page (1 of 3)









#### AGENDA: Sept 24, 2025 from 10:00pm - 4:00pm (ET)

START TIME	TOPIC	PRESENTER
12:40pm (ET)	Welcome Back	Thomas DeMichael
	FSP NASA Team Introductions	NASA FSP Project Manager
12:50pm (ET)	NASA Fission Instrumentation & Controls for Space (FICS)	Robert Okojie
	2024 FICS Workshop Outcomes	John Wrbanek
	Live FICS Database	Phil Neudeck
	FICS Working Group	NASA Glenn Research Center
	<ul> <li>'Draft' NASA I&amp;C Technology Development Path for Fission Surface Power</li> </ul>	
	System	
	Instrumentation & Controls: Evaluation of Instrumentation Sensors and	
	Electronics	
:30pm (ET)	Risk Reduction Activities for Stirling Controllers and Stirling Power System	Christopher Barth
	Development	NASA Glenn Research Center
1:50pm (ET)	Davier Management and Distribution	David Pike
1.30pm (E1)	Power Management and Distribution	NASA Glenn Research Center
2:10pm (ET)	10 Minute Break	





Continued on the next page (2 of 3)









AGENDA: Sept 24, 2025 from 10:00pm - 4:00pm (ET)

START TIME	TOPIC	PRESENTER
2:20pm (ET)	Testing the Effects of Lunar Dust on FSP Radiators at Glenn Research Center	Ronald Leibach NASA Glenn Research Center
2:40pm (ET)	Irradiation testing of Stirling PCS Organics and freeze tolerant heat rejection fluids	Tyler Steiner NASA Glenn Research Center
3:00pm (ET)	Metal Vaporization risk of superalloys in vacuum at high temperature for long endurance	Kaiser Aguirre NASA Glenn Research Center
3:20pm (ET)	10 Minute Break	
3:30pm (ET)	Advanced Closed Brayton Cycle modeling for FSP	Thomas Lavelle NASA Glenn Research Center
3:50pm (ET)	FSP NASA Efforts—Question and Answers/Wrap up	Thomas DeMichael NASA FSP Program Manager
4:00pm (ET)	END OF WEBINAR Thank You for your participation and time!	











# Fission Surface Power Technology Maturation Webinar Clarification



The following presentations are **solely** based on the 40-kW Fission Surface Power Project of the NASA Space Technology Mission Directorate.

The presentations are **ONLY** for public reporting and archiving purposes of the 40 kW NASA Fission Surface Power Technology Maturation activities.

The presentations do not imply, suggest, infer, advocate to represent or promote the recent NASA Directive to procure a 100 kW FSP system.









# **Key Design Trades for a Near-term Lunar Fission Surface Power System**

Lee Mason<sup>1</sup>, Lindsay Kaldon<sup>1</sup>, Sebastian Corbisiero<sup>2</sup> and DV Rao<sup>2</sup>

<sup>1</sup>NASA Glenn Research Center, Cleveland, Ohio <sup>2</sup>Idaho National Laboratory, Idaho Falls, Idaho

#### Background

- NASA/DOE team formed to conduct design trades for a near-term FSP system based on the requirements and goals stated in the 2021 FSP Phase 1 Statement-of-Work
  - Team members included Glenn Research Center, Idaho National Lab, Los Alamos National Lab
- The government studies were performed in parallel with three separate contractor-funded Phase 1 FSP projects:
  - Lockheed Martin/BWXT
  - Intuitive Machines/Xenergy
  - Westinghouse/Aerojet-Rocketdyne
- The design assumptions and analyses were informed by numerous prior FSP design studies, including:
  - Fission Surface Power System Initial Concept Definition, NASA/TM-2010-216772
  - A Deployable 40 kWe Lunar Fission Surface Power Concept, NETS-2022
- The primary goals of the NASA/DOE studies were:
  - Acquire insights to help the government team be a smart buyer
  - Identify risks and opportunities to inform government technology investments
  - Develop FSP concepts that can be shared with NASA architecture study teams
  - Collect data to guide/inform future flight system requirements

**TABLE I.** Phase 1 Design Requirements (DR) and Design Goals (DG).

DR-1	Power	40 kWe for 10 yr	DG-1	Stowed Volume	4m dia. x 6m length
DR-2	Launch & Landing Loads	7.63 g-rms launch, 4 g landing	DG-2	Total Mass	6000 kg including margin & growth
DR-3	Radiation Protection	<5 rem/yr at 1 km	DG-3	Power Cycles	Multiple on/off cycles
			DG-4	User Load	0 to 100%
			DG-5	Fault Tolerance	At least 5 kWe after fault
			DG-6	Transport- ability	Can be removed from lander and relocated

### **Key Design Assumptions**

- The NASA/DOE team established a set of FSP design assumptions based on the goal to deliver a FSP system to the moon in the late 2020s or early 2030s
  - The design assumptions were made after evaluating a variety of alternatives and prior studies
  - The assumptions are not intended to prescribe the future flight system, but rather be representative of the range of potential systems that could be implemented
- The design assumptions are strongly influenced by the current Technology Readiness Level (TRL) of the major FSP subsystems and components:
  - Subsystems/components considered TRL5:
    - Reactor fuel element (UN, <1400K, <1% burnup)</li>
    - Reactor heat pipes (Na, <1200K)</li>
    - 10 kWe-class Stirling power conversion (<1100K)
    - Water-based heat rejection & composite radiators (400-500K)
  - Subsystems/components considered TRL4:
    - Moderator element (YH, <1100K, ≤10<sup>21</sup> n/cm2)
    - Radiation shield (LiH/B4C/W)
    - Reactor Instrumentation & Control
    - 10 kWe-class Brayton power conversion (<1100K)
    - High voltage PMAD (240Vac-3000Vac-120Vdc)
- GRC's parametric system model EZ FSP Sizer was used to evaluate the system performance and mass sensitivities for all the design permutations evaluated in this paper

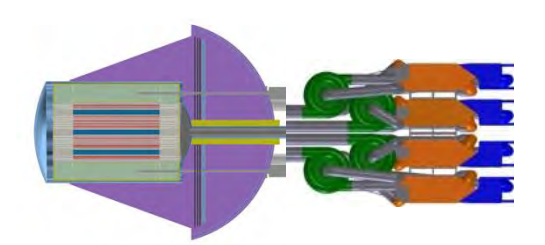
**TABLE II.** Key Design Decisions.

	1	1	
	GC-Brayton	HP-Stirling	
Reactor fuel and	19.75% enriched UN fuel pins, YH		
moderator	moderator		
Reactor heat transport	Direct gas-	Na heat pipes	
method	cooling	iva neat pipes	
Power conversion	40 mol. weight	Helium	
working fluid	HeXe	Henum	
Cycle hot-end temp	1100 K	1050 K	
Cycle cold-end temp	390 K	420 K	
Peak cycle pressure	1.5 MPa	7.5 MPa	
Power string number	4 x 25%; first failure results in no less		
and size	than 75% power output		
	Pumped H2O heat transport;		
Heat rejection approach	composite radiator panels with		
	embedded Ti/H2O heat pipes		
	240 Vrms alternator output, 3 kVac/1		
PMAD approach	kHz step-up, 1 km transmission, 120		
	Vdc load interface		
	<10 MRad at 1m (pwr conv), <300		
Radiation limits kRad at 10m (controller), <5		oller), <5 rem/yr at	
	1km (crew hab)		

#### **FSP Technology Approaches**

# A) Gas-cooled reactor and Brayton power conversion

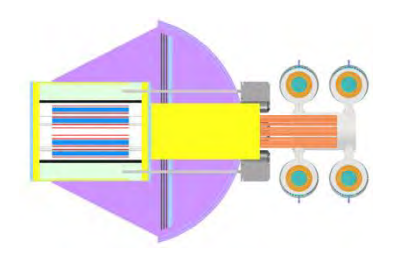
- Direct-gas HeXe coolant, 1.5 MPa, 40 g/mol
- 1100 K turbine inlet
- Four 25% converter strings



**Gas-cooled Brayton** 

# B) Heat pipe reactor and Stirling power conversion

- Na heat pipes and NaK primary heat exchanger
- 1050 K heater head
- Four 25% converter strings



**Heat Pipe Stirling** 

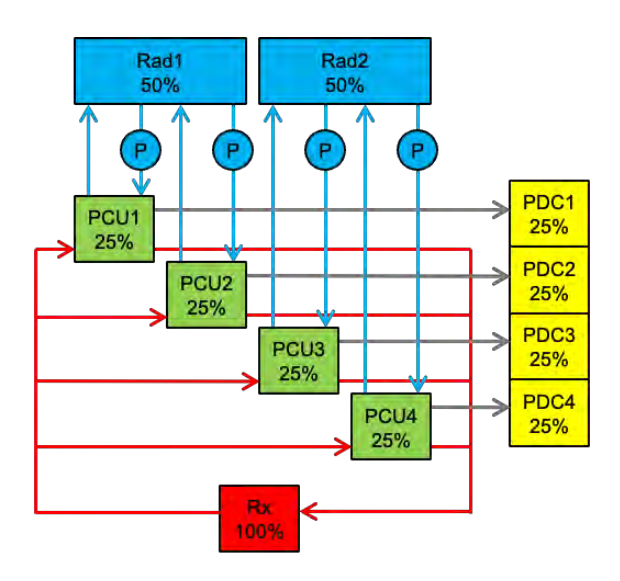
FSP provides 40 kWe Net at User Interface

#### **Common Assumptions:**

- <u>Fission reactors</u> use ceramic (UN) HALEU pin fuel and YHmoderator
- <u>Directional radiation shield</u> with 36° included angle providing
   410 MRad at 1m PCS, <300 kRad at controller, <5 rem/yr at 1km crew area
- Heat rejection via pumped H2O fluid loop and composite radiator panels with embedded Ti/H2O heat pipes sized for 270K lunar sink
- PMAD converts 240 Vrms
   alternator output to 3 kVac for 1
   km transmission with step down to 120 Vdc at load
   interface

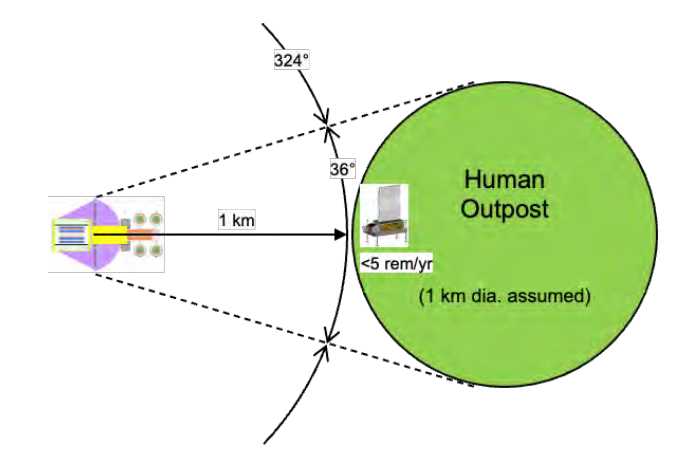
#### **FSP System Architecture**

- Four, parallel power conversion strings with converter-dedicated radiator loop and PMAD channel
  - First failure results in no less than 75% power
  - Trades performed to assess 4x25%, 2x50%, 4x50%, 2x100%



- Directional radiation shield based on hypothetical 1 km dia. human outpost with FSP User Interface Pallet located at 1 km boundary
  - Crew and associated equipment would be located beyond 1 km boundary (dose 

    1/r2)
  - Actual crew dose further attenuated by time on surface (33 days), time in habitat, time/distance of EVAs
  - Crew radiation limit based on NASA STD-3001, <2 rem (20 mSv) per mission year</li>



#### **GRD Reactor & Shield Materials**

Los Alamos National Laboratory

#### Selection of Materials and Technologies

High Fidelity Full-Scale Reactor Design Assessments Formed the Basis for Down Selection Decisions.

- Reactor Nuclear Fuel
  - Metal Alloy Fuels (U10Mo)
  - Ceramic Fuel Pellets (UO<sub>2</sub>, UN and UC)
  - Micro-engineered Ceramics (TRISO, BISO)
- Moderators and Reflectors
  - Beryllium compounds (Be, BeO and B2C)
  - Metal Hydrides (ZrH<sub>1.6</sub>, YH<sub>1.8</sub>, Y.Zr.H<sub>1.8</sub>)
- Shielding
  - Tungsten, Boron Carbide (B<sub>4</sub>C or WB<sub>4</sub>C)
  - · Lithium Hydride and Hafnium Hydride
  - · Advanced: B.Al.Ti.Hydride in WB4C

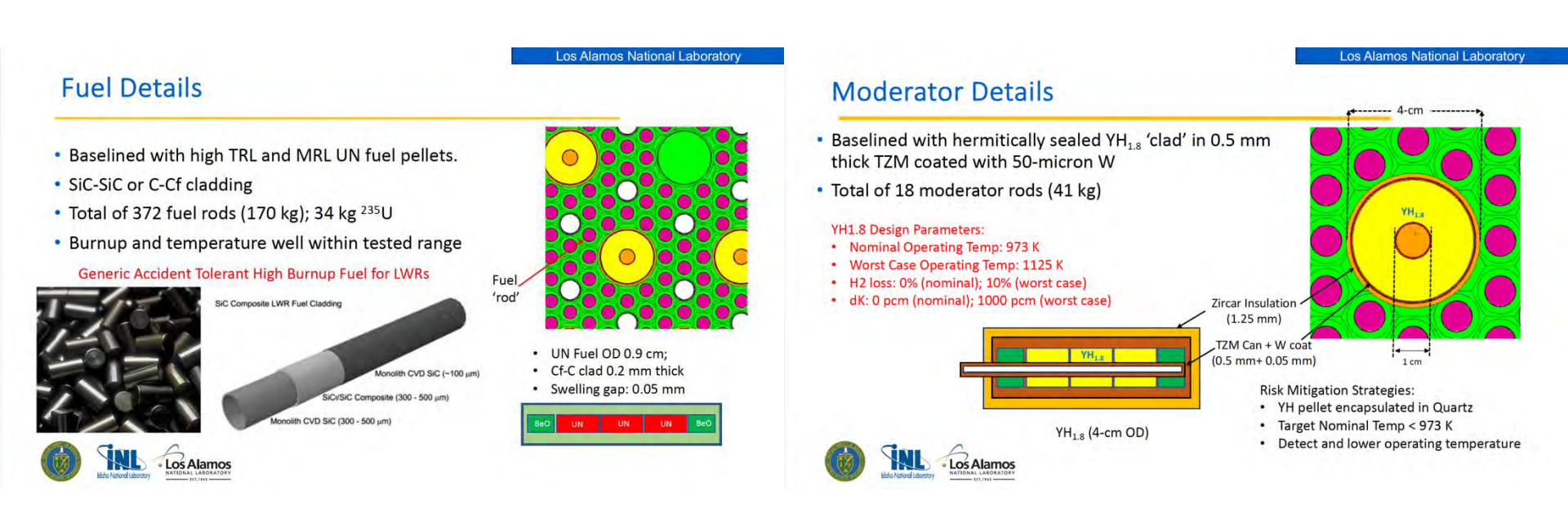




- Heat Transfer Technologies
  - Pumped Liquid Metals (NaK, Na)
  - High Temperature Heat Pipes (K, Na)
  - Direct Cycle Gas Cooled (HeXe, CO2, N2)
- Operating Temperature
  - Low (<1000 K)</li>
  - Intermediate (1000-1200 K)
  - High (>1200 K)
- Structures, piping and vessels
  - Haynes 230, TZM (Mo-Alloy)
  - Carbon-Carbon or composite carbides

Industry Phase-I parametric analyses confirmed several of the important down-select decisions

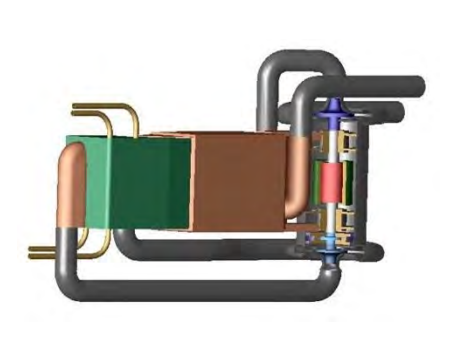
#### **GRD Fuel & Moderator**



#### **Power Conversion Options**

#### Closed Brayton

- 4x 11.7 kWe converters
- HeXe working fluid (Mol Wt. 40)
- 1100 K turbine inlet
- 1.5 MPa peak pressure
- 240 Vrms, 2 kHz, 3-phase output
- 20% converter efficiency
- 300 kg per converter
- 90 x 50 x 40 cm volume envelope





Both use high-temperature Parasitic Load Radiator (PLR) for power control

#### Free-piston Stirling

- 4x 12.6 kW converters (2 alternators per converter)
- He working fluid
- 1050 K heater head
- 7.5 MPa peak pressure
- 240 Vrms, 50 Hz, 1-phase output
- 29% converter efficiency
- 250 kg per converter
- 110 x 30 x 30 cm volume envelope





#### Radiator Architecture

#### **GC-Brayton** 180 kWt total radiator heat load (45 kWt per Brayton) • Two radiator wings; each wing serves two Brayton converters with shared H2O fluid manifold Polymer composite radiators with embedded Ti/H2O heat pipes 9 panels per wing; 18 panels total, each panel 2.5x2m 180 m2 total radiator area ~900 kg subsystem mass

# Rad9 Rad8 Rad7 Rad6 Rad5 Rad4 Rad3 Rad2 Rad1 379K 270K Tsink

#### **HP-Stirling**

- 120 kWt total radiator heat load (30 kWt per Stirling)
- Two radiator wings; each wing serves two Stirling converters with shared H2O fluid manifold
- Polymer composite radiators with embedded Ti/H2O heat pipes
- 7 panels per wing: 14 panels total, each panel 2.5x2m
- 140 m2 total radiator area
- ~700 kg subsystem mass

Stirling2

Stirling1

Rx (175 kWt) Stirling4

Stirling3

#### **Key Technologies:**



**Ti-H2O Heat Pipes** 

Rad7

Rad6

Rad5

Rad4

Rad3

Rad2

270K Tsink

Composite Structure



**Flexible** 

Interconnects

Scissor **Deployment** 



**Shared Manifold** Concept



Brayton4

Brayton3

Brayton2

Brayton1

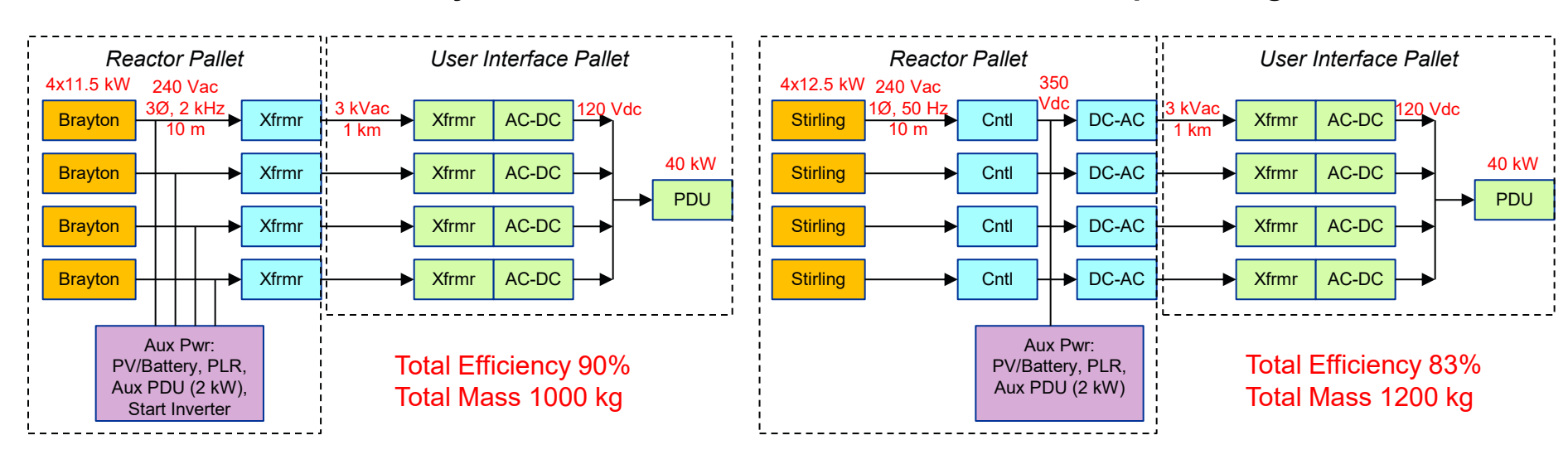
Rx

(230 kWt)

#### **PMAD Architecture**

#### **Gas-cooled Brayton**

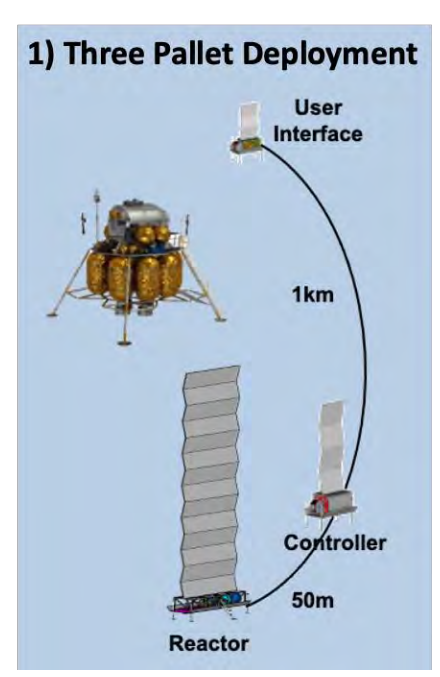
#### **Heat Pipe Stirling**



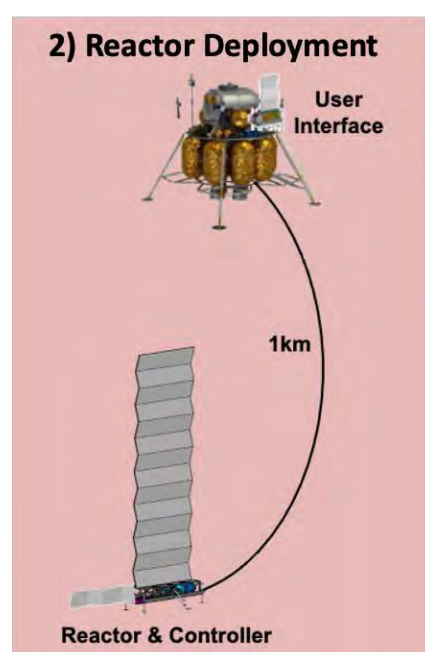
User Interface PMAD equipment is identical for both options

### Mission Integration Options

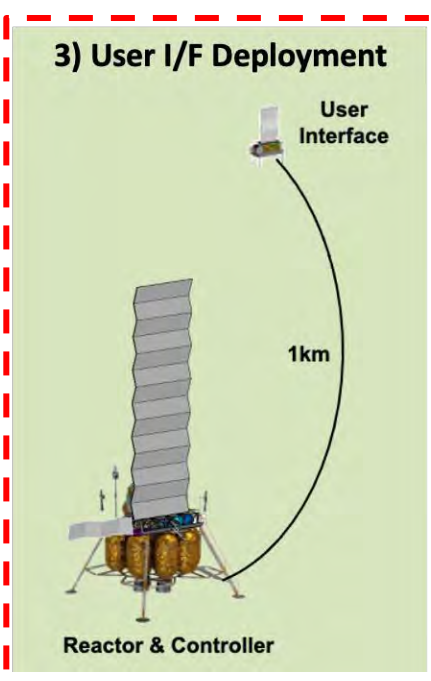
- 1) Three Pallet
  Deployment: Off-loading
  and deployment of three
  separate pallets reactor,
  controller, and user
  interface (DAC1)
- 2) Reactor Deployment:
  Off-loading and deployment
  of combined reactor &
  controller pallet while user
  interface remains on
  delivery lander (DAC2)
- 3) User Interface
  Deployment: Off-loading
  and deployment of user
  interface pallet while reactor
  and controller remain
  on/with delivery lander
  (DAC3)



Highest FSP mass & greatest deployment complexity, but lander can be reused.



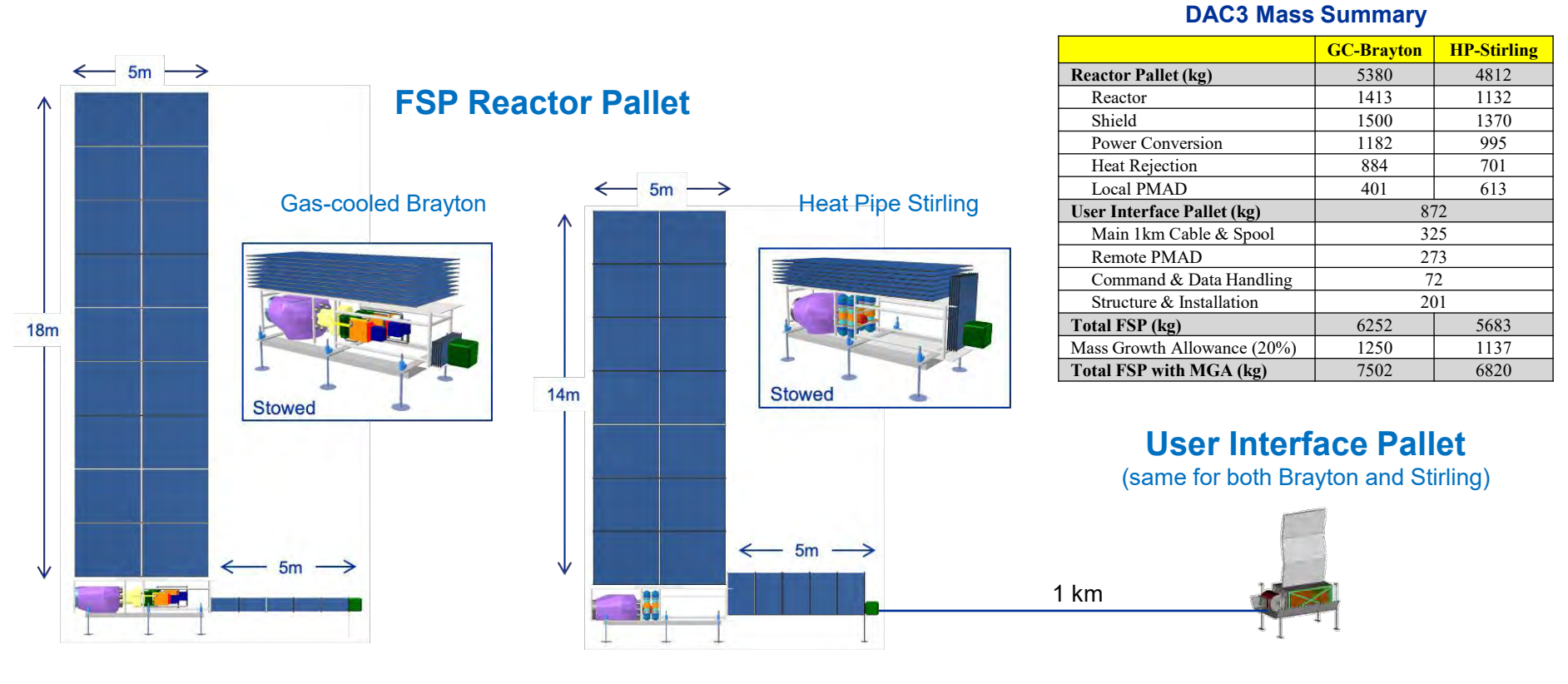
Single, large deployment and lander must be dedicated to serve as power interface node.



Lowest FSP mass & easiest deployment, but lander must support long-term reactor ops.

**Reference Approach** 

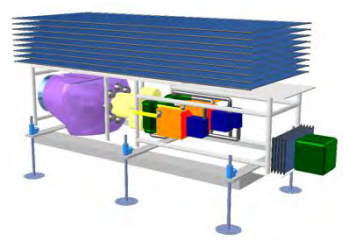
#### **DAC3** Design Layouts



### Preliminary DAC3 ConOps

#### Deliver two-pallet 40 kW FSP on Human-class Deliver Lander (HDL) with co-manifested utility rover

- Reactor Pallet (RP) includes reactor, shield, power conversion, main radiator, controller, 3000 Vac step-up transformers, auxiliary power system, parasitic load radiator
- User Interface Pallet (UIP) includes 1 km cable (pre-connected to RP), step-down transformers, 120 Vdc power distribution unit, command & data handling
- Lower two FSP pallets and rover to surface from HDL
- FSP startup to full power (takes about 8 hrs)
- FSP commissioning/tech demo phase (very notional)
  - Radiation Characterization
  - **Power Setpoint Changes**
  - Power String Shutdown & Restart
  - Reactor Temperature Excursions
  - RP Shutdown & Restart
  - **Lunar Day/Night Transients**
- Verify UIP functionality while co-located with RP
- Transport and install UIP at designated operating site
- **Potential FSP re-configurations (very notional)** 
  - UIP could be re-located to maximize utility (within constraints of 1 km cable and 36° shield angle)
  - High-voltage cable extender could be added to 1 km cable and UIP could be moved to farther location (with some power loss due to increased length)
  - Secondary power distribution node could be added on UIP output channel to extend service to multiple smaller users



Stowed RP ~6t, ~2x2x6m



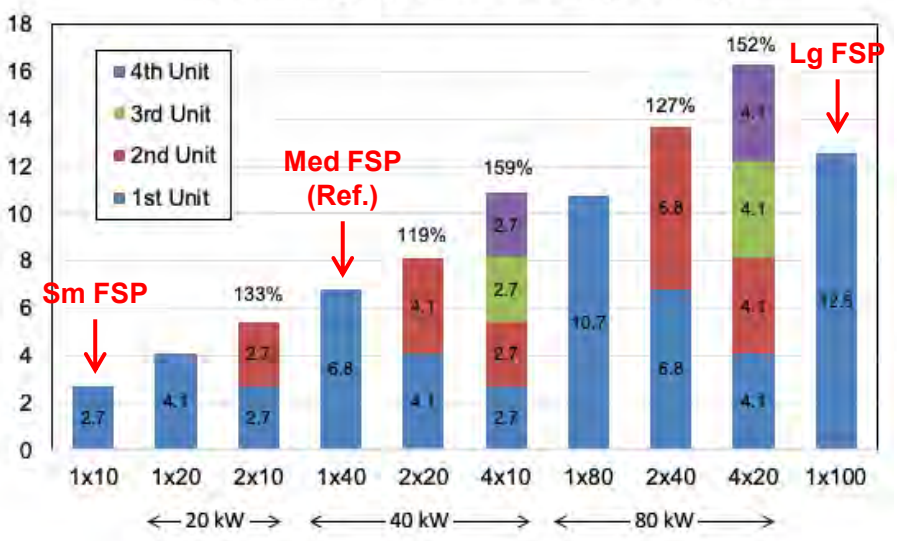
Stowed UIP ~1t, ~1x1x2m



#### Some What Ifs...

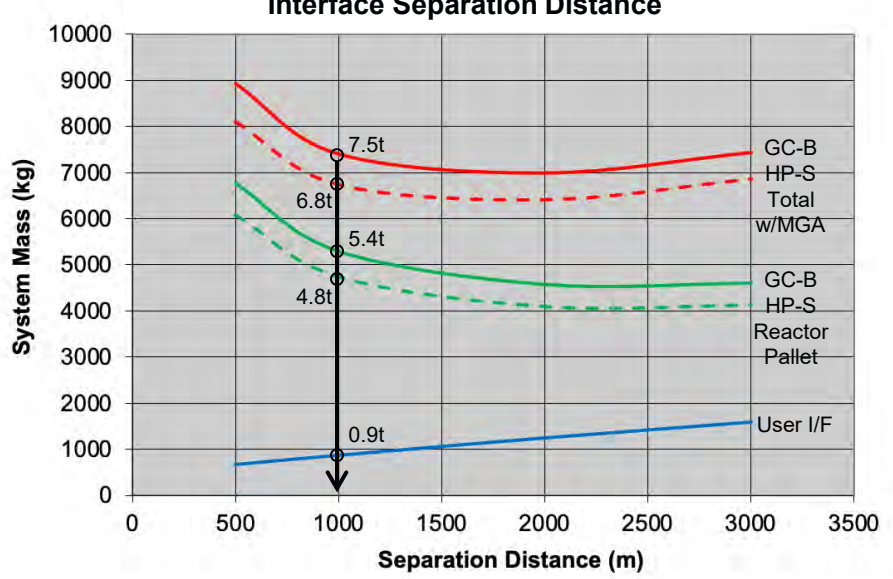
 What if the FSP system power changes?





• What if the user interface distance changes?

DAC3 FSP Mass Sensitivities with Varying User Interface Separation Distance



#### Summary

- An internal NASA-DOE study team performed trades and evaluated design concepts in parallel with three contractor teams that are responding to the same FSP system requirements and goals.
- The 40 kWe FSP concept developed by the government team weighs about 7t (including MGA) based on a configuration where the reactor pallet remains with the delivery lander and the user interface pallet is deployed 1 km away.
- The HP-Stirling approach offers a 10% mass advantage over the GC-Brayton option.
  - The HP-Stirling system also provides the benefit of lower reactor thermal power and reduced radiator area.
  - The GC-Brayton system simplifies the PMAD architecture, which is manifested in higher PMAD efficiency and lower gross power generated for the same net power delivered.
- Trade studies were performed to assess FSP system performance for a variety of configurations and design parameters.
  - A notional concept-of-operations was developed for a baseline configuration which provides a starting point for future, more-detailed studies.
  - Several "What If" analyses were performed to assess the system mass sensitivity for different power levels and cable lengths.
- The focus on the two specific FSP variants in this paper does not preclude the possibility of other options going forward.
  - The HP reactor could easily be adapted to work with Brayton conversion by employing a hot-end, gas plenum heat exchanger.
  - Another potential variant is a pumped liquid-metal cooled reactor that could be coupled to either Brayton or Stirling.
  - The government study team will continue to explore design variants as the project moves ahead and welcomes additional ideas from outside sources.





#### Venkateswara Rao Dasari

Venkateswara.Dasari@inl.gov | https://www.fsp.inl.gov

#### Caitlin Kohnert

Caitlin@lanl.gov

Approved for general distribution per LA-UR-25-29481 & INL/MIS-25-87819









# Basis for Nuclear Technology Maturation Analysis of Design Alt. formed basis for Govt. TechMat



#### Background

- FSP Power was increased to 40 kWe for 10-year operation
  - Preference: technologies and design features that are extensible to MW-class
- A design assessment is underway to revise previous DOE assessments to this power level
- Concepts being analyzed include
  - Yttrium Hydride Moderated Ceramic Fuel HP Reactor
  - Yttrium Hydride Moderated Ceramic Fuel HeXe Gas-Cooled Reactor
  - Krusty derived HALEU UMo Fast Metal HP Reactor
- Ceramic fuel forms include sintered pellets and coated fuel particles
- Power conversion systems include Stirling and Brayton systems

# Objectives of the alternative design assessments

- Identify and Prioritize Technology and/or Materials Gaps
  - Reconcile with industry findings
- Develop a multi-year technology maturation strategy to achieve mission infusion readiness
  - Delineate between Industry initiatives and Laboratory R&D
- Perform shielding and concept-of-operation analyses
  - Enable decisions related to location of deployment and ground-based reactor control
- Host Technology Interchange Meetings
  - Share data widely with the industry teams









# Technology Readiness Levels vary considerably

- NASA
- TRL for the nuclear fuel is sufficiently high. MRL is limited by lack of market signal. Government led fuels technology maturation R&D is NOT required.
  - Well characterized fuel forms pellets of UO<sub>2</sub> or UN and plates of U10Mo exist. DOE's ARDP/ATF and RERTR projects are establishing fuel infrastructure for manufacturing HALEU forms of these fuels.
  - Additional confirmatory testing would be needed for UN and U10Mo at expected burn up conditions; requirement exacerbated for HEU fast spectrum reactors
  - Test reactors exist to perform confirmatory testing in thermal spectrum reactors. ATR, MITR, etc.
- Reliable high temperature metal hydride moderators are important to achieve weight limits for HALEU fueled FSP designs while retaining both PCS options. Government led technology maturation is a high priority
  - BeO by itself is unlikely to achieve weight limits; thermally segmented Be moderator may be able to perform but requires a complicated thermal management scheme
  - Some industry teams as well as DOE's microreactor project are advancing metal hydride moderators.
  - A government-led national laboratory R&D is recommended to assure TRL 5/6 readiness











# Technology Readiness Levels vary considerably



- Current technology readiness level for instrumentation and controls is low. Government-led R&D to identify and mature reliable I&C architecture (in-core vs ex-core) is recommended
  - Independent size, weight and power (SWAP) assessments for the integrated architecture.
- Shielding takes more than 50% of reactor weight. LiH is essential to keep shielding weight manageable. R&D into fabrication and qualification of LiH is recommended











# Starting point for FSP Moderator Technology Maturation



Powder

DOE's MRP demonstrated and established expertise for Fabrication, characterization of YH

Thermal stability was demonstrated

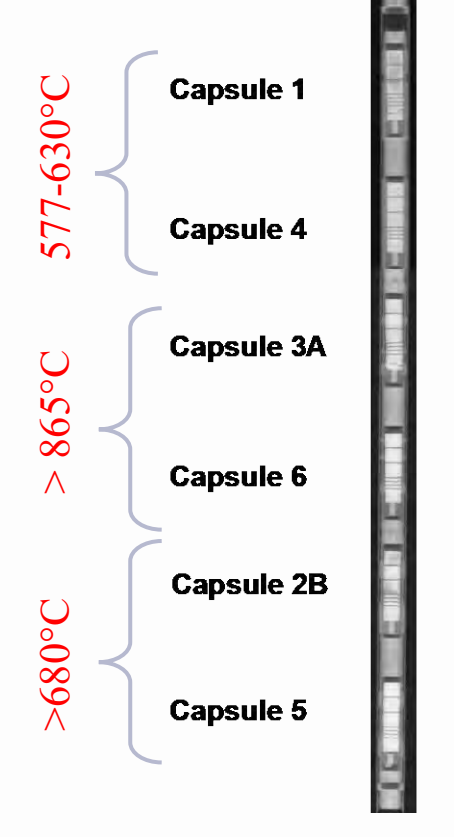
at > 900-C

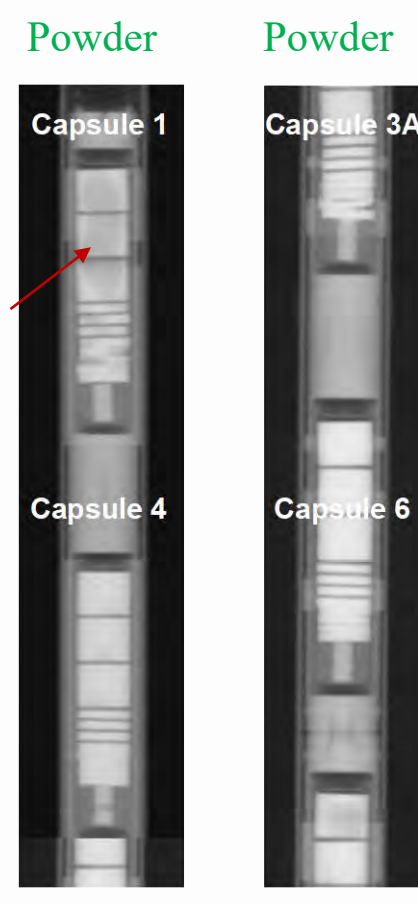
#### Focus of FSP maturation is

- net-shape fabrication;
- long-term thermal testing; and
- Neutron irradiation

Idaho National Laboratory

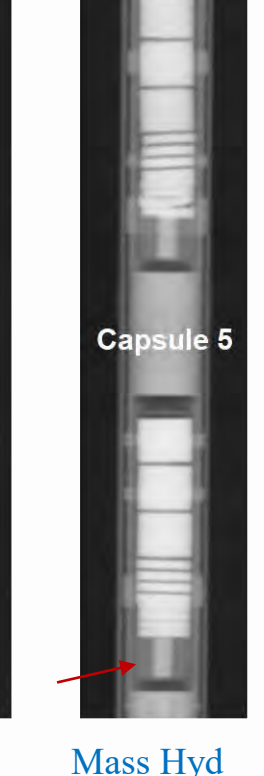






Mass Hyd

Neutron Radiography of ATR irradiated YH samples









Mass Hyd

# Solid State Moderators

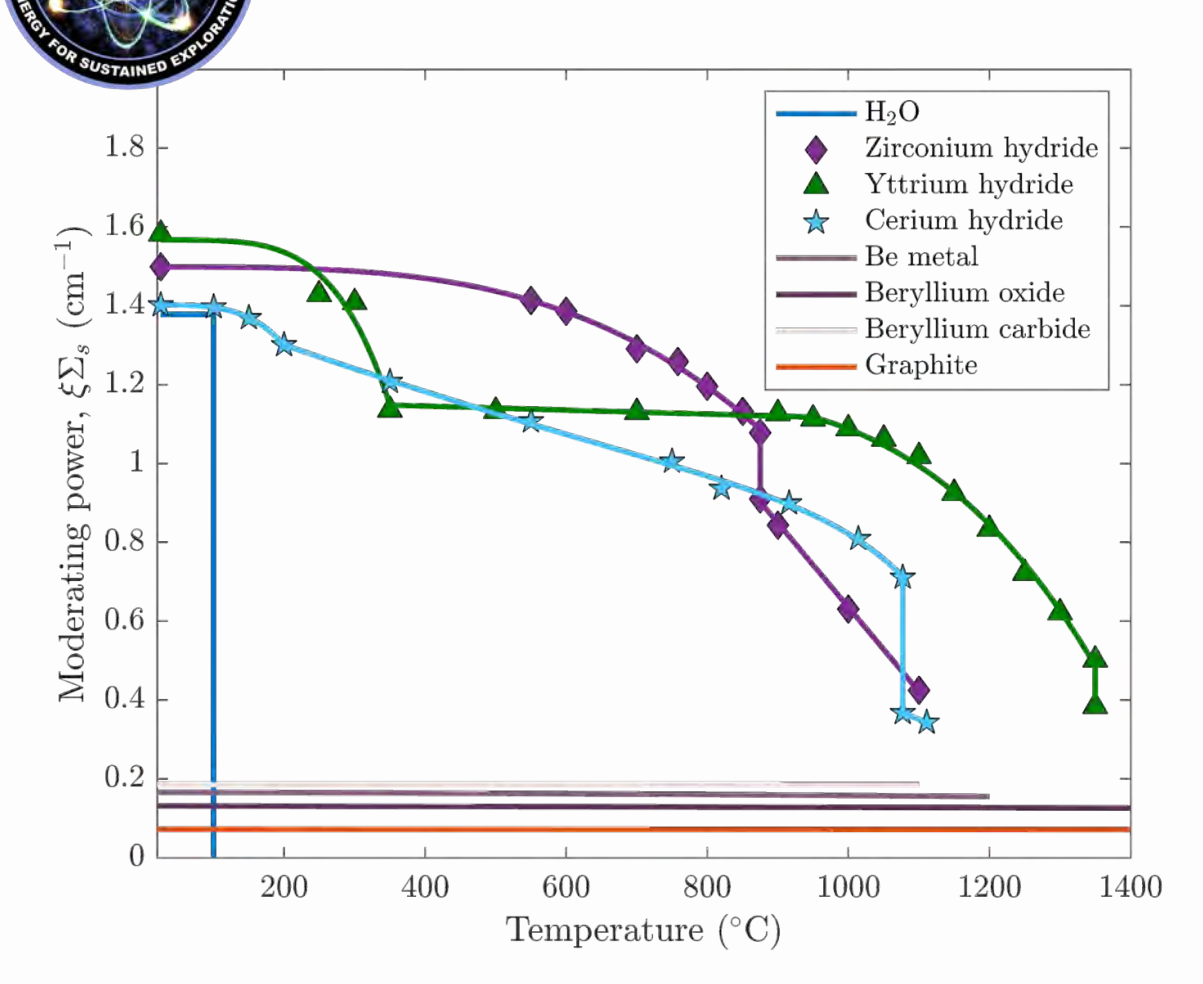
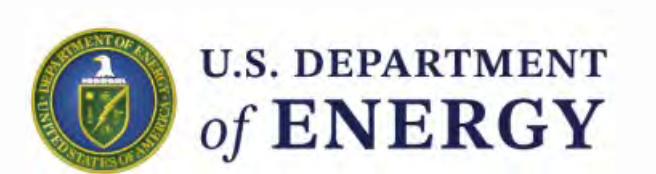
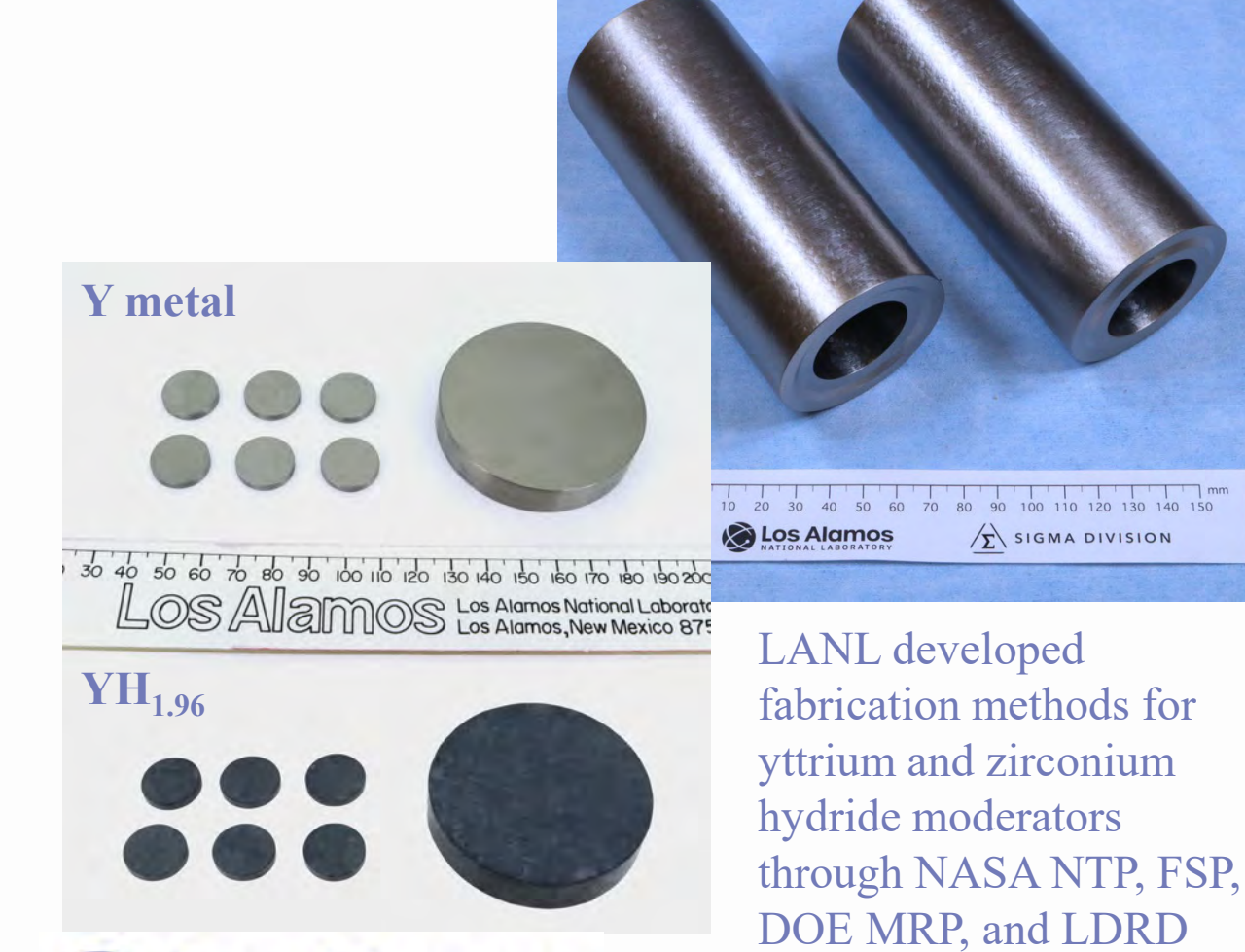


Figure by Adi Shivprasad







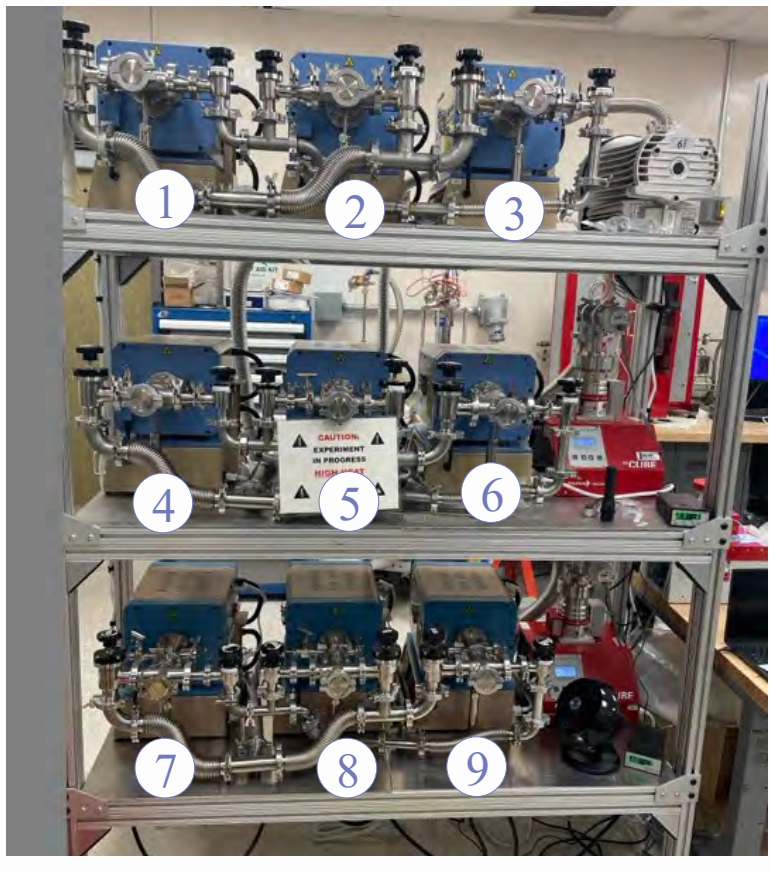
**ZrH**<sub>1.85</sub>

National Laboratory

# EN AUSTAINED ENTORS

# Hydride Moderators Need Cladding

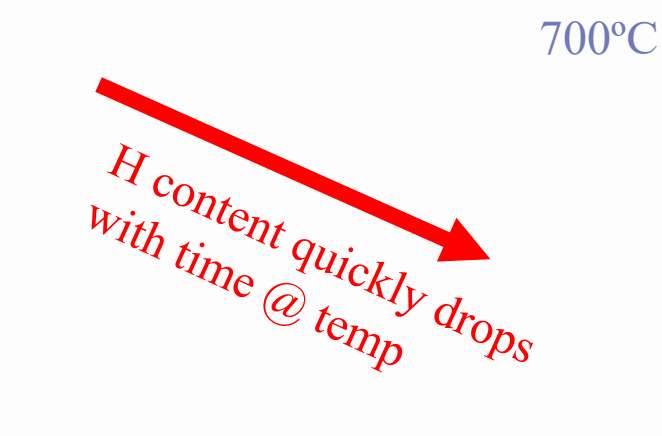




LANL setup an array of thermal testing vacuum furnaces to test moderator prototypes









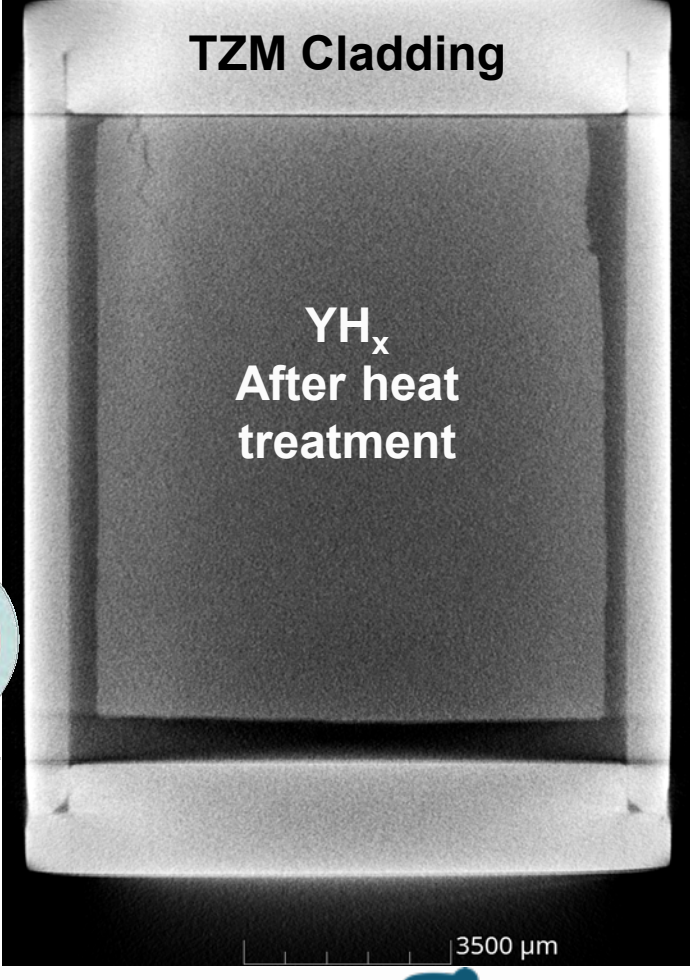
Tests on yttrium hydride without cladding showed rapid hydrogen loss

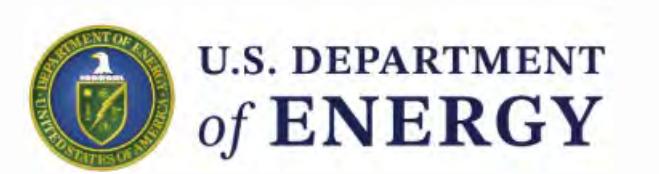




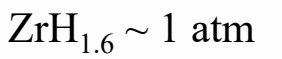
# Hydride Moderators Need Cladding

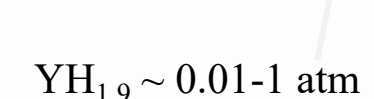


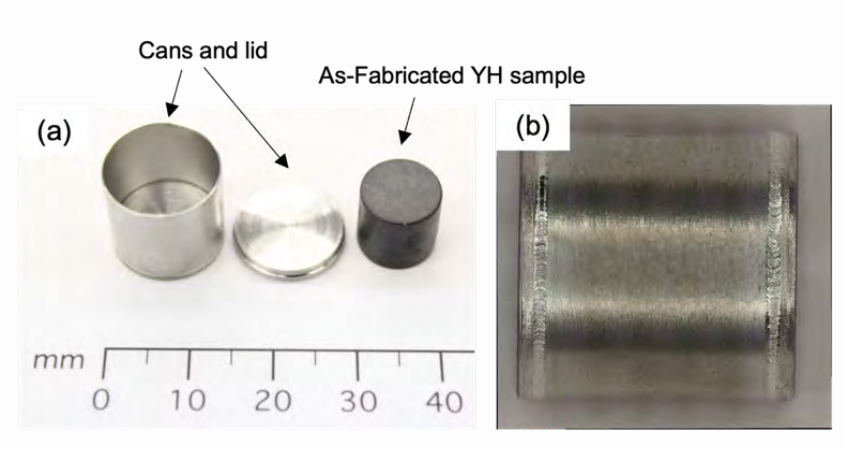












LANL fabricated and thermally tested





#### Refractory Metals & Ceramics Provide Opt. Hydrogen Retention Temperature [°C] 1000 750 300 500 Possible base metals Temperature [K] 2000 1500 1200 1000 500 TZM FeCrAl-APMT Inconel 718 Permeability [mol/(m\*s\*Pa<sup>0.5</sup>)] 10 $Al_2O_3$ 316 SS Cr2O3 FeCrAl-APMT SiC -e [1/C] 304 SS TiC Inconel 800 ZrC CTE×10 nconel 617 c-BN Inconel 600 TiN ZrN CrN **AICrN** 10<sup>-20</sup> TIAIN 0.50 1.25 1.50 1.75 2.00 1.00

• Primary concepts are **quartz** and **TZM** (Mo, 0.5% Ti, 0.1% Zr) cladding

1000/T [K-1]

- Oxidized FeCrAl was attempted but difficult to weld. Cannot oxidize after welding without desorbing hydrogen.
- W coated TZM was attempted and does improve retention. Surface preparation and coating method are important.
- Argonne National Lab developed a multilayered Cr/Al<sub>2</sub>O<sub>3</sub> coating concept







200

600

Temperature [ ° C]

800

1000

1200



Si<sub>3</sub>N<sub>4</sub>



# Quartz Cladding Offers Superior Hydrogen Retention



- INL developed a method for sealing hydrides in quartz (Fused Quartz from Technical Glass Products)
- A molybdenum foil is used as an interaction barrier between the hydride and glass
- LANL performed thermal testing on the quartz clad moderator element









# Weld Development and Quality is Needed for Hydrogen Retention

Weld Development for 0.5 mm wall thickness ESPI TZM







- LANL used E-Beam welding to develop leaktight welding method on 0.5 mm and 1.0 mm wall thickness TZM
- Compared results with LANL developed SWIFT model of H retention in a clad moderator

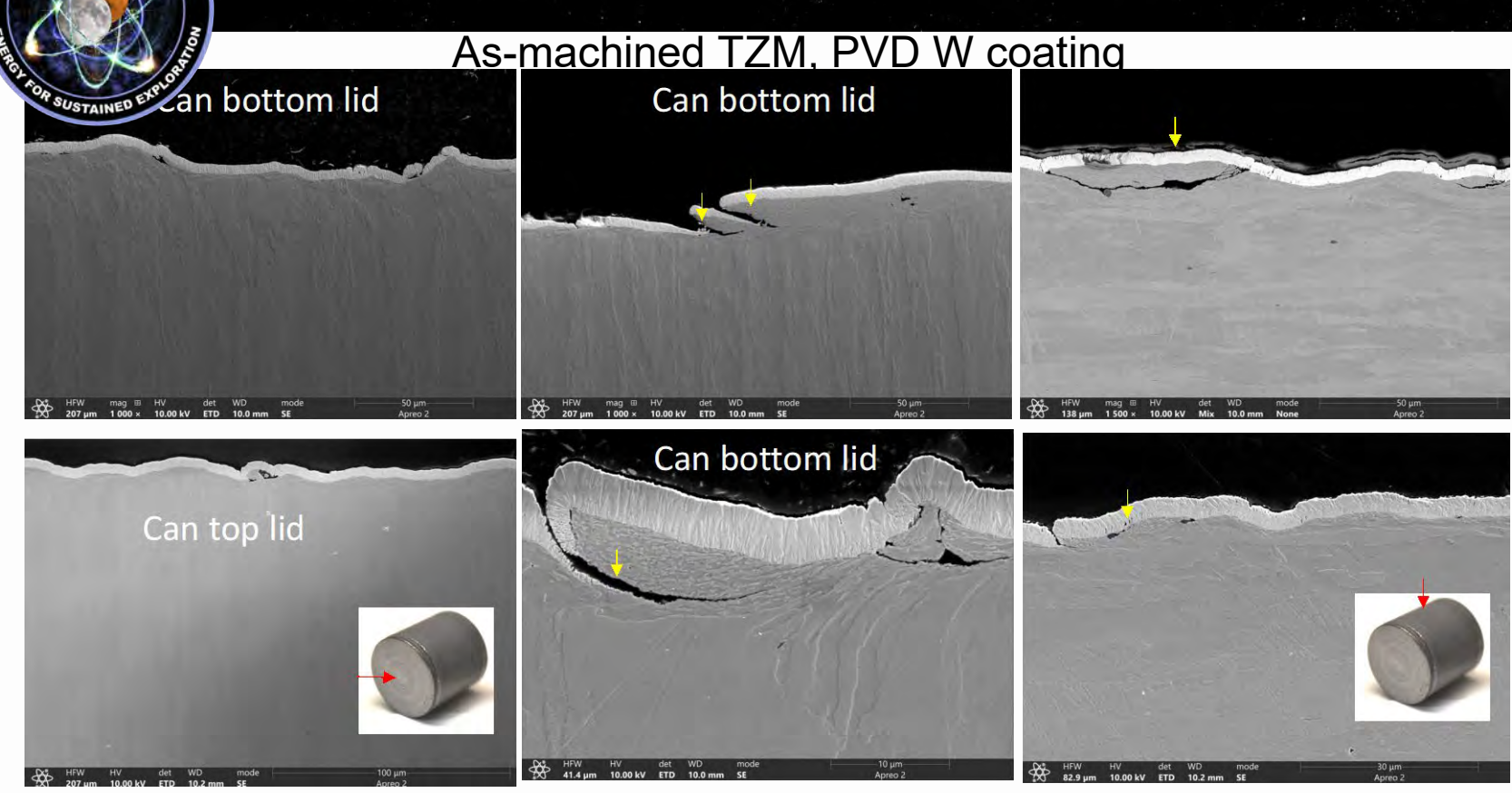




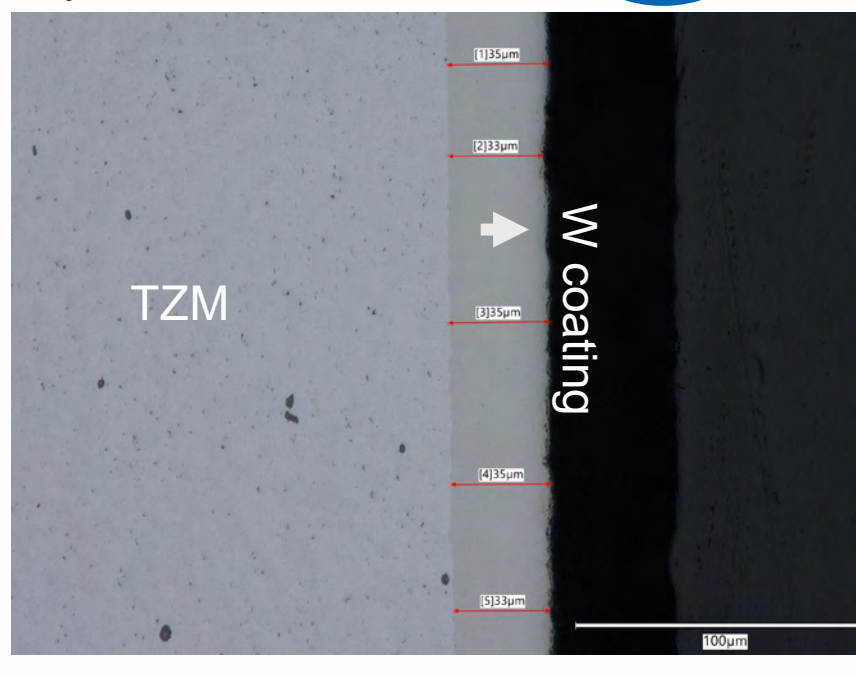




# Tungsten Coating is also effective. But needed some maturation







- As-machined TZM surface is rough and difficult to coat, leading to H loss
- Polished surface is easier to coat uniformly
- CVD coating provides the smoothest coating with best microstructure for H retention
  - CVD Vendor was ATL in the UK
- You do not want a porous, cracked or nonuniform coating







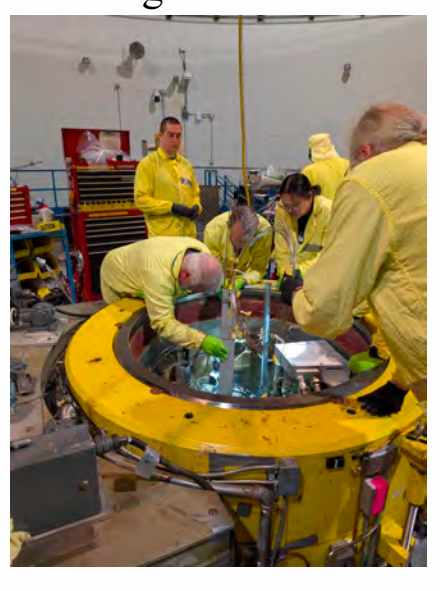


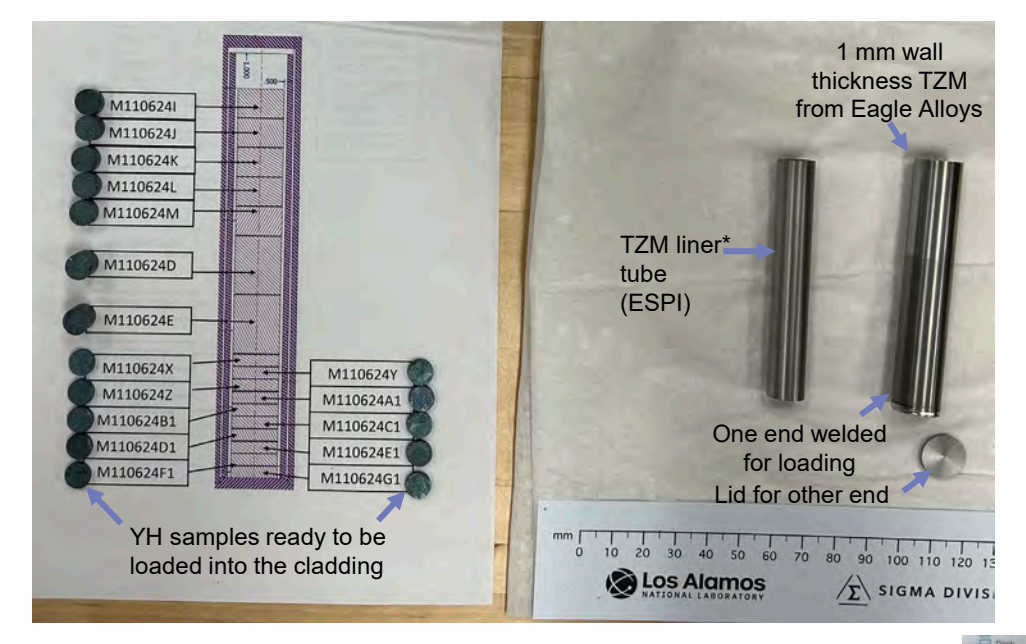
# Irradiation Testing of Moderator Elements

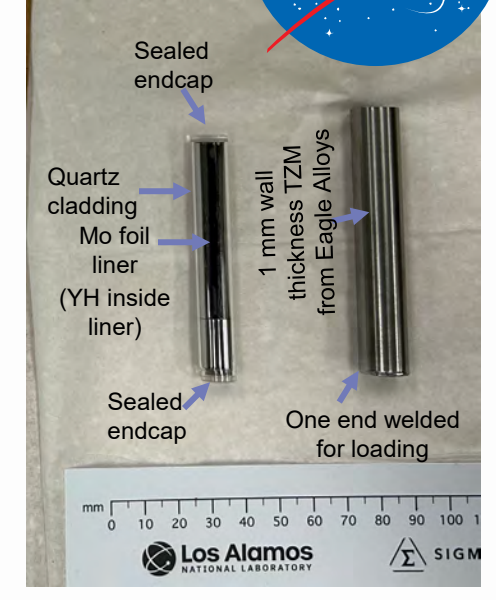


Moderator element prototypes in titanium holder

Initial insertion and alignment







Sealed quartz

endcap

- Irradiations performed at MITR
- Two cladding concepts tested: YH in TZM and YH in quartz+TZM. Two temperatures: 700C and 800C.
- Irradiations will stop at  $\sim 0.6$  dpa at the end of September
- Hoping to transfer samples to ORNL and use other funding mechanisms to characterize















# INL Designed Shake Testing Fixture & Performed Tests on Ti in Quartz



1) Encapsulated surrogate specimens in quartz



2) Designed a test fixture



3) Installed fixture on shake table



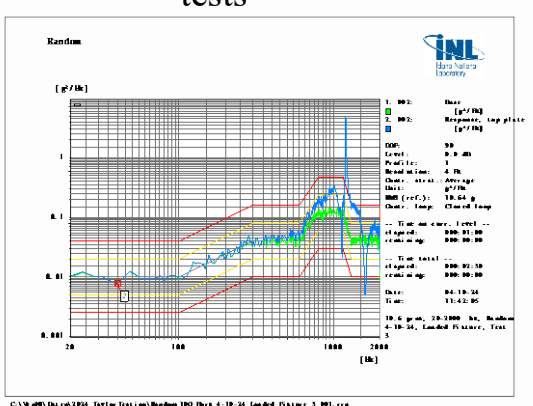
4) Mounted accelerometers



5) Protoflight test parameters

Test	Prototype Dauffootoe	Protoflight Qualification	Acceptance
Structural Leads*	1,35 x Limit Land	1,25 s LimitLoad	1,0 x Limit Load
Centrituge/Static Load* Sine Burst	1 minute 5 cycles (() hall level per seis	20 seconds 5 cycles (§ full-level per axis	30 seconds 5 system (§ 3.4 lev per axis
Acquatics Level Duration	Limit Level + 3dB 2 minutes	Limit Level = 3d8 1 minute	Linit Level 1 minute
Randore Vibration Levil <sup>®</sup> Duration	Limit Level + 308 2 minutestasis	Linit Level = 3d9 1 minutologis	Linit Level 1 minutalaxis
Sine Vibration* Lovel Sincep Rate	526 x Linit Level 2 octivin	1.85 x Limit Level 4 oct/min	Limit Level 4 octimin
Mechanica I Direck Actual Device Directated	2 actuations 1,4 x Limit Level 2 x Each Axis	2 actuations 1,4 x Limit Level 1 x Each Axis	1 actuations Limit Level 1 x Each Asis
Thermal-Hacuum	Maximin, predict. ± 10°C	Maximin predict.	Max, Inin, predict + 5°C
DMC & Magnetics	As Specified for Moston	Same	Some
2.5 on a limite. Derytion Note: Test break for well are 5.25 x Limit Level far 2 - As a minimum, the set is 3 - The sweep-direction shou if a sine sweep is used to resiste environment, a far for over stress.	ments, berytum, bonder both qualification and ac- vell shall be equal to origi- ity to the evaluated and chos- selledy the bads or other saler sweep nate may be o	I and composite shucker leptance testing water than the workman as to minimize the risk of equipments, safter than positioned, e.g., 6-8 oction	<ol> <li>including motal male ship level.</li> <li>damage to the hardway to simulate an oscillate in to reduce the polar</li> </ol>
<ol> <li>Shorter durations may be due to foot by firstations, to demonstrate that the to all test measurements he condities.</li> </ol>	If a shorter duration is ur root loading condition to	ed then the diver time a a been achieved within t	t wad shot be suffice to specified townsor

6) Performed shake tests



7) Examined specimens after each test



8) Leak checked specimens

Rodlet	Leak rate (atm.cc/s)		
size	Before test	After test	
2	1.5 x 10 <sup>-5</sup>	1.5 x 10 <sup>-5</sup>	
4	2.5 x 10 <sup>-5</sup>	2.1 x 10 <sup>-5</sup>	
6	3.1 x 10 <sup>-5</sup>	3.5 x 10 <sup>-5</sup>	
12	3.4 x 10 <sup>-5</sup>	4.8 x 10 <sup>-5</sup>	

#### **Conclusions**

- Quartz may be a feasible cladding material.
- Quartz cladding merits further investigation.











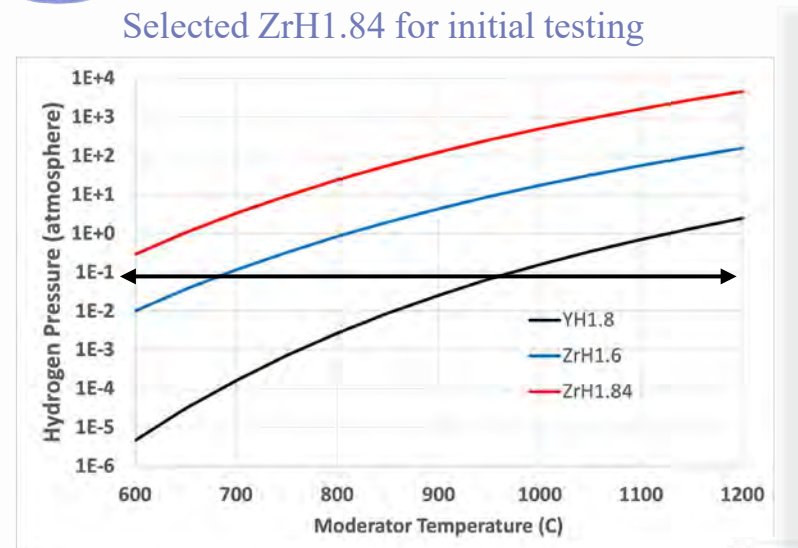
# Quartz Burst Testing was Performed



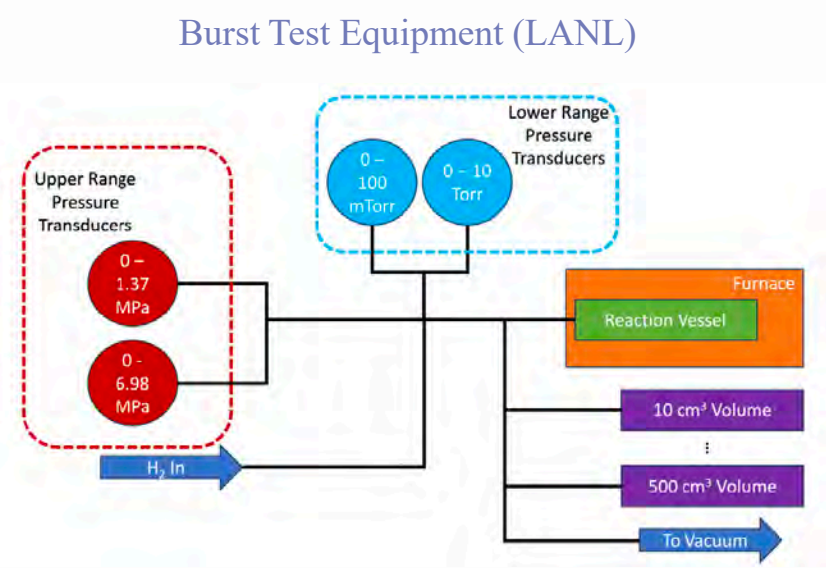
Can quartz or other clads withstand excessive pressure build up if temperature rapidly build up?

Modes of Failure for Cladding

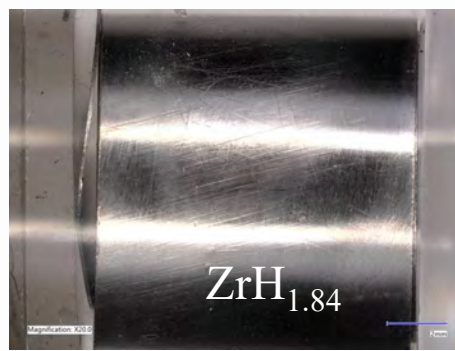
Idaho National Laboratory

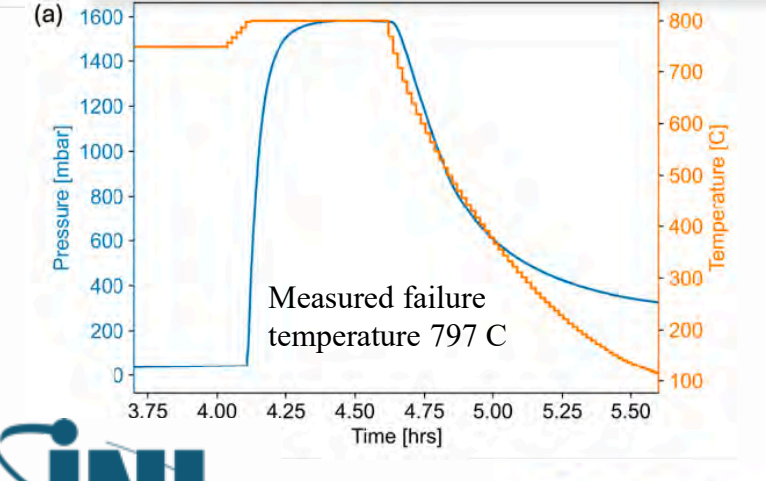


hoop stress end cap stress @ corners dome cap flat cap  $\sigma_{ih} = \frac{\sigma_q t}{r} \quad \sigma_{ie} = \frac{2\sigma_q t}{r} \quad \sigma_{if} = C_e \frac{\sigma_q t^2}{r^2}$ 



Burst Test Sample (INL)





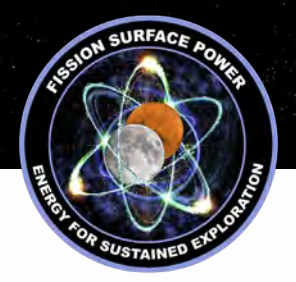
#### Conclusions:

- Predicted 1-cm diameter quartz failure temperature for ZrH1.84 is 775-815 C.
- 5-cm diameter YH1.8 encapsulated in 1 mm thick quartz can withstand rapid heat up as high as 1100 °C
- Additional testing ongoing.











## **Fission Surface Power Shielding**

Alex Levinsky, Ph.D. and DV Rao, Ph.D. Russell Johns, Miriam Kreher Ph.D., Alexis Maldonado, Robert Weldon Ph.D., Denton Reel, Brianna Musico. Ph.D., and Josh Smith PhD.

FSP Webinar, September 24, 2025





Approved for general distribution per LA-UR-25-29495 & INL/MIS-25-87819







# **Outline**



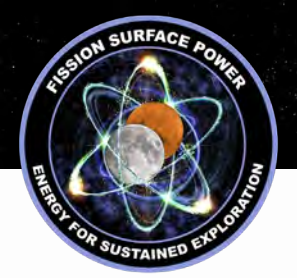
- Project Goal
- Approach
- Results
- Possible Next Steps











# **Project Goal**

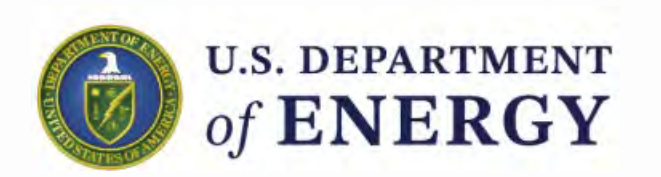
NASA

- Shielding is critical for protection of humans and sensitive equipment from reactor radiation
- Shielding has a significant contribution to reactor size and weight

The project is focused on minimizing the shielding size and weight via a combination of design, materials, configuration and reactor location while keeping the crew and sensitive equipment safe.

The project goal is to increase Technology Readiness Level (TRL) and Manufacturing Readiness Level (MRL) of FSP shielding components.





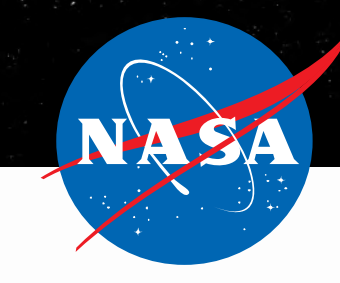








# **Approach – Modeling and Simulation**



### Material

# **Shielding Configuration**

### Location

Assessment of different materials

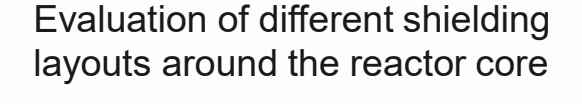


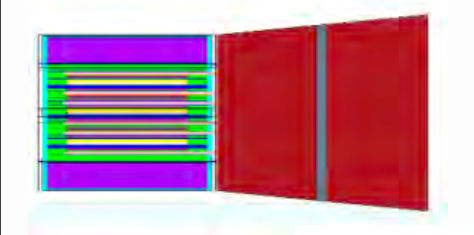
Lithium Hydride

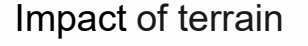
Boron Carbide

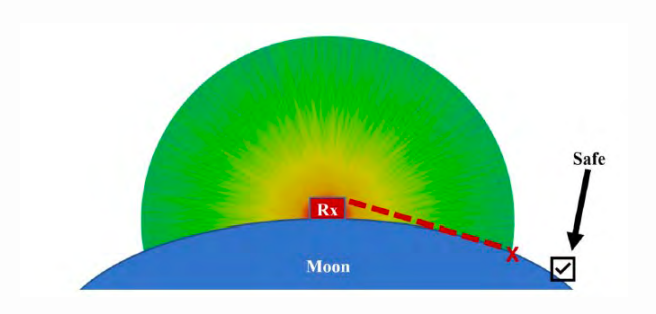


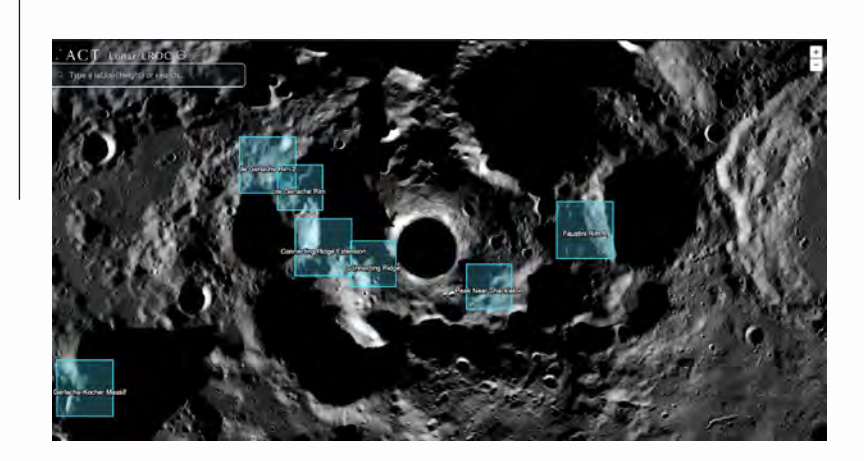


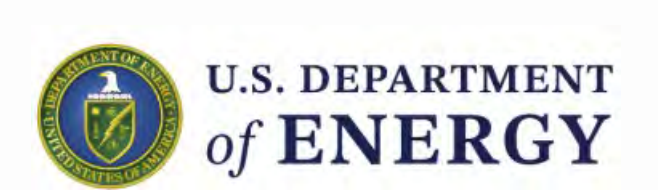












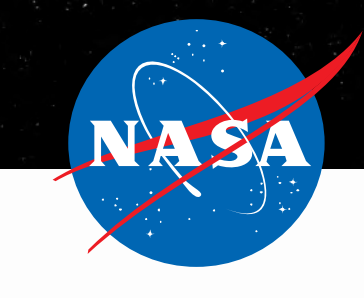








# **Approach – Manufacturing**





### Method

**Evaluation of** manufacturability

Cold isostatic press



Additive manufacturing

### **Specification Limitations**

Shape, size, parameters (density, purity, etc.), and quality control (tolerance, profile, etc.)





### **Supply Chain**

Sourcing location, available quantities, and price

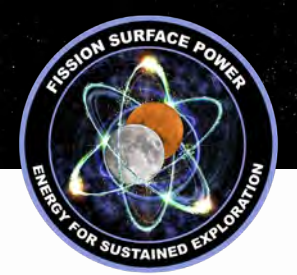












# **Approach – Experiments**



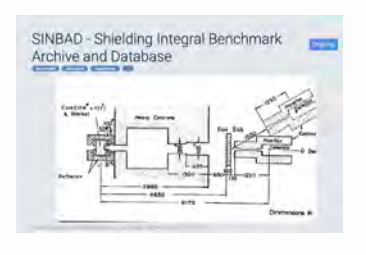
### **Test and Measurements**

# **Computer Code and Data Validation**

# **Uncertainty Quantification and Reduction**

Neutron counter









Reduction in uncertainty associated with the radiation dose and corresponding shielding material thickness







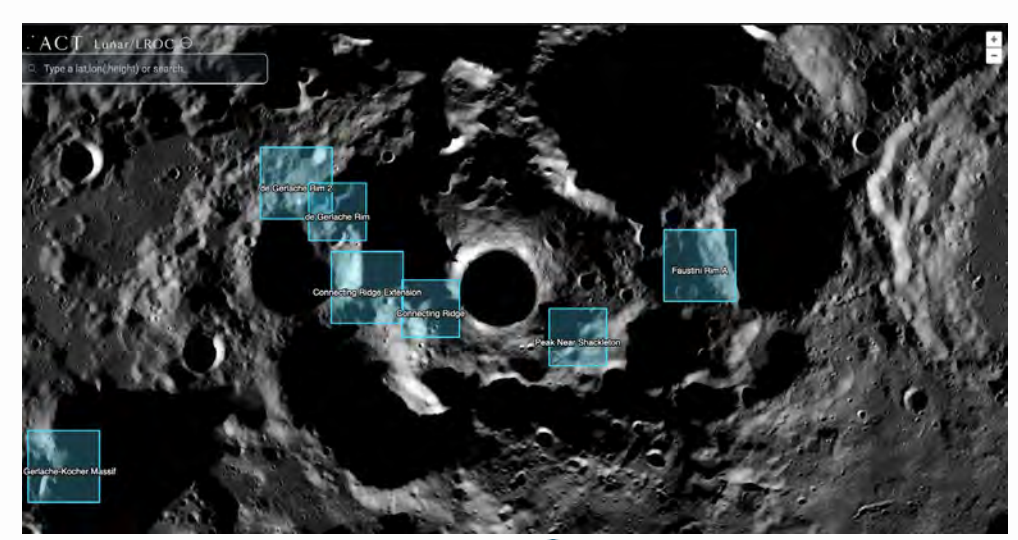


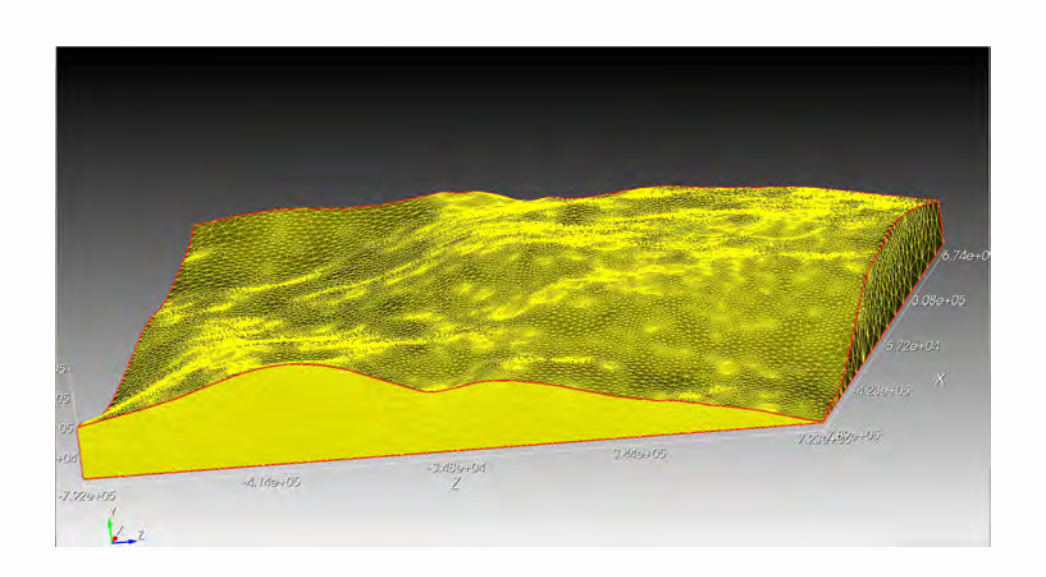


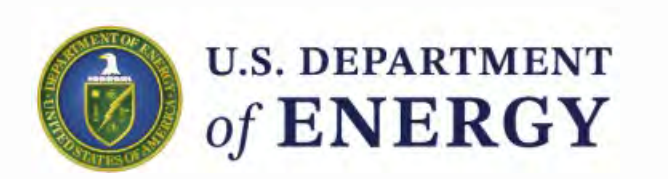
# Results – Modeling and Simulation Monte Carlo Radiation Transport Analysis – Material Selection and Shield Design

NASA

- Radiation transport analysis using MCNP 6.3 and ENDF VII.1
- Criteria: dose to electronics, sensitive components, and humans
- The following analyses was performed:
  - Calculations for a set of materials using a fixed design-base configuration
  - Evaluation of the different shield shapes and determination of the best shield configuration and layout
  - Assessment of the Lunar terrain impact









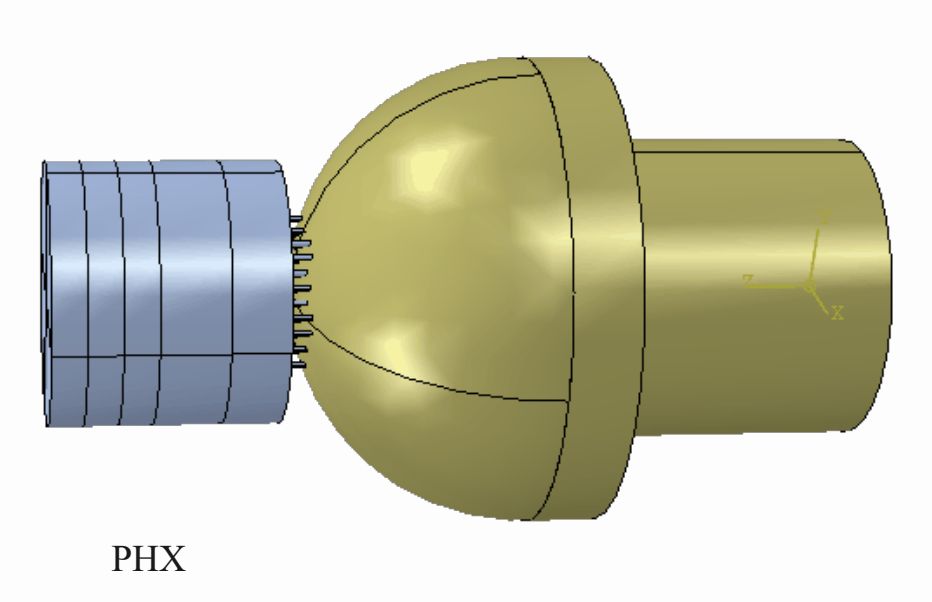






# Results – Modeling and Simulation Thermal Analysis – Shielding Material Temperature Assessment





- Thermo-mechanical model in Abaqus with ability to be coupled with MCNP 6.3
- Temperature distributions for reactor and shield were estimated



The reactor surrounded by shield











# **Results – Manufacturing**

- Assessment of manufacturing methods and manufacturing and supply chain evaluation of the major material candidates was performed
- These materials include B4C, LiH, WB4, WC, and their composites
- Samples of different thickness were manufactured to assess their material properties and perform radiation testing

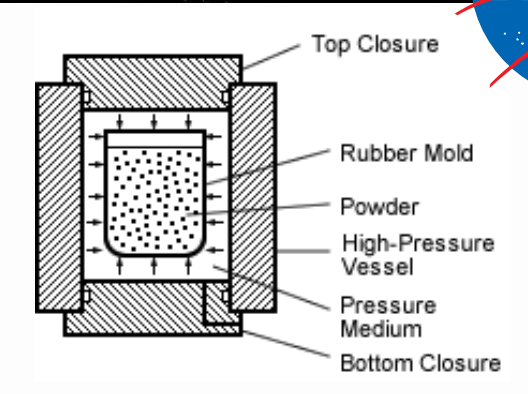
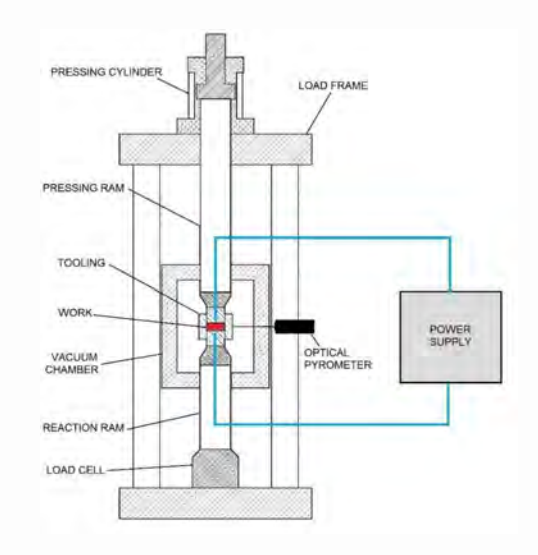


**Fig.** Example diagram of a cold isostatic press, used for consolidation\*
\*Figure taken from Kobelco.co.jp











# **Possible Next Steps**



- Performed work is applicable and extendable to major considered reactor designs and power levels
- All current results will be captured in the report (preparation is in progress)
- Any future work in the field should be focused on the following area:
  - Modeling and simulation:
    - Assessment of alternative placements of the reactor on the Moon
    - Impact of location on the shield modification and simplification'
    - Structural analysis of the shield materials
    - Thermal analysis of the shield materials for the different power levels
    - Implications of shield manufacturing and encapsulation if needed on its performance
    - Impact of radiation and material changes on its performance
  - Testing
    - Radiation testing with gamma and neutron sources
    - Irradaition testing to accumulate the required radiation doses
  - Manufacturing
    - Fabrication of net shape shielding components
    - Encapsulation of shield components if needed
    - Shield assembling techniques











# References



- Fission Surface Power, https://inl.gov/fsp/
- https://www.sciencemadness.org/smwiki/index.php/File:Lithium\_hydride\_crystal\_by\_ChemicalForce.jpg
- https://www.technical-ceramics.com/en/materials/boron-carbide/
- https://sheffieldgaugeplate.co.uk/blog/tungsten-blades/
- <a href="https://www.msesupplies.com/products/mse-pro-60t-electrical-cold-isostatic-press-cip-with-50mm-id-vessel-and-safety-shield">https://www.msesupplies.com/products/mse-pro-60t-electrical-cold-isostatic-press-cip-with-50mm-id-vessel-and-safety-shield</a>
- https://www.fastercapital.com/content/Tolerance-Design--The-Tolerance-Factor--Designing-for-Optimal-Qualityof-Conformance.html
- https://araxchemi.com/en/what-is-the-degree-of-purity/
- https://www.linkedin.com/pulse/what-supply-chain-management-why-important-modern-high-pat-rajen-
- LA-UR-18-29563, C.E. Moss, M.A. Nelson, R.B. Rothrock, and E.B. Sorensen, "MC-15 Users Manual".
- https://www.oecd-nea.org/jcms/pl\_32139/sinbad-shielding-integral-benchmark-archive-and-database
- https://www.nndc.bnl.gov/endf-b7.1/
- <a href="https://www.nndc.bnl.gov/endf-releases/?version=B-VIII.1">https://www.nndc.bnl.gov/endf-releases/?version=B-VIII.1</a>











# **FSP Instrumentation and Controls—DOE Lab Team**

For Space Applications



### Venkateswara Rao Dasari

Venkateswara.Dasari@inl.gov | https://www.fsp.inl.gov

### N. Dianne Bull Ezell

bullnd@ornl.gov | (865)-804-3545 ORCiD: 0000-0001-9334-5822 https://www.ornl.gov/group/nuclear-experiments

Approved for general distribution per INL/MIS-25-87819











# Radiation Environment Operational Experience

Slide courtesy: Jarvis Caffrey (NASA-MSFC)



## DEFENSE

Very short durations
Very high rate
Neutrons + Gammas

## **SPACE**

Variable Duration
Low-mid rates
Charged Ions

### TERRESTRIAL

Long duratio
Variable rates

Neutrons + Gammas



### **SPACE NUCLEAR**

Variable Duration
Variable Rates
Neutrons + Gammas







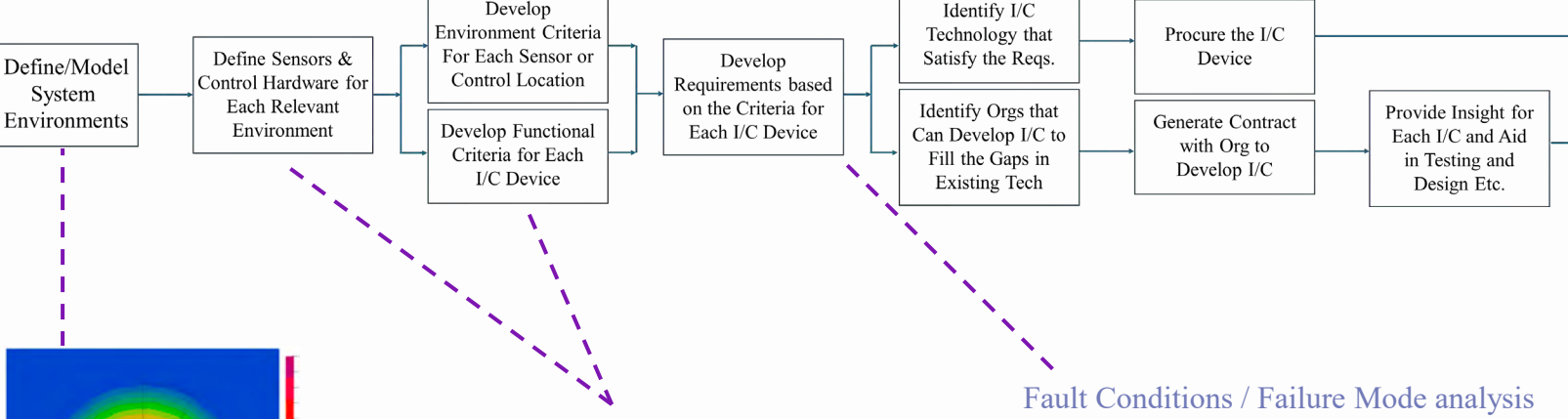




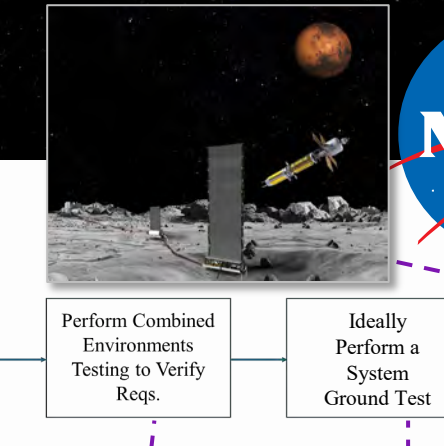
# **I&C Roadmap for Technology Maturation**

PI: Dianne Ezell (ORNL); Tyler Steiner (NASA-GRC); Jarvis Caffrey (NASA-MSFC)





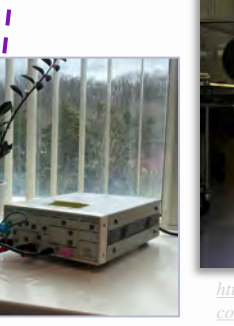
Sauce .	fed:	Wheel .	tendos falavo (IM-	Oleganya (166				
Pierry	Product Factorial See Even	Display	Street Arting (After principle Souther Advance Cons)	And anastroly Ching form Eventure     All Type (m) To liver group:     All Type (m) To liver group:     Debricon these a variety for an almost one group of all groups, will then beautiful.     Application of Neutron Speciety I vine group in prysical				
	Propries Fractions Loss (Impac)	0.0-04	Start SHAT districted the Salary experimental	Make the Salary automorphism is in the UNA				
	Paper / Acros Ma	beck	Manager DRAF	State organization Consideration Frontings     And Country organization of Anthony Consideration     September of Securing State     Securing Consideration of the General Consideration of Anthony     Securing Consideration of Consideration				
	langen	Directal.	The tase of DKAI	And an investigation of prices of extrements  - And Traps should be done proper  - December & diagnost in the second constraint of distinct in the format in the format in the format in the constraint of the prices of expectation of expectation of expectations.				
	944	District Market	Million Long. High screams or place	Add property () (Song-drawn if recovery     Add Tops cript for their grappy     Selection of problem to also shows only only of drawn or all forces     They found change resources position to UV				
Fun Assembly	Successed Filter	Olive 6k	See 1907 take carriery and many					
	Price in the	Double	Kith demand blockey     Stable Sorter	The minimization is form of that processing of the PATHOP (processing).  If you described the following the first processing of the processing of the processing of the processing of the pathological processing or processing of the pathological processing or processing or processing or pathological processing or proce				



Perform Functional

Testing to Verify







https://aerospaceamerica.aiaa.org/departents/space-nuclear-power-seriously/

Repeat for each sensor, location/environment, combine testing as much as possible





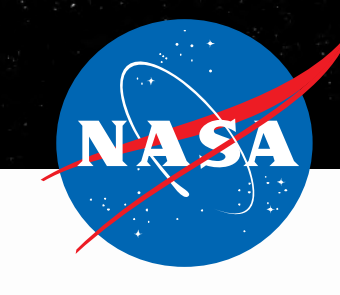
SNP I&C GRD







# **I&C** Technology Maturation



- Proposed Topics Identified as "Risk Items" for FSP:
  - Radiation Power Monitoring
  - Actuators
  - Temperature Sensors
  - Pressure Sensors
  - Radiation Hardened Electronics (unfunded ORNL)
  - Fiber Optic Sensing (unfunded ORNL)
  - Autonomous Controls (unfunded INL/ORNL)
  - In-core Radiation Detectors and Power Inferencing (unfunded INL)











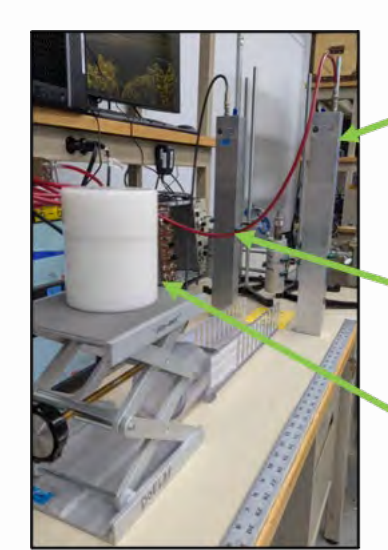
# Reactor Power Monitoring: Ex-core Radiation Detection

PI: Ryan Fronk (INL)

- Radiation detection is crucial for realtime monitoring of reactor operation.
- Goal: Qualify commercially-available radiation detector systems for operability in space using real-world measurements.
  - Differentiate between reactor-born radiation from space-born (i.e. background) radiation,
  - Integrate ML-based analysis software (SPOCK) into reactor operation and safety control,
  - Predict detector life expectancy, calibration drift, etc.
     over time and mitigate any adverse effects,
  - Integrate and demonstrate detector response to radiation with actuator and controls testbed.



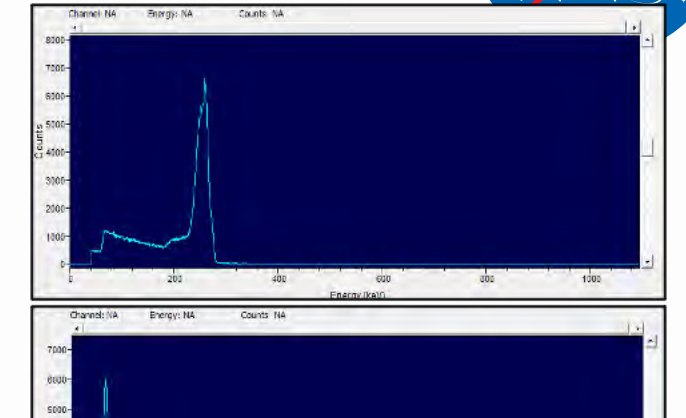




Witness Charged-Particle Detector.

Neutron-Sensitive Ex-Core Reactor Monitor Sensors.

Moderated Cf-252 Neutron Source. Distance, intensity, and energy emission spectrum is iterated through testing.



 Depicted are the measured reaction-product spectra as reported by the 3He detector (Top) and the 6Li-Foil detector (bottom). Each show good signal-to-noise ratios.

- Exploring <sup>3</sup>He- and <sup>6</sup>Li-Foil Sensors for Stand-Off Neutron Detection and Reactor Power Monitoring
  - <sup>3</sup>He: Industry standard for neutron detection, very high detection efficiency, flight tested on multiple NASA missions,
  - 6Li-Foil: Low cost, low back-fill pressure alternative to 3He. Possibility of neutron-insensitive witness detectors, sensitivity to directional orientation, etc. for greater background subtraction.



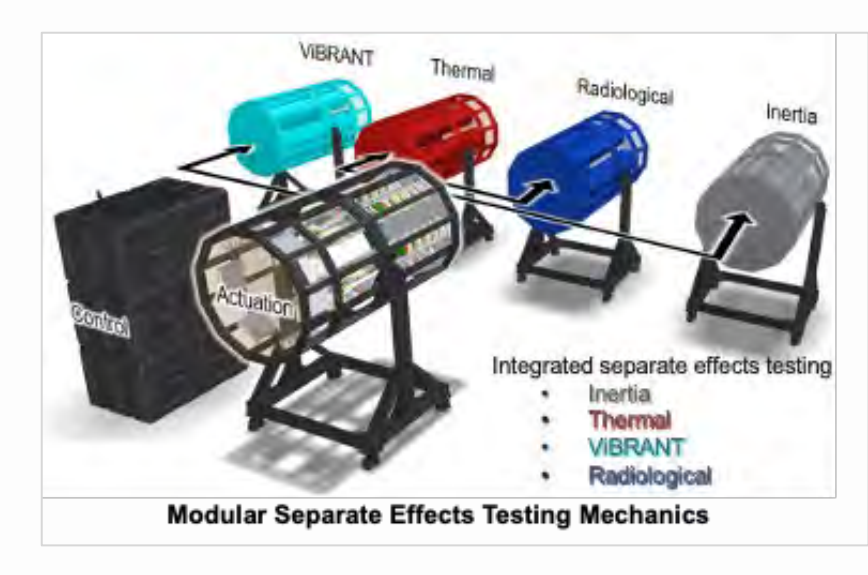




# **Actuators: Testbed Developments for Autonomous Controls**

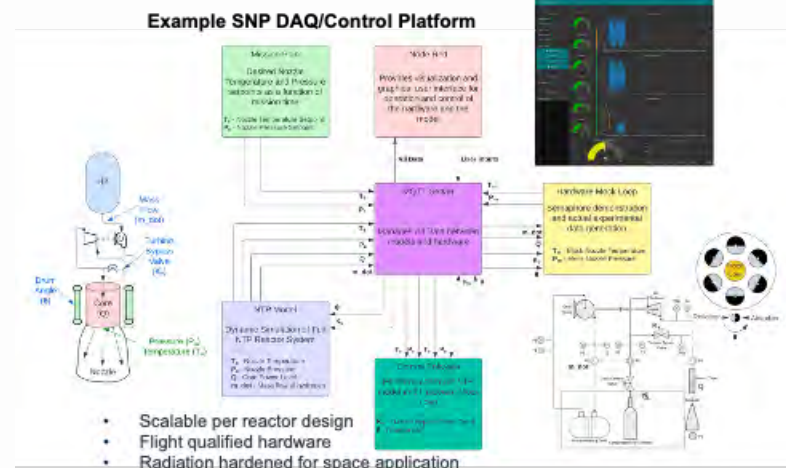
PI: Tony Crawford (INL)

- Actuator hardware and software for reactor control has never operated per FSP mission
- Goal: Build hardware-in-the-loop testbed to evaluate long term operation and develop autonomous controls
  - Integrated separate effects testing
  - Gravitational effects testing
  - Flight-ready, deployable data acquisition and control hardware





Environmental Loading (lateral and vibration)













STARTUR

FSP reasoning:

STEADY STATE

SSCV CONTROL OF TEMP

Communication

SHUTDOWN

# **Autonomous Controls**

#### Space Nuclear Power Autonomous Control Algorithm and Control Element Test Bed

Wilson, Brandon, et al. "Space Nuclear Power Autonomous Control Algorithm and Control Element Test Bed.", Mar. 2024. https://doi.org/10.1109/AERO58975.2024.10521158

https://ntrs.nasa.gov/api/citations/20140001436/downloads/20140001436.pdf

Long-term operation (PRA decision making)

COOL DOWN

#### Autonomous Control of Space Nuclear Reactors

Autonomous operation and safety are addressed simultaneously.

John H. Glenn Research Center, Cleveland, Ohin

Nuclear reactors to support future robotic and manned missions impose new and innovative technological requirements for their control and protection instrumentation. Long-duration surface missions necessitate reliable autonomous operation, and manned missions impose added requirements for failsafe reactor protection. There is a need for an advanced instrumentation and control system for space-nuclear reactors that addresses both aspects of autonomous operation

The Reactor Instrumentation and Coutirol System (RICS) consists of two functionally independent systems; the Reactor Protection System (RPS) and the Supervision and Control System (SCS). Thorough

and, upon sensing a system anomaly, automatically takes the appropriate actions to prevent an unsafe or potentially unsafe condition from occurring. The RPS encompasses all electrical and mechanical devices and circuity, from sensors to armation device output terminals

The SCS contains a comprehensive data acquisition system to measure rontinuously different groups of variables consisting of primary measurement elements, transmitters, or conditioning modules. These reactor control variables can be categorized into two groups: those directly related to the behavior of the core (known as nuclear variables). and those related to secondary systems (known as process variables). Reliable closed-loop reactor control is achieved

tion from tions by ma in order to The RIC

dancies tha ration, ele tional inde complies of a muchan availability is intended puter (the where the a

The RICS inherent is also integra desector (V provides th Table 1. Major technologies for auton

Technology category Major technologies Notes/examples Deep Space 1: asteroid detec-Navigation and control tion, orbit updates Chang'e 4 lunar landing, Per-Terrain-relative navigaseverance entry, descent, and Computer vision systems near earth object exploration, Perception and sensing Mars rovers (Spirit, Curiosity) LiDAR and laser ranging 8-9 Havabusa2 terminal descent. Mars 2020 field-programmable gate array enhanced sensing OSIRIS-REx touch-and-go Robotic arms and manip-Robotic systems sampling at Bennu Surface mobility (rovers) 9 Sojourner obstacle avoidance. modern rovers Al for decision-making ESA OPS-SAT deep learning, AI and ML NASA image processing Brain-inspired computing 3-4 ESA Advanced Concepts Team research, experimental High-bandwidth commu-NASA CAPSTONE peer-to-Comms and data peer navigation Onboard data processing 8-9 ESA FSSCat Al chip for filter-Solar panels and battery Widely used in low Earth orbit Power management and deep space missions Radioisotope thermoelec- 9 Deep space missions (e.g., Voy-

TRL Scale: 1 (basic principles) to 9 (flight-proven). Estimates are based on deployment in missions and research status as of

CUI//SP-NUC

ORNL/SPR-2025/3826

Space Reactors Autonomous Roadmap

ager, Cassini, New Horizons,

Supports AI/ML in space, radiation-hardened designs

Curiosity)



radeep Ramuhalli lesley C. Williams lichael D. Muhlheim nathan McConnell . Dianne Bull Ezell

pril 2025

RTMENT OF ENERGY

https://inldigitallibrary.inl.gov/sites/sti/Sort 64742.pdf

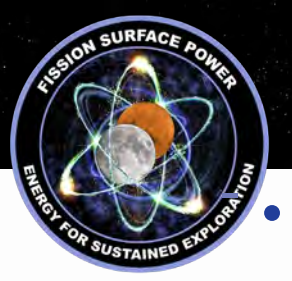
Autonomous controls are a requirement – currently low TRL for terrestrial reactors







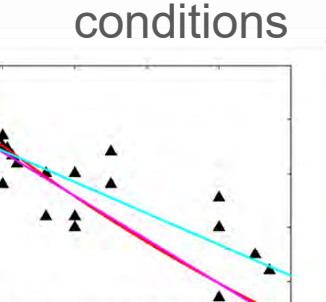




# **Temperature Sensors: In-core and Near-core**

PI: Richard Skifton (INL)

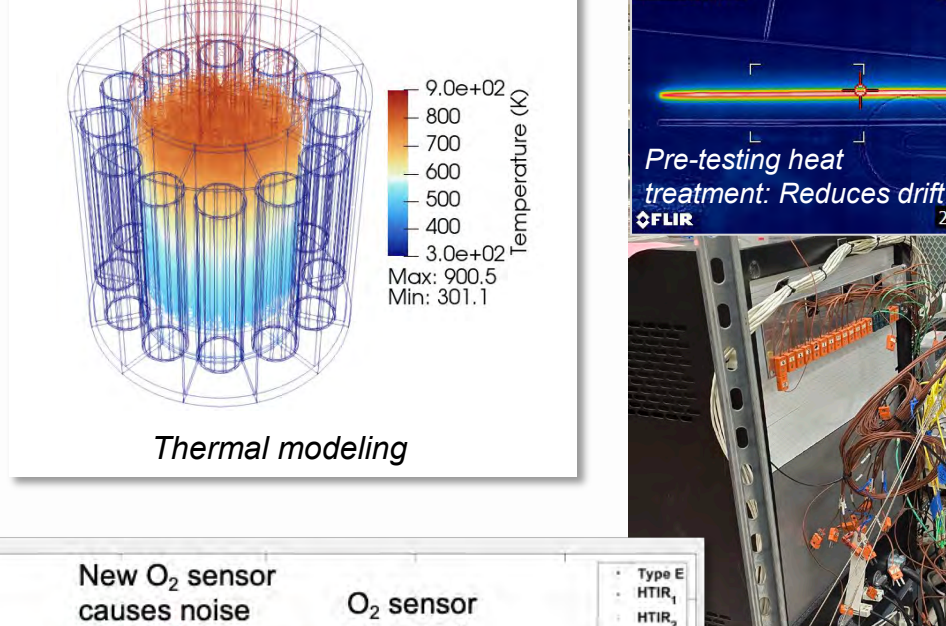
- Temperature detection crucial for reactor operation and monitoring
- Goal: Demonstrate long-term survivability of HTIR-TC
  - Predict life expectancy and drift over time through continuous furnace testing
  - Irradiation demonstration at FSP relevant

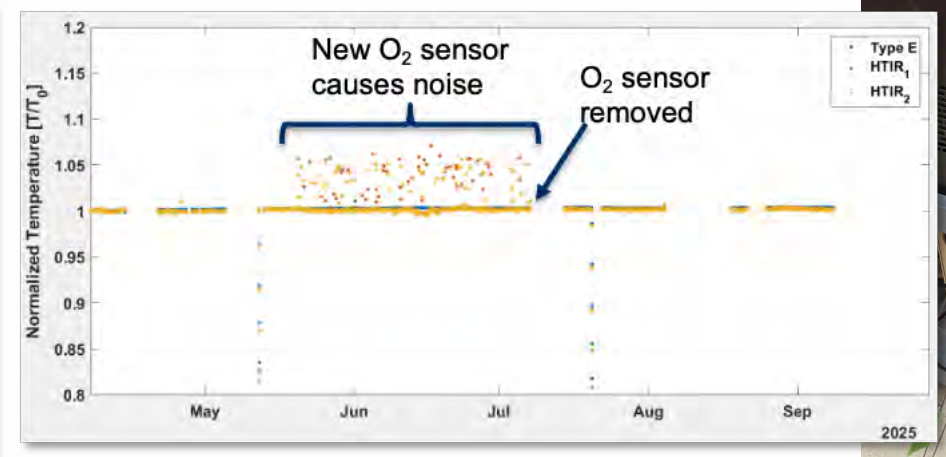


Thermal Fluence (10<sup>21</sup> N/cm<sup>2</sup>)

Halden-Conroy:  $D=-100(1-e^{(a(b-\phi))})$   $0.25 \le \phi \le 1$  a=0.067 b=0.25  $1 \le \phi$  a=0.104 b=0.52 Halden-General Electric:  $D=-8.1(\phi-0.25)$  General Electric:  $D=-5.8\phi$   $0 \le \phi$ 

Shake down of differing empirical models showing drift of "Type D" thermocouples [Riley, 2023] during irradiation tests over the foregoing 30 years











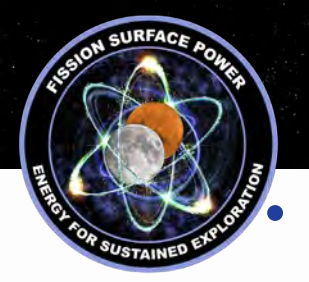


Furnace and

TC inserts

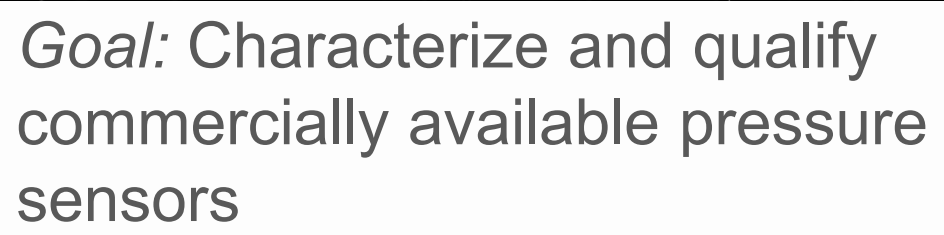
and Cold
Junctions

~103°C



# Pressure Sensors: Near-core (Rad-hard)

PI: Joshua Daw (INL)



- Market-survey of COTs
- Single vendor identified with viable option

Vender	Bast Model	Technology	Pressure	Temperatore Limit	Radiation Rating	WeightMass	Electronics	Cost	Delivery	Link	Neivs
PCB.	175A33	Plezoelectric (dynamic only) or silicon on supphre piezoresistiye	Up to 3000 PSI	ири тексі.	NA	3.1 uz	482006	5927 without electronics	6 wooks	https://www.pcb.com/pr oducts?m=176A33, https://www.pcb.com/pr oducts?m=482C05	A DESCRIPTION OF THE PARTY OF T
Kistler	NA.	Piezoelectric (dynamic prity) or stition on papphine piezorosistive (of filed)			NA						Strain gauges used for force sensors. May be ab to customize, but development needed
Kuma	ETUT-312(M)		Up to 5075 PSI	Lie to 196. G	NA	15 grams				https://kuite.com//asset s/media/2017/06/ETL 1 -312.pdf	
Physical Acoustics	NA.										Zonalmy-onth-omo-went
Harold Schaevitz	NA.	Plezoelectric idynamic only), discensor sacphire prezonesstva LVDT/Belows	Up to 72500 psi		LVDTs are highly rad interant, other technologies are not railed	Sensor described					1.47 militarian yada mas malami munin 1400 manifesia manifesi manife malami jami nima
Stellar Technology	STIMO	77	Up to 10000 PS	UA III 2000	"Space Rated"	10 02	"Rad hard" incorporated into sensor. "Electronics manufactured to NASA 8739.3"			hitps://www.stellurtech. com/product/scace- rated-pressure- transducer-senes- sc1300*	Waiting on quote/mapone
Sigma-notics	SST 64X-RT	Strain gauge on daptragm	Up to:	De as 400F	10 Mrad	*0.4 nz	Not needed, in- line electronics ruln radiation tolerance	\$3K tor seriedt, \$30K with electronics (not needed)	20 media	https://www.sigmanotic s.com/products/prossure-transducers/sst-54v- if-sone-transducer/	Vishay's M-Bond 610 use for bonding strain gauge limiting factor for temperature and rad tolerance, have current SBIR with NASA for DAG development
Sergonetics	SEN-160	Silicon on supphire piezoresistive diaphragm, Built in RTD	Up to.	the resympt	777		oyanan.c			0.30000	Waiting on quotalmsports
Ultra Energy	NP9000		Up to 2500 PSI	de au engi-	35 MRud					hitps://www.udra.energy/ media/stuprs.ua/np9000- cetreme-en/uorimen/- pressure-transducers- march/24.1.pdf	Waiting on quotalnespons
Suprock Technologies	Custom Prototype	Shain gauge on disphiages	Variable by design	2906K	"Stable" in high reuman and gamma	97	Custom amplifer/DAQ, tailored to sensor	Sensor –22K Biectronics –44K		https://suprocktoch.org/ innovations/	Purchesa Undervillay





Suprock Developed High-temperature and Radiation-resistant Pressure Sensors. <u>Note this</u> is a proprietary design and development

- Benchtop Testing and Irradiation planned under NSUF Super-RTE at MIT research reactor
- Sensors built upon request to meet needs of application











# Summary of progress / Looking forward



- Radiation: testing completed application specific software still in progress
- Actuators: Hardware procured assembly in progress
- Temperature: 2<sup>nd</sup> year of testing completed; drift model adjusted to account for new data – more data would strengthen the model
- Pressure: commercial sensors acquired irradiation pending Jan/Feb 2026

- Based on 40kWatt / 10 year mission
- Adaptable for any reactor power requirements or mission ops
- Technology gaps still exist:
  - Radiation hardened electronics
  - Fiber Optic sensing
  - Robust Autonomous Controls
  - In-core radiation detection
  - So many more...











# FSP INSTRUMENTATION and CONTROLS Evaluation of Instrumentation Sensors and Electronics

Robert Okojie<sup>1</sup>, Philip Neudeck<sup>1</sup>, John Wrbanek<sup>1</sup>, Susan Wrbanek<sup>1</sup>, Liang-Yu Chen<sup>2</sup>, Carl Chang<sup>3</sup>, and Norm Prokop<sup>1</sup>, and Philip Ugorowski<sup>3</sup>

<sup>1</sup>NASA Glenn Research Center, Cleveland, OH 44135

<sup>2</sup>Ohio Aerospace Institute, Cleveland OH 44135

<sup>3</sup>HW5-LLC, Cleveland OH 44135

robert.s.okojie@nasa.gov

NASA Fission Surface Power Project.

Fission Surface Power (FSP) Technology Maturation Webinar Series 9/24/25

### **Motivation**



- Unlike terrestrial nuclear power plants (NPPs) and emerging Small Modular Reactors (SMRs), the lunar FSP system is more compact, autonomous, and a prescribed 10year life.
- Instrumentation must be compact, rad-hard, and high temperature (~800 °C) durable.
- Failing lunar FSP reactor sensors would not have the luxury of replacement.
- From FSP instrumentation reliability standpoint, the sensor technologies are currently not commercially available for deployment.

# **Objectives:**

### Evaluate heritage SoA unshielded:

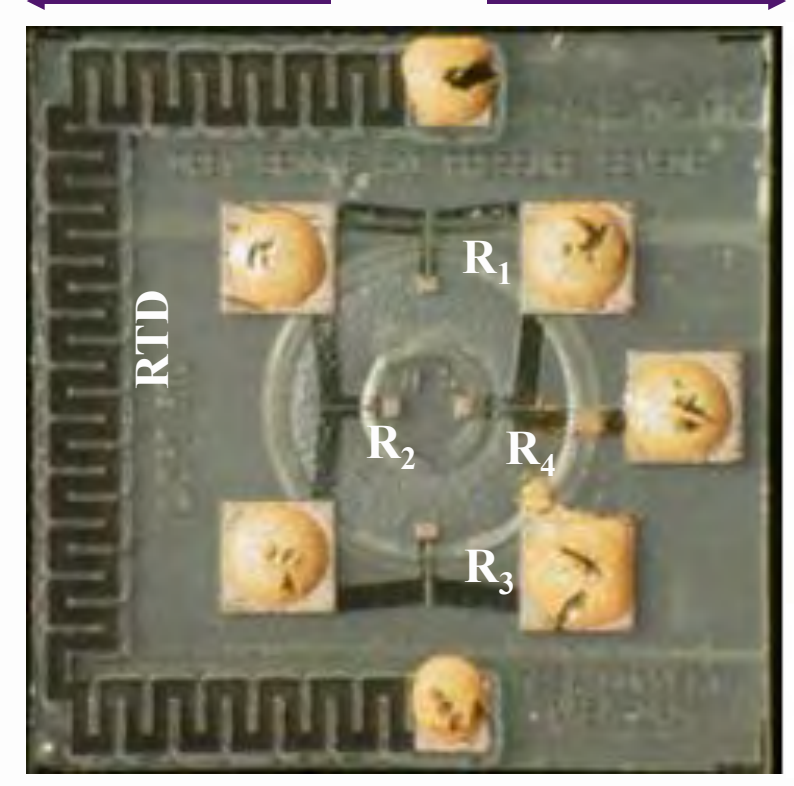
- 1. On-chip integrated 4H-SiC pressure/temperature sensors. (Tested to 800 °C)
- 2. Multi-functional thin-film sensors. (temperature, strain, heat flux). (Tested to 1000 °C)
- 3. 4H-SiC Integrated Circuits. (Tested to 500 °C).
- 4. Use results as baseline reference to develop more robust sensors and electronics for future reactor applications.

# Pressure Sensor: Quick Overview of the Wheatstone Bridge Circuit





4 mm



Input current

In a perfect world,  $R_1=R_2=R_3=R_4$ Therefore,  $V_{out}=0$  (Balanced Bridge)

In an imperfect world,  $R_1 \neq R_2 \neq R_3 \neq R_4$ Hence,  $V_{out} \neq 0$  (Unbalanced Bridge, **Zero-Offset**)

As a piezoresistive pressure sensor

$$V_{gross}(T,P) = V_{\underline{Z}P0}(T) + S(T)P$$

Zero-Offset Voltage

Pressure Sensitivity

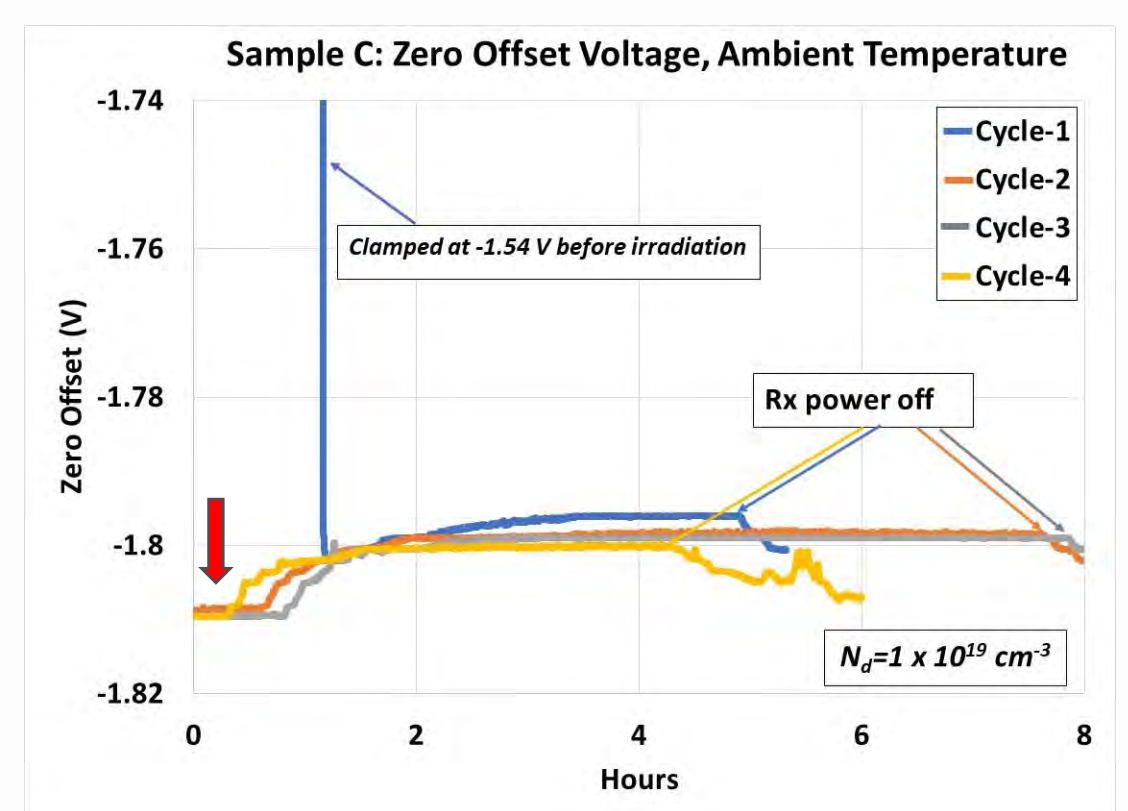
4H-SiC Integrated pressure/temperature sensor view of the SiC sensor chip showing co-located RTD and pressure sensor.

- These parametric variables largely govern sensor reliability and accuracy.
- Temperature effects on these parameters make combined analysis complex.
- Hence, de-coupling is required for effective analysis.
- This presentation focuses on the radiation effects on the Zero-Offset and

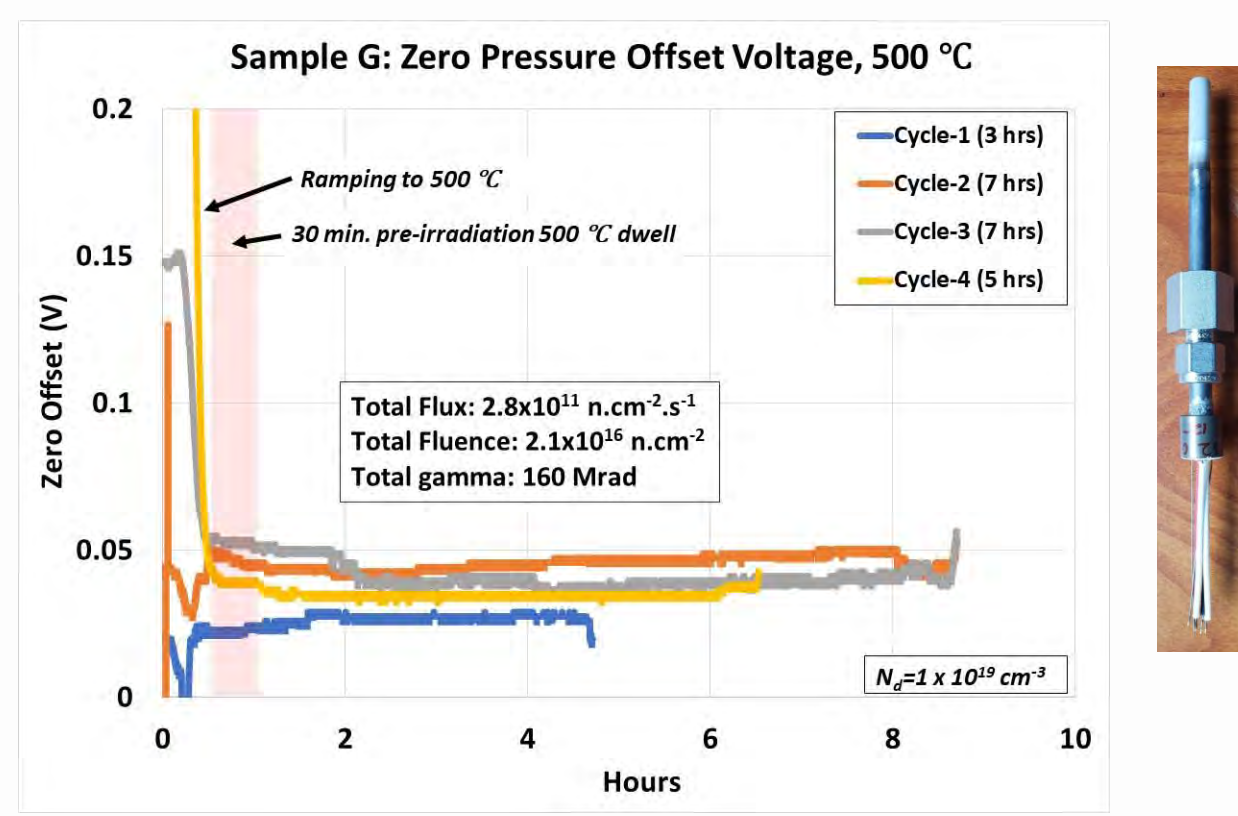
# OSURR: Radiation Effects on Zero-Offset, Ambient and 500 °C



### Sample-C



### Sample-G



### **Ambient Temperature**

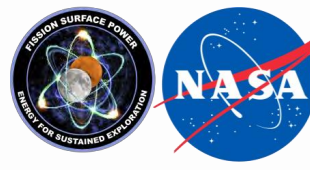
- Offset rises to "steady-state." Likely gamma heating
- Drifts at steady-state, more in Cycle-1.
- Offset returns to reference before next cycle.

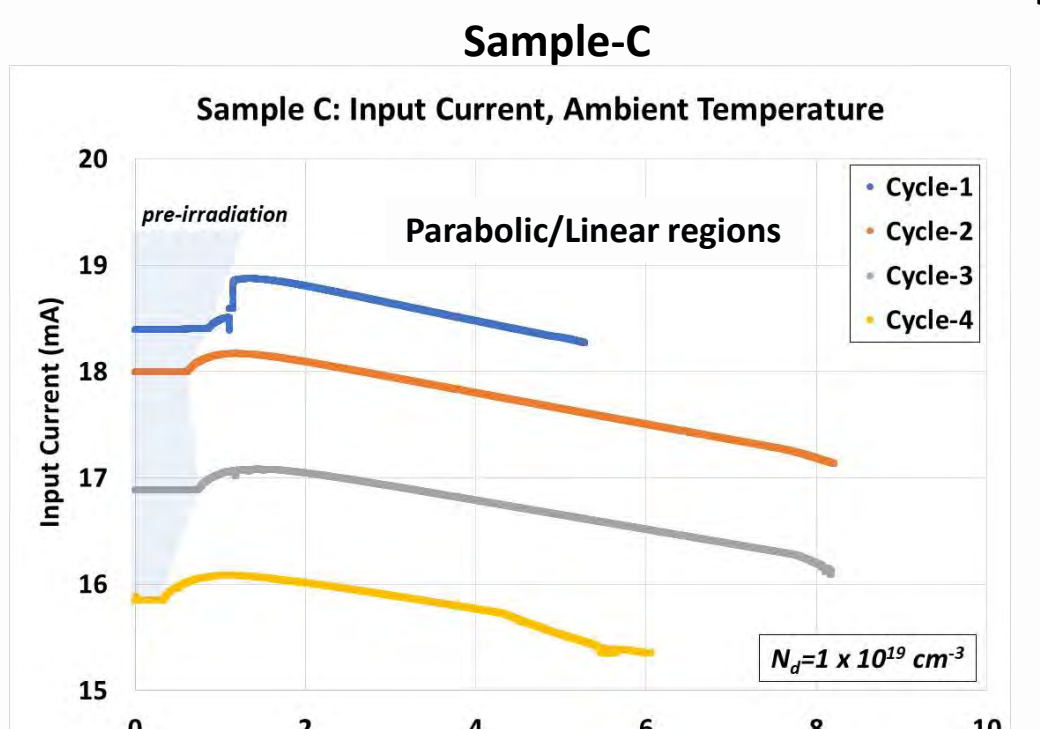
### Irradiation after 500 °C, 30 minutes of dwell time

- No rise in offset at irradiation. Gamma heating suppressed.
- Minimal drifts at steady state, except Cycle-3 initially.
- Shifts before next cycle.

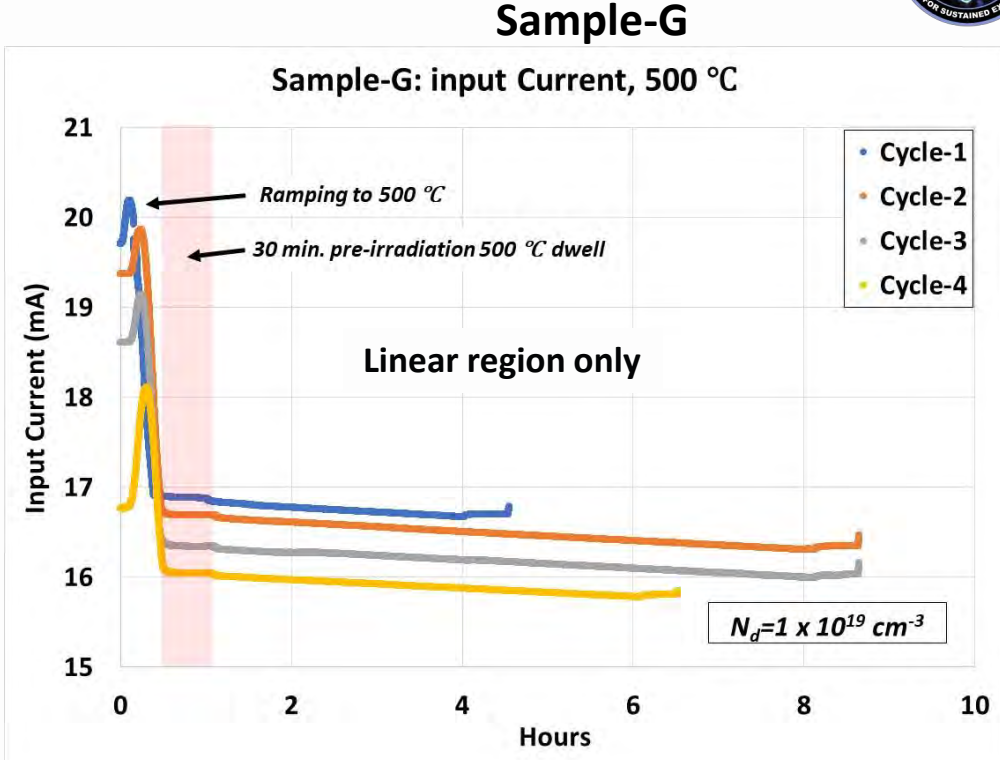


OSURR: Radiation Effects on Input Current, Ambient and 500 °C





Hours



### **Ambient Temperature**

- Parabolic rise and quasi-linear negative slope.
- Current drops after each cycle-Resistance increase.
- Slopes of all cycles exhibited systemic behavior.

### Irradiation after 500 °C, 30 minutes of dwell time

- Only linear region present during irradiation.
- Current drops after each cycle-resistance increase.
- Slopes of all cycles exhibited systemic behavior.
- Slopes flatten with reactor off.

**Irreversible current drop confirmed carrier removal > degrades semiconductor electronics** 

# **Summary/Conclusion from OSURR Campaign**



> Evaluated unshielded State of the Art integrated SiC pressure/temperature sensors at OSURR.

### At ambient,

- Minimal shifts in zero-offset and returned to pre-irradiation values-Minimal degradation.
- Some drifts at steady-state.
- Two charge transport mechanisms identified-initial parabolic, followed by negatively sloped.
- Negative slopes with identical trends.
- Permanent drop in current from cycle to cycle.

### ➤ At 500 °C,

- Shifts in zero-offset and non return to pre-irradiation 500 °C values.
- Only one charge transport mechanism observed-negatively sloped current seen at 500 °C.
- Consistent drop in current with increasing cycle associated with neutron-induced carrier removal.
- Results of unshielded sensors considered worst case-Baseline to guide future improvements.
- FSP-Class Instrumentation sensors and electronics would require new and innovative concepts (materials, shielding, better understanding of physics of charge transport in high radiation fields to minimize carrier extraction rate during reactor lifetime).



# **Evaluation of NASA GRC FSP Instrumentation Sensors and Electronics**

NASA FSP Contract # 80GRC024CA032



# Irradiation of NASA GRC SiC Pressure Sensors, Thin-Film Sensors and Electronics

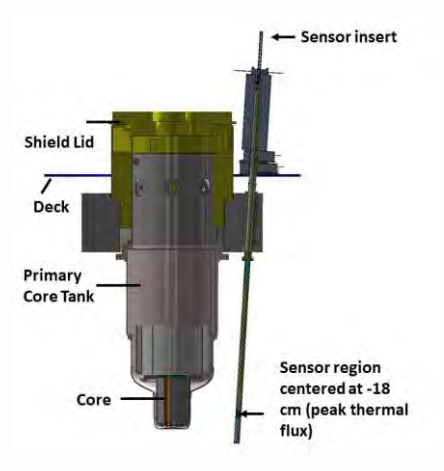


## **Objective**

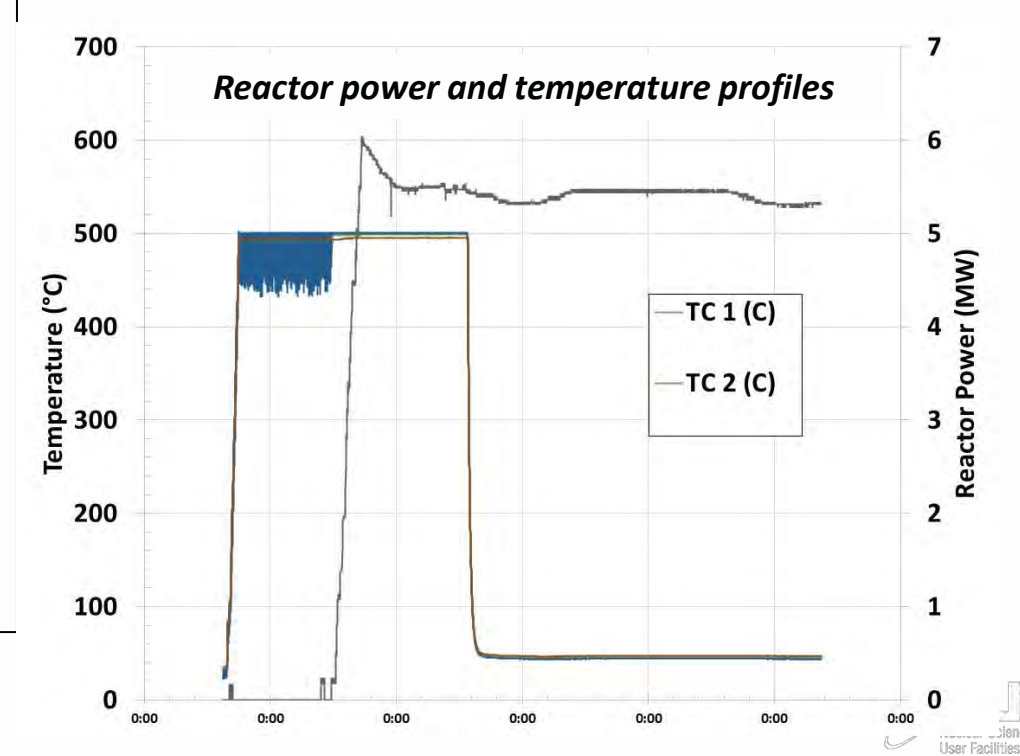
Perform irradiation at temperature of NASA GRC sensors and electronics technologies in the MITR under elevated combined temperature and radiation conditions for the purpose of baselining the TRL, as part of the Fission Surface Power (FSP) Project technology maturation plan.

## **Approach**

- 24 hrs. of In-situ measurements
- Max. thermal flux:  $1x10^{13}$  n/cm<sup>2</sup>-s E<0.1 eV.
- Max fast flux  $2x10^{10}$  n/cm<sup>2</sup>-s E>0.1 MeV.
- Temperature: 500 -800 °C.

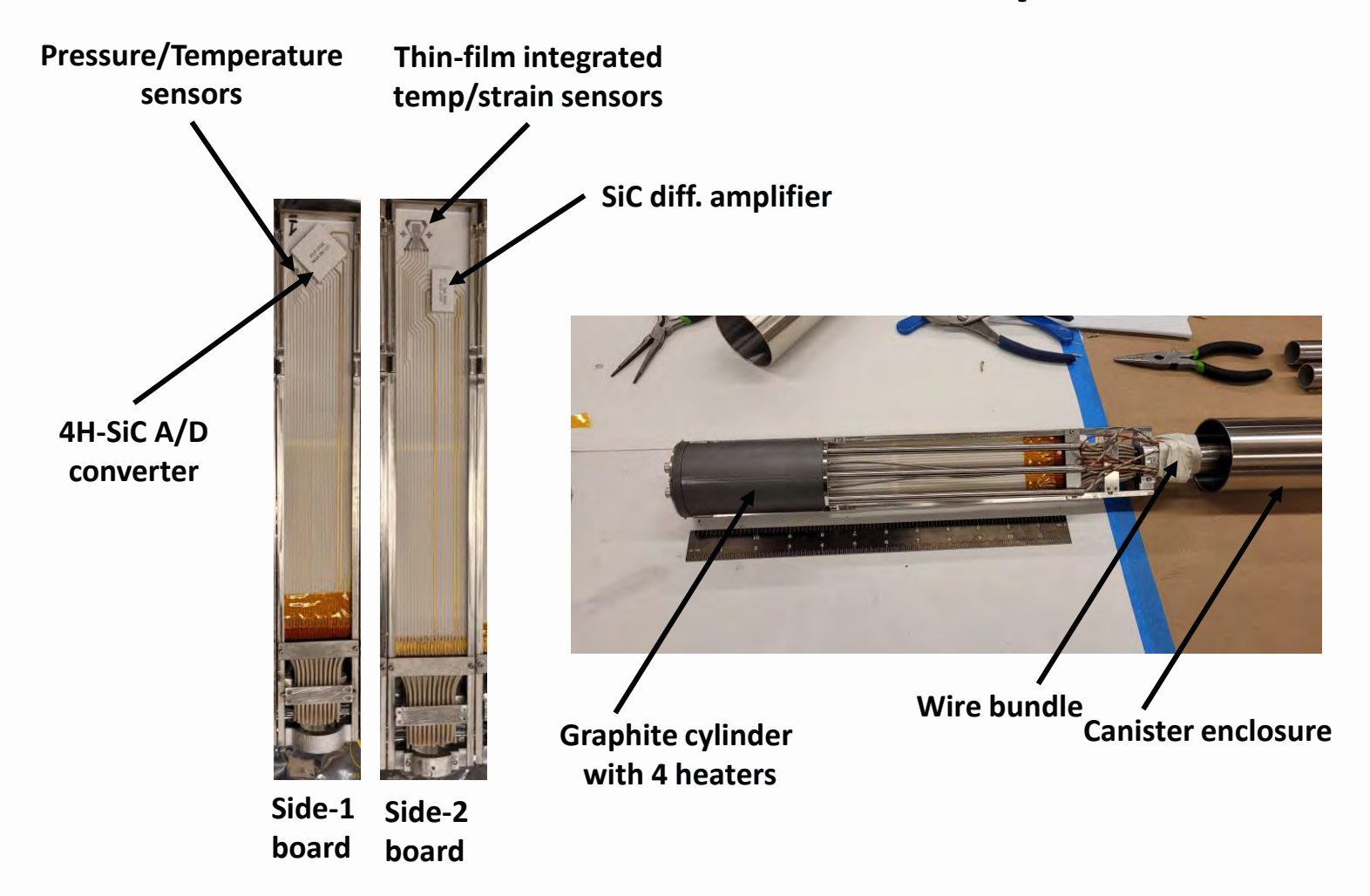


MITR 3GV position relative to core



# **Test Setup**



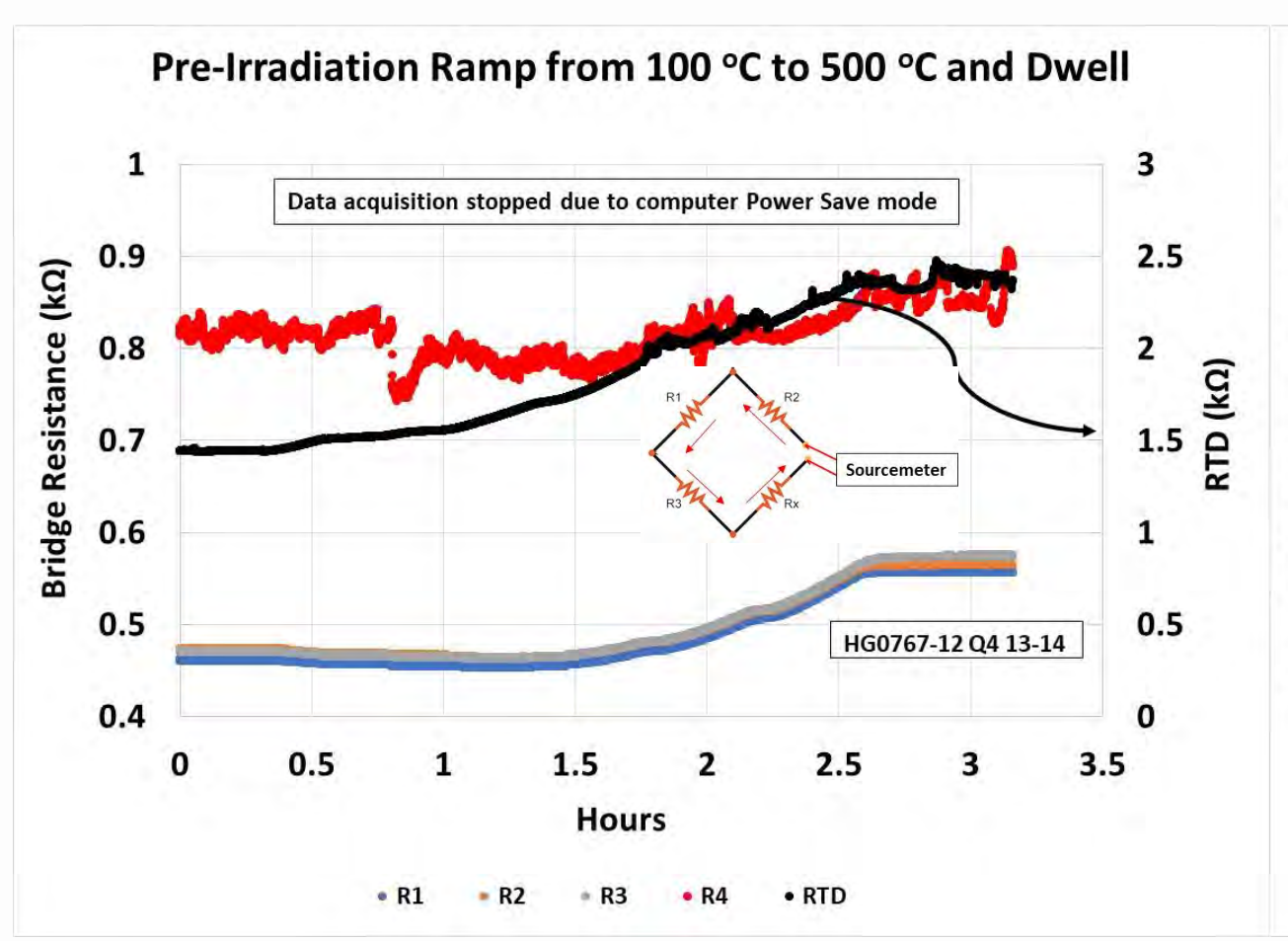


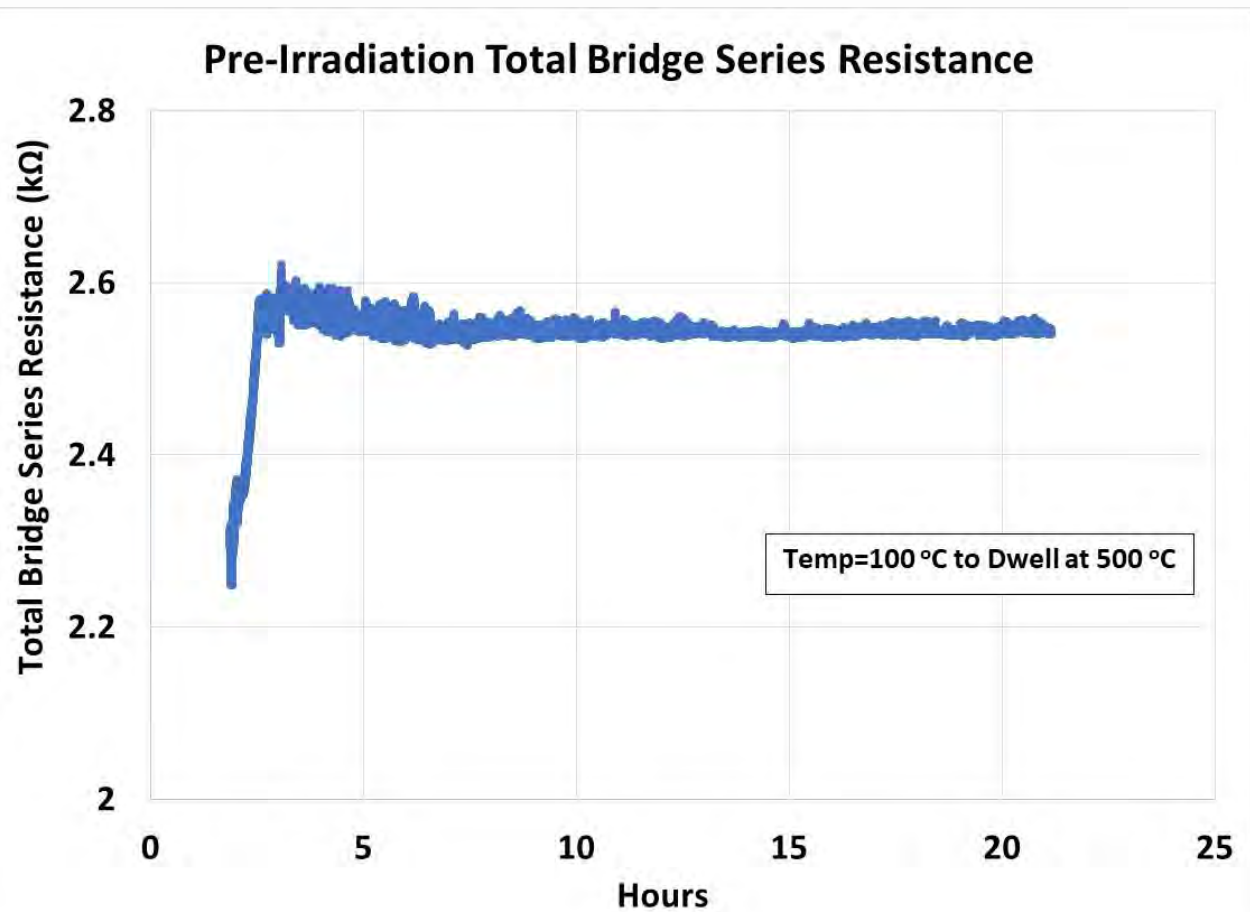


**Test article closure** 

# **MITR: Preliminary Results**





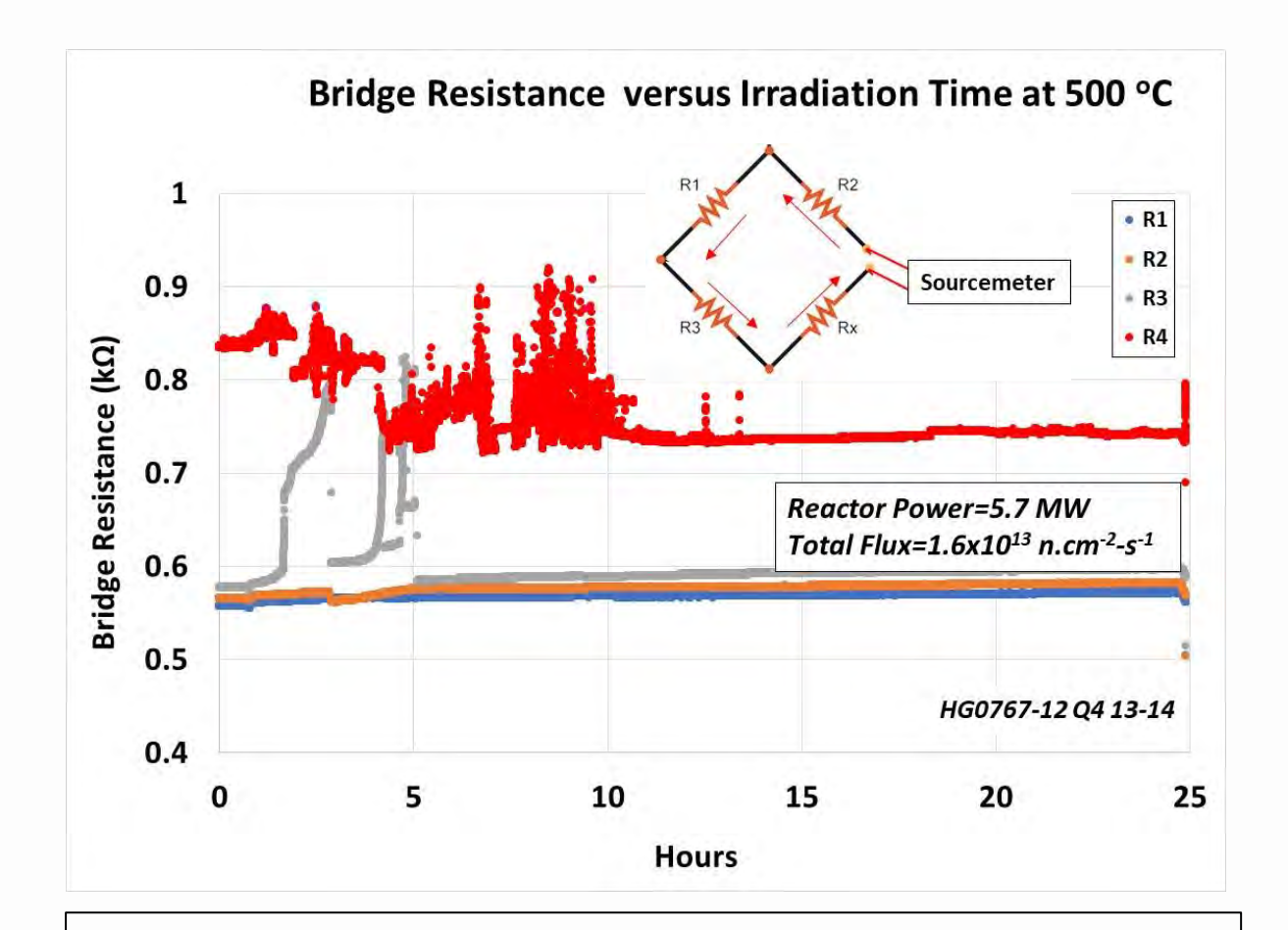


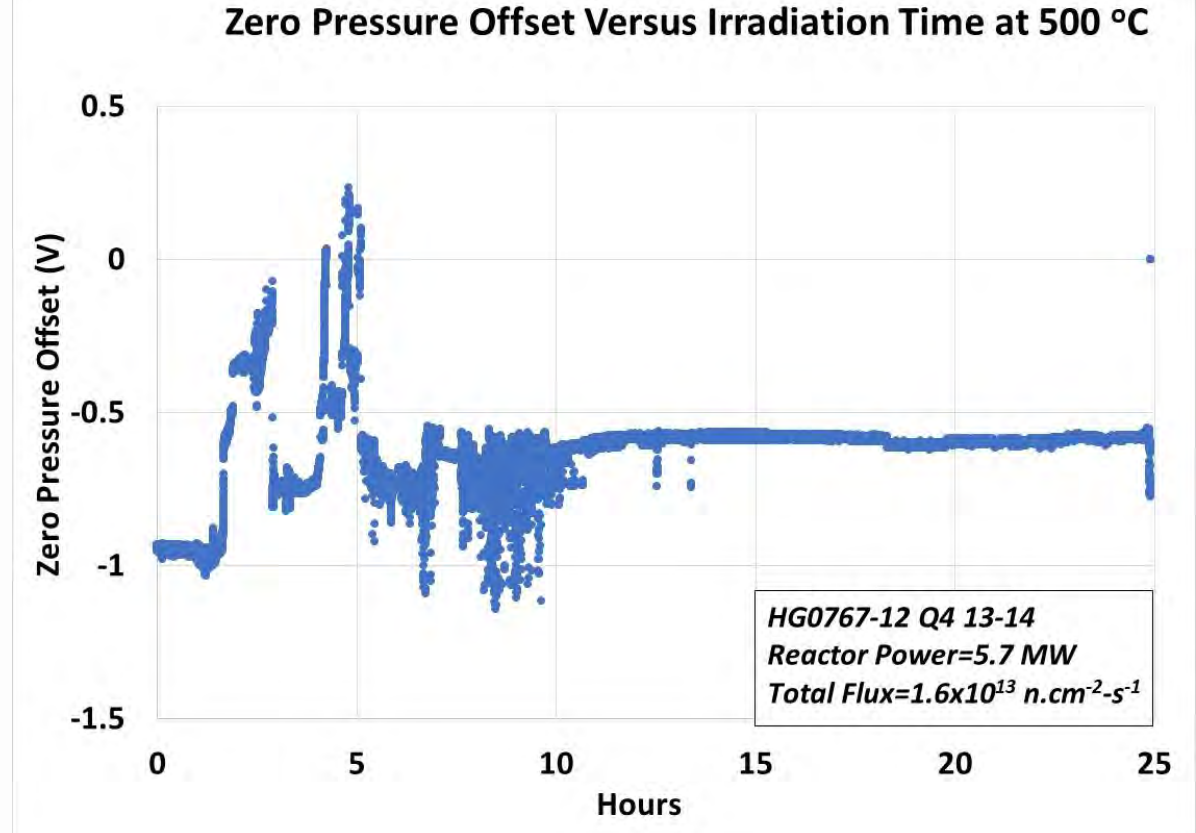
- R1, R2, and R3 tracked very well.
- R4 tracked but noisy. Would contribute to initial instability during irradiation

Aggregate of the individual resistors

# MITR: Preliminary Results (Total Neutron Fluence= 7x10<sup>17</sup> n/cm<sup>2</sup>)







- Noisy R4 contributed to initial instability.
- R3 temporary unstable, then settled.
- R2 exhibited low level instability then settled.
- Overall, increase of ~4 % at 7x10<sup>17</sup> n/cm<sup>2</sup>

- Initial instability due to shaky R4
- Relatively stable zero pressure offset after initial instability.



# **Evaluation of NASA GRC SiC Electronics**

Dr. Philip G. Neudeck

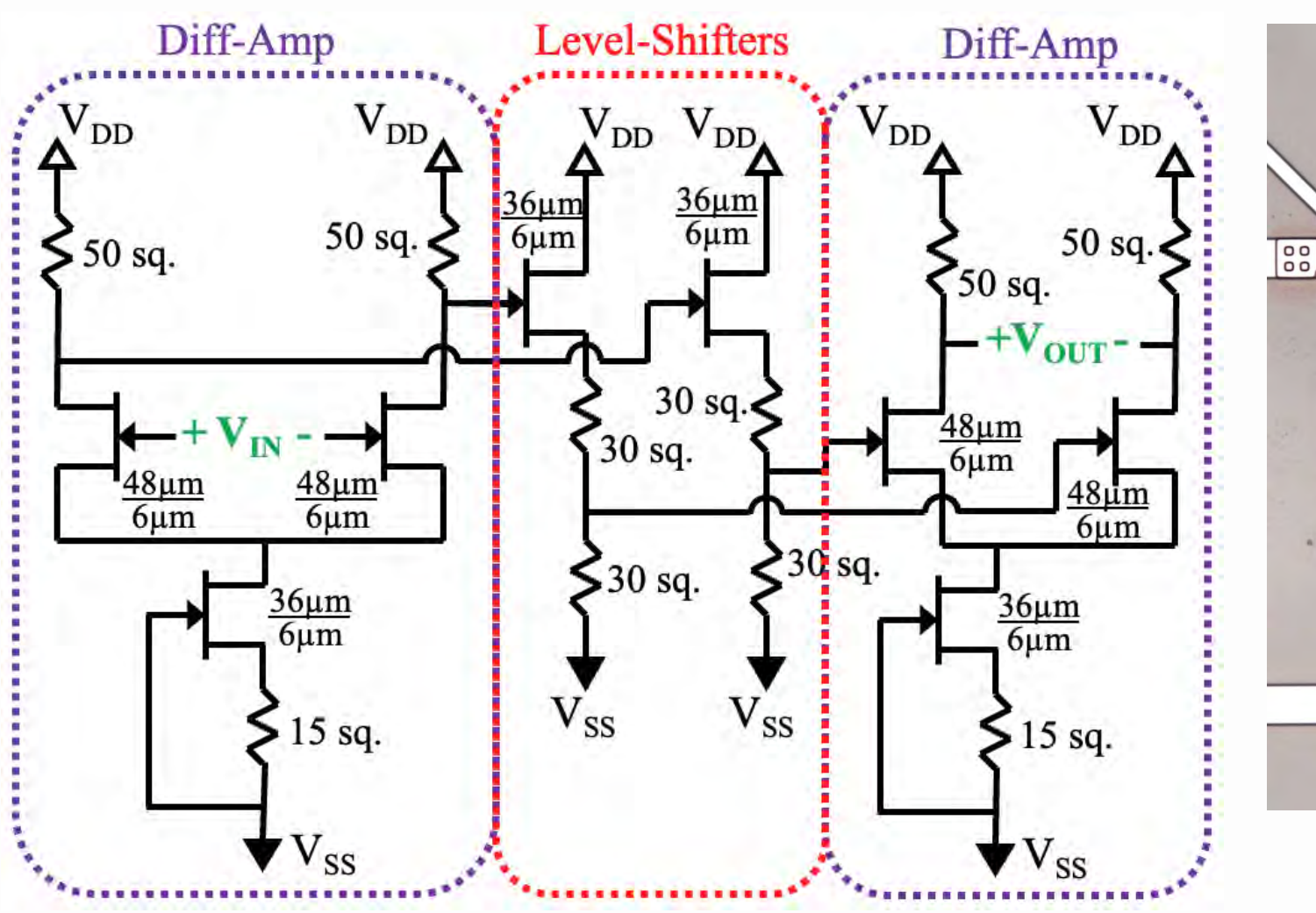


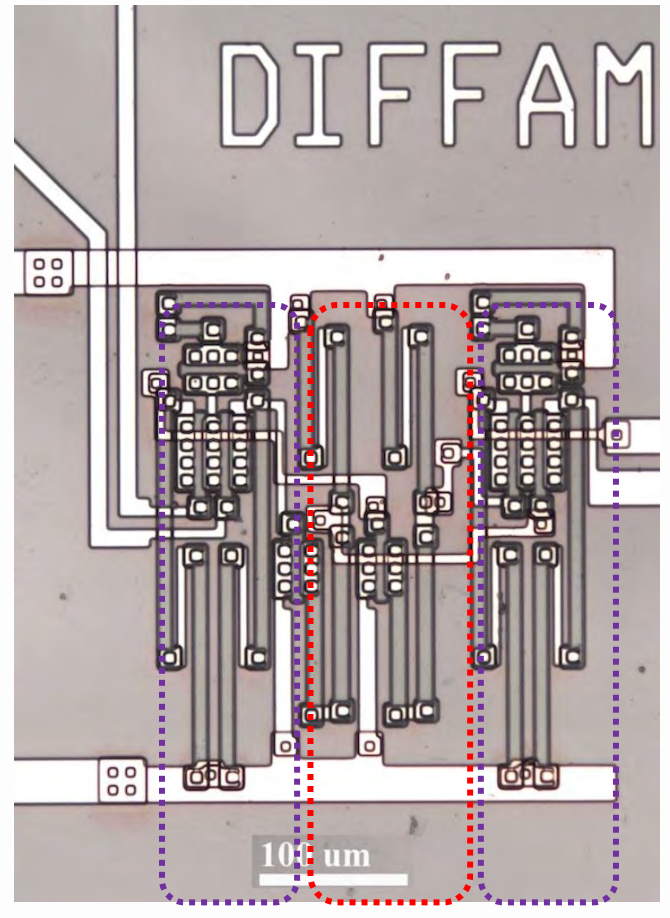
# IC Gen. 10.2 2-Stage Differential Amplifier Integrated Circuit



### **Circuit Schematic Diagram**

### **Optical Microscope Image**

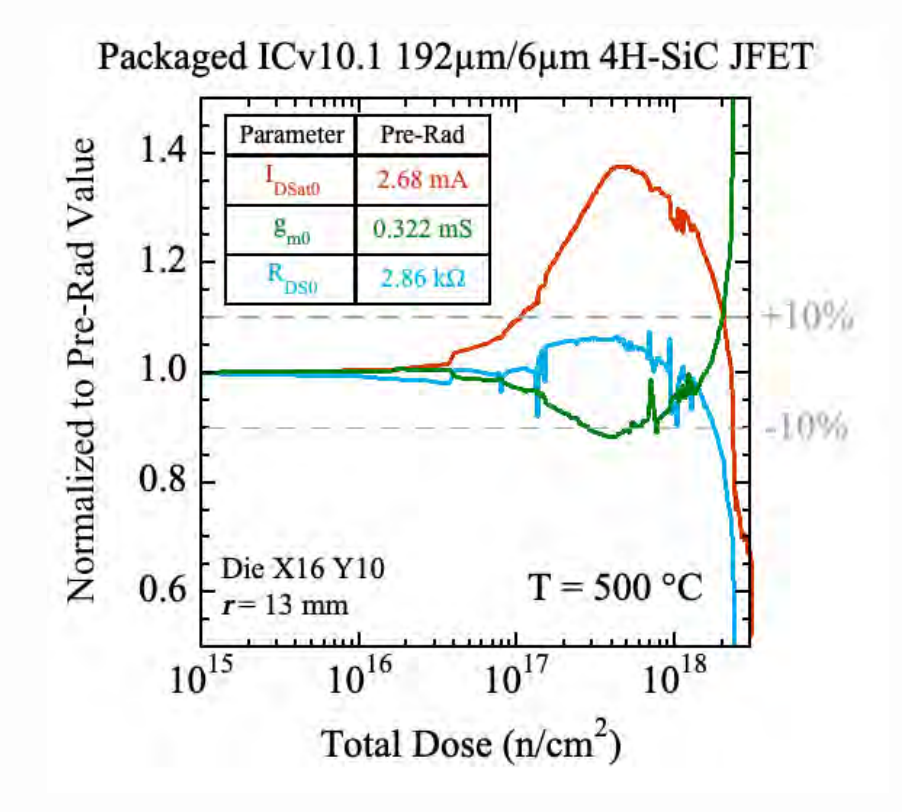




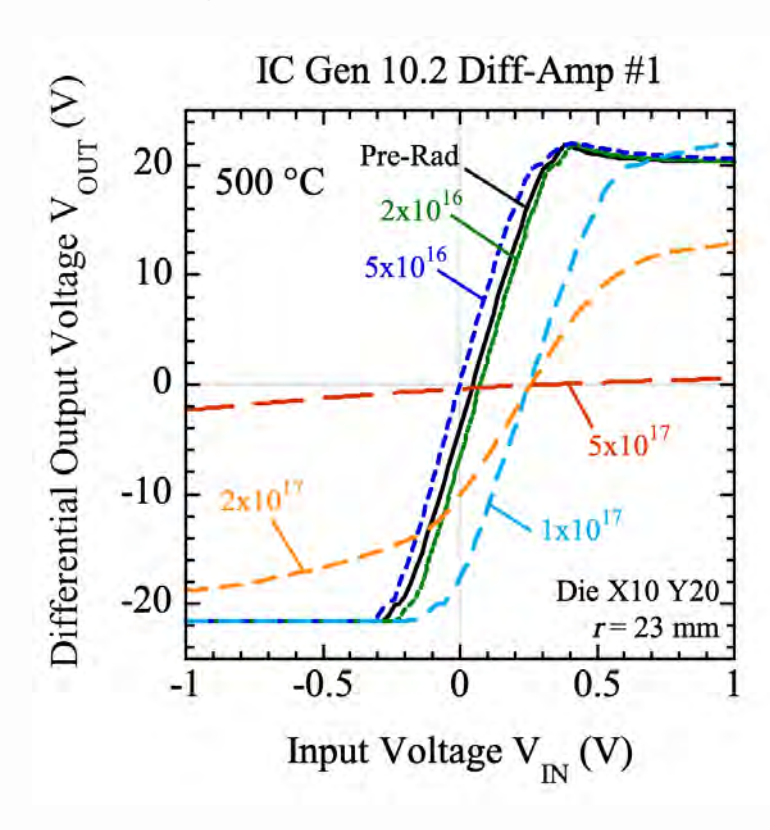
# JFET & Amplifier MIT Reactor Neutron Irradiation Measured Results



### **SiC JFET Electrical Parameters vs Dose**



### **SiC Amplifier Transfer Characteristics**



Stable electrical operation (< 10% change) at 500 °C demonstrated until total flux exceeds 10<sup>17</sup> n/cm<sup>2</sup>



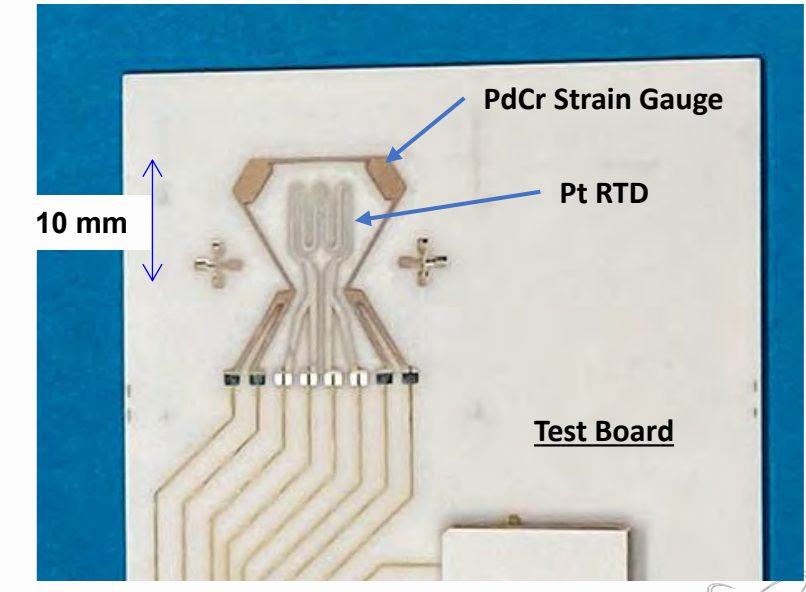
# **Evaluation of NASA GRC Thin-Film Multifunctional Sensors**

John D. Wrbanek



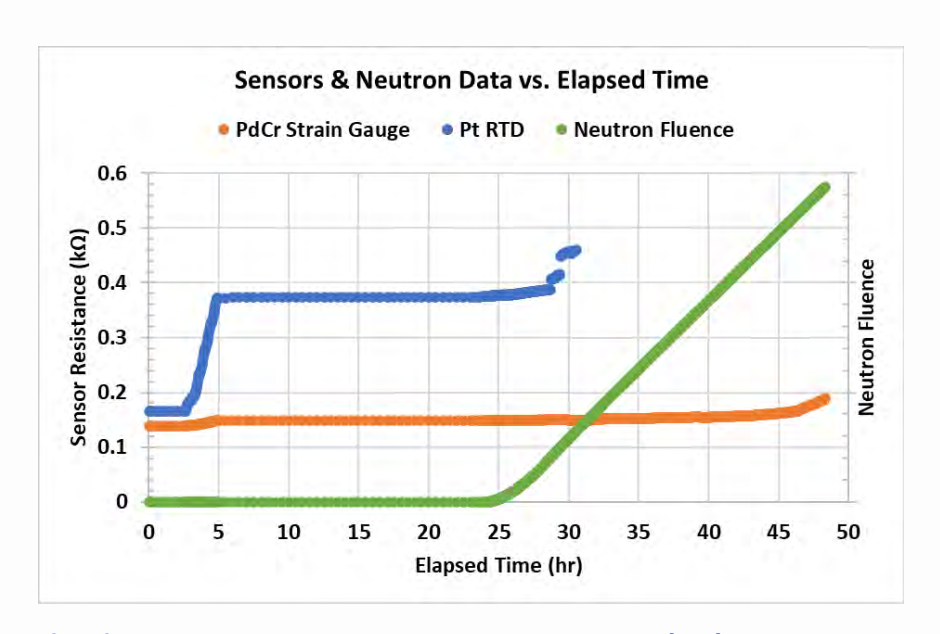
# Thin Film Sensors for Fission Surface Power MIT Reactor Test

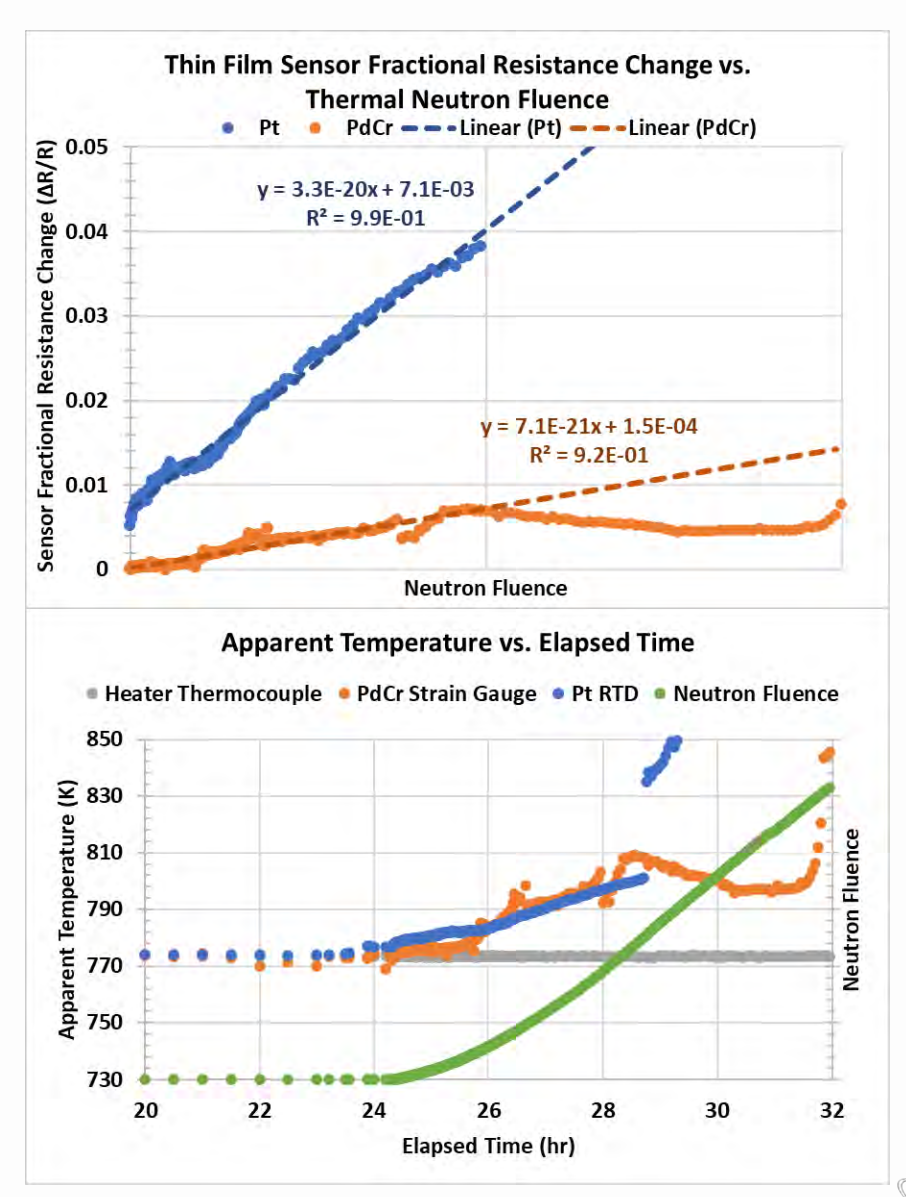
- Background: GRC's Thin Film Physical Sensors have a long history of demonstrated high temperature applications on components in a variety of conventional propulsion test conditions
  - Custom solution for difficult in-situ harsh environment measurements
  - Microns-thin, component surface fabrication significantly reduces sensor mass added to the system (<mg)
  - Improved accuracy and rapid response time with less weight
- FSP Baseline: On-Component Thin Film Physical Sensors selected from those previously demonstrated at 1000°C by GRC for MIT Reactor test
  - PdCr alloy (Pd-13%Cr) strain measurement (Lei, BSSM 1995)
  - Pt RTD temperature measurement (Wrbanek et al., AIAA-2001-3315)
  - Baseline reactor test to establish reliability in high temperature, neutron environments
- · Approach: Sensors fabricated directly on test board
  - 200 nm Pt with Ti bond coat (I/w=133)
  - 1000 nm PdCr (I/w=87)
  - 2 µm Al2O3 overcoat both sensors
- Methodology: Resistances of sensors as indicators of sensor health
  - 4-wire measurements of each @ 1 mA
  - Temperature characteristic (TCR) for each sensor measured against heater thermocouples
  - · Variations in data reveals sensitivity to reactor exposure





- At 500°C, Pt RTD & PdCr Strain Gauge both increase resistance with neutron fluence
- Sensors' resistance changes consistent with apparent temperature increase in the immediate local area
- Pt film began delaminating at high fluences
- PdCr Strain Gauge did not delaminate, but became more unstable at high fluences





## Thin Film Sensors for Fission Surface Power MIT Reactor Test Summary/Conclusion

- Refractory metallic thin film sensors actively tested in high neutron flux high temperature environment
- At 500°C, both Pt RTD & PdCr Strain Gauge thin film sensors perform nominally to high neutron fluence
- Possible heat flux observed due to associated gamma dose
- Thick Cr apparently more effective than thin Ti for adhesion
- PdCr better suited for bridge applications
- Next steps to improve stability and longevity:
  - PdCr bridge circuit
  - Pt w/ Cr vs. Ti
  - Protective overcoat layers beyond Al2O3



## **Development of NASA GRC Radiation Detectors**

Susan Y. Wrbanek



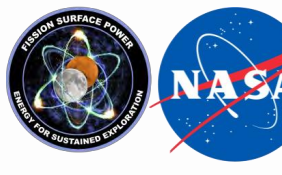


### **Neutron and Environmental Radiation Monitoring**

- Significance: Monitoring neutrons and environmental radiation for power monitoring applications is a critical need for autonomous operations
  - Includes neutrons generated by the reactor core as well as secondary neutrons and ions generated by the Lunar and Martian environment that may impact the unshielded reactor performance
  - Environmental radiation flux dependent on the local geology & typography and direction-dependent based on Sun & Earth positions
  - Near-core conditions and long reactor lifetimes requires robust, rad-hard, thermally stable radiation detectors
- Approach: GRC is examining applications for compact, low noise multidirectional radiation detectors using Wide Band Gap semiconductors (Patents: 7,872,750, 8,159,669, 10,054,691, 10,429,521)
  - GRC has developed large area (2 cm²), low noise (<5 nA) radiation detectors, demonstrated sensitive to alpha particles (1.2 MeV/u) and gamma rays (>25 keV) based on robust, high-temperature capable SiC
  - Demonstrated in repeated refractory chamber tests >120°C as part of SAA3-1804
  - Technology adaptable for long-term monitoring of neutrons and environmental radiation in harsh environments for FSP

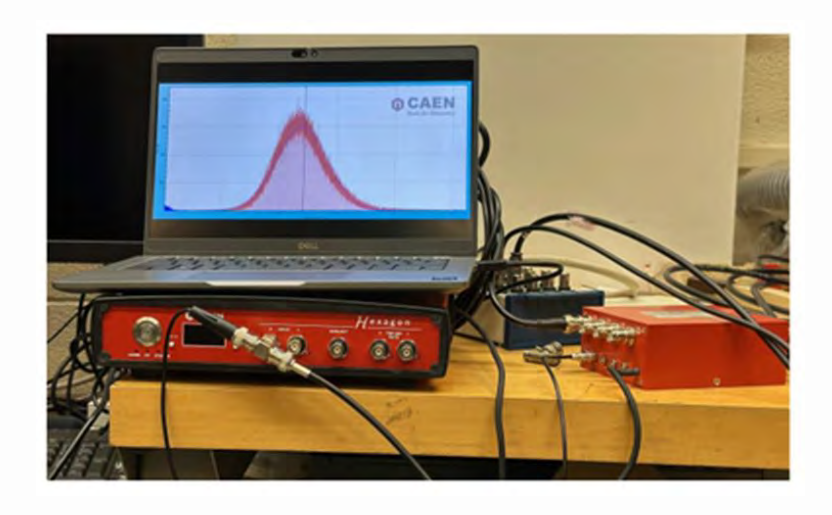
#### FSP Goals:

- Demonstrate SiC-based directional LET detectors in radiation environments to allow reliable long-duration field application of FSP system environmental monitoring
- Fabricate, characterize, and test, SiC-based neutron detectors for high temperature internal reactor environments

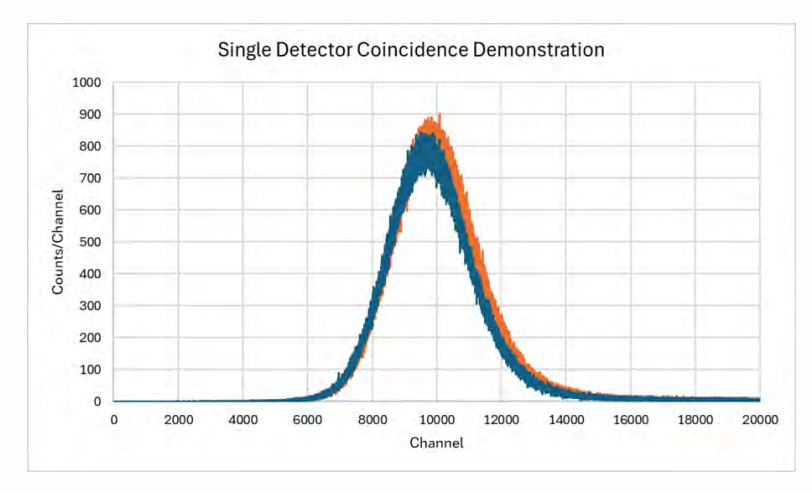


#### **LET Environmental Sensors**

- Fabricated and characterized detectors for harsh environment applications
- Improvements in detector noise and dE/E resolution
- Assembled a portable system for field measurements
- Demonstrated single detector coincidence critical for understanding directionality



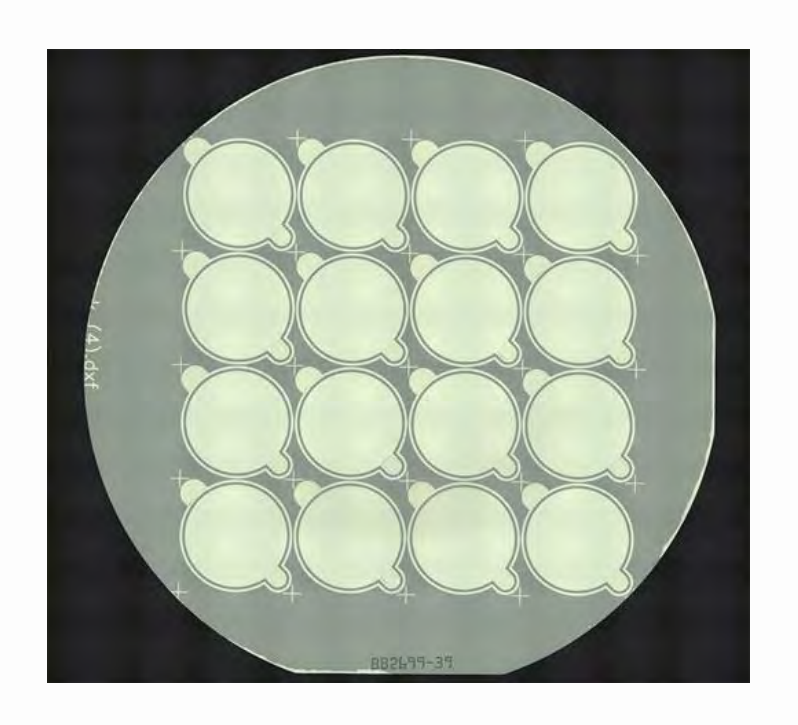


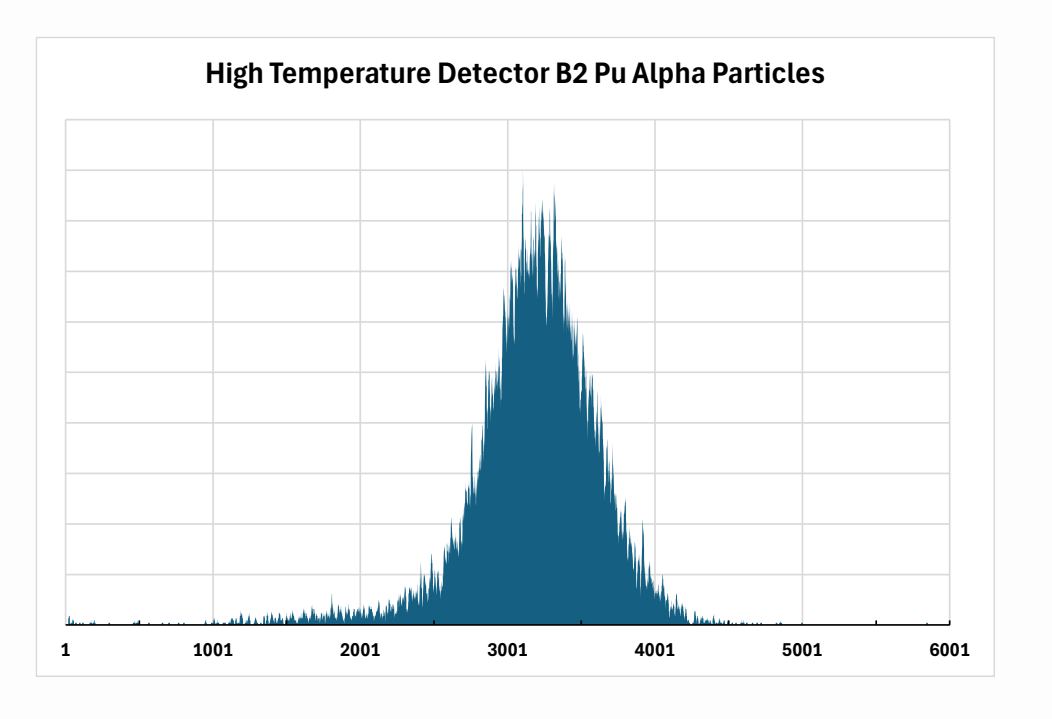


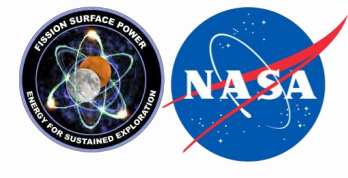


#### **Neutron Detectors**

- Focus on robust detector design for near-core use
  - Long-lived thermal neutron convertor
  - Au-free contacts
  - Detector element demonstrated robust to at least 600°C
  - High temperature packaging
  - Compact pre-amplifier circuit designed for high radiation environments







### **Radiation Summary/Conclusion**

- To Date Progress:
  - Detector element demonstrated robust to 600°C
  - Fabrication in process for longer-lifetime high temperature neutron detectors
  - Front-end amplifier for high radiation environment tests designed
  - Improved noise and energy resolution of large-area LET environment detectors
- Future plans:
  - Reactor test for neutron detectors
  - Packaging designs for reactor applications
  - Characterization of LET environmental detectors for ion, gamma, and neutron sensitivity

#### References:

- Wrbanek, J.D., & Wrbanek, S.Y. (2003) Multi-Aspect Cosmic Ray Ion Detectors for Deep-Space CubeSats, in The Nanosatellite Revolution: 30 Years and Continuing (pp. 505-536) SPIE Press.
- Wrbanek, J.D., Wrbanek, S.Y., Gonzalez, J.M., Osborn, B.A., Large Area SiC LET Detectors for Space Science Applications NASA/TM-2025001636, March 2025

### **In Progress**



#### NASA-FSP Contract # 80GRC024CA032 Continues at MIT

Continue evaluation of **unshielded** NASA GRC integrated P/T sensors, Thin-film temperature/strain sensors, and SiC electronics at-

- ~10<sup>13</sup> and ~10<sup>10</sup> nv thermal and fast fluxes, respectively, at 5.7 MW
- Temperature from 500 to 800 C
- Duration: 24 Hours

#### **NSUF Super-RTE**

Conduct "In-Operando Performance Characterization of On-Chip Integrated SiC Pressure/Temperature Sensors under Irradiation" to understand radiation effects on piezoresistance (sensitivity) at-

- $\sim 10^{13}$  and  $\sim 10^{10}$  nv thermal and fast fluxes, respectively at 5.7 MW
- Temperature from 500 to 800 °C
- Duration: 24 Hours
- Pressure

$$V(T,P) = V_{ZPO}(T) + S(T)P$$

**Offset Voltage** 

**Pressure Sensitivity (Gauge Factor)** 

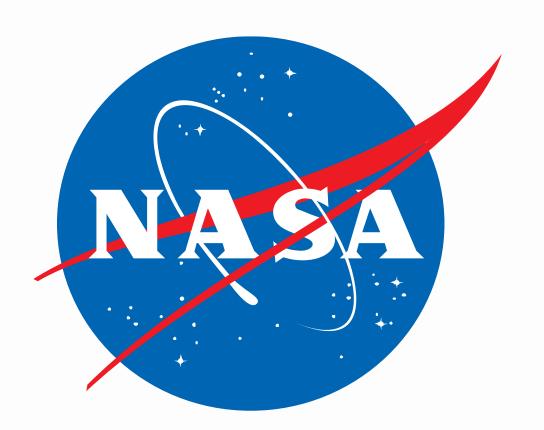
### Acknowledgement



Tiffany Vanderwyst, Ariana Miller, Wentworth T. John, Jose Gonzalez, Tyler Kuluris, Frank Lam, Michael Krasowski, Beth Osborn, Nicole Hofstetter

FSP Project team





### **Key References**

- 1. T. Unruh, "Gap assessment on sensors and instrumentation for advanced reactors." No. INL/EXT-21-63894-Rev000. Idaho National Lab. (INL), Idaho Falls, ID (Univ. 2021.
- 2. P. Calderoni et al,. "Identification of I&C components for fission surface power technology maturation," NL/RPT-23-72809, Idaho National Lab. (INL), Idaho Falls, ID (United States). May 2023.
- 3. <u>H. C. Hyer, D. Giuliano</u>, and <u>C. M. Petrie</u>, "Demonstrating distributed fiber-optic temperature sensors in a simulated gas-cooled reactor outlet," <u>Trans. American Nuclear Society</u>, vol. 129, pages 350-353. 2023.
- 4. R. Skifton, J. Palmer, and A. Hashemian, "Optimized high-temperature irradiation-resistant thermocouple for fast-response measurements," EPJ Web of Conferences 253, 06004 (2021), ANIMMA 2021.
- 5. <u>A.Y. Nikiforov</u>, and <u>P.K. Skorobogatov</u>, "SiC pressure sensors radiation hardness investigations" CERN 2002. <u>8th Workshop on Electronics for LHC Experiments</u>, 404-407. 2002.
- 6. D. A. Goodenow, "Characterization of effects of mixed neutron/gamma irradiation on NASA Glenn SiC piezoresistive pressure sensors," Master's thesis: The Ohio State University. 2007.
- 7. R. S. Okojie, D. Lukco, V. Nguyen and E. Savrun, "4H-SiC piezoresistive pressure sensors at 800 °C with observed sensitivity recovery," *IEEE Electron Device Letters*, vol. 36, no. 2, pp. 174-176, Feb. 2015, doi: 10.1109/LED.2014.2379262.
- 8. F. H. Ruddy, A. R. Dulloo, J. G. Seidel, M. K. Das, Sei-Hyung Ryu and A. K. Agarwal, "The fast neutron response of 4H silicon carbide semiconductor radiation detectors," *IEEE Trans. on Nuclear Science*, vol. 53, no. 3, pp. 1666-1670, June 2006, doi: 10.1109/TNS.2006.875151. 2006.
- 9. A. A. Lebedev et al., "Radiation hardness of the silicon carbide," Materials Science Forum Vols. 433-436 (2003) pp 957-960. 2003
- 10. The Ohio State University Research Reactor: https://reactor.osu.edu/research-capabilities/instrumented-experiments
- 11. D. C. Floyd, T. R. Steiner, E. Hutchins, R.T. Wood, and N.D.B. Ezell, "Steady-state irradiation of characterized instruments for nuclear thermal rockets using in-pile experiment apparatus," *Nuclear Technology*, 208(sup1), S74–S84. <a href="https://doi.org/10.1080/00295450.2021.2011575">https://doi.org/10.1080/00295450.2021.2011575</a>. 2022.
- 12. S. S. Courts, "High level, gamma radiation effects on platinum and silicon diode cryogenic temperature sensors," 2020, IOP Conf. Ser.: Mater. Sci. Eng. 755 012077-
- 13. I. Tsveybak, et al., "Fast neutron-induced changes in net impurity concentration of high-resistivity silicon," IEEE Trans. Nucl. Sci. NS-39/6, 1720-1729. 1992.
- 14. E. Almaz, S. Stone, T. E. Blue, and J. P. Heremans, "The effects of neutron irradiation and low temperature annealing on the electrical properties of highly doped 4H silicon carbide," Nucl. Instr. Meth. Phys. Res. A, 622, pp. 200. 2010.
- 15. A. A. Lebedev et al., "Dependence of the Carrier Removal Rate in 4H-SiC PN Structures on the Irradiation Temperature." Materials Science Forum, vol. 963, Trans Tech Publications, Ltd., 19 July 2019, pp. 730–733. 2019.
- 16. H. Spieler, "Introduction to radiation-resistant semiconductor devices and circuits." AIP Conference Proceedings. Vol. 390. No. 1. American Institute of Physics, 1997.
- 17. V. F. B McLean et al., "Analysis of neutron damage in high-temperature silicon carbide JFETs," IEEE Trans. Nucl. Sci., vol. 41, no. 6. December 1994.
- 18. B. Tsuchiyaa et al., "Radiation induced changes in electrical conductivity of chemical vapor deposited silicon carbides under fast neutron and gamma-ray irradiations," Fusion Engineering and Design 86 (2011) 2487–2490).
- 19. I. Caban, "Review: electrically active defects in 3C, 4H, and 6H silicon carbide polytypes," Crystals 2025, 15, p. 255. 2025.
- 20. S. E. Stone, "A study of the effects of neutron irradiation and low temperature annealing on the electrical properties of 4H-SiC." Master's Thesis, The Ohio State University, 2008.

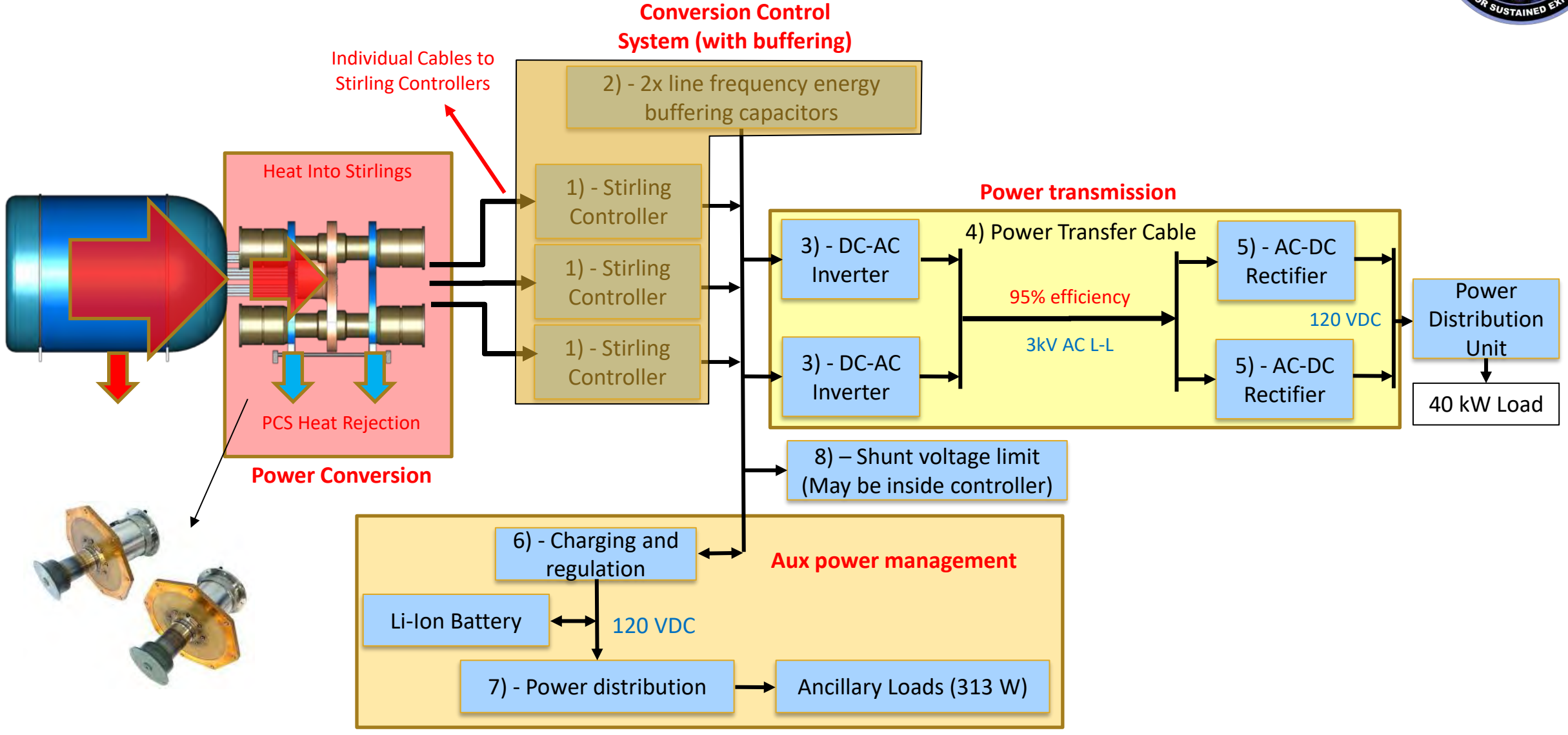


# Risk reduction activities for Stirling controllers and Stirling power system development



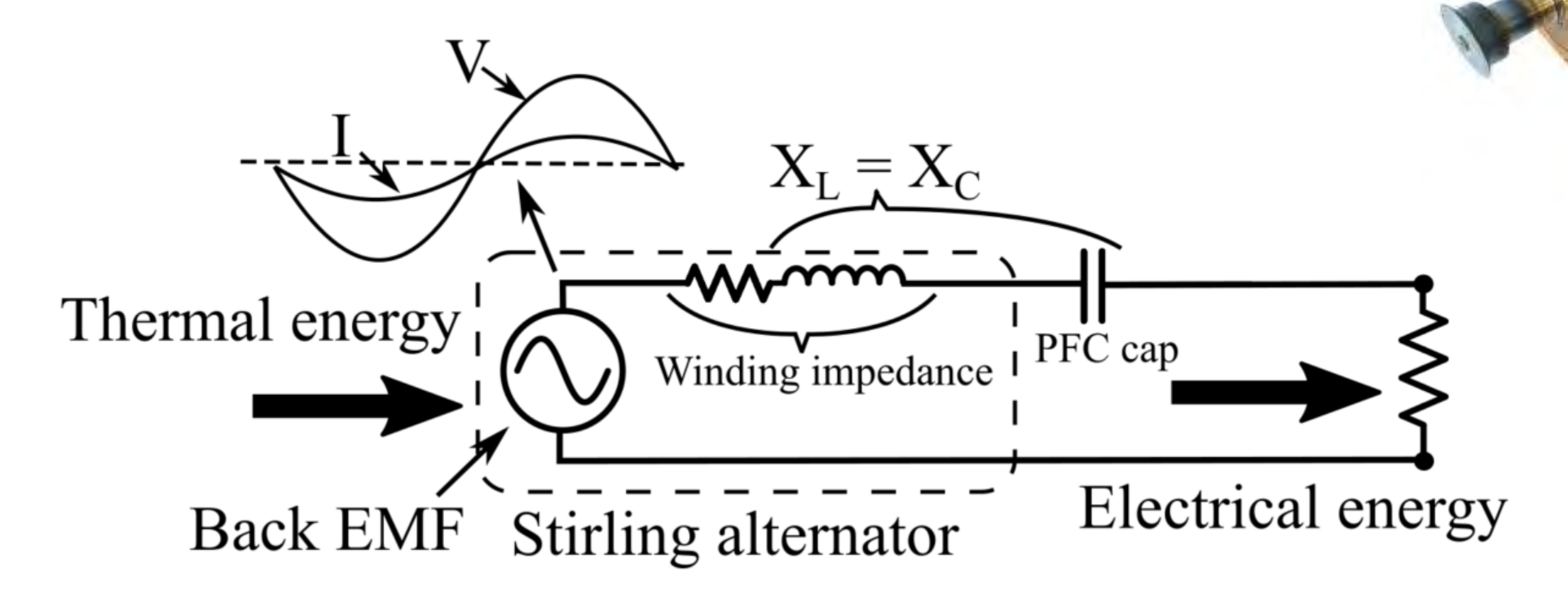
## **Stirling Power Conversion System**





## **Stirling Convertor Control**

- Power factor correction (PFC) negates alternator impedance
  - Can be implemented using a capacitor or active control



Energy balance facilitates stable operation

## Outline



- Core technology risk reduction
  - High-density capacitors
  - Power FETS
- Stirling controller reference design development
  - Control strategy
  - Implementation
  - Operation
- Support for system development
  - ☐ Reconfigurable Stirling simulator
  - 2 kW Stirling testbed
  - Modular Stirling test rack architecture

## Outline



- Core technology risk reduction
  - High-density capacitors
  - Power FETS
- Stirling controller reference design development
  - Control strategy
  - Implementation
  - Operation
- Support for system development
  - Reconfigurable Stirling simulator
  - 2 kW Stirling testbed
  - Modular Stirling test rack architecture

## **Core Technology – Polymer Capacitors**

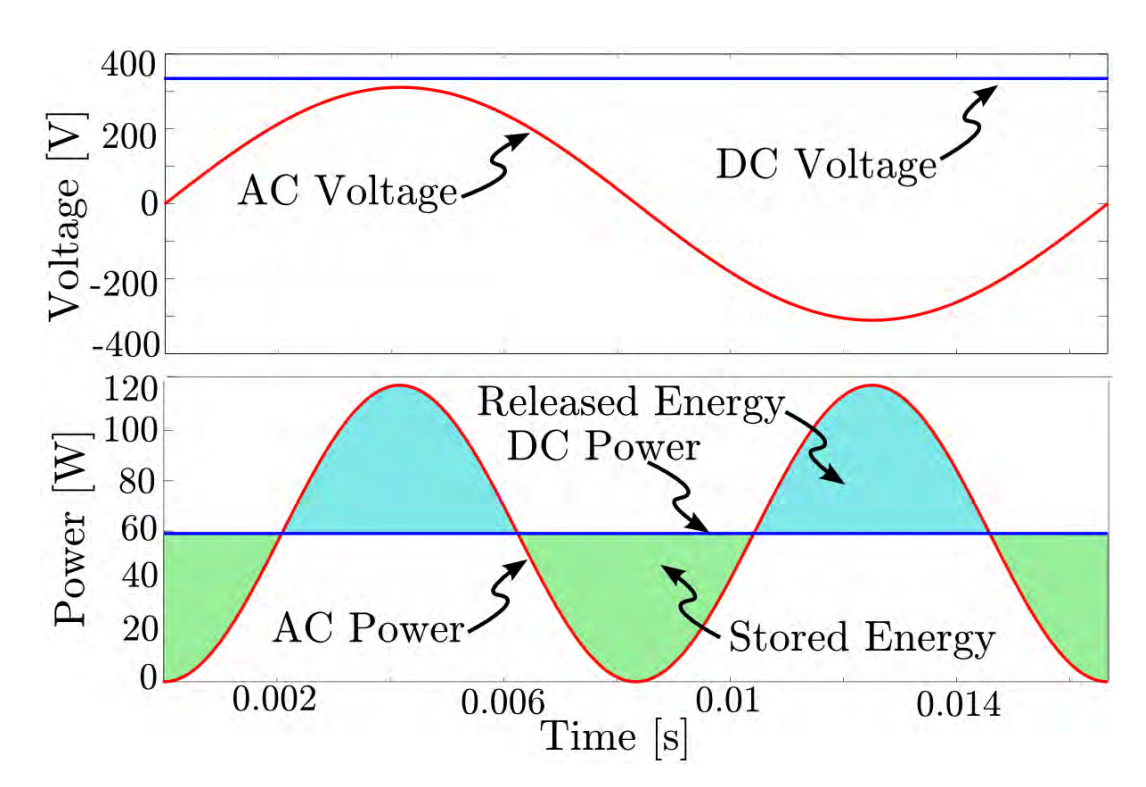


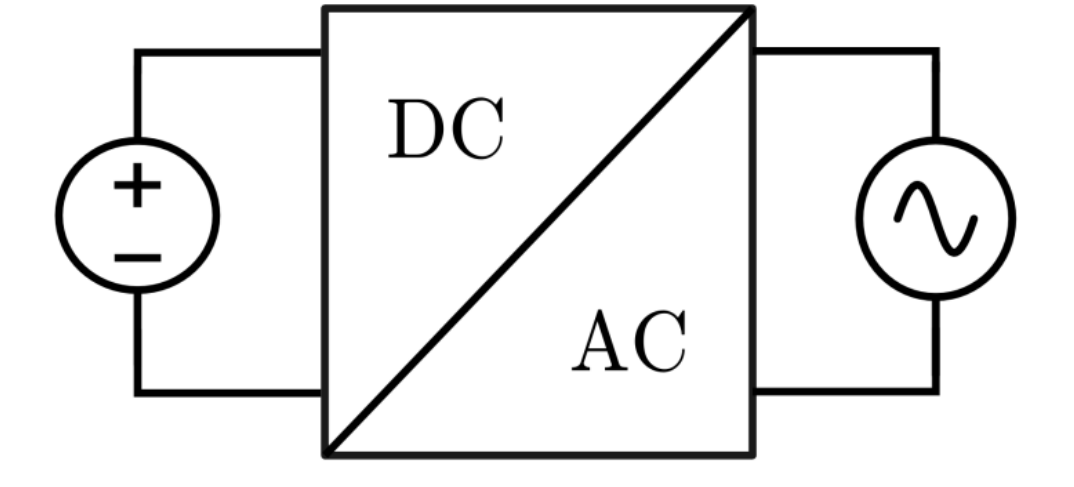
• Instantaneous power mismatch exists between DC and single-phase AC.

$$-\overline{P_{DC}} = \overline{P_{AC}}$$
, but  $p_{dc} \neq p_{ac}$ 

$$-E_{store} = \frac{P_{dc}}{2\pi f_{line}}$$

- 10+ Liters of capacitance required for 10 kW system
  - Volume estimate disregards packing factor and enclosure structure





## **Core Technology – Polymer Capacitors**

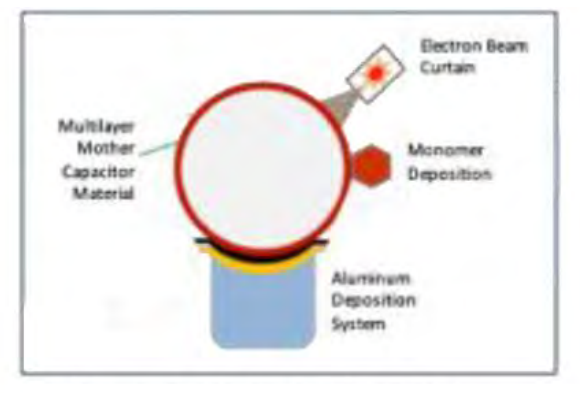
THE RESIDENCE PROPERTY OF THE PROPERTY OF THE

LYCHARGE

- Polymer Multilayer Capacitors
  - Comparable energy density to Type 2 ceramics with lower dissipation factor and <u>zero bias dependence</u> or piezoelectric effect
  - Roughly 50X density improvement over MIL-PRF-39022/12 devices
  - Radiation tolerant (Polypropylene capacitors are susceptible to radiation)
  - Self-healing, fail open, low ESL, low ESR
  - Stable capacitance from -196°C to 200°C
- SBIR Phase 1 & 2 complete and successful
  - Follow-on work prototyped 600 V part for multiple missions
- Capacitors completed "Acceptance Testing"
  - 105 C, 140% of rated voltage for 2000 hours
  - Gamma radiation
  - Moisture
  - Highly Accelerated Life Testing (HALT)
  - AC Characteristics
  - Calculation of reliability acceleration factors
  - Life-dose reactor irradiation of full devices complete
    - 22 Mrad, 2E16 n/cm<sup>2</sup>
    - Electrical life testing to follow
  - Additional testing in process



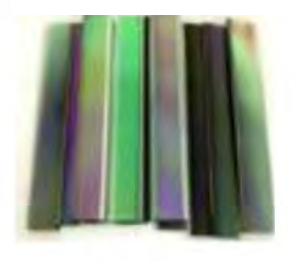
5uF, 1000V NanoLam Capacitor 0.12 J/cm^3 - Nominal 0.042 J/cm^3 - Derated

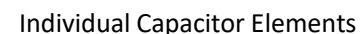


PML Capacitor Process Schematic



Segmented Mother Capacitor Material







**Aluminum Electrodes** 



**Arc Sprayed Termination** 

<sup>[1]</sup> Teverovsky, Alexander A. "Evaluation of Elements used for Manufacturing of NanoLam Metallized Polymer Film Capacitors." (2023)

<sup>[2]</sup> Teverovsky, Alexander A. "Capacitor Tasks 2024", NASA Electronic Parts and Packaging (NEPP) Program, 2025 Electronics Technology Workshop Program

## **Core Technology – GaN E-HEMT**



- Single event effect (SEE) susceptibility has limited voltages in NASA missions [1]
  - Radiation hardened Si MOSFETS lag commercial devices by an order of magnitude
  - Wide-bandgap SiC MOSFETs have proven extremely susceptible to Single Event Effects
- High-power missions with power transmission require elevated voltage to reduce conduction losses and system mass
- Recent testing by NASA has raised confidence in operating GaN E-HEMTs in the space environment [1,2]
  - Acceptable SEE performance at 400VDC
  - Useable at 300 Vdc with derating
  - –NASA Stirling controllers implemented with GaN Enhancement-Mode High Electron Mobility Transistors (E-HEMTs)

TDG650E601TSPF



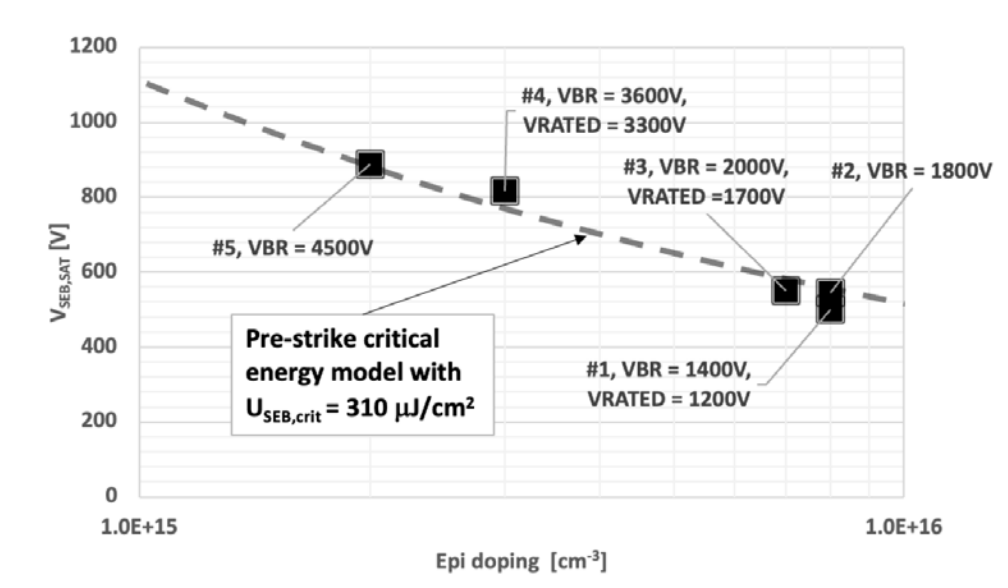
<sup>[1]</sup> Boomer K, Scheick L, Hammoud A. Body of knowledge for Gallium Nitride power electronics. NASA Electronic Parts and Packaging (NEPP) Program Website. 2020 Oct 2.

<sup>[2]</sup> Contact: Jason Osheroff (jason.m.osheroff@nasa.gov), Ansel Barchowsky (ansel.barchowsky@jpl.nasa.gov)

## Core Technology – 1.5kV SiC

THE ROLL FOR SUSTAINED EXPORTS

- Silicon Carbide For High Voltage In Radiation Environments (SHIRE) aims to develop and
  experimentally demonstrate radiation-hardened silicon carbide (SiC) power switching devices
  capable of sustaining single-event burnout (SEB) thresholds of 1500 V or higher under high-LET
  heavy-ion exposure
  - Led by Vanderbilt University, Steven Kosier (PI)
- Builds on prior modeling validated using both newly fabricated and existing devices to save time and cost.
- Epitaxial doping, more than thickness, controls high-LET SEB thresholds in high-voltage devices. **This was new understanding for the field** 
  - Stands in contrast to previous models, which emphasized breakdown voltage or total depletion width as the primary determinants of SEB susceptibility
- SHiRE continuation program will extend these findings to achieve still-higher SEB voltage of 1500 V or greater
- This work marks a <u>significant</u> shift in how SEB is understood and managed in SiC power devices.
  - Transitions the field from empirical derating practices toward first-principles-based modeling
- Three-and-a-half-year effort with annual device fabrication and testing (FY '26 start)
  - First year fully funded



Test data showing correlation between epi-doping and single-event break-down voltage [1]

- Passing ions release energy stored in the Drain-Body Depletion Capacitance
- In SiC, burnout occurs if this energy is greater than the critical energy
- Qualitatively similar to oxide rupture, SEGR

## Outline



- Core technology risk reduction
  - High-density capacitors
  - Power FETS
- Stirling controller reference design development
  - Control strategy
  - Implementation
  - Operation
- Support for system development
  - Reconfigurable Stirling simulator
  - 2 kW Stirling testbed
  - Modular Stirling test rack architecture

## NASA Controller Implementations



Demonstrate suite of Stirling controller and power transmission hardware using leading-edge core technology with path to flight

#### Purpose:

- Validate and document simplified control strategy on high-efficiency hardware;
- > Set benchmark/standard for flight hardware on conversion efficiency and limited complexity;
- Develop functional IP
- Reduce risk of future project cost overruns

#### TRL Advancement:

- > 3-4 for dual-1 kW controller with defined path for flight using radiation-hardened components FY '25
- > 5 for 80 W controller by FY '27

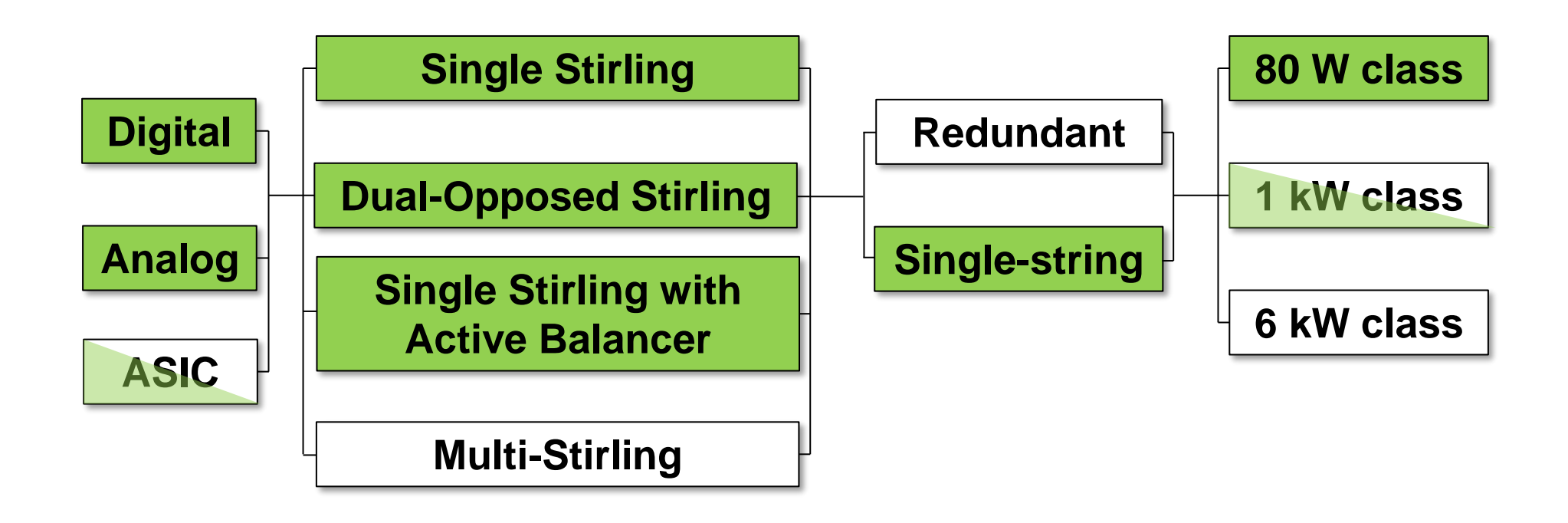
#### Funding:

- Fission Surface Power project (NASA Space Technology Mission Directorate)
- Radioisotope Power Systems Program (NASA Planetary Science Division)
- Additional sources of government and industry collaboration

## **NASA Controller Taxonomy**



- Controller building block designs being developed
- Functionality can be mixed and matched to meet application
- Green blocks have undergone initial demonstration

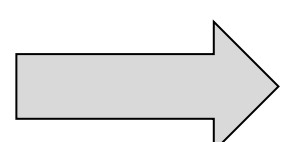


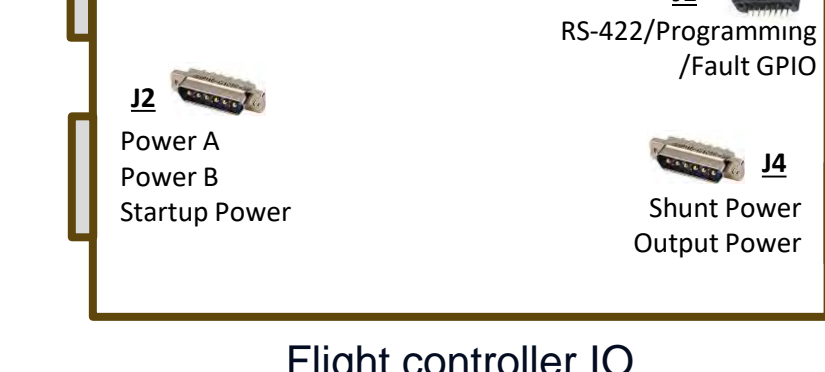
## **Dual 80 W Stirling Convertor Controller**

- Lab prototype developed and validated at NASA Glenn
  - Easy vetting of control functionality due to low voltage
- Integrated system monitoring and data streaming using Bundle Protocol V7 over Serial Line Internet Protocol (SLIP)



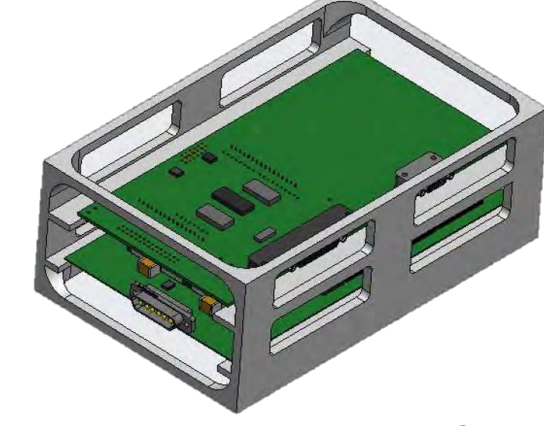
Lab prototype controller





16-ch Temperature

Flight controller IO



FLDTs (X<sub>n</sub> X<sub>n</sub>

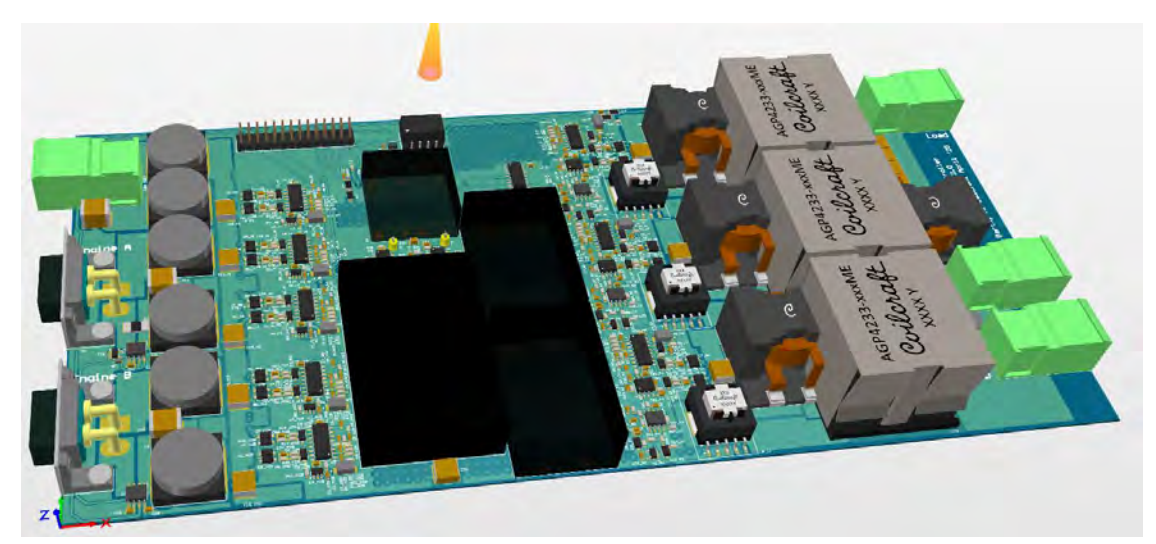
Preliminary controller CAD

Class D flight hardware in development

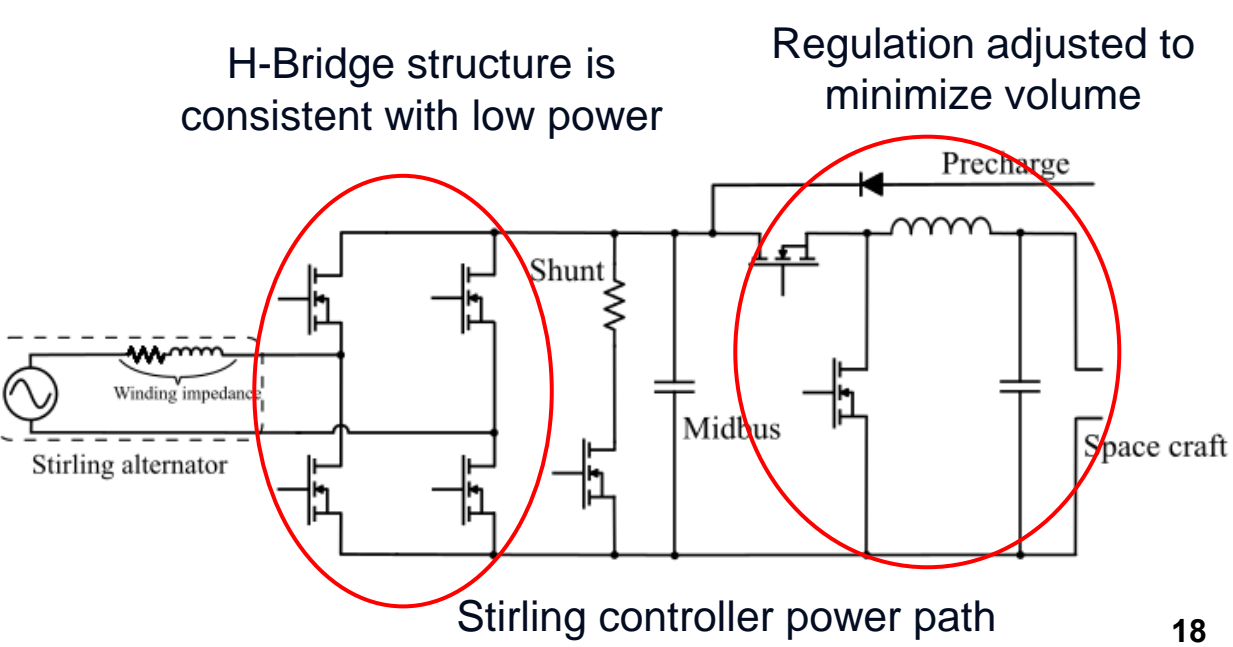
- Enclosure: 4.75" X 7.50" X 2.75"
- Estimated mass: < 2kg
- Estimated hardware delivery: March 2026

## **Kilowatt-class Stirling Convertor Controller**

- Dual-1 kW Stirling controller
  - Path to flight exists and is being refined
  - Builds on Dual-80 W designs
  - Shared control hardware paired with multi-kilowatt power stage



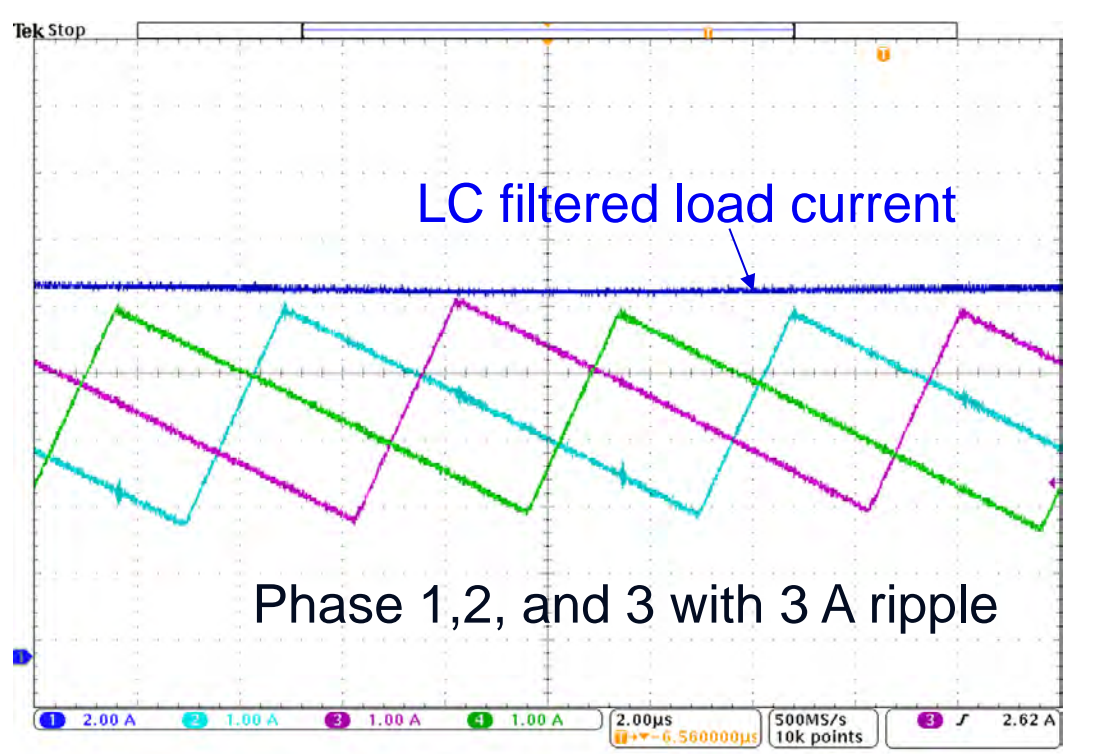
Dual-1kW Controller CAD model



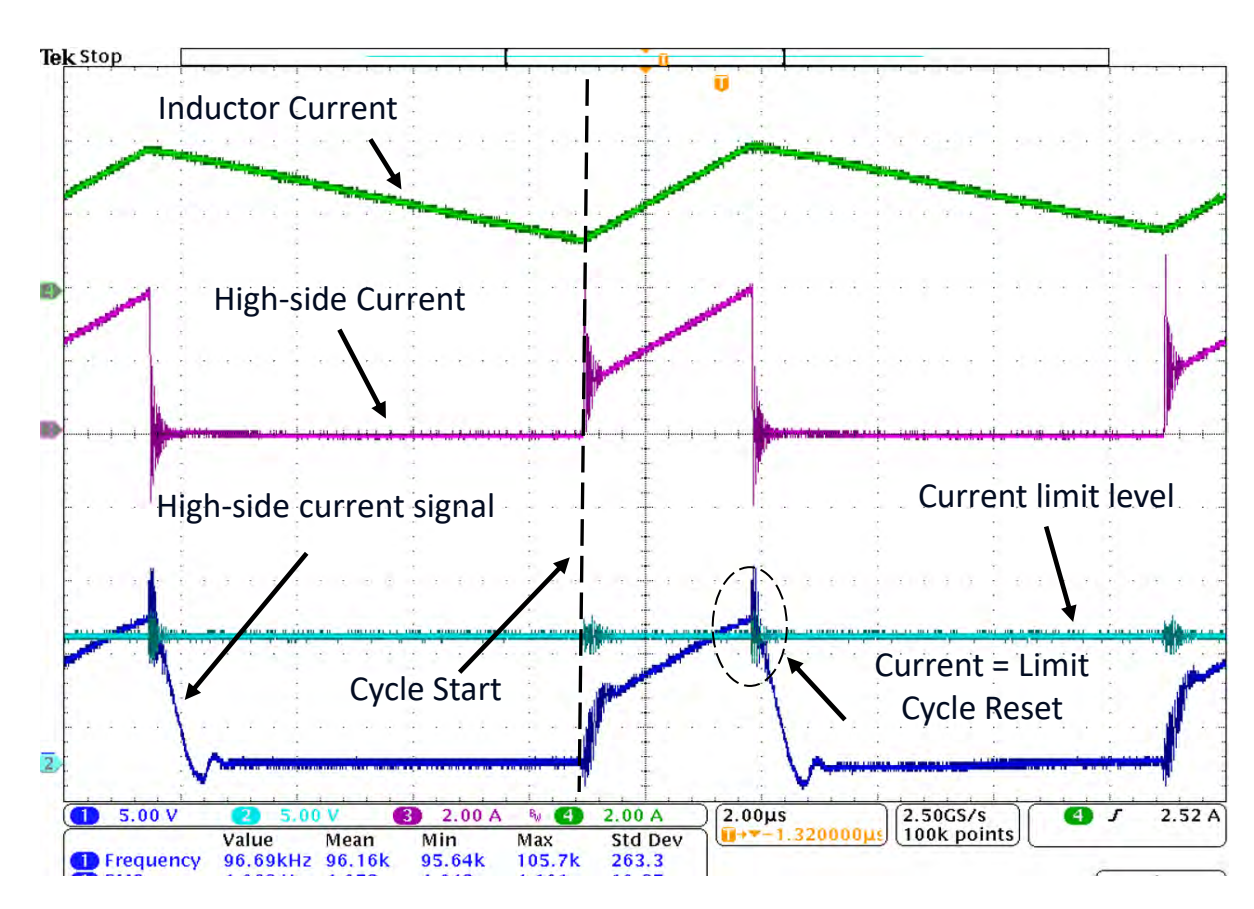
## **Kilowatt-class Stirling Convertor Controller**

EN SURFACE POWER

- Parallel, interleaved buck regulator used to reduce filter size
  - High-ripple buck currents combined into reduced ripple output
- Peak current mode control
  - Accurate current between phases
  - Inherent electrical isolation between control and current sensing



3-phase interleaved buck converter as well as combined signal with low ripple at light load



Scope screenshot of single-phase DC peak current control

## Outline



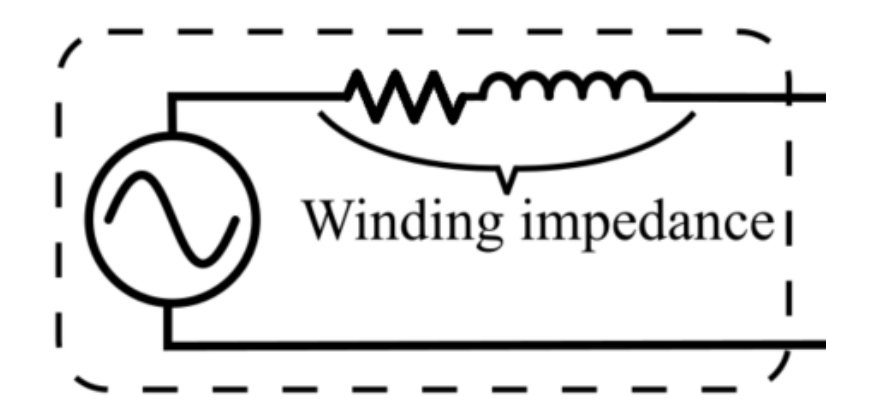
- Core technology risk reduction
  - High-density capacitors
  - Power FETS
- Stirling controller reference design development
  - Control strategy
  - Implementation
  - Operation
- Support for system development
  - ☐ Reconfigurable Stirling simulator
  - 2 kW Stirling testbed
  - Modular Stirling test rack architecture

## **Stirling Simulators**

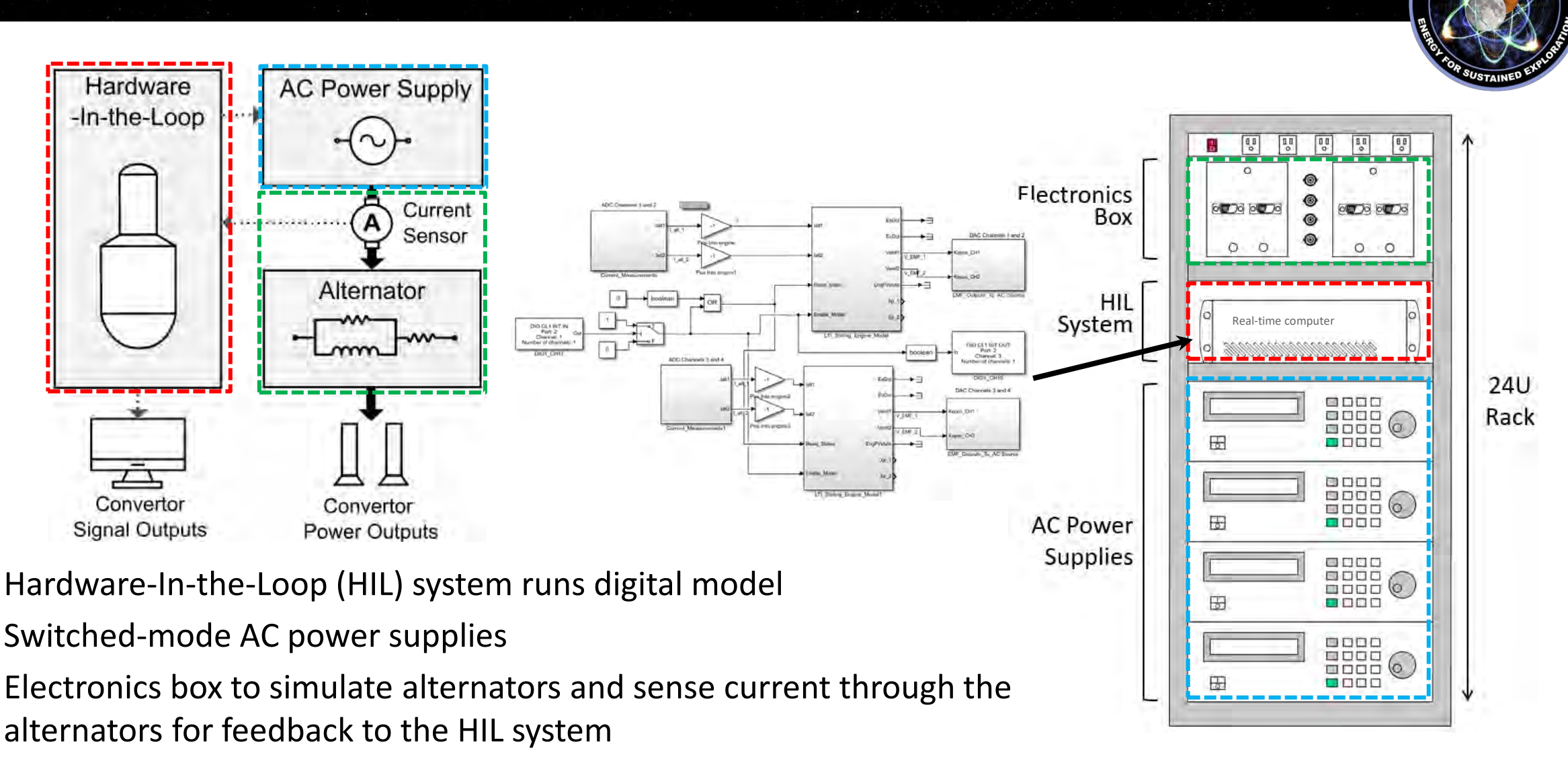


## Objectives

- Test Stirling electrical power systems without risking damage to Stirling convertor hardware
- Save time required to heat and cool Stirling convertors at the start and end of controller testing
- -Simulate any free-piston Stirling convertor
- -Simulate multiple convertors
- Reconfigurable to different types Stirling convertors with minimum modifications



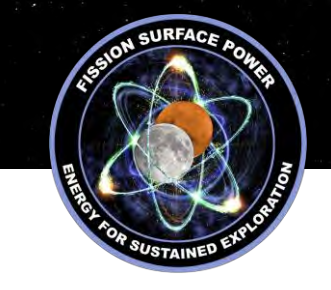
## Multi-Convertor Configurable Simulator (MCCS)



Yang, Donguk Max, Christopher Barth, Ronald Leibach, Michael Casciani, and Luis A. Rodriguez. "Multi-Convertor Configurable Simulator for Dynamic Radioisotope Power Systems." In 2023 IEEE Aerospace Conference, pp. 1-6. IEEE, 2023.

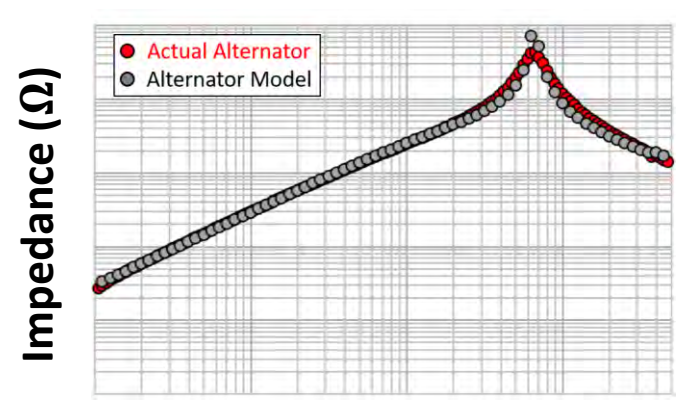
Yang, Donguk Max, and Brett Shapiro. "Development of System Identification Testing Method for Stirling Convertors." Nuclear and Emerging Technologies for Space (NETS 2025). 2025.

## Multi-Convertor Configurable Simulator (MCCS)

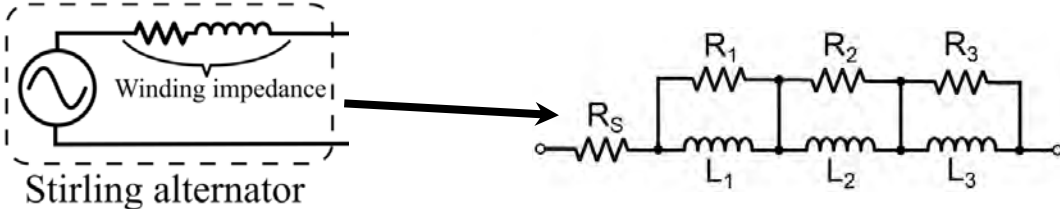




#### **Alternator Modeling**



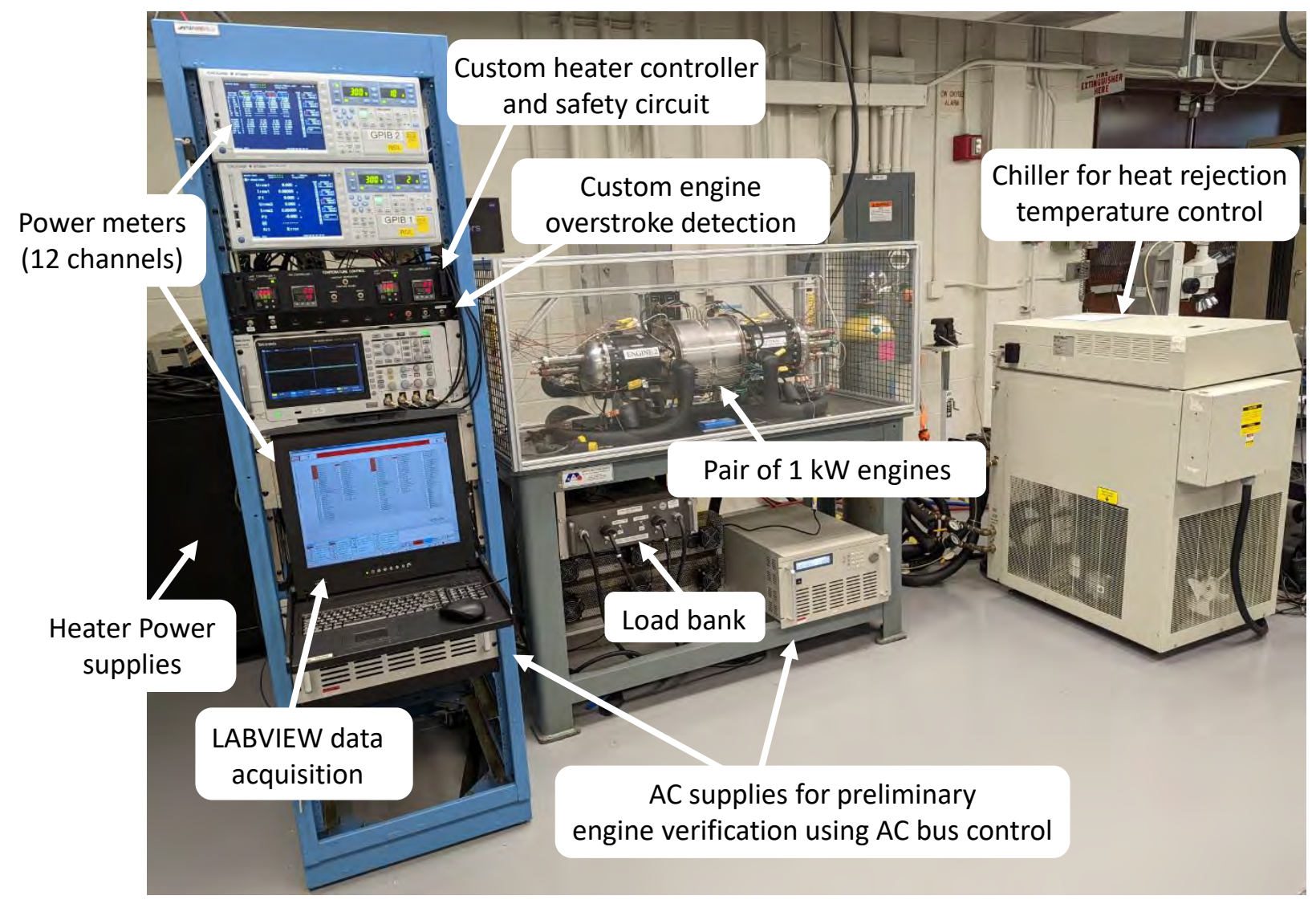
#### Frequency (Hz)



- Hardware system includes an RL array to reproduce high-frequency alternator characteristics
- Switching between Stirling engines requires changing engine models and alternator configuration
- Low-cost, transferable computation solution being developed to facilitate tech transfer

## **Kilowatt-class Stirling Convertor Testbed**





Kilowatt-class Stirling convertor testbed

## **Kilowatt-class Stirling Convertor Testbed**



- Dual-opposed 1 kW Stirling convertors
  - Electrically heated for ease of operation

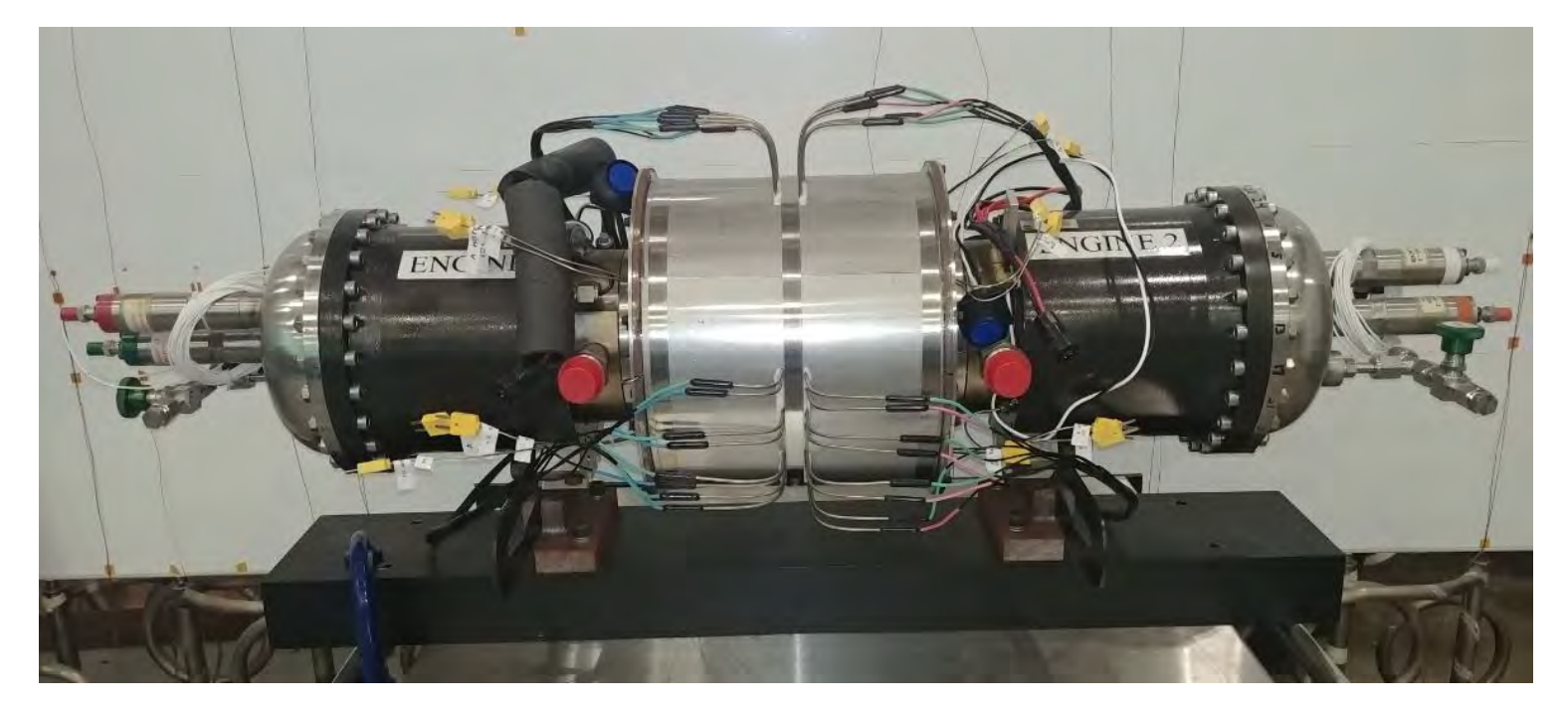


Photo of P2A engine pair. Units are 1 kW each

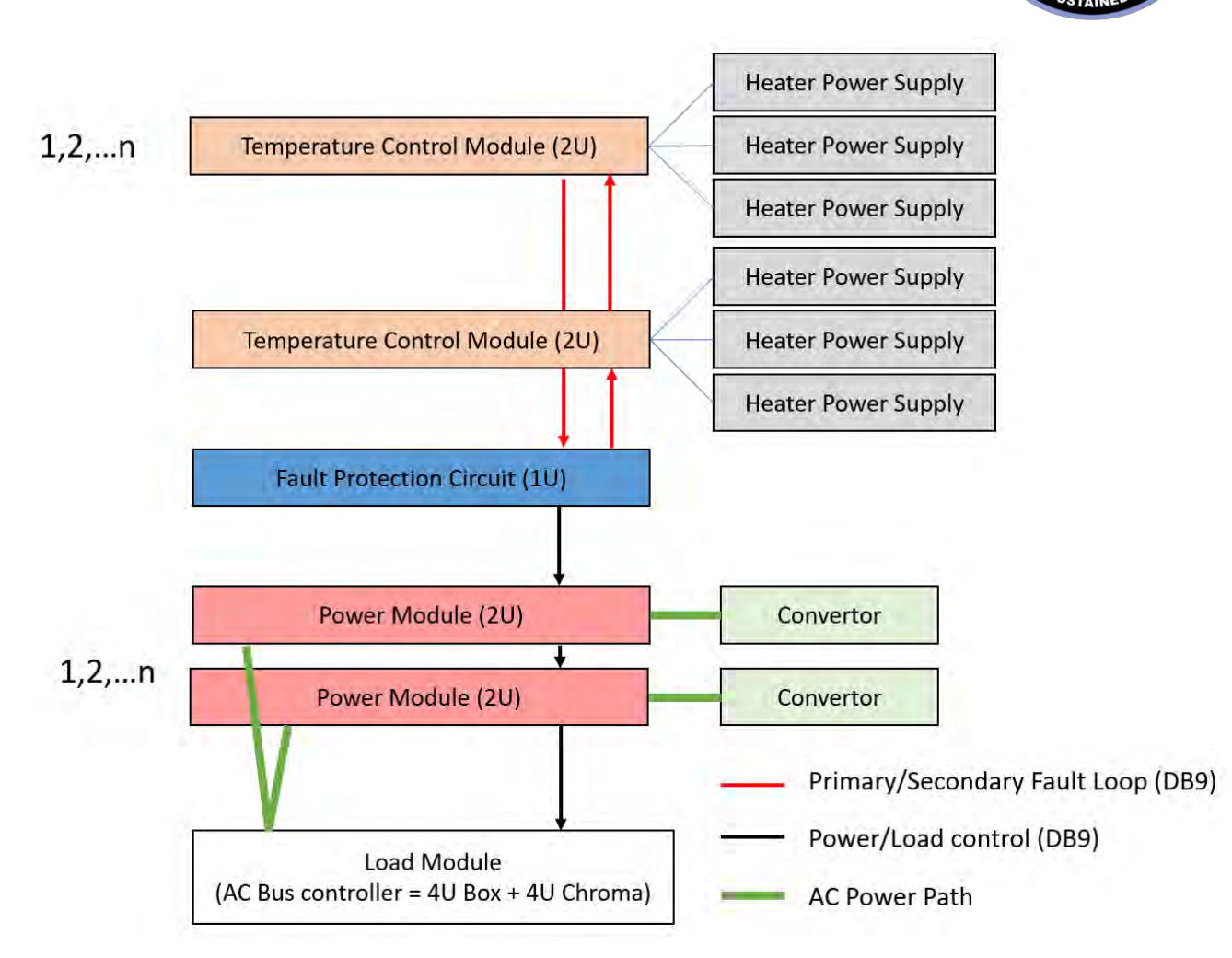
## Outline

THE PORT OF SUSTAINED ENGINEERS

- ☐ Core technology risk reduction
  - High-density capacitors
  - Power FETS
- Stirling controller reference design development
  - Control strategy
  - Implementation
  - Operation
- ☐ Support for system development
  - Reconfigurable Stirling simulator
  - 2 kW Stirling testbed
  - Modular Stirling test rack architecture

## Stirling Convertor Hardware Safety and Support

- Stirling convertor verification and controller testing requires a robust support system to protect Stirling engines from damage
  - System testing will result in engine damage without protection
- "Modular Support Rack" developed to dramatically reduce project ramp-up costs
- Hardwire safety logic protects against
  - Engine hot-end overheat or chilling
    - Heaters disabled and engine stalled after cooling
  - Engine piston over stroke (due to controller malfunction)
    - Engine immediately stalled and heaters shut down
  - Building power loss
    - Engine control maintained with backup power source (building-level uninterruptable power source)
- Design iterated three times and batch of hardware in fabrication



Partial block diagram of modular rack system

## **Modular Rack Design**

- –Integrated Fault Protection Circuit (FPC) module includes:
  - Four analog channels to enforce bi-polar limits on piston stroke and vibration (with disable option)
  - Automatic emergency shutdown
  - Power path control interface (Controller vs. AC bus)
  - -Temperature control module:
    - All temperature and hardware temperature limit controllers for a single Stirling







Temperature Control Module

## Modular Rack Design



#### Power Path Module

- Routes power path between power factor correcting capacitors, AC bus controller, H-bridge controller, and two distinct stall loads
- Configurable for both low voltage (~25V) and high voltage engines (~240V) engines
- Series interconnect for multiple engines

#### Load Module

- "AC bus" interface connection for multiple engines
- Includes step-down transformers for compatibility with low-current AC supplies
- Disconnects AC supply in the event of a fault



Power path module

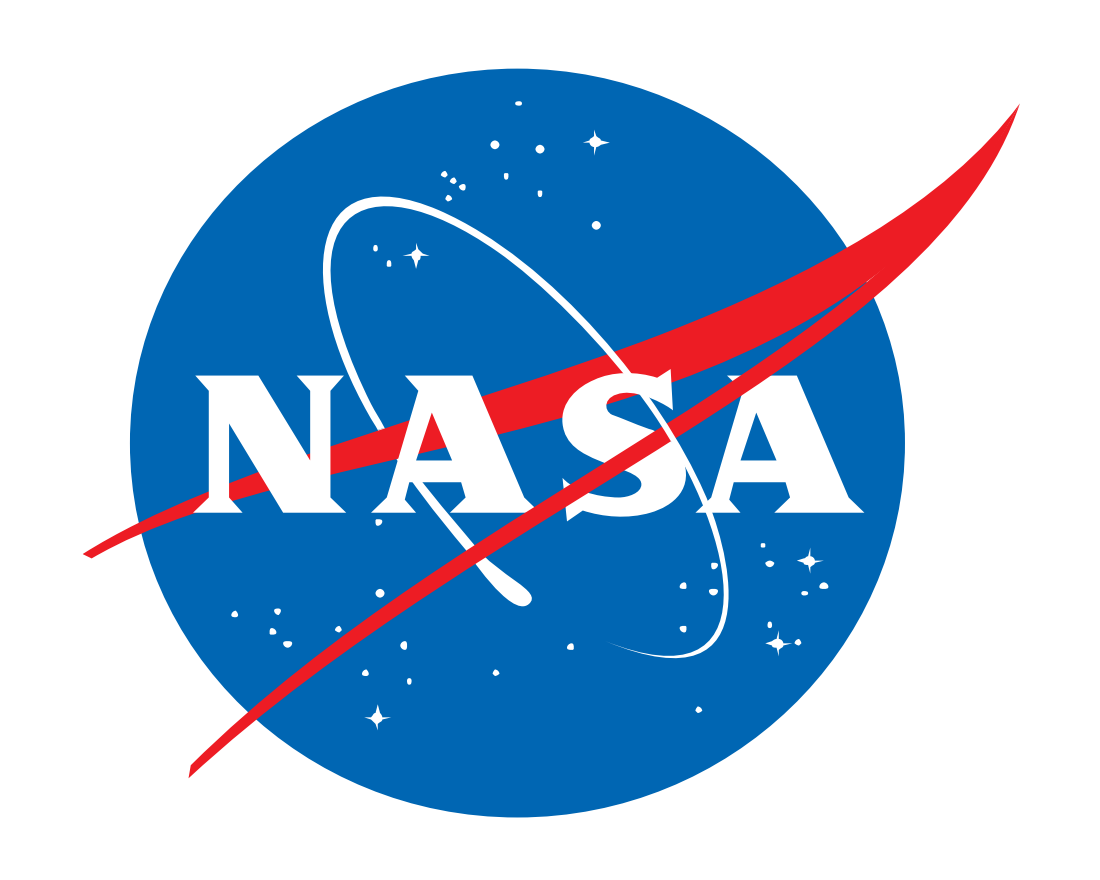


AC Bus/load module front and rear

## Outline



- Core technology risk reduction
  - High-density capacitors
  - Power FETS
- Stirling controller reference design development
  - Control strategy
  - Implementation
  - Operation
- Support for system development
  - Reconfigurable Stirling simulator
  - 2 kW Stirling testbed
  - Modular Stirling test rack architecture



Contact: Christopher.b.barth@nasa.gov



## **Backup Slides**

### Stirling Systems Require a Large Buffering Capacitance



Minimum capacitor volume can be estimated as a function of energy storage

$$-W_{buffer}(J) = \frac{P_{Avg}}{2\pi * F_{Stirling}} = C V_{avg} \Delta V$$

- Average terrestrial film cap power density: 0.03 J/cm<sup>3</sup>, 12.7 J/kg [1]
  - Existing Class S capacitors for space have a significantly lower density
- •5% discharge allows a ~10% utilization of capacitive energy storage. [2]
  - Volume for 10 kW:  $\frac{10 \text{ kW}}{2\pi * 60 \text{ Hz}}$  (J) \*  $\frac{1 \text{ cm}^3}{0.03 \text{ J}} * \frac{1}{0.10} = 8841 \text{ cm}^3 = 8.8 \text{ liters}$ 
    - This is only the dc link capacitance and assumes <u>zero</u> voids and <u>no</u> interconnections.

[1] C. B. Barth, T. Foulkes, I. Moon, Y. Lei, S. Qin and R. C. N. Pilawa-Podgurski, "Experimental Evaluation of Capacitors for Power Buffering in Single-Phase Power Converters," in *IEEE Transactions on Power Electronics*, vol. 34, no. 8, pp. 7887-7899, Aug. 2019.

Capacitor density spot checked Oct 8<sup>th</sup>, 2019 with Kemet Polypropylene C4GADUD5300AA3J: 0.0244 J/cm^2, 27 J/kg

[2] S. Qin Et Al "A High Power Density Series-Stacked Energy Buffer for Power Pulsation Decoupling in Single-Phase Converters," in *IEEE Transactions on Power Electronics*, vol. 32, no. 6, pp. 4905-4924, June 2017.

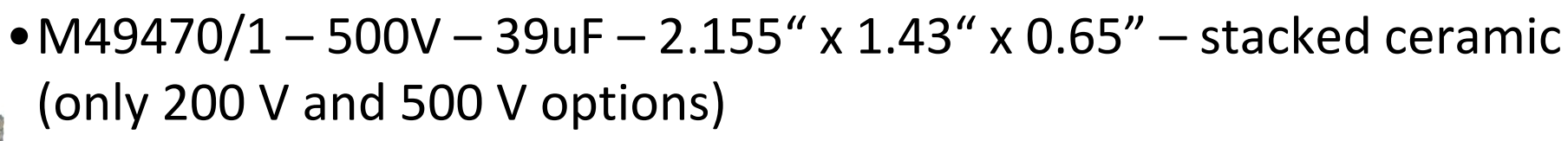
### Capacitor Volume for 10 kW system



- DC link requires 10.4 mF of capacitance at 160 V
- Using EEE-INST-002 as guidance for capacitor choice
  - 266 V device required for 160 V operation with 40% voltage derating
- M83421/6 400V 2uF 1"x2.5" polypropylene

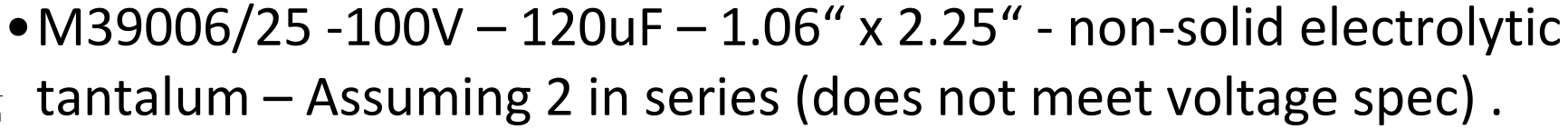


-5,200 capacitors, 13000 in<sup>3</sup> = 213 L





- Capacitance value will derate ~35% to 25 uF at 160 V
- -416 capacitors, 833 in<sup>3</sup> = 13.6 L
- Ceramics have reliability concerns





- 173 capacitors, 437 in<sup>3</sup> = 7.16 L



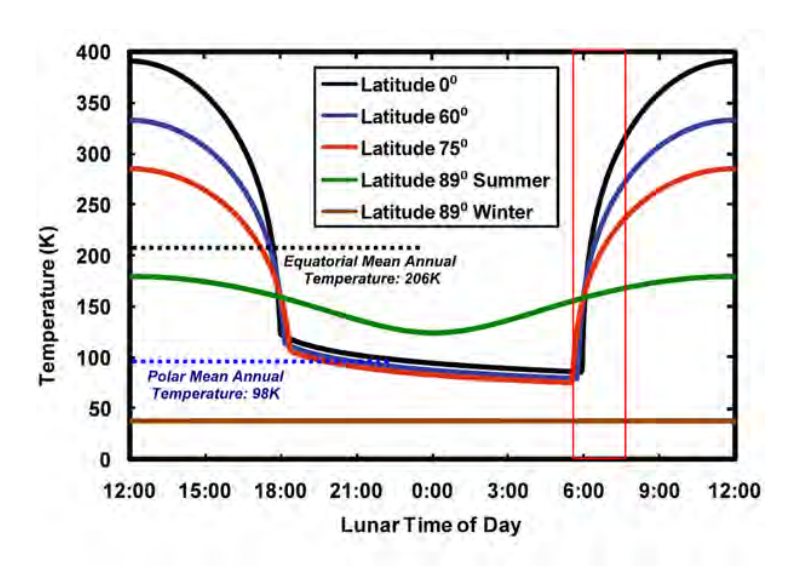
# Fission Surface Power PMAD

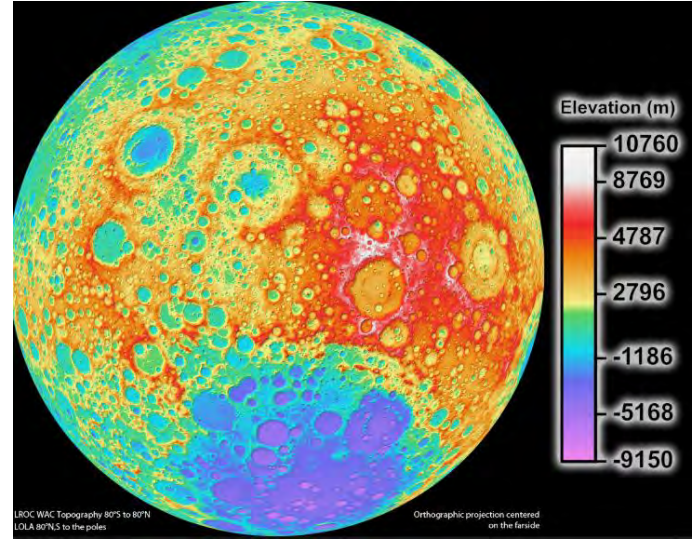
David Pike
PMAD Lead Engineer
NASA Glenn Research Center, Cleveland, OH
FSP Technology Maturation Webinar Series
September 24, 2025



### Lunar Environmental Challenges

- Radiation environment: cosmic rays, solar wind, solar flares; comparable to in-space environment (similar degradation expected to GEO)
- Temperature extremes: -173 to +127 C near the lunar equator and down to -247 C inside the craters and cold traps
- Large thermal gradients that may occur across an asset during sunrise and sunset
- Dust: jagged crystalline, can be expelled at high velocity on landing/takeoff
- Topographical: uneven surfaces, craters, high slope areas, low density surface dust
- Variations in conditions based on equatorial, polar, or permanently shadowed areas. Design solutions for the lunar south pole may not be acceptable as operations move towards the equator
- Hard vacuum: with no atmosphere, components will off-gas and functionality may be affected or compromised completely
- Insulating lunar regolith: unlike the earth, the moon is non-conductive, meaning that terrestrial grounding conventions may not apply
- Component reliability: harsh environment will likely degrade components

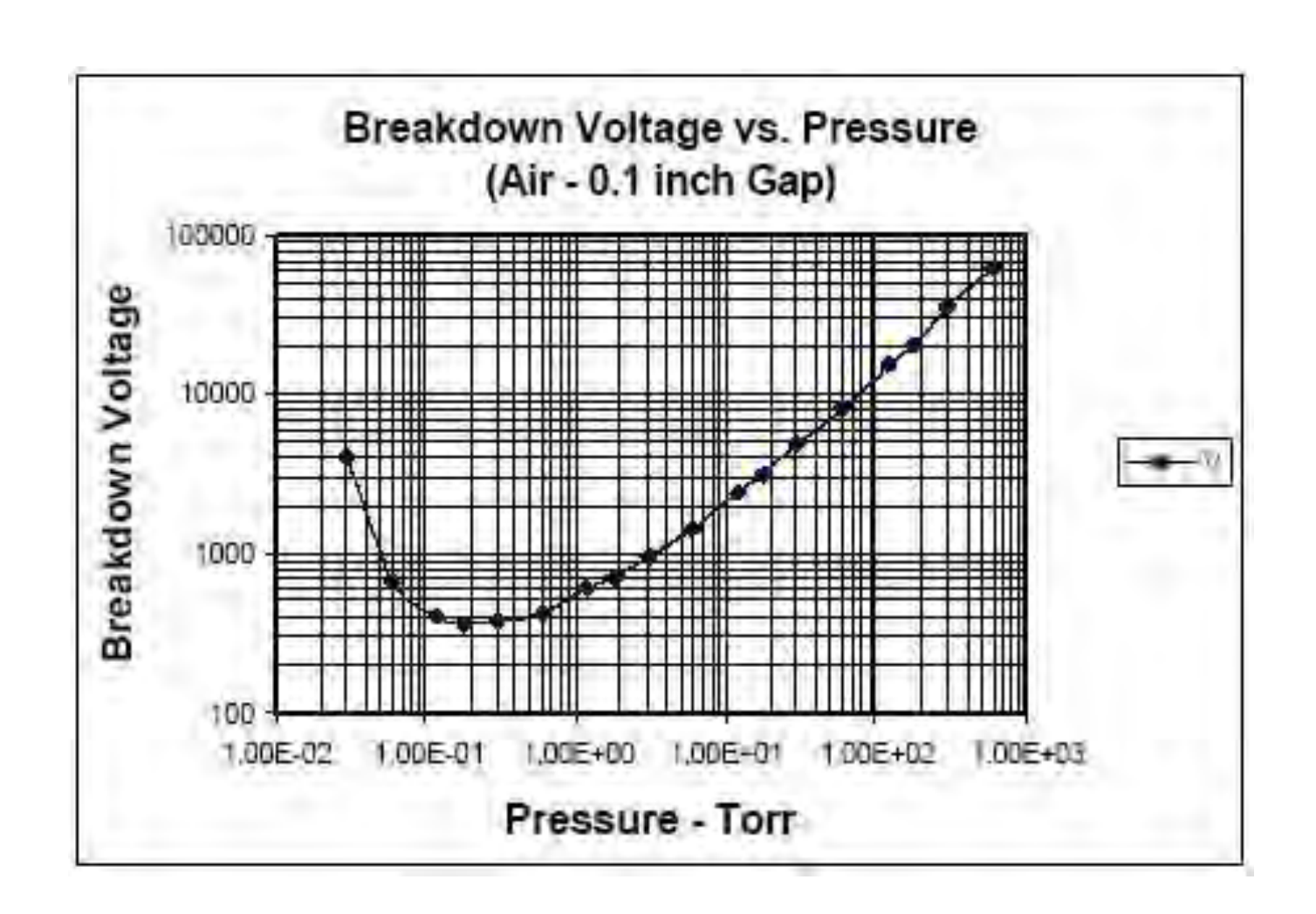






### **MOSFET Limitations in Space**

- MOSFETs are critical switching devices, required for power management and distribution (PMAD) hardware
- MOSFETs can fail due to TID radiation, SEE radiation, thermal environment, or Paschen breakdown (arcing between component conductors)
  - TID, Paschen breakdown issues, and thermal issues can be solved with engineering
  - SEE cannot be shielded
- Space-rated MOSFETs have been limited to 120VDC operation
  - Space station uses 120VDC

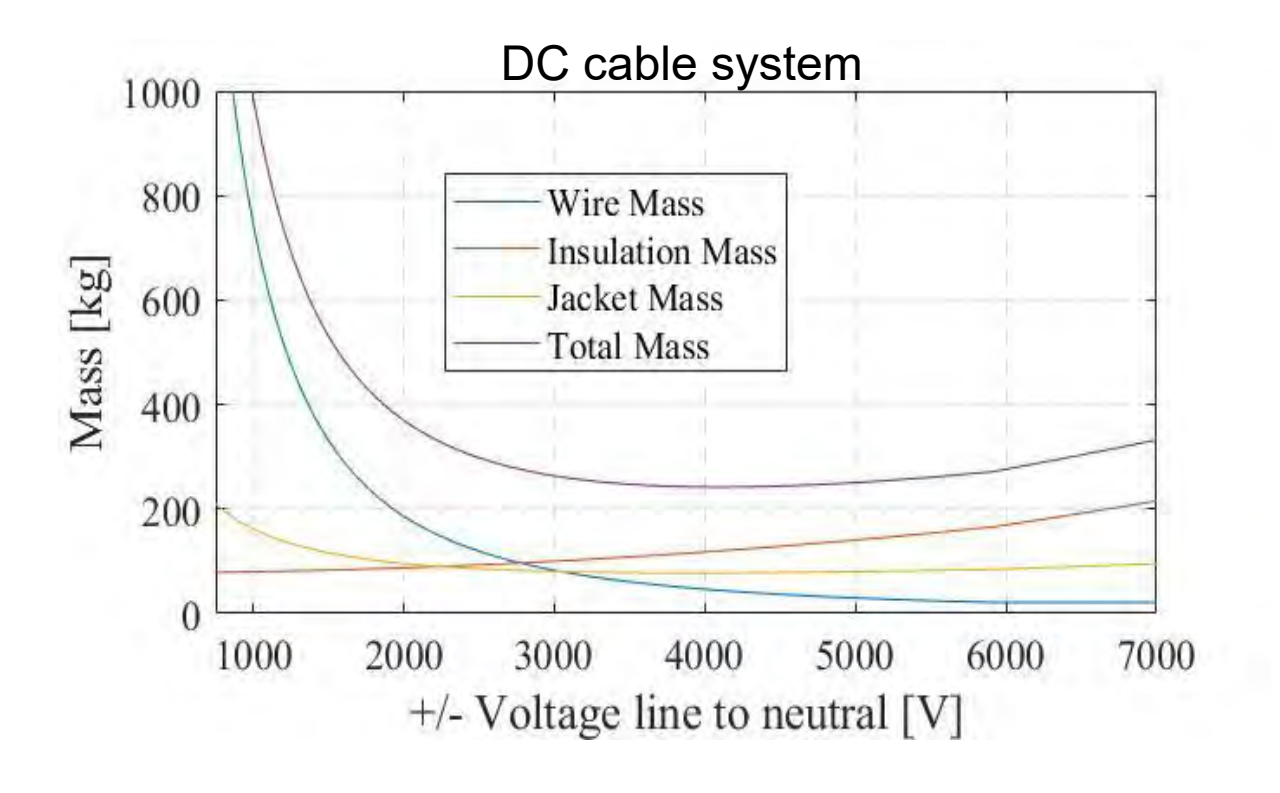


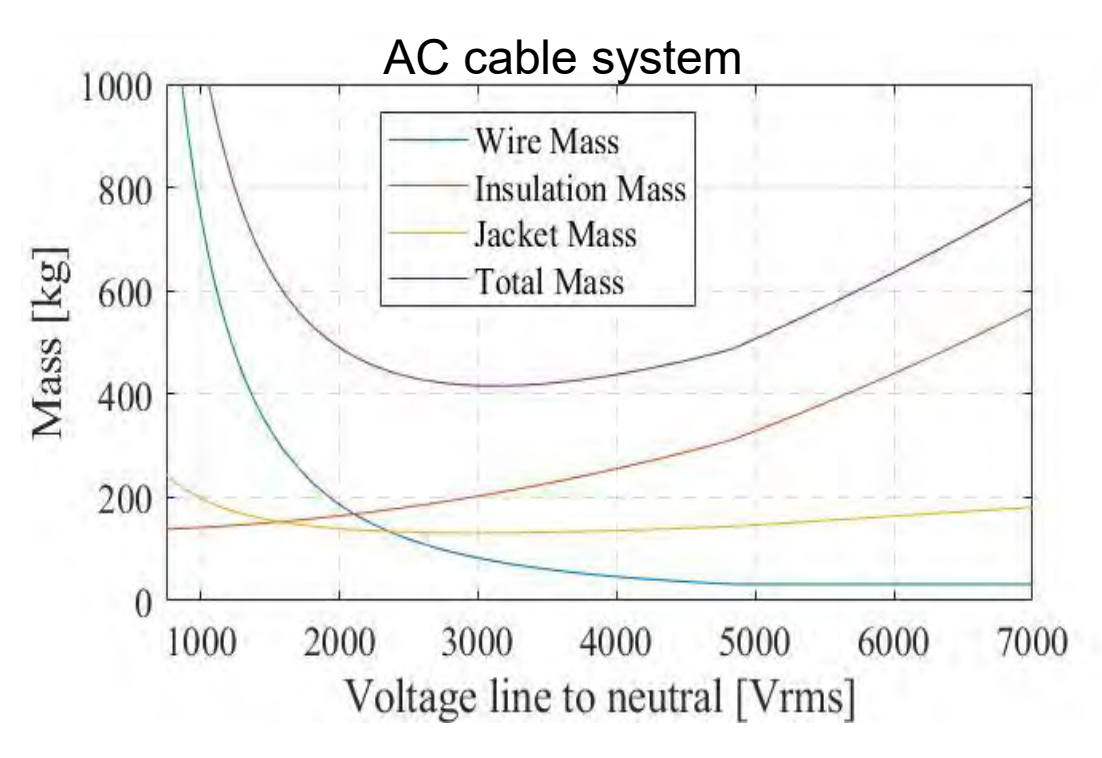
### AC vs. DC Power Transmission



#### Assumptions:

- Cable sized for transmission of 43 kW a distance of 3 km with 95% efficiency
- Cable power loss limited to 0.7 W/m
- Fission Power Mass estimates: 1689 kg/10 kW core power conversion, 2691.4 kg/10 kW



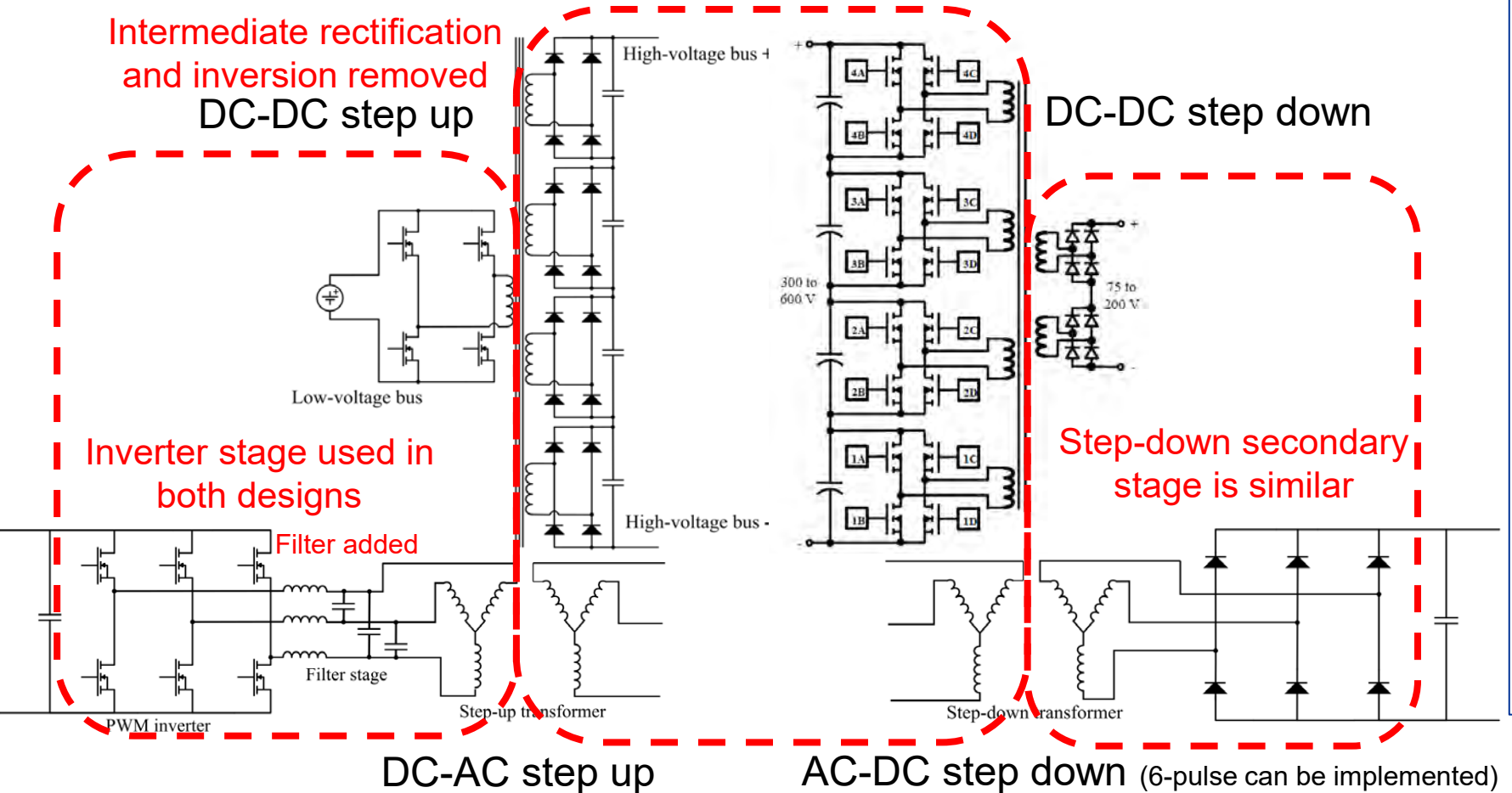


- 1) Christopher Barth, PhD and Pike, David. LUNAR POWER TRANSMISSION FOR FISSION SURFACE POWER. Cleveland: NASA Glenn Research Center, 2022.
- 2) Trade Studies Report Nuclear Fission Power System, Document No.: NFP-RPT-0017, May 14th, 2020 version

### AC vs. DC Power Transmission



- Input and output stages are similar for both designs
- Intermediate rectification and inversion are removed for AC
- DC requires more parts & higher risk of system failure



### **Auto Balancing Series Stacked** converter (ABSS)

- Inherent isolation
- # Active Switches =  $4 * ceiling \left[ \frac{Vdc}{Vsw} \right]$ 
  - 24 switches rated at 175 V = 1050 V
  - 6 levels required for 175 V switches and 1 kV bus
    - o 250 V switches derated to 175 V

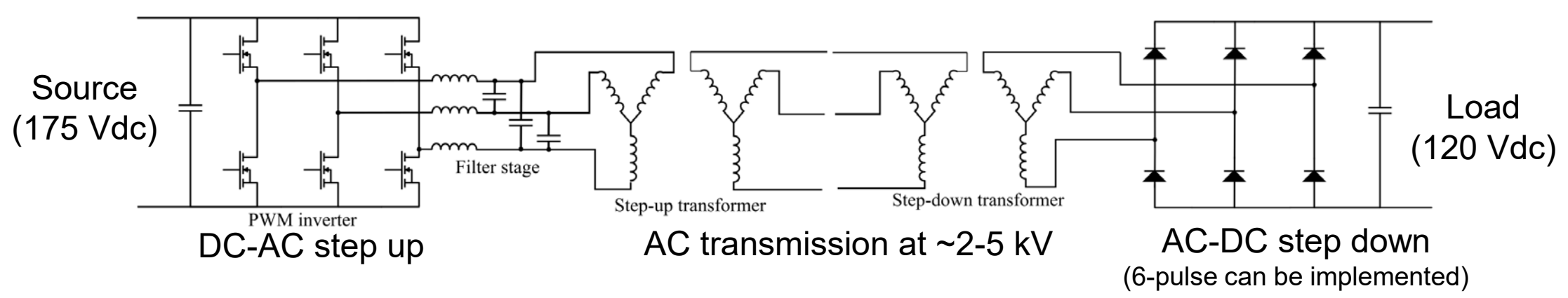
AC-DC step down (6-pulse can be implemented)

1) Christopher Barth, PhD and Pike, David, LUNAR POWER TRANSMISSION FOR FISSION SURFACE POWER, Cleveland: NASA Glenn Research Center, 2022.

### AC vs. DC Power Transmission



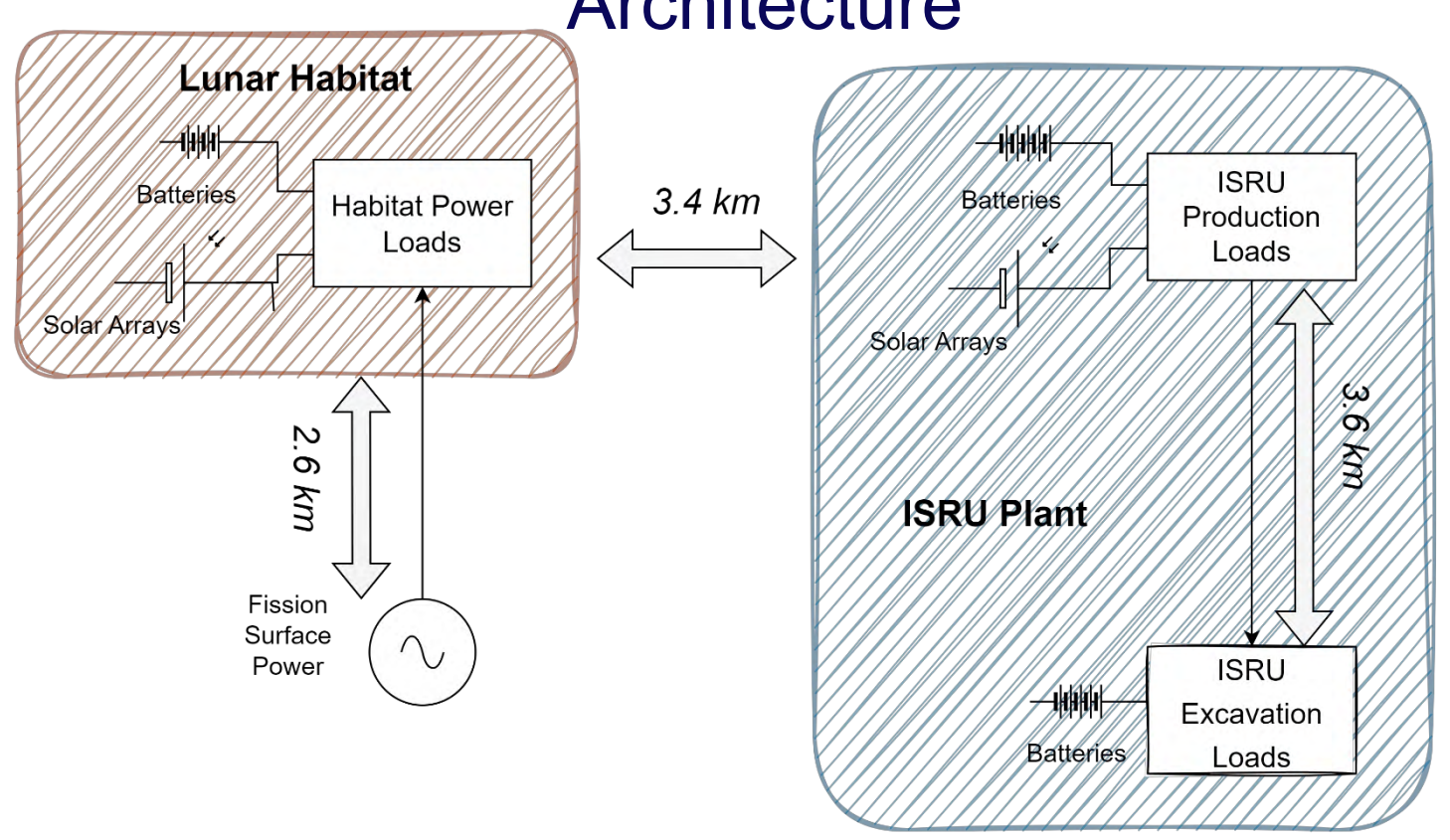
- Simplifies voltage step-up and step-down
  - AC transmission allows use of existing flight-rated switches without stacking (175 Vdc)
  - Eliminates the need for high voltage capacitors
- Modest frequency (1-5 kHz) AC transmission options have been proposed and preliminarily evaluated [1-3]. AC and DC system masses are comparable.
- AC transmission voltage can be easily changed (by changing turns on transformer) based on distance without changing power electronics
- Additional work is in process at GRC to evaluate cable insulation degradation under AC transmission



- 1) K. J. Metcalf, "Power management and distribution (PMAD) model development," NASA Contractor Report CR-2011-217268, Boeing Corporation, Canoga Park, CA, Nov. 2011 (118 pages)
- 2) K. J. Metcalf, R. B. Harty, and J. F. Robin, "Issues concerning centralized vs. decentralized power deployment," NASA Contractor Report CR-187121, Rockwell International, Rocketdyne Division, Mar. 1991 (120 pages)
- 3) T. Kerslake, "Electric power system technology options for lunar surface missions," Tech. Rep. NASA TM-2005-213629, NASA Glenn Research Center, Cleveland, Ohio, Apr. 2005



# Government Reference Example: Baseline Lunar Power Architecture



- Note: This is not an actual system architecture, rather it is a notional architecture that resembles key
  characteristics of interest:
  - 10 km total line distance and ~100 kW of total power
  - FSP separated at least 1 km from other assets
  - 3-5 km distance between ISRU excavation (located in PSR) and ISRU production plant (crater rim, peaks of eternal light)



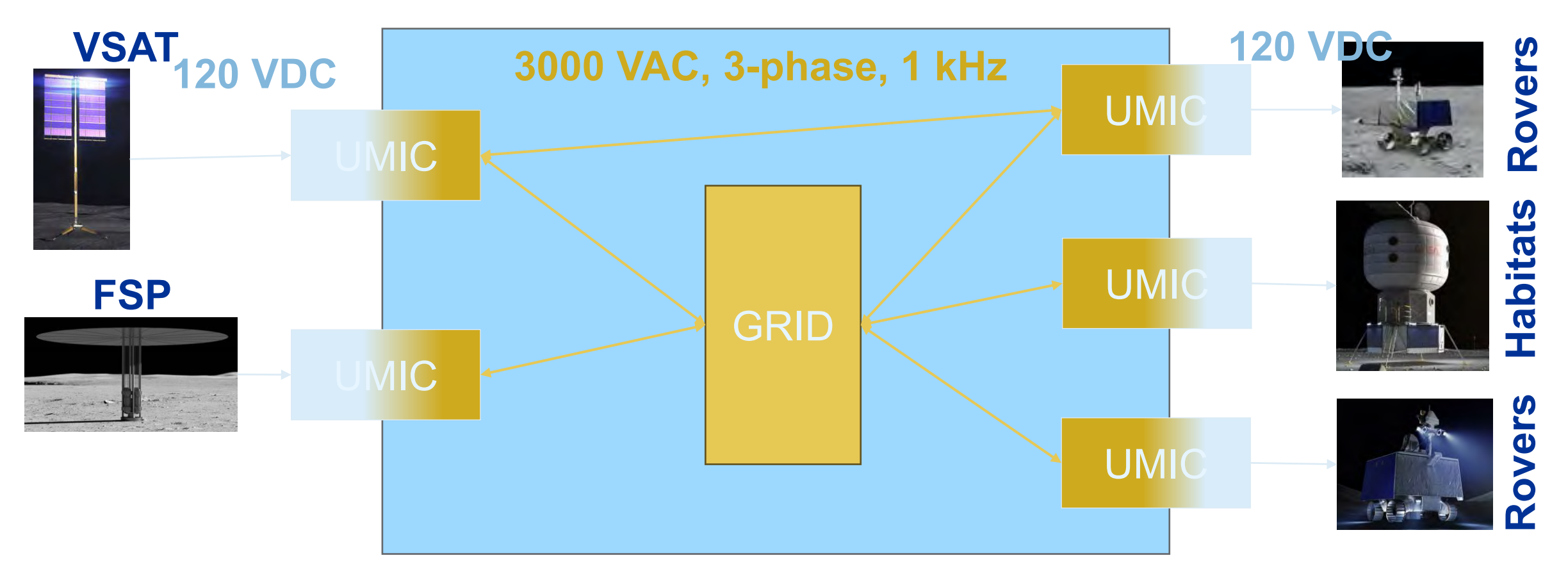
### **Brayton Integration**

- Some Brayton alternator topologies lend themselves well to high frequency 3Φ AC output
  - Homopolar Inductor, Wound Rotor, Rice-Lindell can directly connect
  - Permanent Magnet and Switched Reluctance cannot directly connect
    - Would require an inverter
  - Could be integrated into a microgrid optimized for the natural output
    - Significantly higher efficiency than using inverters
    - Other inverters can follow the inertia of the alternator
- Terrestrial microgrids prefer to have some rotating machinery to offer inertia to a grid
  - A Brayton alternator could be used to serve this purpose on a lunar microgrid



### Universal Modular Interface Converter Concept





- The UMIC enables long-distance power transmission and a power grid
  - Connects power sources and loads together over-long distance and allows for a power grid as the system evolves.
  - Source and loads design to current 120 VDC and 28 VDC power standards



### **UMIC** Design

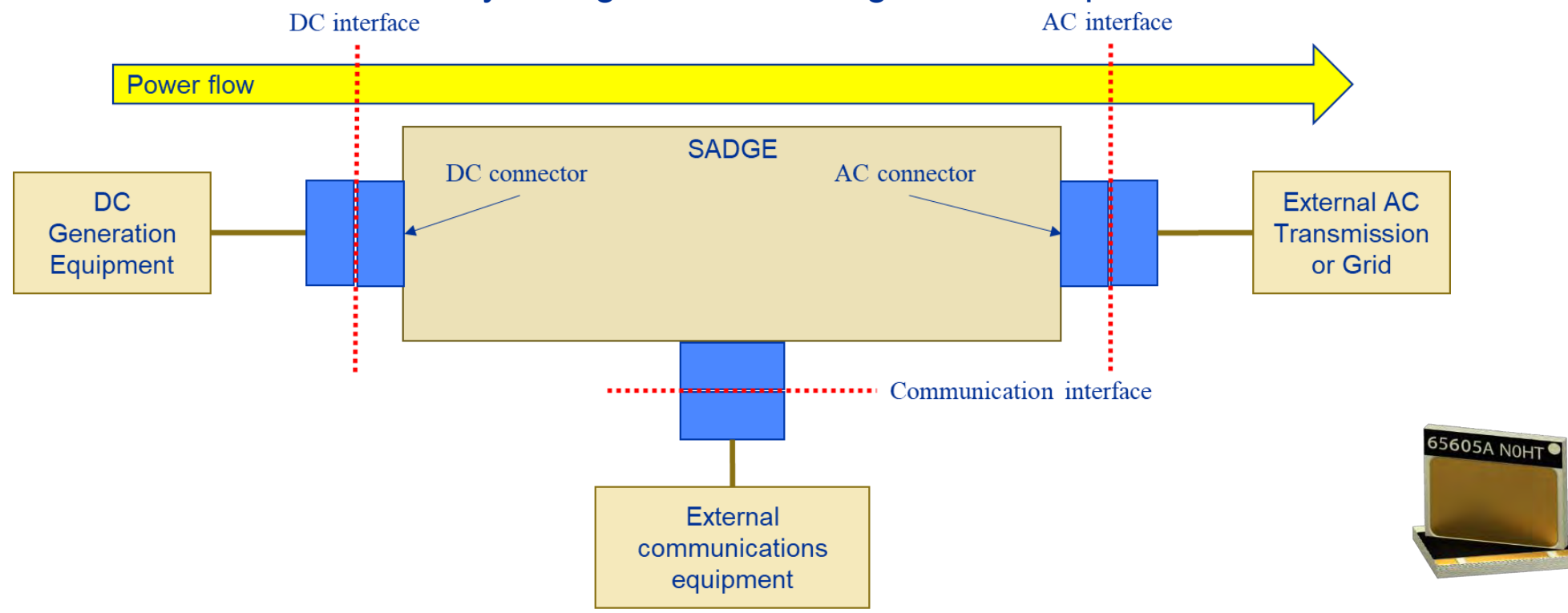
- Bidirectional 120 VDC to 3 kVAC converter
  - Modular in 1 kW units up to 10 kW
  - Controller independent of processed power specifications
  - AC transmission specifications match results of FSP transmission studies (3 kVAC 1 kHz)
  - DC not a good fit at 120 VDC
    - Low DC voltage costs significant mass
- Minor redesign allowing for higher DC voltage could be a good fit for FSP needs
- FSP can use single direction converters





### Standardized Adapter for Dedicated Generation Equipment (SADGE) Operating Parameters

- 300 VDC to 3 kVACrms, 3 phase, 1 kHz, >3 kW
- GaN MOSFET (GS-065-060-5-T-A) can only be used to 325 V
  - Converter is intended to operate at 275-325 VDC
- Redesigned UMIC based on the higher DC input voltage and unidirectional power flow
  - Similar control scheme; only change based on single direction power flow

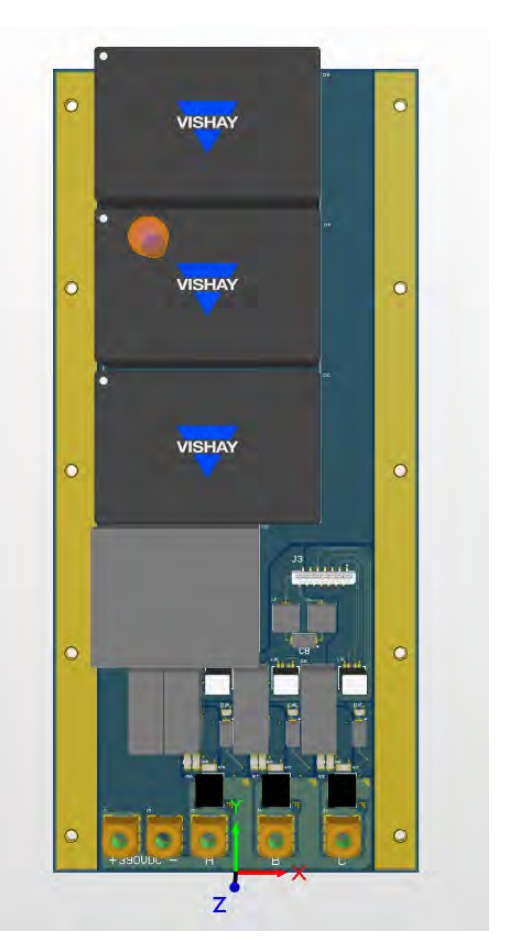


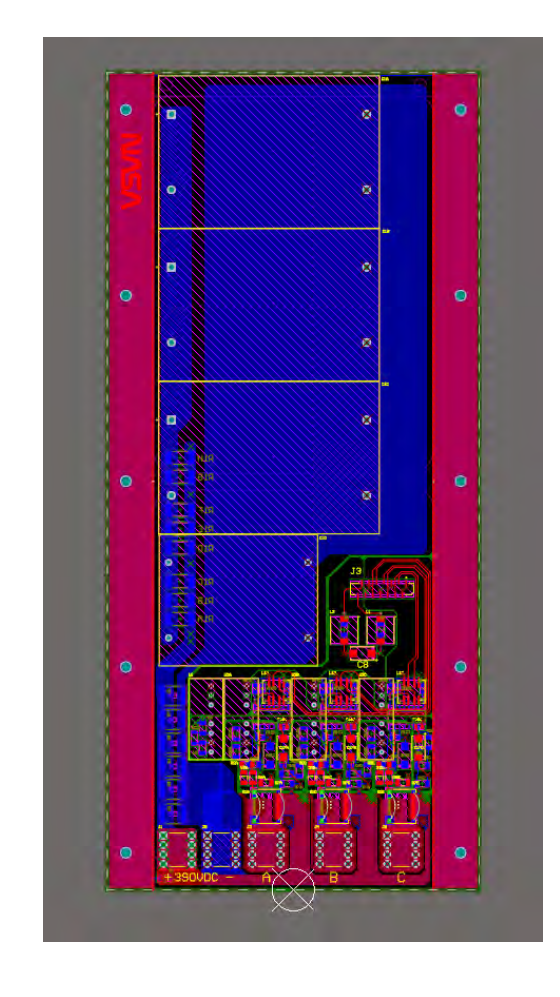


### SADGE Inverter: Initial Design

- Operating parameters
  - Successfully benchtop tested at 325 V, 3 kW
  - Redesigning to address issues faced by UMIC team in TVAC testing

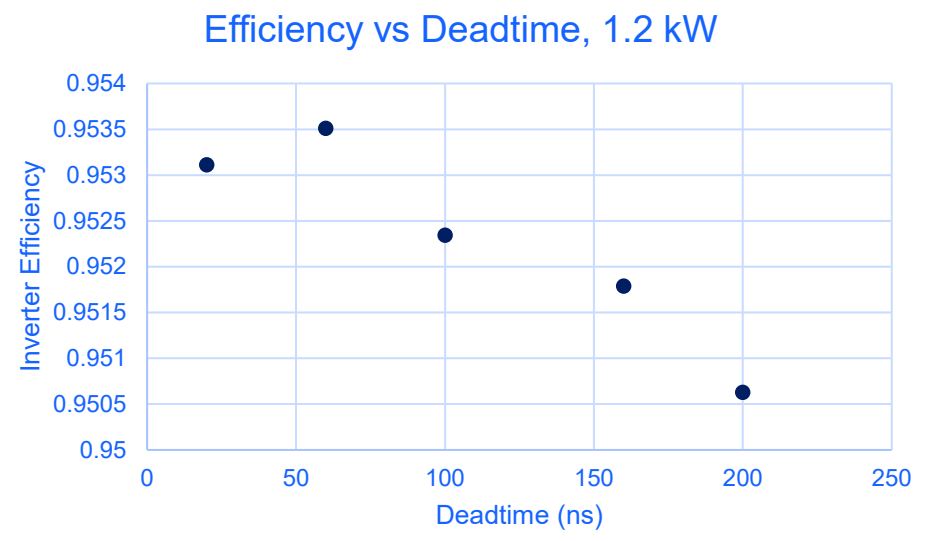






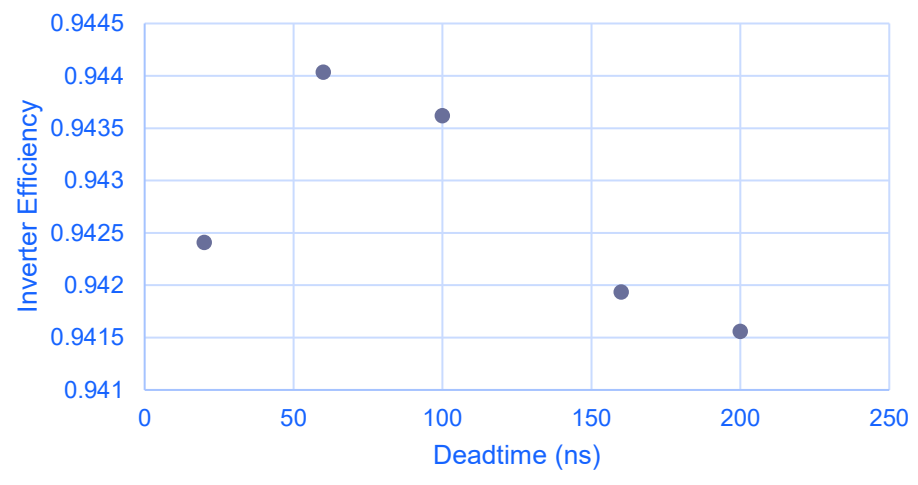


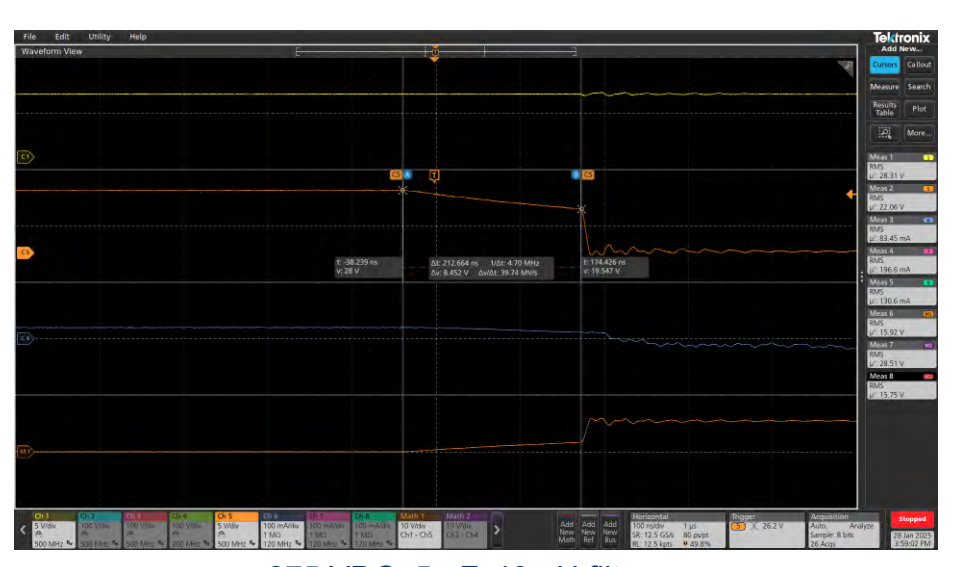
### Deadtime optimization





### Efficiency vs Deadtime, .9 kW



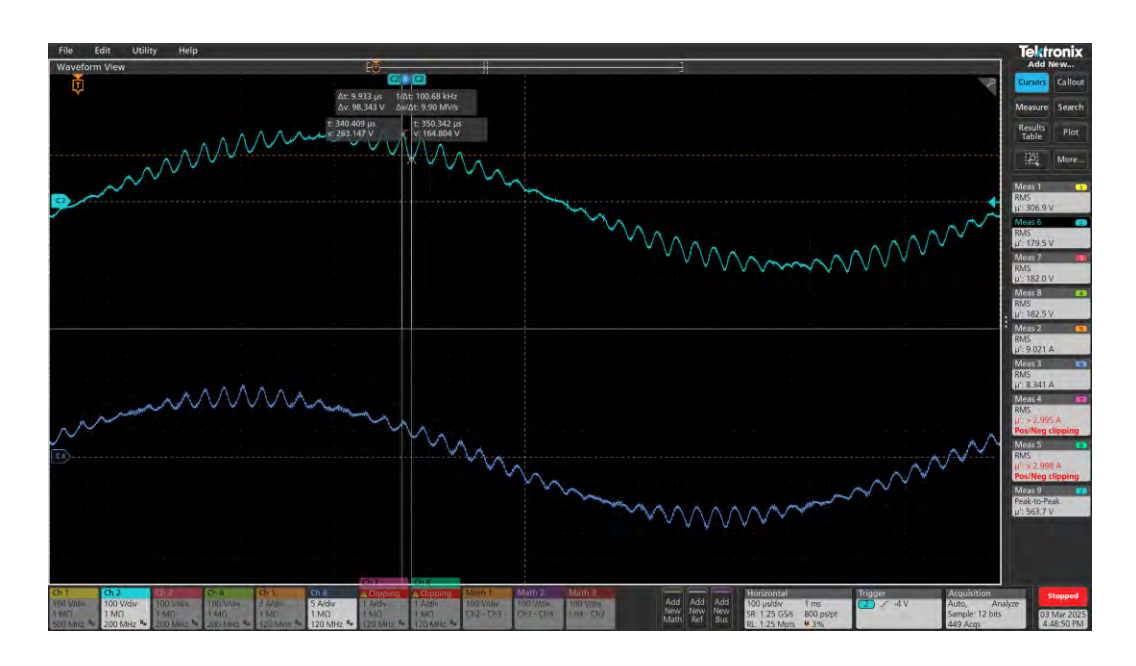


275 VDC, 5  $\mu$ F, 40  $\mu$ H filter

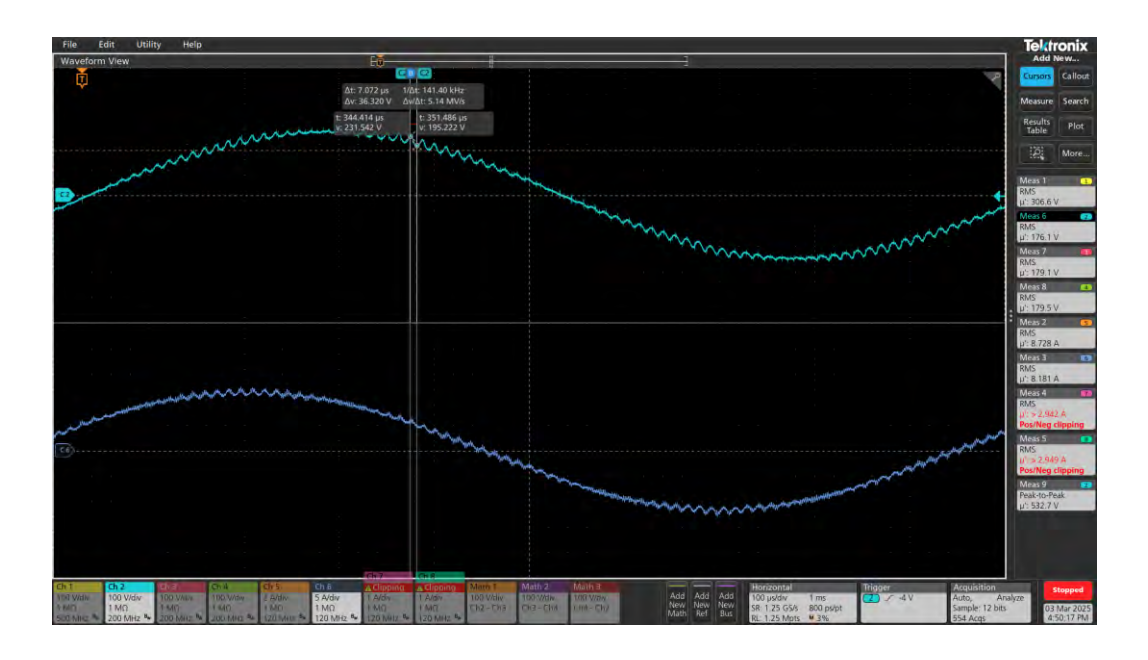


### Filter and Switching Optimization

300 VDC, 100 ns deadtime, 1 µF, 80 µH filter, 2.6 kW



50 kHz switching frequency 98.3% efficient 17.4% ripple

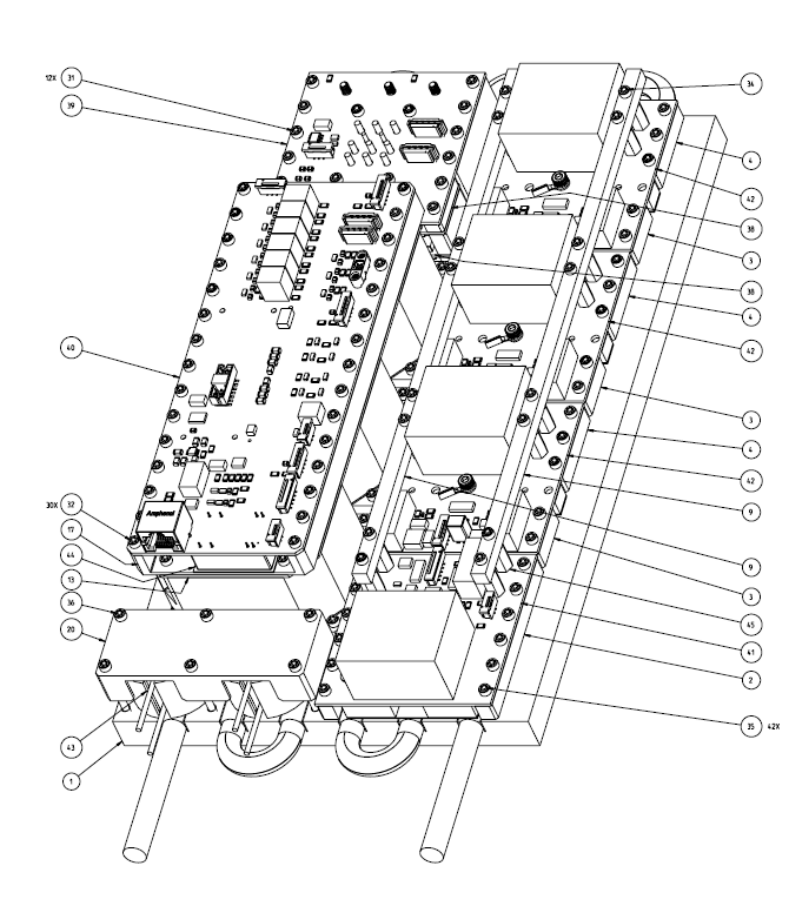


80 kHz switching frequency 97.9% efficient 6.8 % ripple



### **SADGE Inverter: Revision 1**

- Redesigned for optimal cooling of MOSFETs and other thermally critical components
- **Benchtop testing** to occur upon completion of assembly, FPGA reprogramming, and GUI updates
- Design intended to survive Shock and Vibe testing, as well as TVAC testing







### SiC MOSFET Development

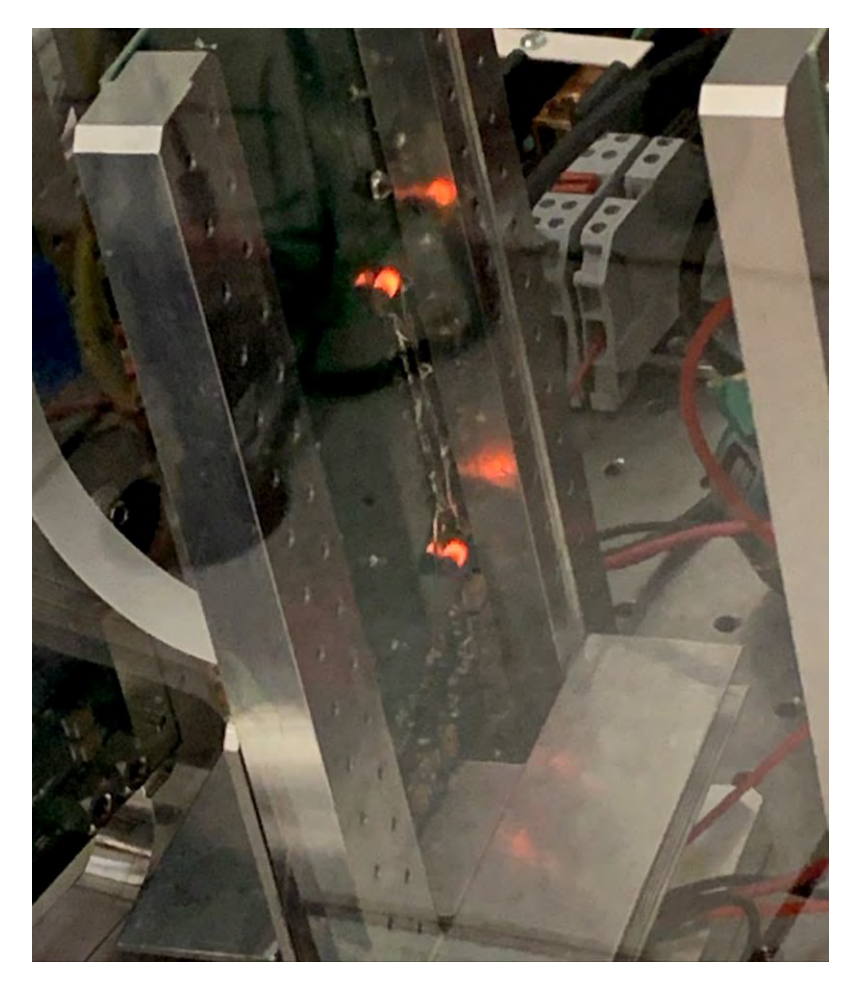
- Vanderbilt University is working on cutting edge research regarding SEE tolerance of SiC MOSFETs
- Preliminary research indicated performance in SEE environment at 900 VDC
  - Represents an improvement of 3x over state of the art
- Design improvements to device make 1.5 kV+ feasible
  - Contract in place to occur over ~3.5 years
  - Would allow for NASA to explore DC transmission

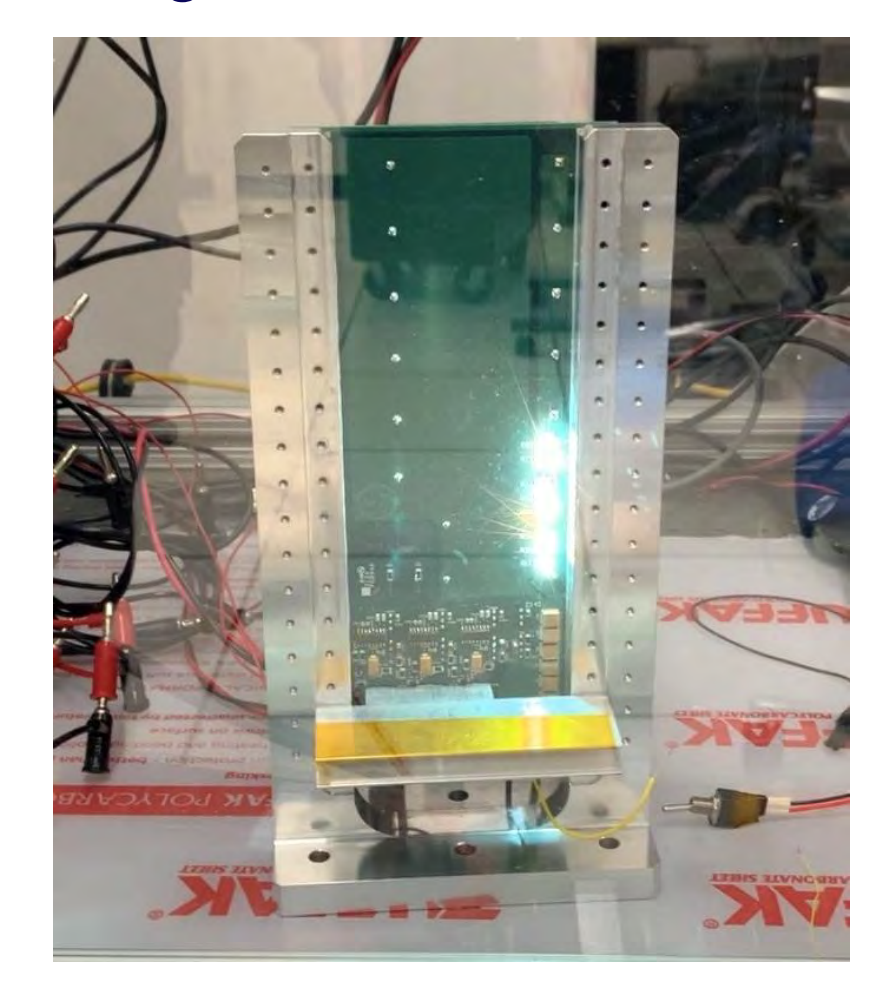




### Questions?

### david.c.pike@nasa.gov







### Fission Surface Power (FSP) Project

Testing the Effects of Lunar Dust on FSP Radiators at Glenn Research Center

Fission Surface Power Tech Mat Webinar

September 24, 2025

NASA Glenn Research Center Cleveland, Ohio

Ron Leibach Glenn Research Center

### **Background**



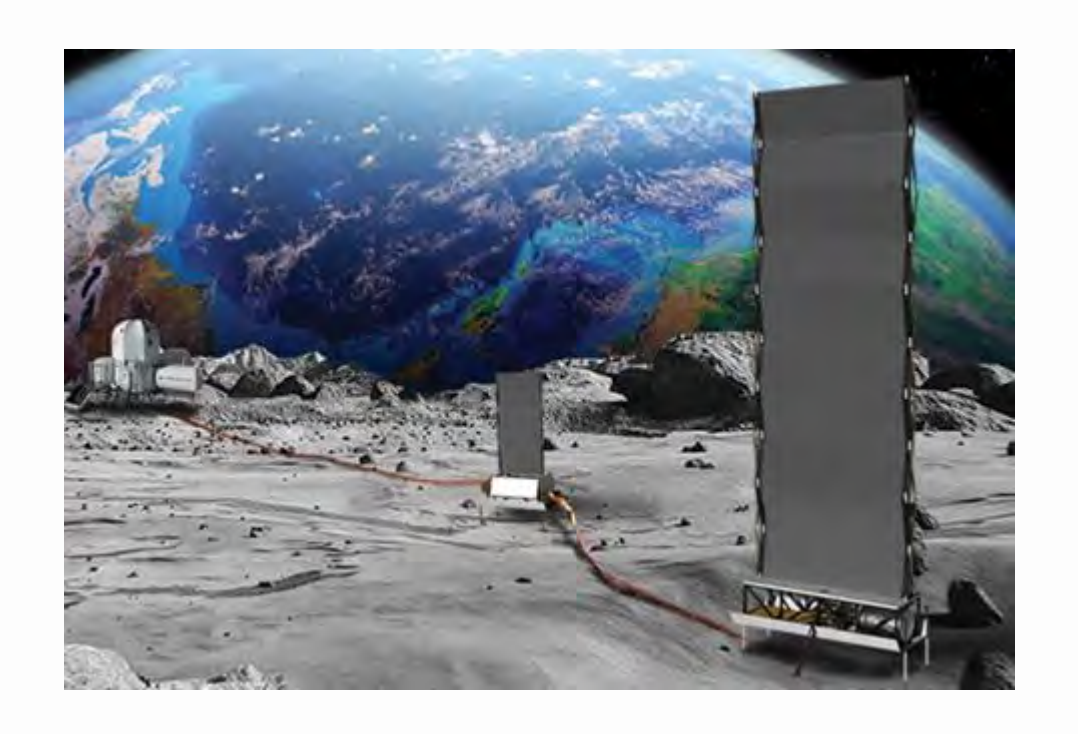
- FSP systems in the 10s of kW range may require thermal control area in the hundreds of m<sup>2</sup>
- Dust as a mission detriment has been studied since the Apollo missions
- The effects of dust on radiator heat rejection performance have not been fully characterized
- It is advantageous to pin-point methodologies for studying dust-radiator phenomena



### Purpose



- The Risk of Radiator Dust Demonstration (R2D2) effort serves to create an in-house platform for regolith testing to assess the risk of regolith on heat rejecting radiators.
- The goal of Phase I was to create a generalized test platform for depositing dust on an operating radiator.
- Phase II studies will be focused studies to characterize specific dust-radiator phenomena



### Phase I

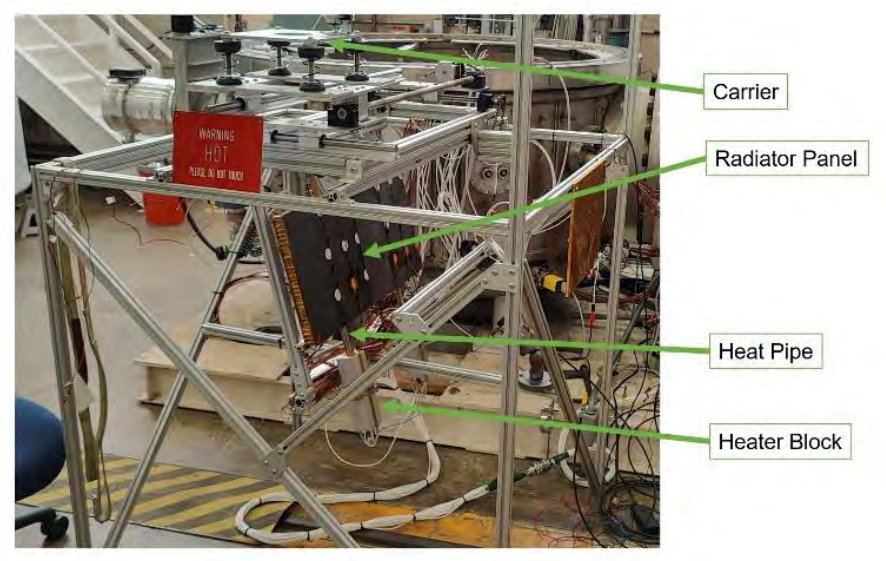
TO REAL PROPERTY OF THE PROPER

- The Phase I study examined the dust-radiator phenomena caused by dust saturation, heat, and voltage bias.
- This was a quick turnaround high level view, which allowed us to design two Phase II experiments.



### Methodology

- 1. Radiator assemblies are installed in aluminum frame beneath a dust deposition system.
- 2. Entire test rig placed in a vacuum chamber, Radiators are brought to operational temperatures.
- 3. Control heater power supply output such that the heat pipe condenser reaches 200C.
- 4. The deposition system releases JSC-1A atop of the radiator surface. Thermal response is studied via IR imaging and a thermocouple array.
- 5. A DC voltage bias is adjusted by 25 V.
- 6. Repeat.



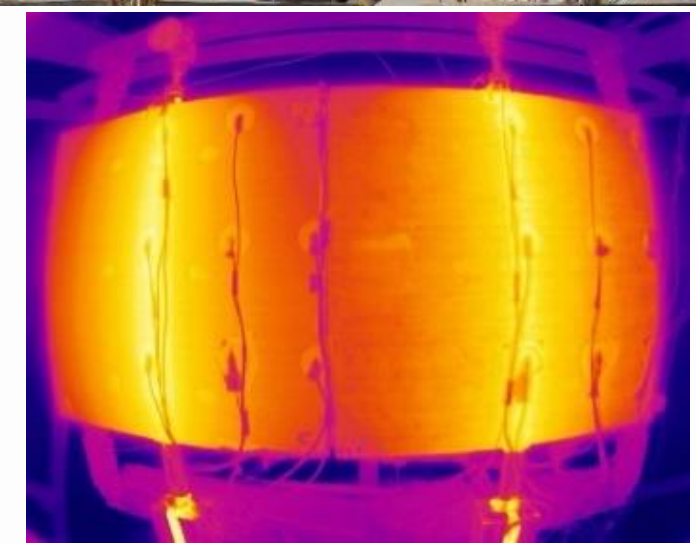


### Instrumentation



- 22 TCs per radiator assembly
  - 9 per facesheet (2x facesheets per assembly)
  - 4 per heat pipe
  - All temp data recorded by DAQ
- IR camera
  - Allows for higher resolution thermal profiles
  - Calibrated by TC data
- Heater power measured from power supply readout





### Test 1



0-100 V sweeps performed with no issues.

### **Lessons learned**

• Dust is being deposited despite camera visuals



### **Lessons Learned**

- Dust adheres as low as 0 V
- There is no indication that additional dust adheres past the first sweep



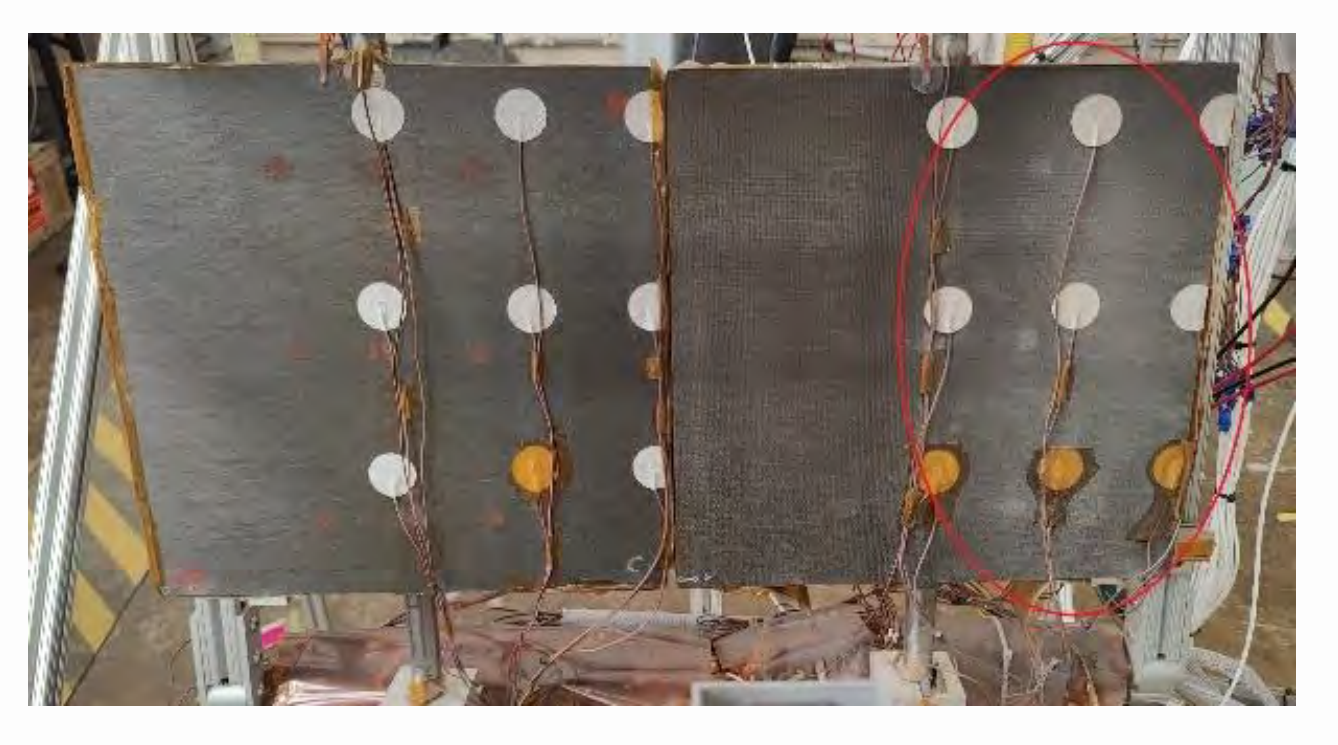
### Test 3



75 micron sieve swapped for 250 micron sieve to alleviate concerns that not enough dust was being deposited

#### **Lessons Learned**

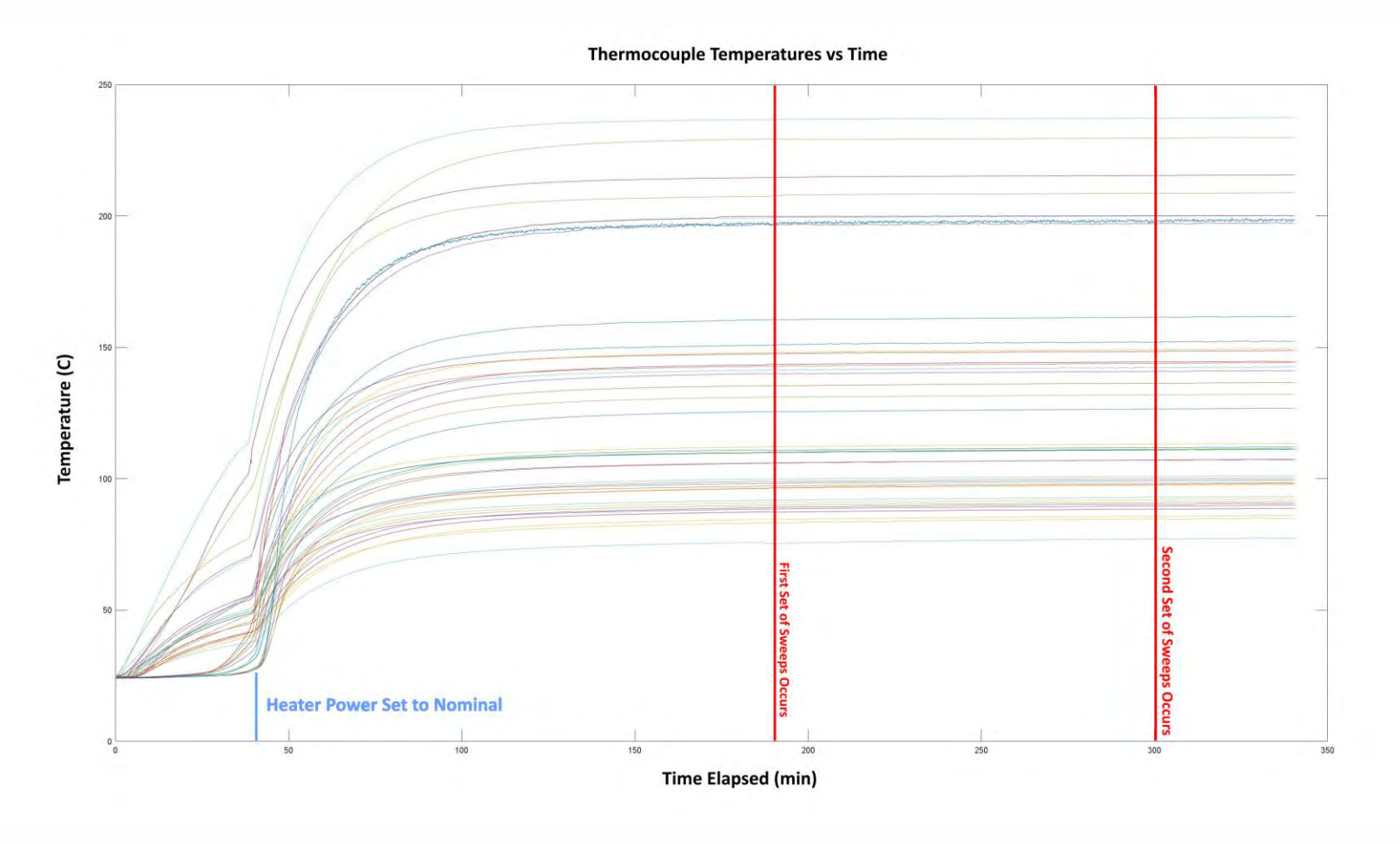
- Dust volume must scale with sieve size
- No indication that dust adhesion increases w/ deposition volume



### Results



Figure shows total thermocouple dataset over time.



### Results

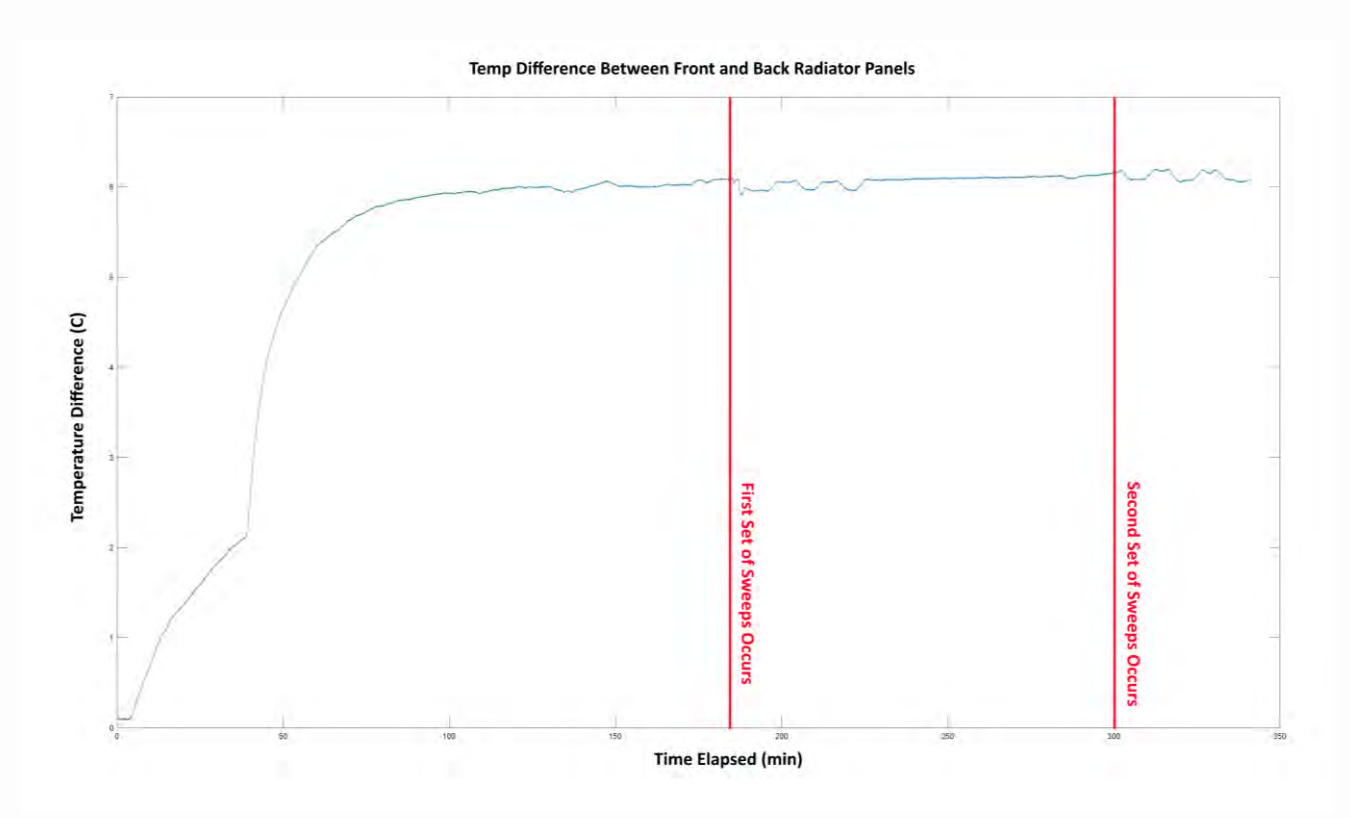


Changes in temperature due to power input will vary both front and back temperature, while dust deposition will *only* affect the temperature of the front facesheet.

Therefore, to study thermal response, look at  $T_{front}$ - $T_{back}$ 

- Pre-deposition  $T_{front}$ - $T_{back}$  = 6.07C
- Post-deposition  $T_{front}$ - $T_{back}$  = 6.09C

We can conclude that more focused studies must be performed to observe an accurate thermal response.



### Results



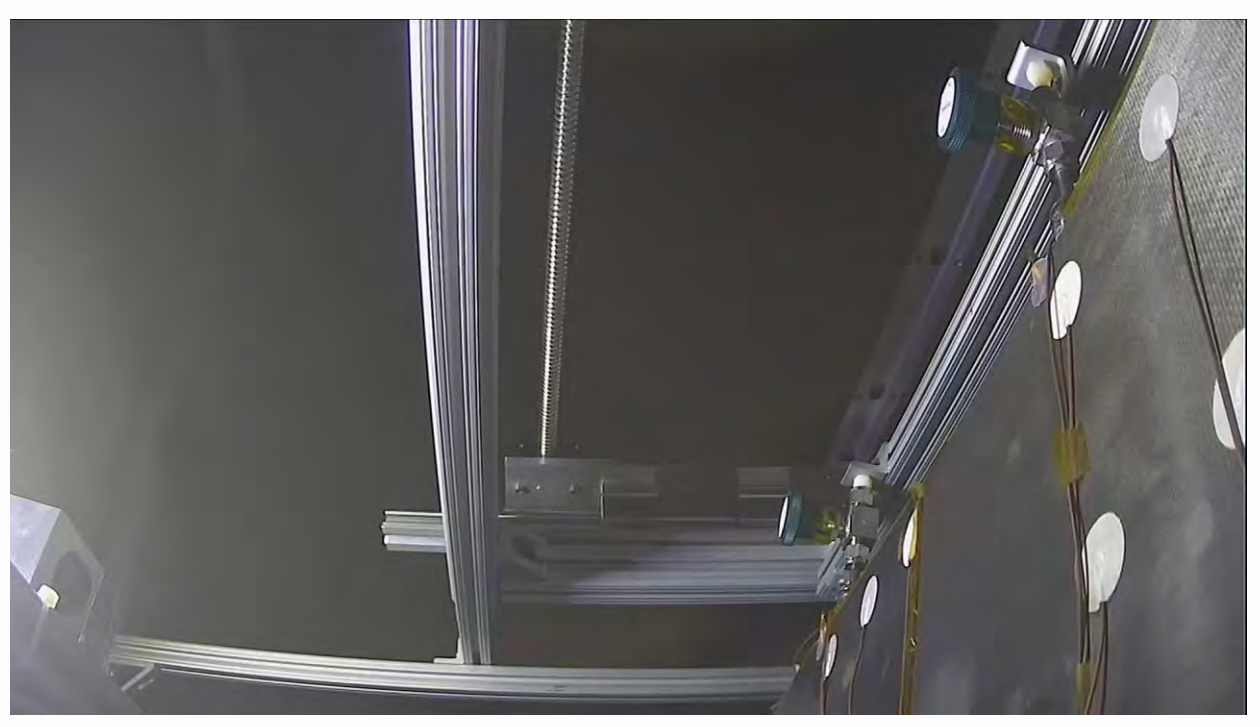
Test video shows that the panel saturated almost instantly

This implies that the test was not capable of applying the magnitude of charge required for increased saturation.

#### Conclusion

We need to implement studies A and B:

- A) Manual saturation thermal response study
- B) Ionic charge induction to force saturation study



### Phase II



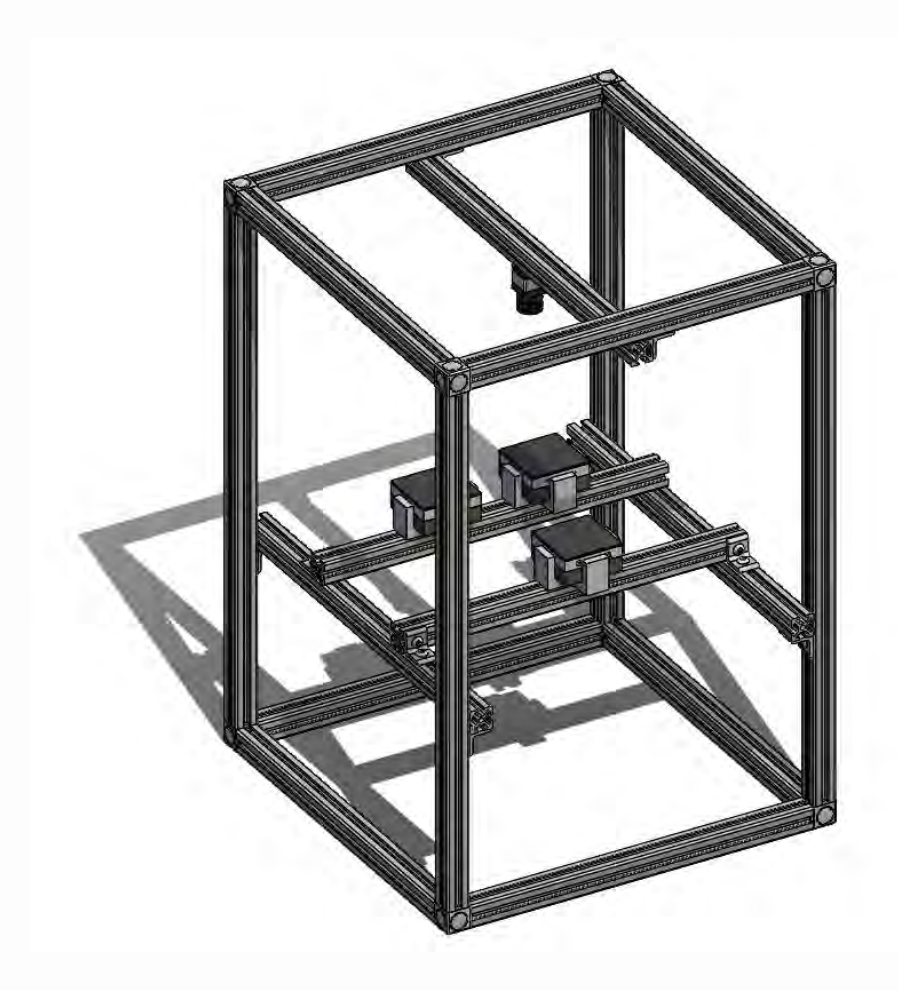
The next phase consists of two lower level experiments meant to characterize known radiator-dust phenomena.

#### Study A:

- Dust saturation mass vs thermal performance
- Solar absorptance vs thermal performance

#### Study B:

- lonic charging vs dust saturation mass
- Operating temperature vs dust saturation mass



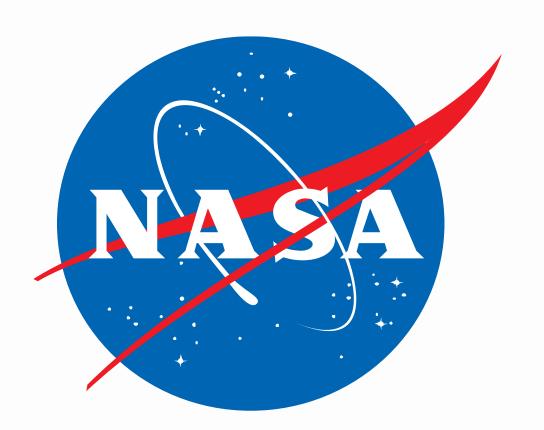
### **Thank You**



Questions?
Contact me via email at:
ronald.j.Leibach@nasa.gov

### Collaborators:

- Greeta Thaikattil
- Jim Sanzi
- Meghan Bush





## **Dynamic Power Convertor Organics Irradiation**

FSP Technology Maturation Webinar Series



#### Context

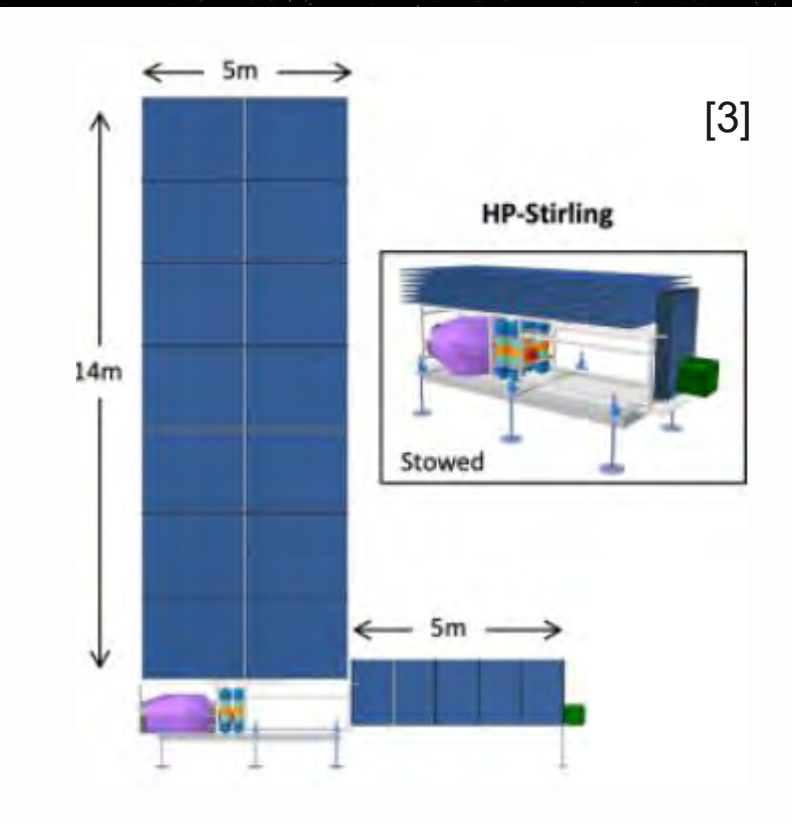


- Dynamic power conversion system for 40 kWe Fission Surface Power
  - Using Sunpower (SRSC) design as representative Stirling PCS
    - O-rings
    - Heat shrink
    - Wire insulations
    - Threadlocker
    - Dry lubricant
    - Potting
- Radiation effects of-interest in organics
  - Cross-link
    - Increase tensile strength
  - Chain scission
    - Embrittlement
  - Outgassing
    - Potentially liberate volatile species
- Conflicting results in literature
  - "The present lubricant is not a satisfactory choice for this service condition [4 Mrad] and a substitute must be found." Golliher, Pepper; Organic materials ionizing radiation susceptibility for the outer planet/solar probe radioisotope power source.<sup>1</sup>
  - "The solid lubricant-coated samples experienced no systematic or statistically significant changes in weight, appearance, or physical/chemical properties as a function of irradiation under the conditions [15 Mrad] studied. Bowman, Shin, Mireles, Radal, Qualls; Radiation specifications for fission power conversion component materials.<sup>2</sup>

#### **Environment**

EN SUSTAINED EXPORT

- FSP dose at PCS:
  - 10 Mrad [3]
  - 5x10<sup>14</sup> n/cm<sup>2</sup> [3]
- PCS temperature:
  - 1100 K hot-end [3]
  - 380 K alternator housing [4]
- Stirling convertor:
  - · Helium working fluid
  - 600 psig
- Synergistic lifetime testing
  - Common containment environment
  - Relevant charge pressure
  - Relevant charge gas
  - Relevant material ratios
  - Complete list of susceptible materials
  - FSP lifetime radiation exposure + margin
  - PCS temperature
    - · During irradiation
    - 8 months continuous thermal aging after irradiation







#### **Past Work**



#### **ASC** organics

- 2009: Stirling Alternator Radiation Test Article [2]
  - Sandia NL GIF (Co-60)
  - 40 Mrad
  - 400 K
  - Alternator components only
  - Short in alternator
- 2011: Coupon testing [5]
  - Oak Ridge NL HFIR GIF
  - 14 Mrad
  - 400 K
  - Complete list of organics
  - Mostly insignificant degradation

- 2010: Coupon testing [2]
  - Texas A&M Univ. TRIGA
  - 5.4 Mrad + 5x10<sup>14</sup> n/cm<sup>2</sup>
  - 400 K
  - Most organics
  - Mostly insignificant degradation
- 2011: Synergistic testing [5]
  - Texas A&M Univ TRIGA
  - 14 Mrad + 5x10<sup>14</sup> n/cm<sup>2</sup>
  - 400 K
  - 515 psig helium environment
  - 5 months, 16 months
  - Most organics
  - Some degradation

- FSP dose at PCS:
  - 10 Mrad [3]
  - 5x10<sup>14</sup> n/cm<sup>2</sup> [3]

#### **Current Work**



• 2017: "The highest service temperature of the final candidates shall be further validated by the synergistic durability life testing (SDLT)" [6]

#### **SRSC** organics

- 2025: SDLT
  - Ohio State University Research Reactor
  - 22 Mrad + 2x10<sup>16</sup> n/cm<sup>2</sup>
  - 375 K, 395 K, 415 K
  - 600 psig helium environment
  - 8 months at listed temperature levels
  - Complete list of organics at relevant ratios in common containment

- FSP dose at PCS:
  - 10 Mrad [3]
  - 5x10<sup>14</sup> n/cm<sup>2</sup> [3]

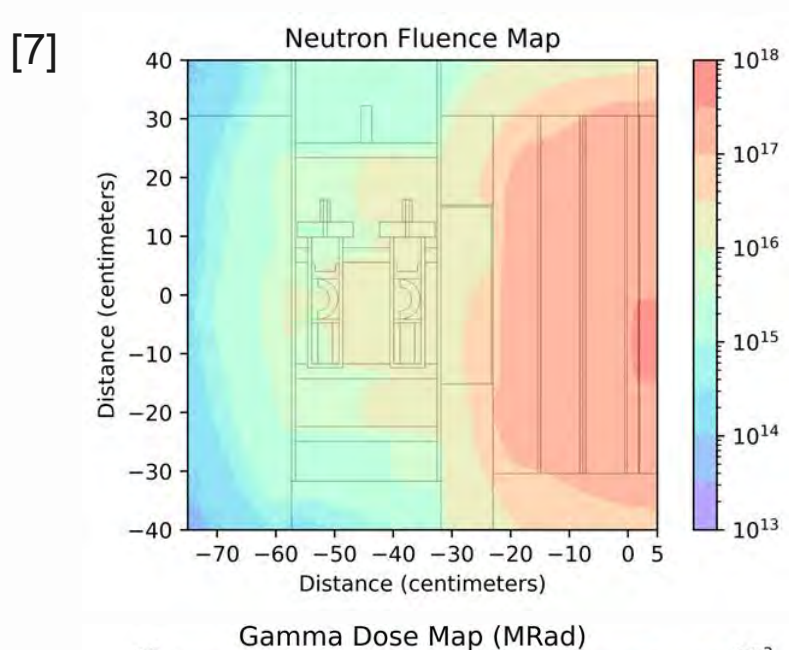
#### **Process**

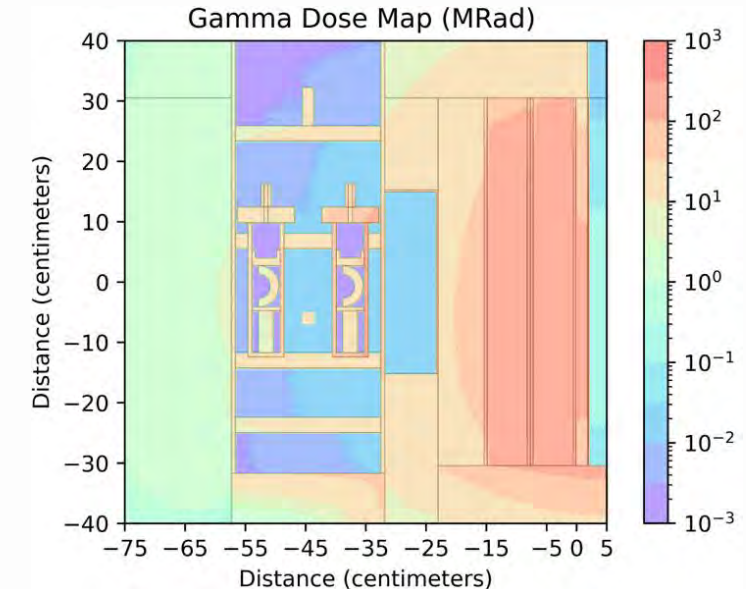
SURFACE PORTER

LESSON SURFACE PORTER

REGISTATINED ENVIRONMENT

- Model
  - Thermal
  - Mechanical
  - Radiation
- K-type TCs and band heaters
- 1. Pre-test material examination
- 2. Out-of-pile verification test
- 3. In-pile test
- 4. Post-test thermal aging (we are here)
- 5. PIE



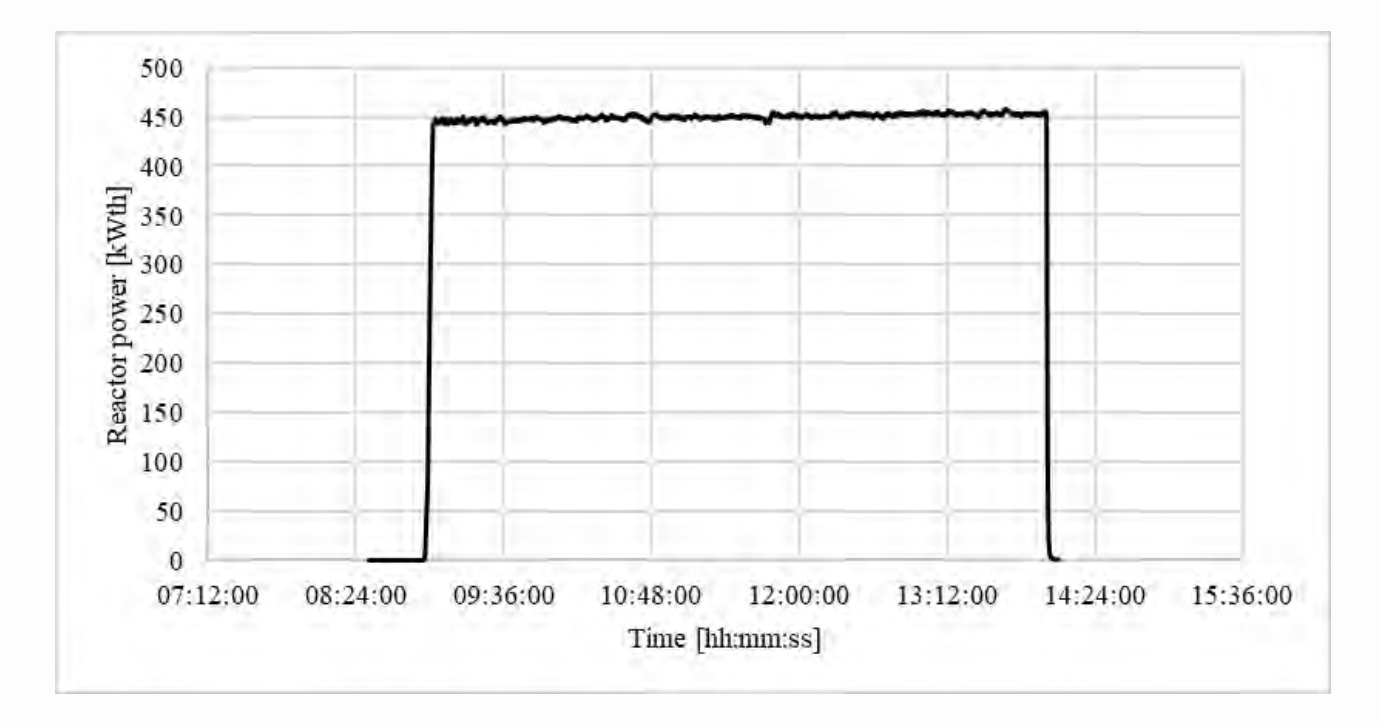


## **Test Matrix**



RI

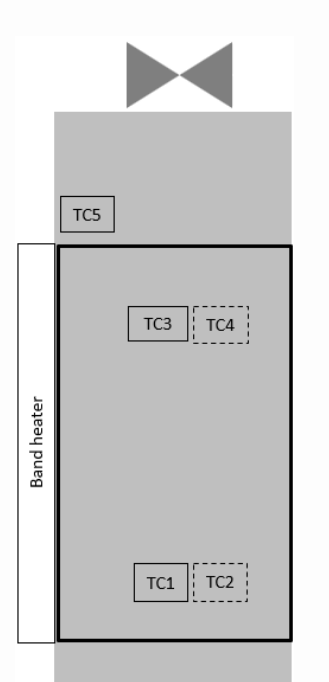
Vessel	Temperature [K]	Time [mo]	Pres [psig]	Expected neutron fluence [n/cm²]	Target gamma dose [krad]	TCs
4	415	8	600	2E16	2.2E4	5
3	395	8	600	2E16	2.2E4	5
2	375	8	600	2E16	2.2E4	5
0-along	N/A	N/A	N/A	2E16	2.2E4	0
1-control	Ambient	8	600	0	0	5

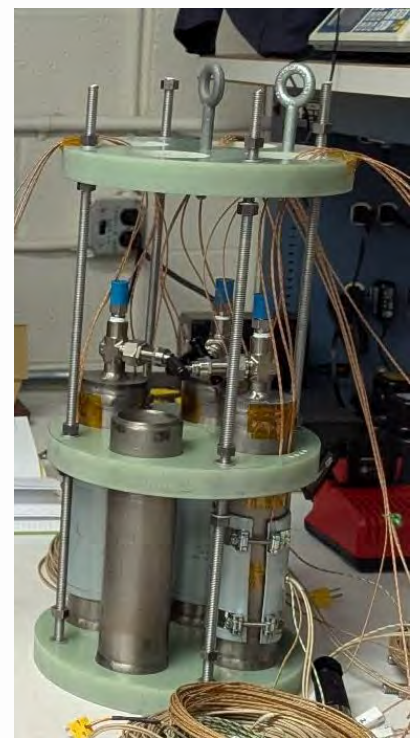


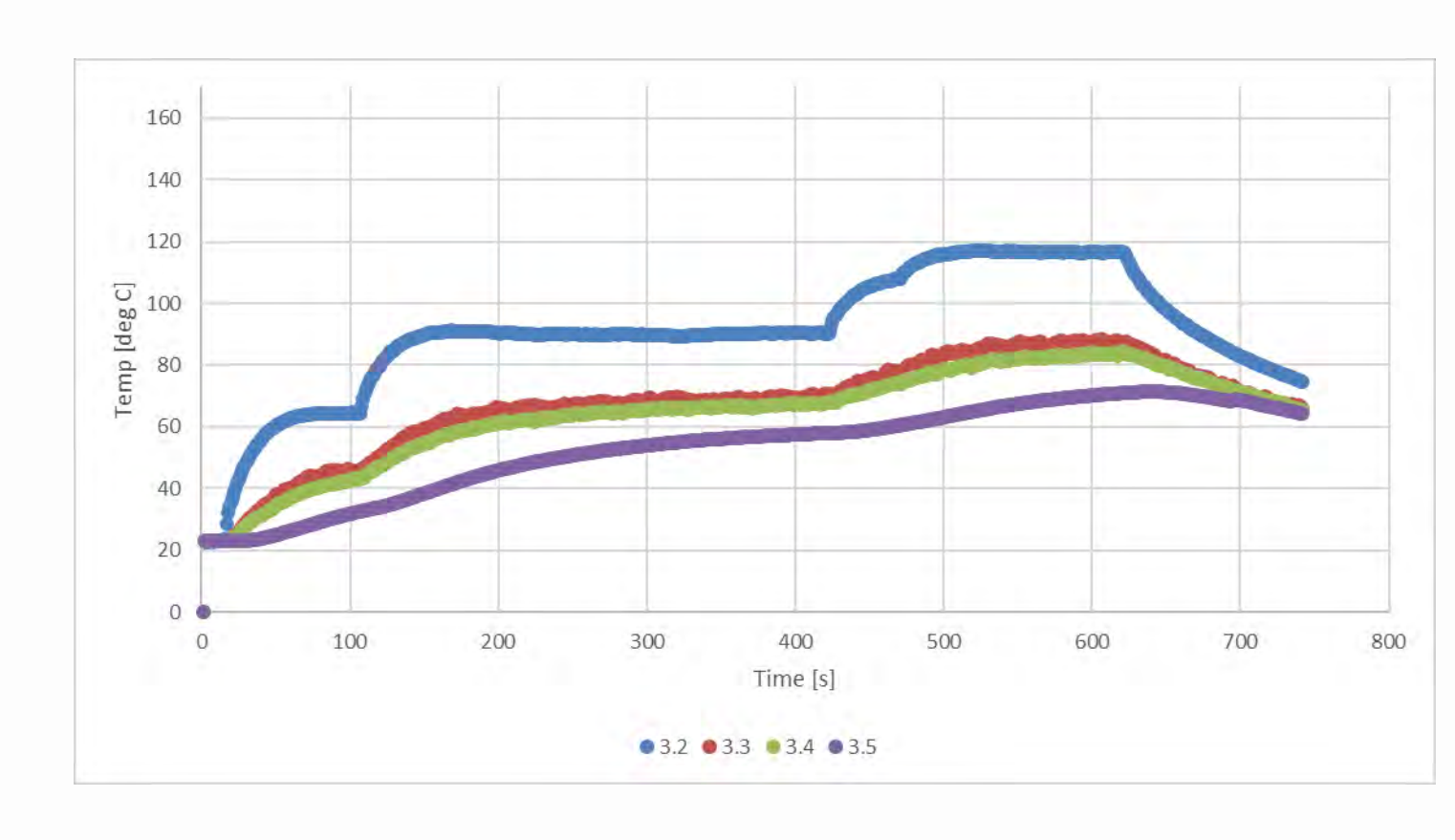
## **Test Execution: Pre-Irradiation Out-of-Pile**







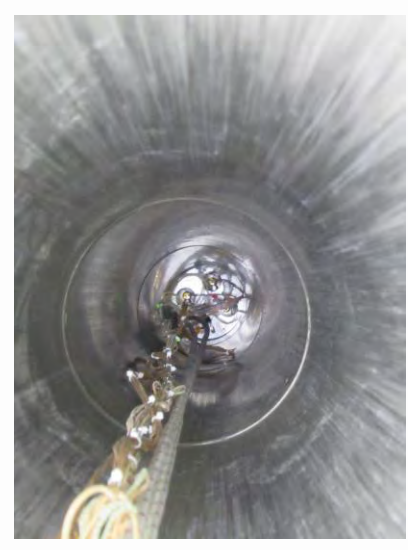




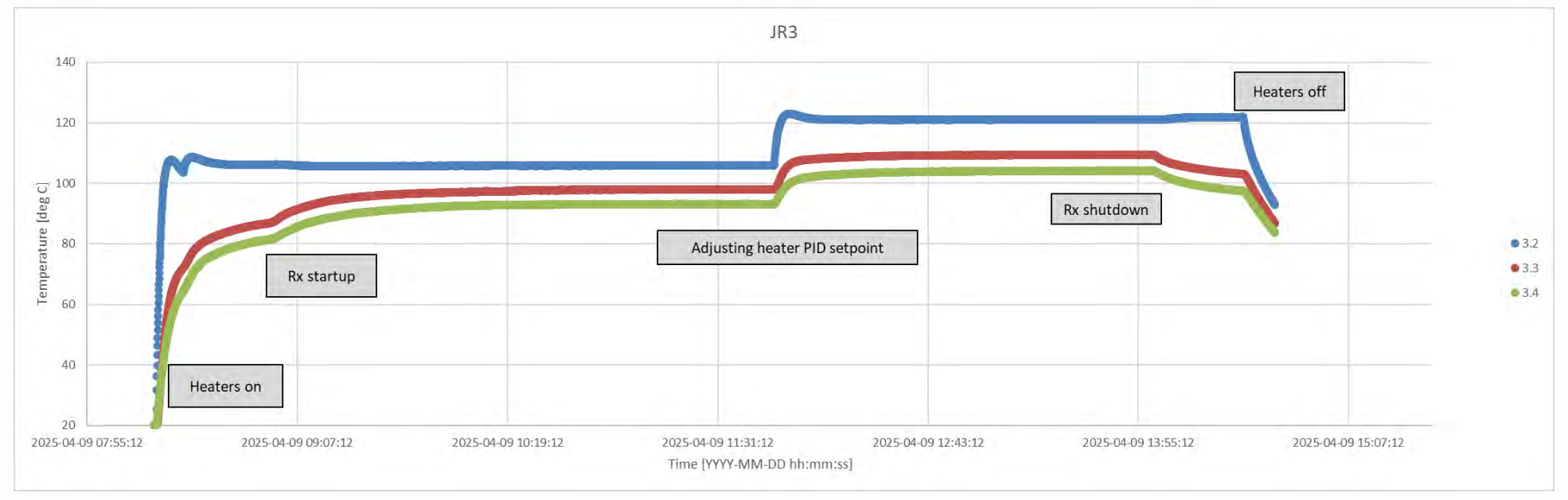
#### **Test Execution: In-Pile**







- Indium foil ridealong
  - Post-irradiation gamma spec + count → 5x10<sup>15</sup> n/cm<sup>2</sup>
    - (At bottom of farthest vessel)



### Test Execution: Post-Irradiation Out-of-Pile





0.40 mrem/hr at console13.0 mrem/hr on contact

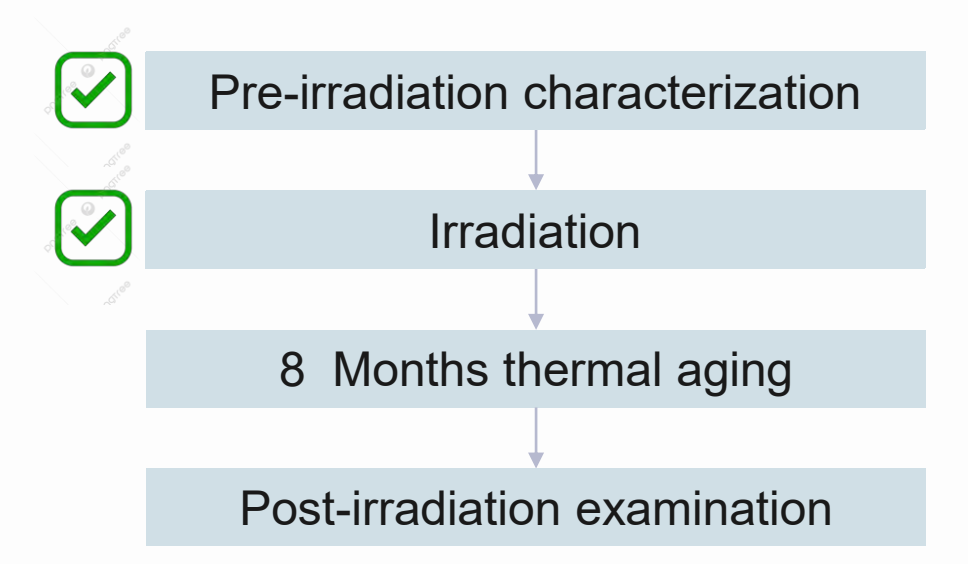


0.20 mrem/hr at console1.6 mrem/hr at concrete

- 8 month thermal aging:
  - 375 K, 395 K, 415 K

## **Material Analysis**



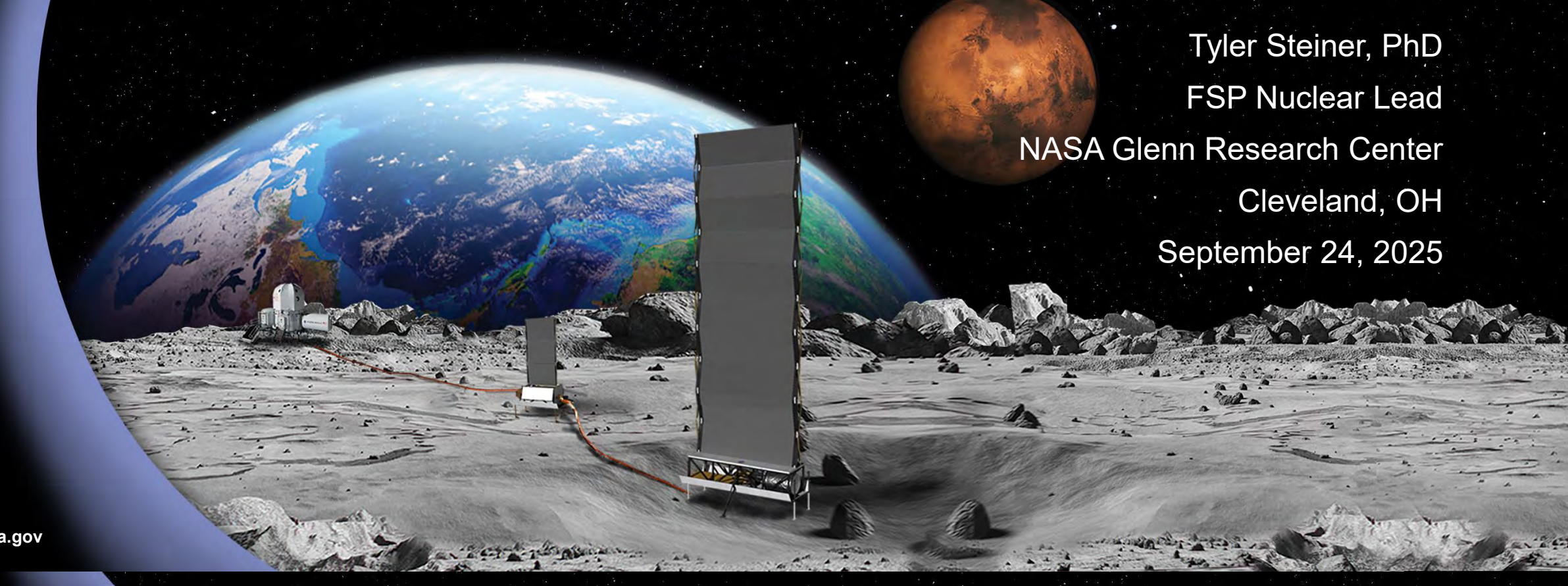


- Weight, dimensional changes & density
- OM/SEM surface microstructures
- FT-IR spectral changes
- Thermal properties
- Functional properties (coef. of friction, scratch)
- Outgas composition



## Radiator Working Fluids Irradiation

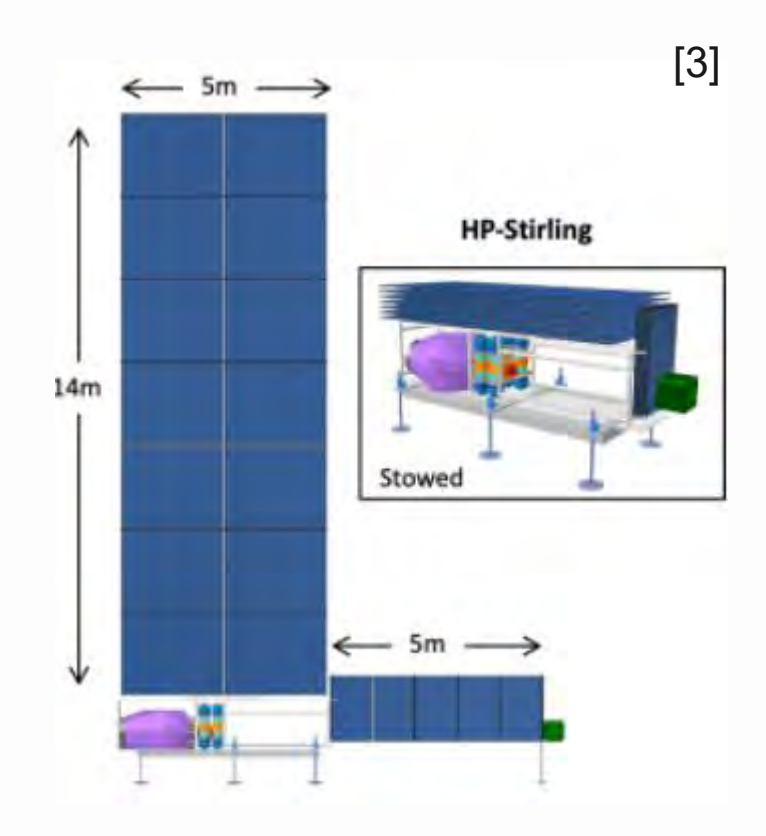
FSP Technology Maturation Webinar Series



#### Context



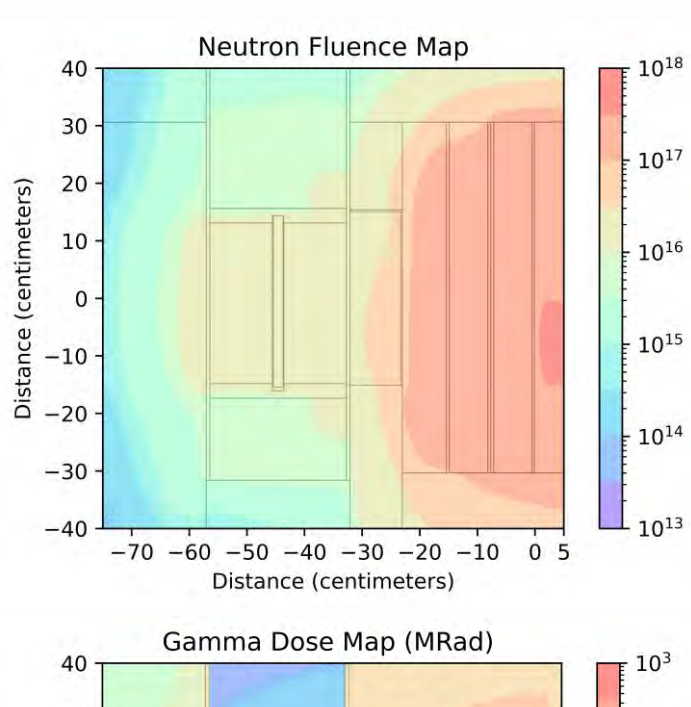
- FSP dose at radiators:
  - 10 Mrad [3]
  - 5x10<sup>14</sup> n/cm<sup>2</sup> [3]
- Radiator temperature:
  - 420 K inlet [3]
- GRD radiator:
  - Titanium H<sub>2</sub>O heat pipes
  - Polymer matrix composite panels
- H<sub>2</sub>O poses potential freeze risk
  - Freeze-tolerant fluids were irradiated
    - Radiolysis: Ionizing radiation → dissociation of molecules
    - Heat pipes used as radiator surrogate

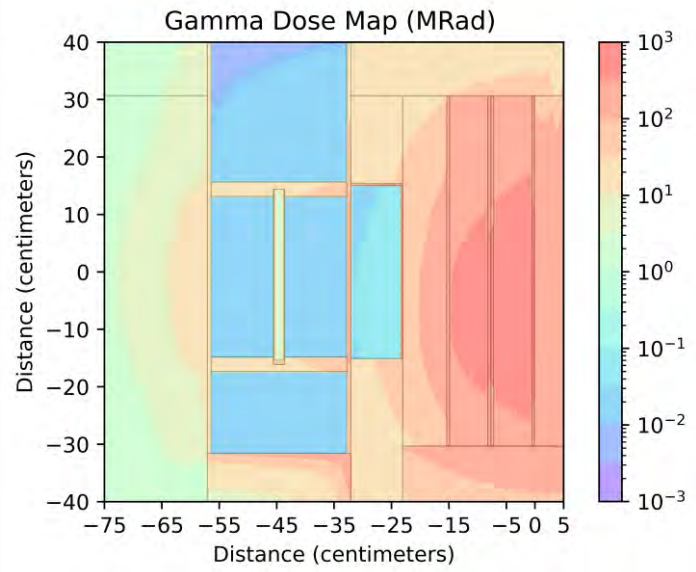


#### **Process**

EXERCISE SOLUTION SURFACE SURFACE SURFACE SURFACE SURFACE

- Model
  - Thermal
  - Mechanical
  - Radiation
- K-type TCs and coil heaters
- 1. Out-of-pile verification test
- 2. In-pile test
- 3. PIE?



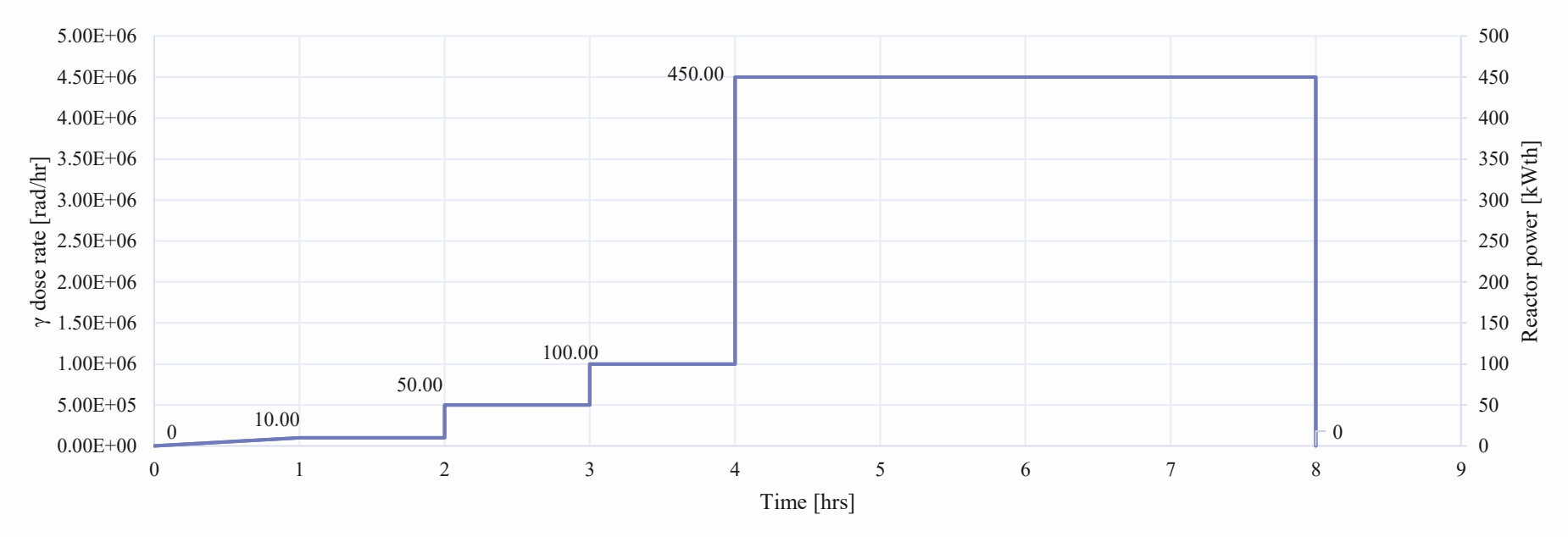


## **Test Matrix**





Fluid	Heat pipe	Qty	Temperature [K]	Expected neutron fluence [n/cm²]	Target gamma dose [krad]	TCs
Α	Ti	2	415	2E16	2.4E4	4x2
В	Ti	2	415	2E16	2.4E4	4x2
H <sub>2</sub> O	Ti	2	415	2E16	2.4E4	4x2
Α	Ti	1	415	0	0	4
В	Ti	1	415	0	0	4
H <sub>2</sub> O	Ti	1	415	0	0	4

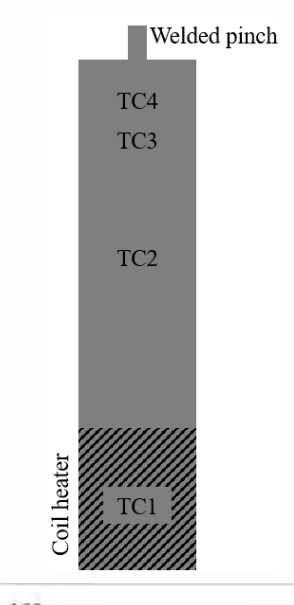


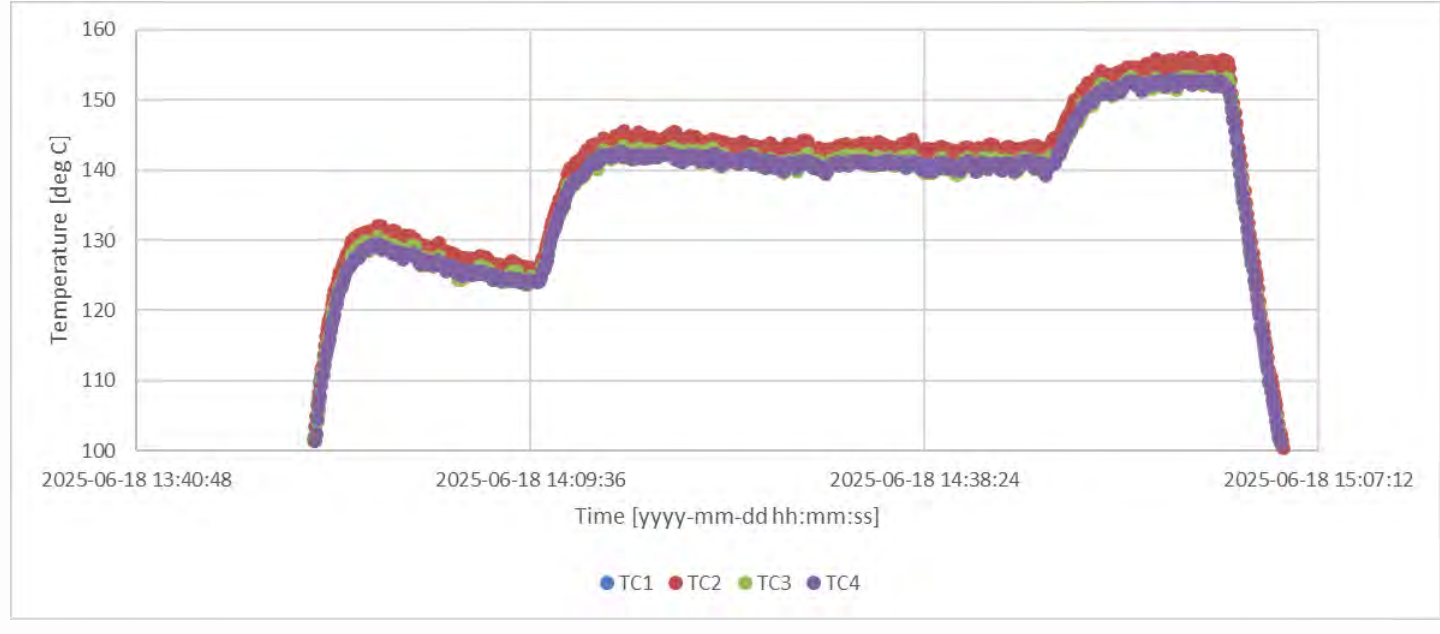
## **Test Execution: Pre-Irradiation Out-of-Pile**



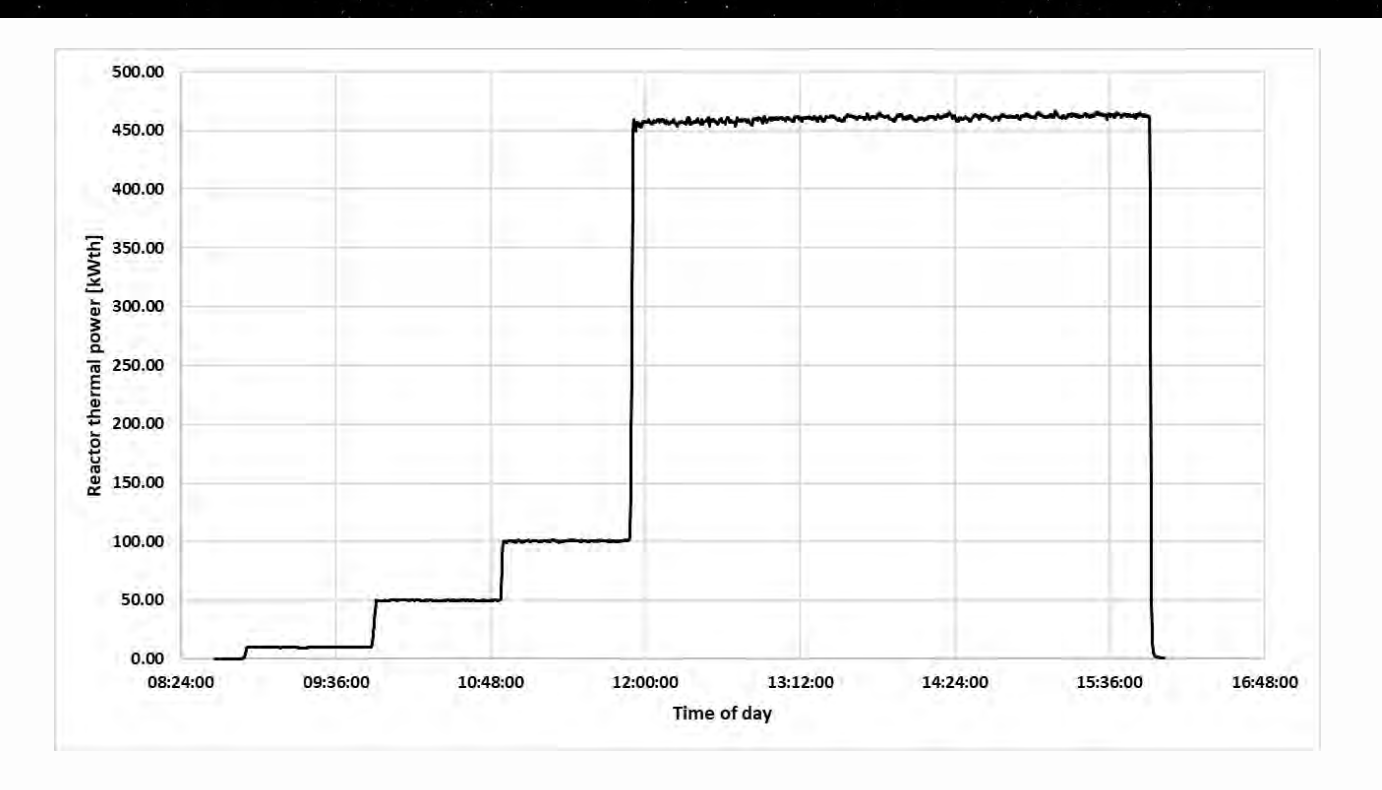


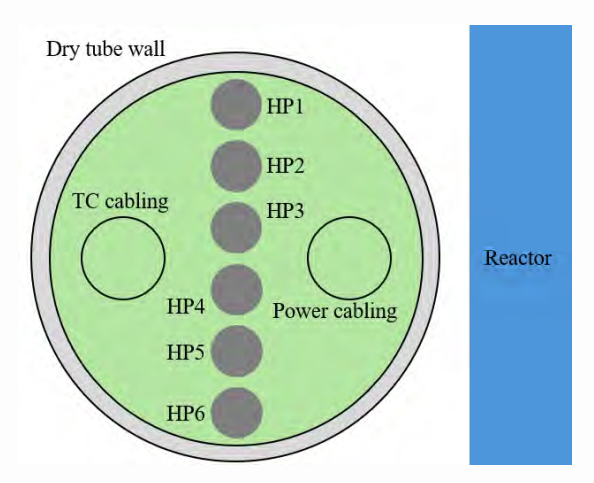






## **Test Execution: In-Pile**





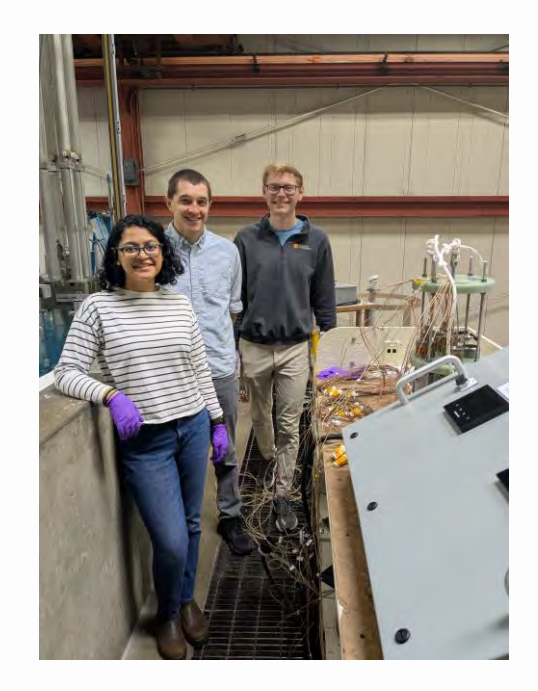




## **Summary**



- Conducted 2 irradiation experiments:
  - Organics in a Stirling convertor
    - Results pending thermal aging February 2026
  - Freeze-tolerant radiator working fluids
    - Results to be published in near future





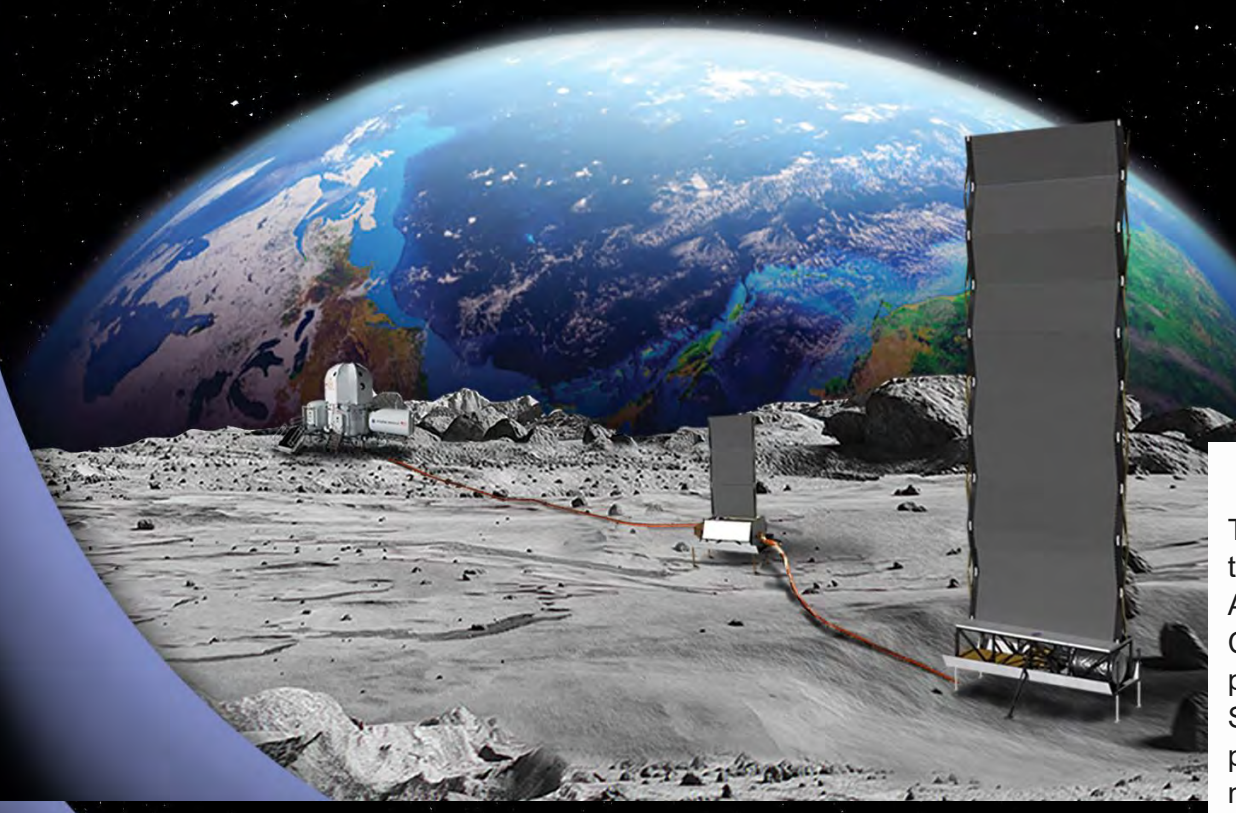
#### References

- 1. Golliher, Pepper; Organic materials ionizing radiation susceptibility for the outer planet/solar probe radioisotope power source. 2000.
- 2. Bowman, Shin, Mireles, Radal, Qualls; *Radiation specifications for fission power conversion component materials*. 2011.
- 3. Mason, Kaldon, Corbisiero, Rao; *Key design trades for a near-term lunar fission surface power system.* 2025.
- 4. Steiner, Goodell, Stang; Relevant environment demonstrations of Sunpower robust Stirling convertors for radioisotope powered missions. 2024.
- 5. Shin; Evaluation and validation of organic materials for advanced Stirling convertors (ASCs): overview. 2015.
- 6. Shin, Scheiman; Screening of high temperature organic materials for future Stirling convertors. 2017.
- 7. Hansen, Steiner, Wilson, Barron; Design methodology of a pressurized irradiation test apparatus for Stirling convertor organics in a fission surface power system. 2025.



www.nasa.gov

# Alloy Vaporization in Vacuum FSP Technology Maturation Webinar Series



Kaiser W. Aguirre
FSP Materials and Processes Lead
NASA Glenn Research Center
Cleveland, OH
September 24, 2025

#### **Notice for Copyrighted Information**

This manuscript is a work of the United States Government authored as part of the official duties of employee(s) of the National Aeronautics and Space Administration. No copyright is claimed in the United States under Title 17, U.S. Code. All other rights are reserved by the United States Government. Any publisher accepting this manuscript for publication acknowledges that the United States Government retains a non-exclusive, irrevocable, worldwide license to prepare derivative works, publish, or reproduce the published form of this manuscript, or allow others to do so, for United States government purposes.

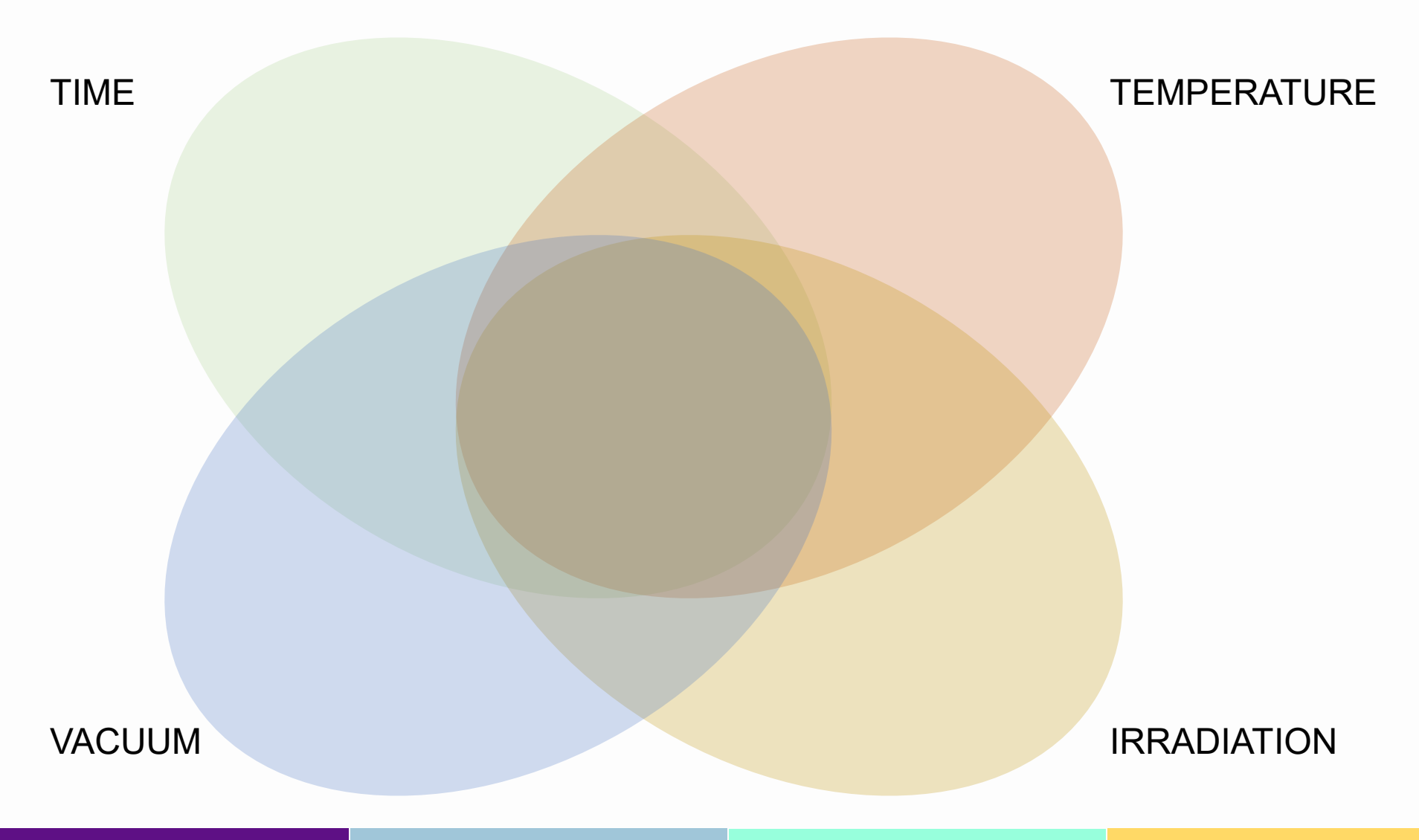
#### **Overview**



- 1. Introduction
  - 1. Context
  - 2. Vaporization
- 2. Applicability to FSP
  - 1. Element vs. Alloy
  - 2. CRES 316
  - 3. Hastelloy N / INOR-8
  - 4. Hastelloy B2
  - 5. Haynes 25
  - 6. Haynes 188
  - 7. Haynes 230
- 3. Possible Solutions
- 4. NASA GRC Efforts

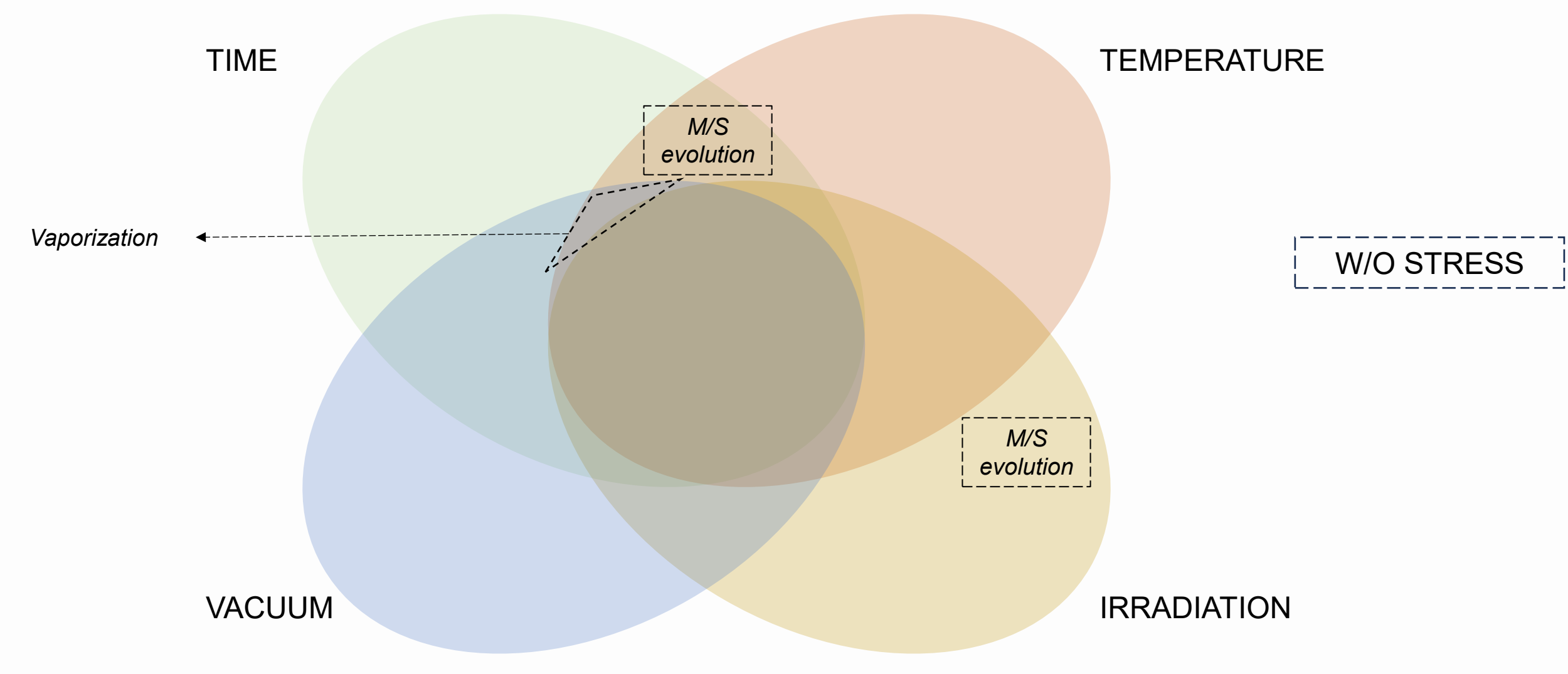




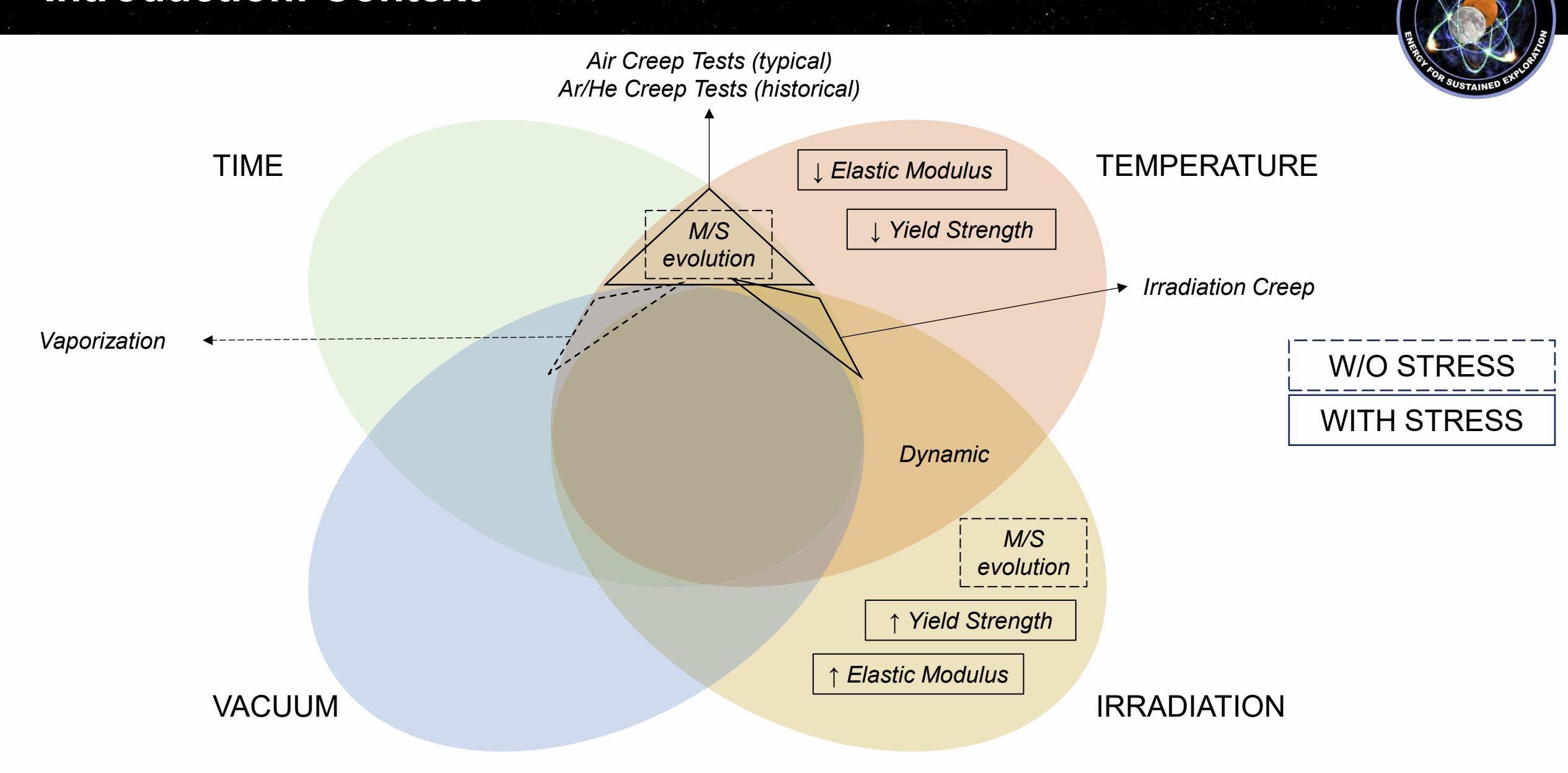


www.nasa.gov Introduction Applicability Solutions GRC



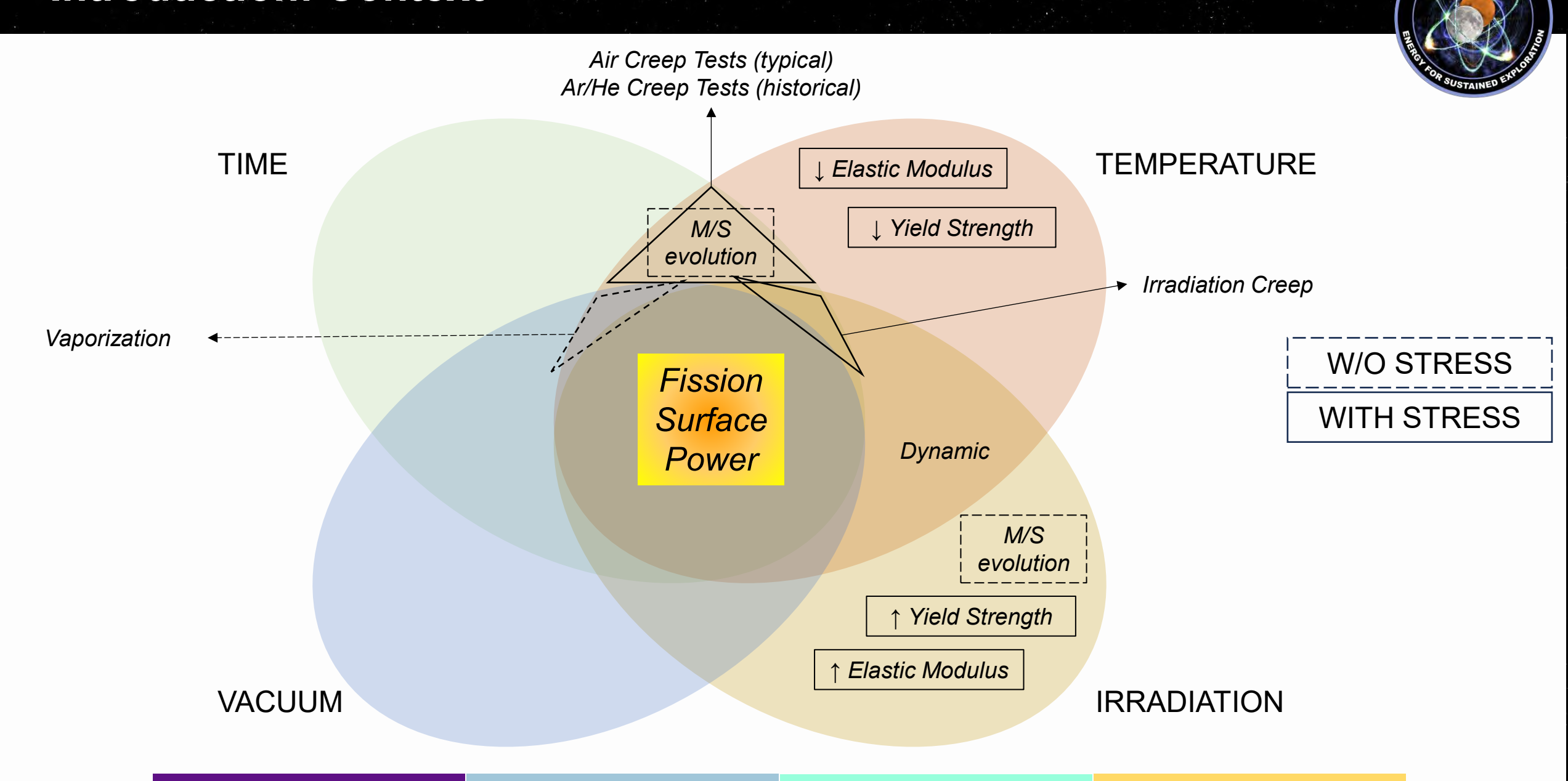


www.nasa.gov Introduction Applicability Solutions GRC

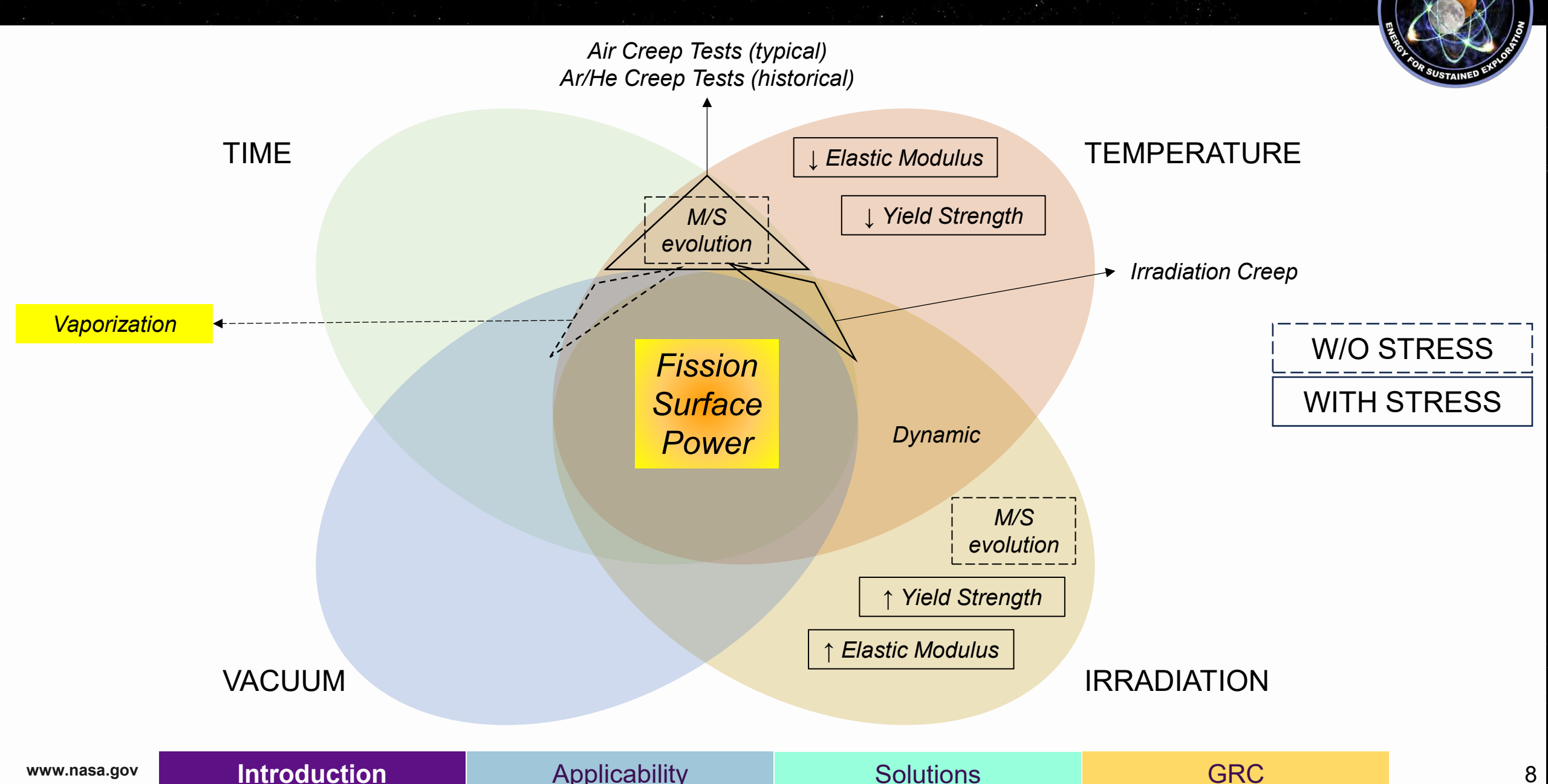




6







**Applicability** www.nasa.gov Introduction **Solutions GRC** 



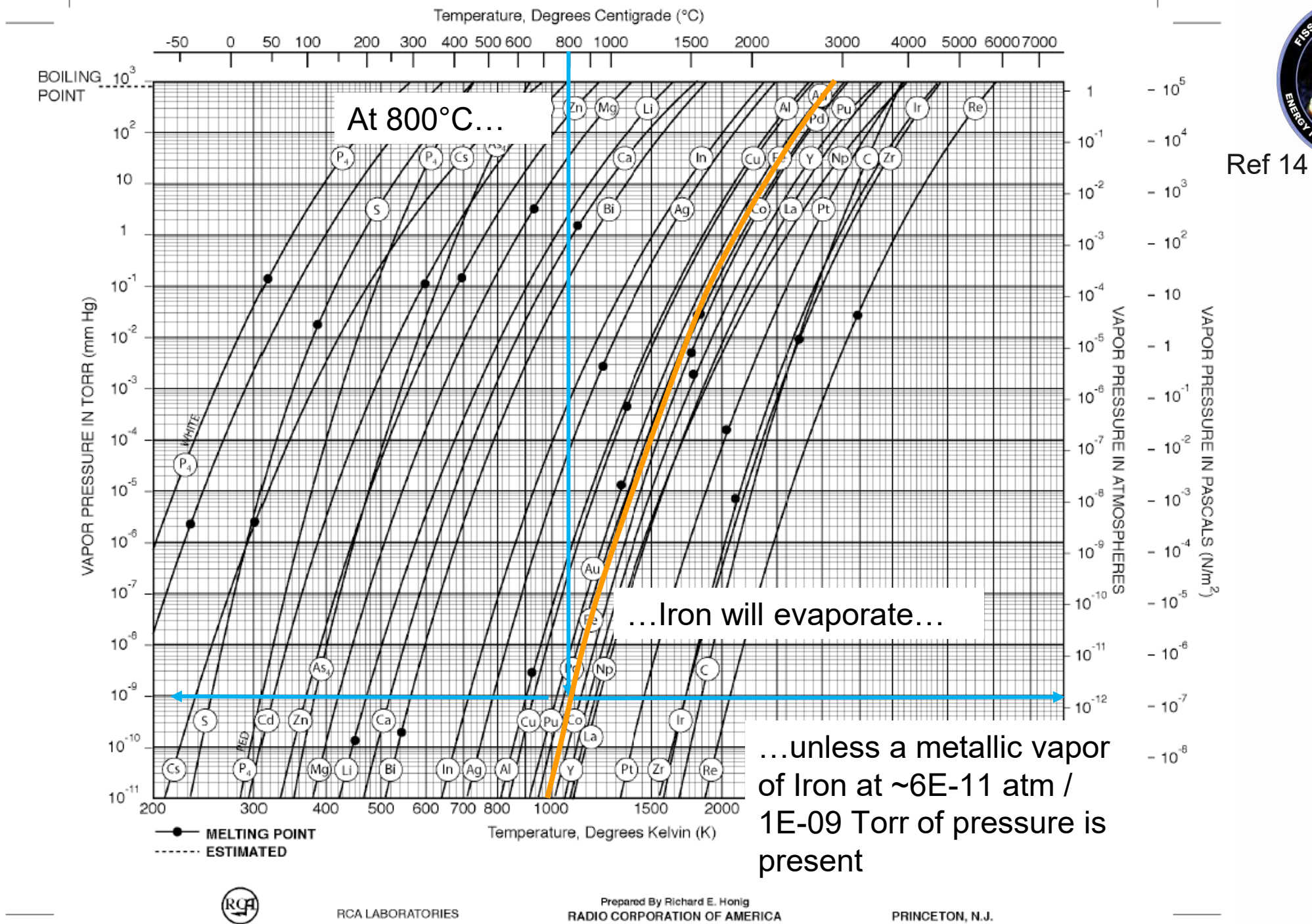
# **Introduction** *Vaporization*

## Introduction: Vaporization

- 1. Just like water can evaporate below it's boiling point, metals can evaporate below their boiling points.
- 2. Just like ice can sublimate from solid to gas, metals can sublimate from solid to gas.
- 3. Just like water evaporation is suppressed when there is a high pressure of water vapor in the air (= humidity), metallic evaporation/sublimation "vaporization" can be suppressed with a high enough pressure of metallic vapor.
- 4. The pressure required to suppress vaporization is the Vapor Pressure (VP).
  - 1. VP is a function of temperature.
  - 2. VP is unique to each element\*.
  - 3. High VP means vaporization is faster.

\*In compounds, local bonding matters.

10



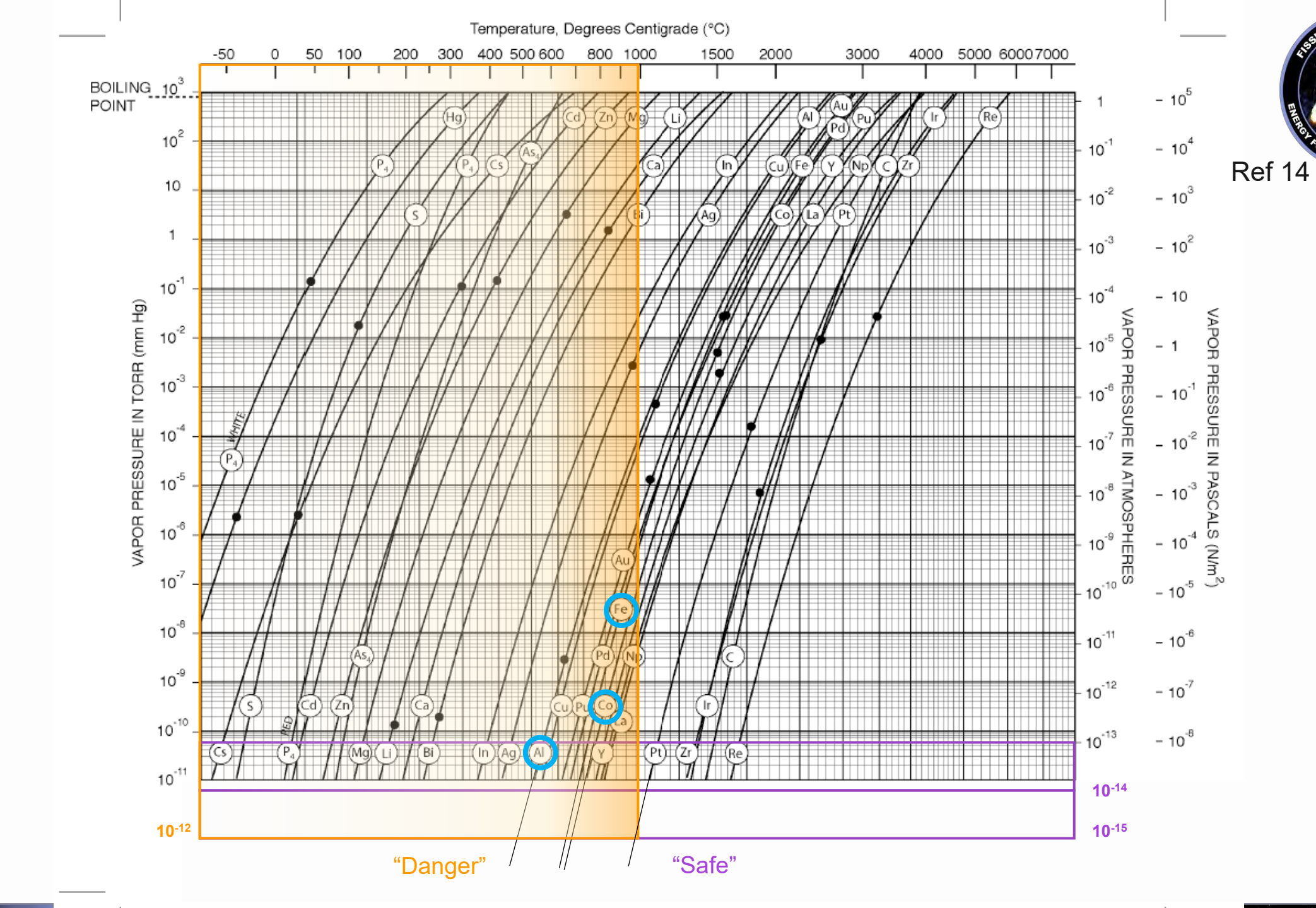
www.nasa.gov

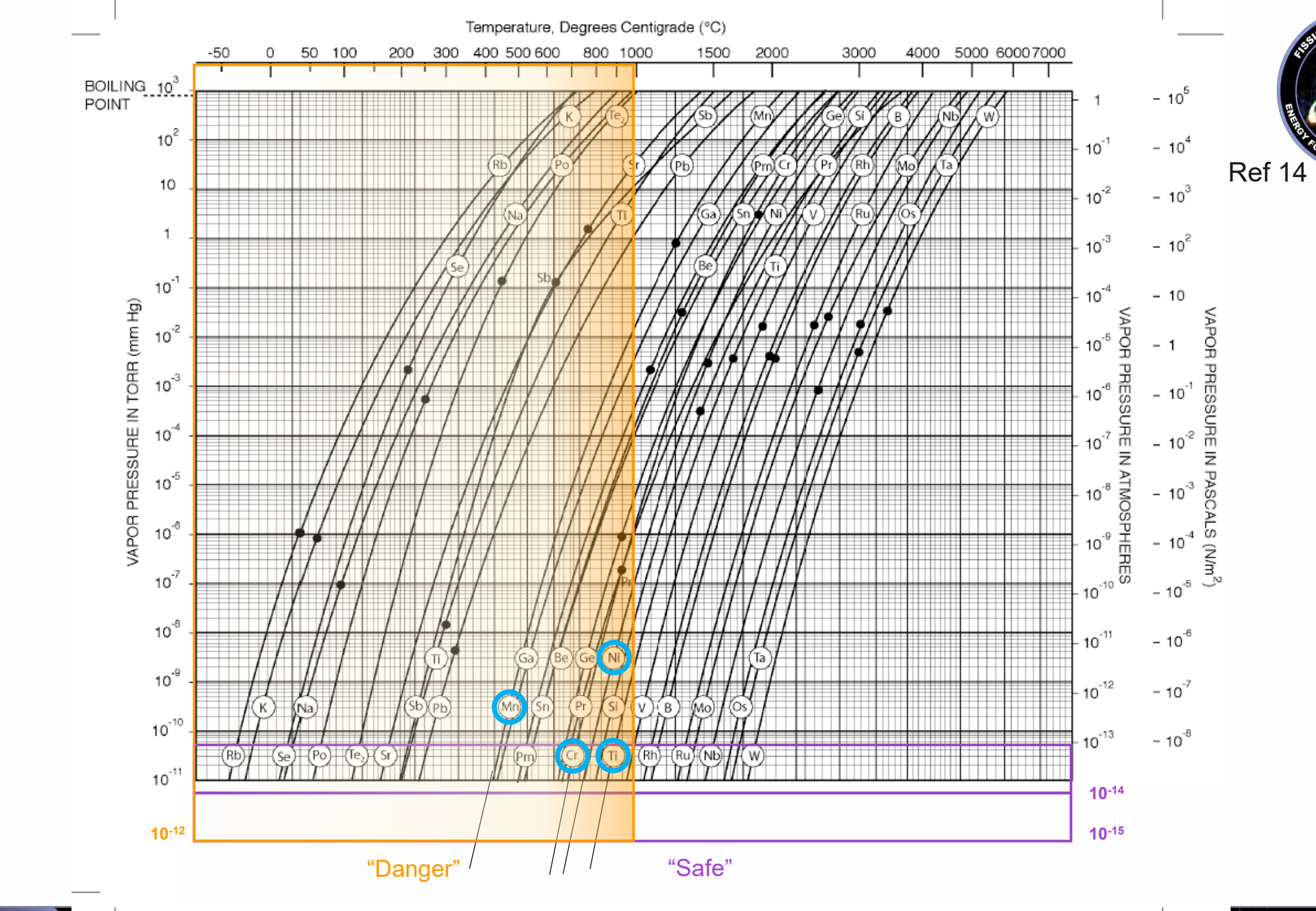
### Introduction: Vaporization



12

- The high-temperature region of interest for 40 kWe FSP is ~700°C to ~1000°C.
- 2. Pressure on the lunar surface is ~3E-15 atm and is mostly comprised of solar wind products.
- 3. At FSP-relevant temperatures and lunar pressure, the following elements will vaporize:
  - 1. Aluminum
  - 2. Iron
  - 3. Cobalt
  - 4. Manganese
  - 5. Nickel
  - 6. Chromium
  - 7. Titanium
  - 8. Others





## Introduction: Vaporization

Select Alloys From MMPDS / ASME BPVC	Approximate composition, atomic %						
WIMPUS / ASIME BPVC	Fe	Cr	Со	Ni	Mn	Al	Remainder
Inconel 625	4	24		63			9
Inconel 718	22	19	0.5	50		1	7.5
Inconel 740H	1.5	26	16	50	0.5	2	4
Haynes 230	1	10	2	82	0.5	0.5	4
Nitronic 50 / XM-19	55	23		11	5		6
CRES 316	67	16		9	2		6
CRES 310Cb	51	26		20	1		2

www.nasa.gov Introduction Applicability Solutions GRC

15



# Applicability Element vs. Alloy

## Applicability to FSP: Element vs. Alloy



17

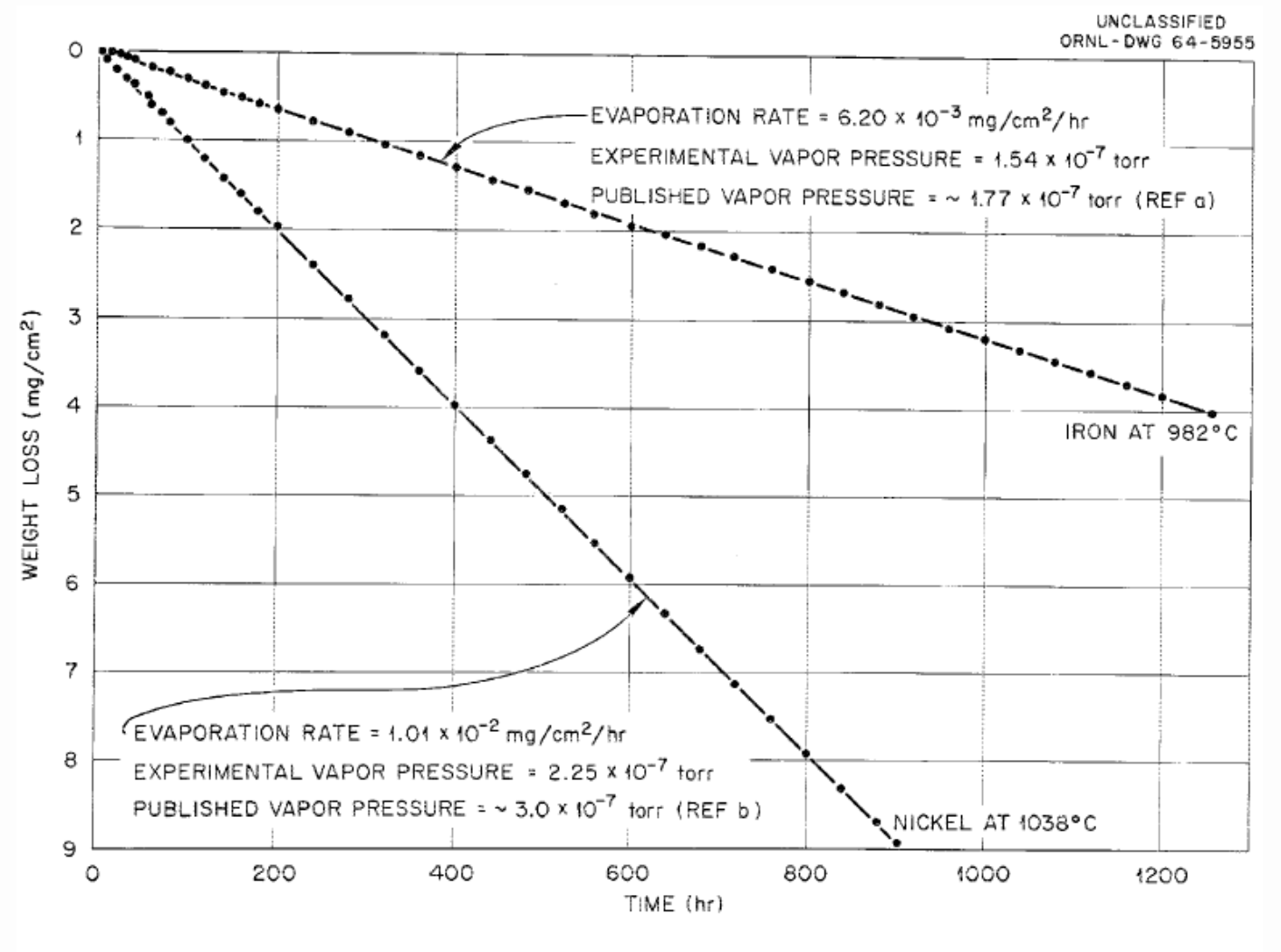


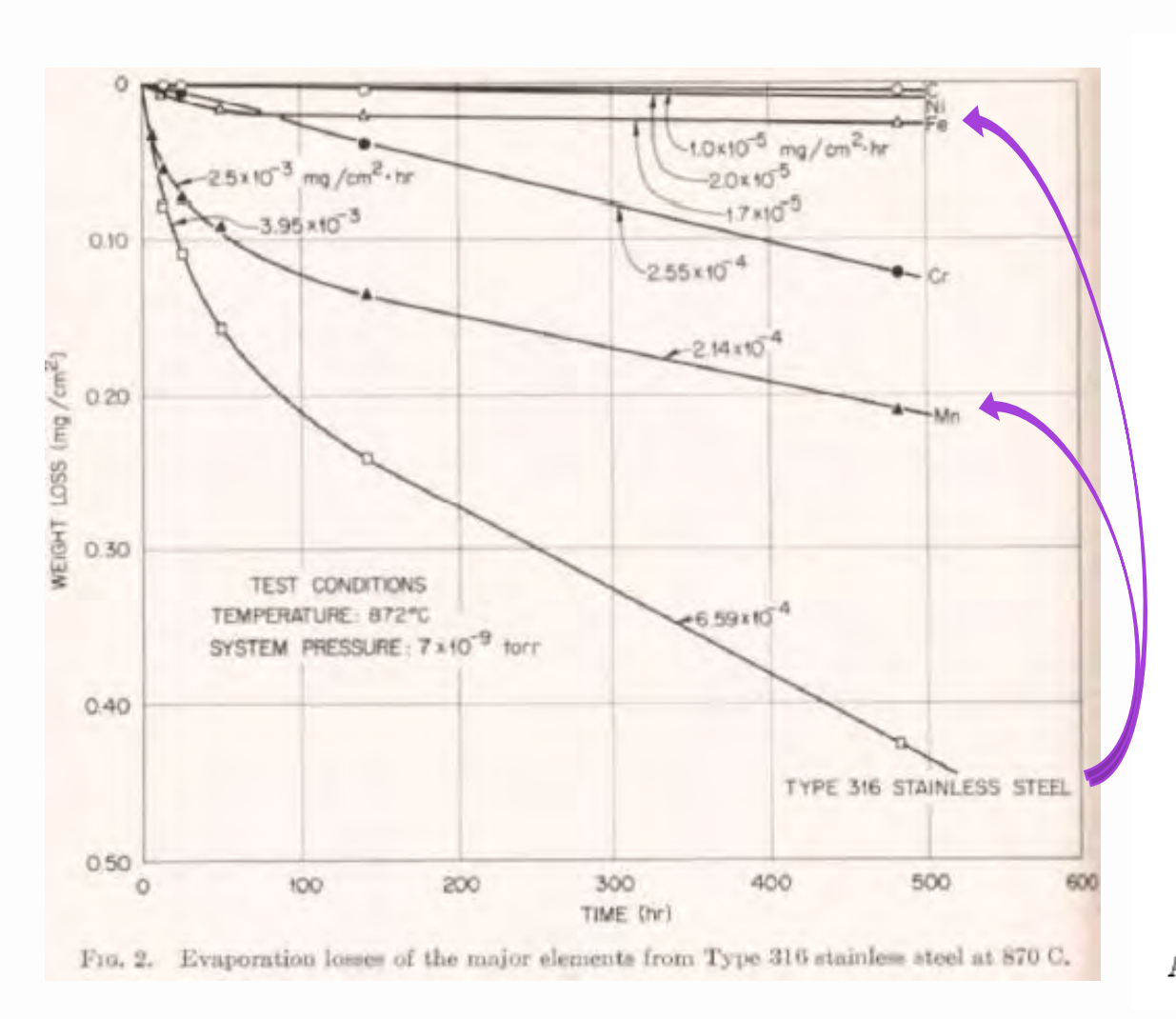
Fig. 3. Evaporation of Iron and Nickel at 982 and 1038°C, Respectively. Refs: (a) J. F. Elliott and M. Gleiser, Thermochemistry for Steelmaking, Vol. 1, p. 270, Addison-Wesley, Reading, Mass., 1960. (b) E. A. Gulbransen and K. F. Andrew, Trans. Met. Soc. AIME 221, 1247 (1961).

www.nasa.gov Introduction Applicability Solutions GRC



18

Ref 1,3



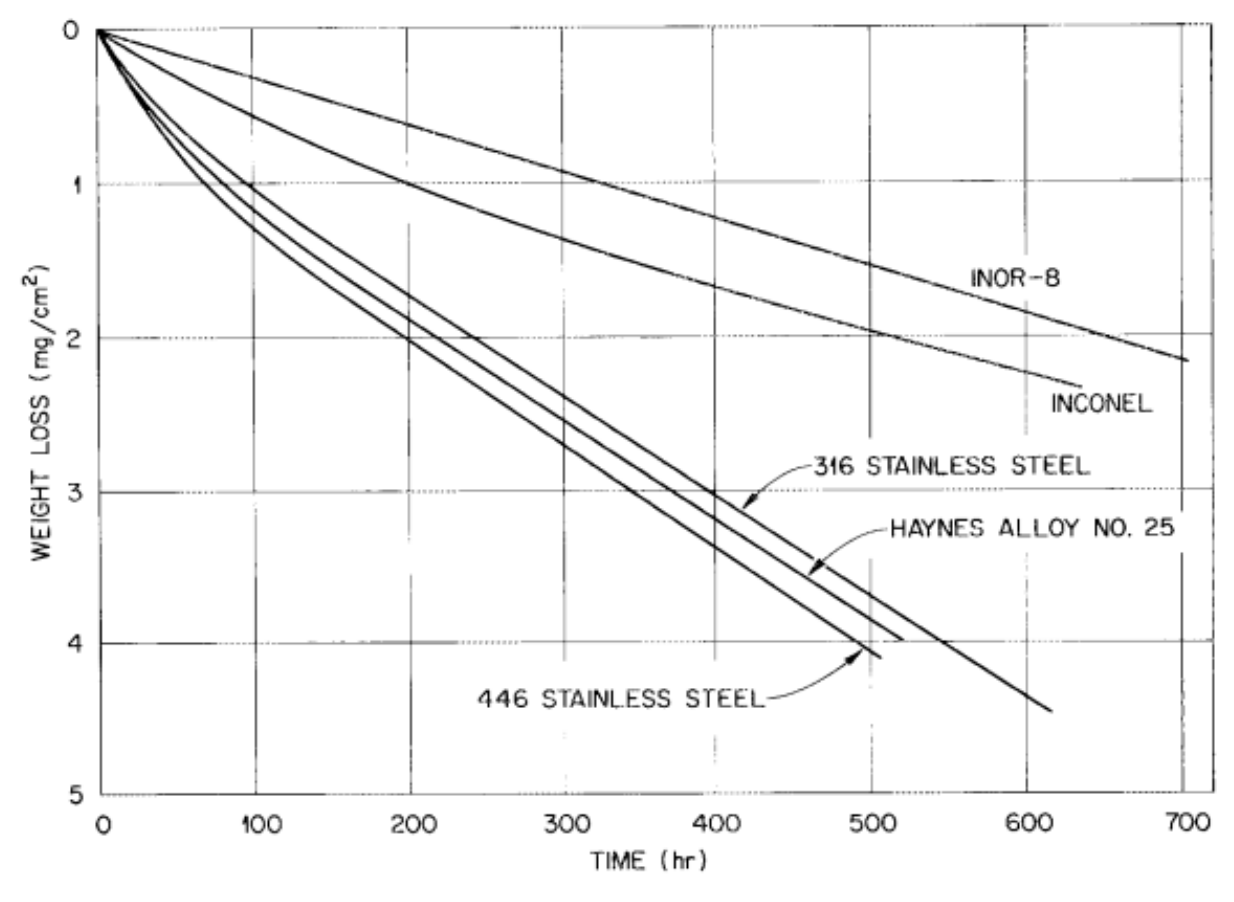


Fig. 6. Evaporation Losses of Iron-, Nickel-, and Cobalt-Base Alloys at 872 and 982°C and Approximately 5  $\times$  10  $^{-7}$  to 5  $\times$  10  $^{-9}$  torr.

#### **Applicability: Element vs. Alloy**



19

Ref 1

Table 5. Evaporation Rates and Length of Transient Periods of Type 316 Stainless Steel as a Function of Temperature

	Shor	t-Term Te	sts	Long-Term Tests									
Testing Temperature (°C)	Temper- Dura-		ation e ( <sup>2</sup> /hr) (0 <sup>-4</sup> Final <sup>b</sup>	Test Dura- tion (hr)	Evapora Rate (mg/cm <sup>2</sup> × 10 Initial	/hr) [	Average ength of ransient Period (hr)	Decrease from Initial to Final Evaporation Rate (%)					
982	616	114.0	66.4	956	120.0	65.9	30	45					
927	598	39.8	21.9	1832	42.3	20.5	50	52.6					
872	61.3	30	6.59	3453	26.8	3.9	80	85.4					
760				1321	6.56	0.528	200	93					

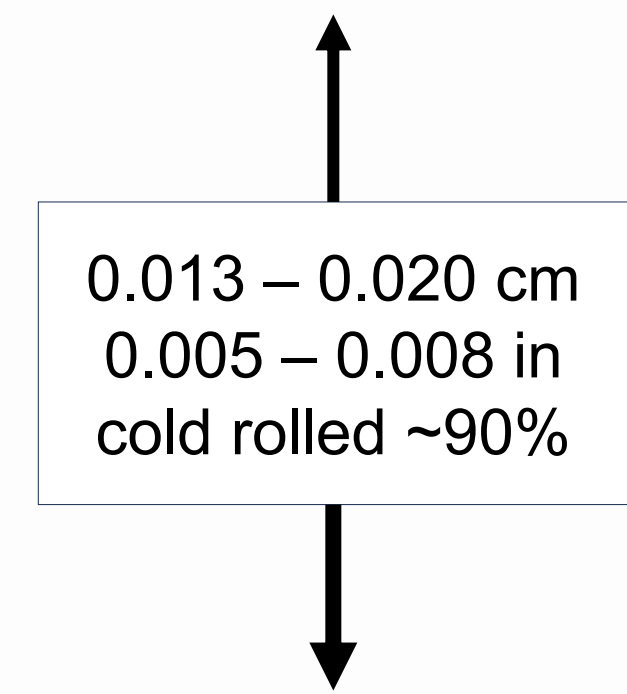
Maximum rate during initial 50 hr of test.

bRate during final 50 hr of test.





Ref 1



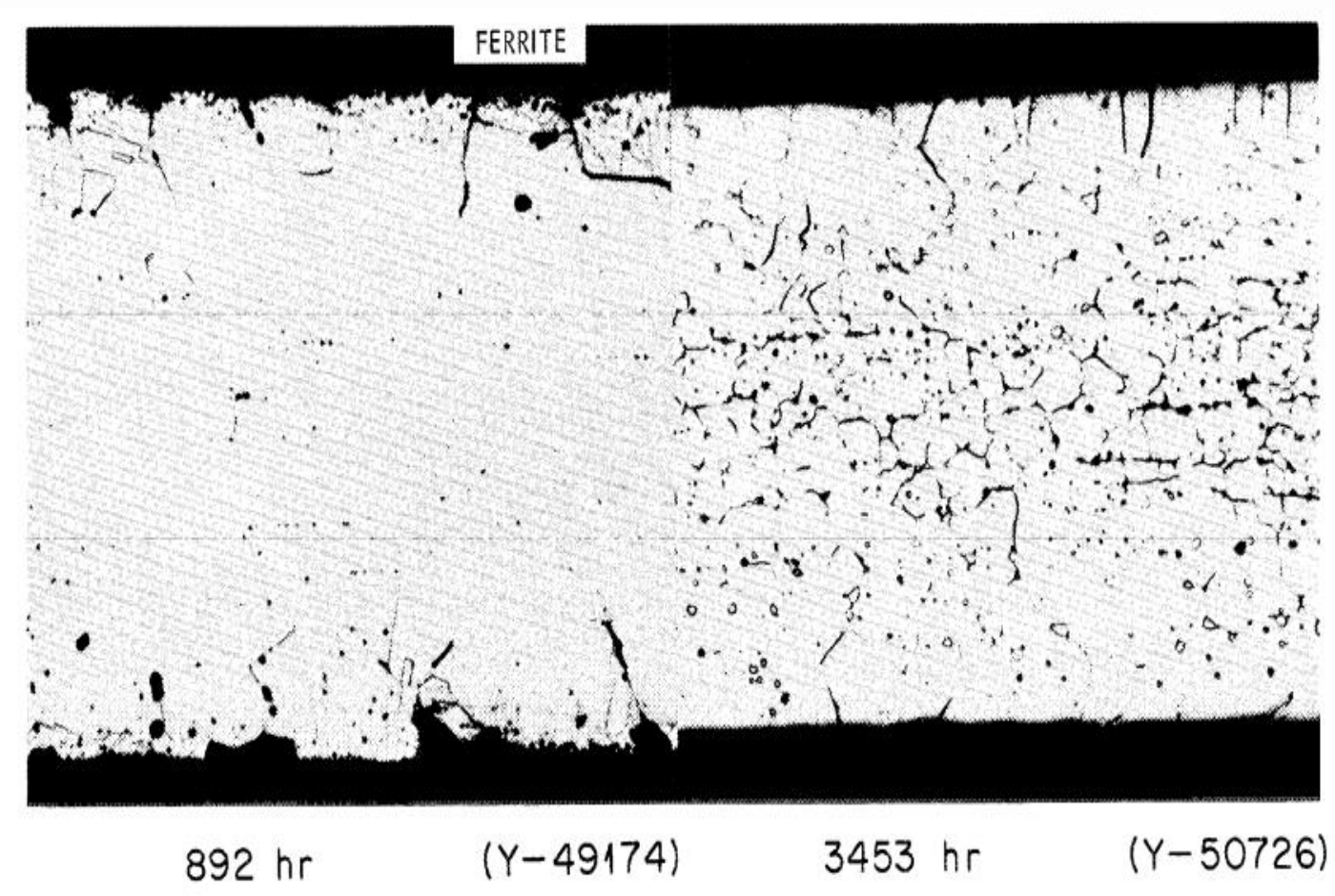


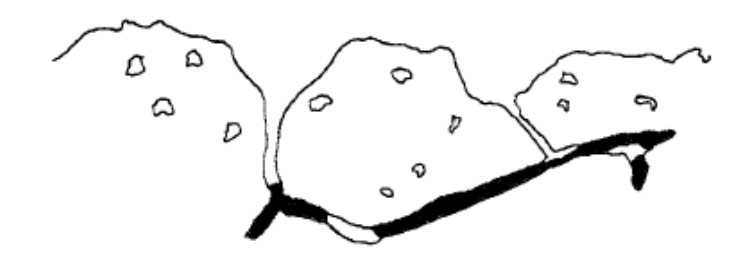
Fig. 12. Cross Section of Type 316 Stainless Steel Evaporation Tested at  $872^{\circ}\text{C}$  and  $8\times10^{-9}$  torr for 892 and 3453 hr, Respectively. Etchant: glyceria regia.  $500\times$ 



22

Ref 1

- (a) AS POLISHED SURFACE
- (b) BEGINNING OF GRAIN
  BOUNDARY EVAPORATION
  AND VOID FORMATION
- (c) BEGINNING OF SURFACE
  ROUGHING AND FORMATION OF
  GRAIN BOUNDARY GROOVES



(d) CONTINUED WIDENING OF GROOVES, VOID FORMATION, AND GRAIN BOUNDARY EVAPORATION



(e) AFTER LONG TIMES, PRODUCTION OF SMOOTH SURFACES AND NEARLY TOTAL GRAIN BOUNDARY EVAPORATION WITH VOID COALESCENCE ACCOMPANIED BY SPECIMEN THINNING

Fig. 11. Evaporation Sequence for Thin Specimens of Type 316 Stainless Steel Exposed to High Vacuum Between 800 and 1000°C.



23

Ref 4

Table 4. Chemical Analyses of Deposits Evaporated from Type 316 Stainless Steel at 872°C and 7 × 10<sup>-9</sup> torr

Element	Vapor Pressure of Element (torr)	Analyses <sup>a</sup> of Original Alloy (wt %)	-									
	( COFF)	(WC /O/		75,	14.2		100	700				
Mn	8 × 10 <sup>-4</sup>	1.67	77.72	71.24	70.2	68.1	59.85	50.88				
Cr	$2.5 \times 10^{-6}$	17.05	3.18	3.84	4.40	7.91	19.95	29.4				
Si	$7 \times 10^{-7}$	0.74	0.712	0.971	1.31	1.45	1.51	1.70				
Fe	$1.5 \times 10^{-8}$	64.03	1.29	1.33	2.39	4.86	9.03	12.27				
Ni	4 × 10 <sup>-9</sup>	13.28	1.01	1.4	1.62	1.71	1.83	1.95				
C	5 × 10 <sup>-19</sup>	0.05	7.53	4.32	3.93	2.11	1.70	1.41				
Мо	3 × 10 <sup>-14</sup>	2.25	ъ	b	ъ	ъ	ъ	b				

<sup>&</sup>lt;sup>a</sup>See Table 1 for original composition.

<sup>&</sup>lt;sup>b</sup>Not detected.

Ref 3

24

Microstructural evolution during vacuum exposure at 760 – 980°C for 1 – 3000 hrs of .005 to .063" sheet

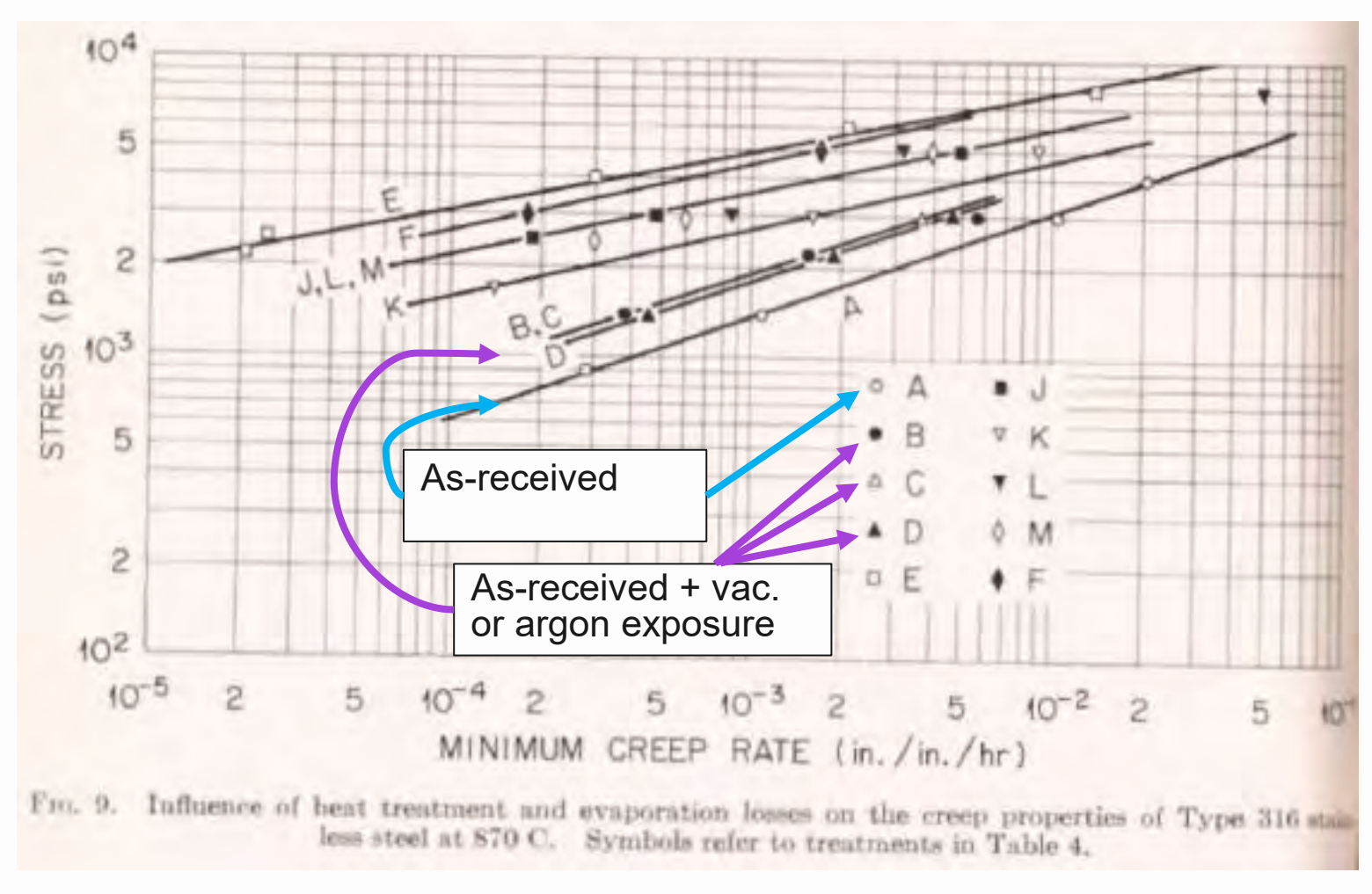
- Subsurface voids, grain growth, grain-boundary "grooving" at surface, disappearance of precipitates along grain boundaries
- For exposure of 870°C for 892 hrs and 980°C for 650 hrs, ferrite forms on surface
  - Attributed to loss of austenite-stabilizing Mn
    - There is also loss of C
  - Ferrite not present after longer-duration 870°C (1456 hr) and 980°C exposures
    - Attributed to ferrite → austenite transition from high Cr loss and low Ni loss
    - May be due to vaporization of ferrite
  - When ferrite formed on surface, evaporation rate approached pure Fe
- Tests >2000 hrs exhibit nearly continuous voids at grain boundaries
- Above 870°C, surface oxides deteriorate at intersection with grain boundaries
  - Presumed to be C reacting with O to form CO

THE RESIDENCE OF THE PROPERTY OF THE PROPERTY OF SUSTAINED EMPLOYED

25

Ref 3

Specimens exposed to various conditions then creep tested in Ar gettered with Zr at 870°C



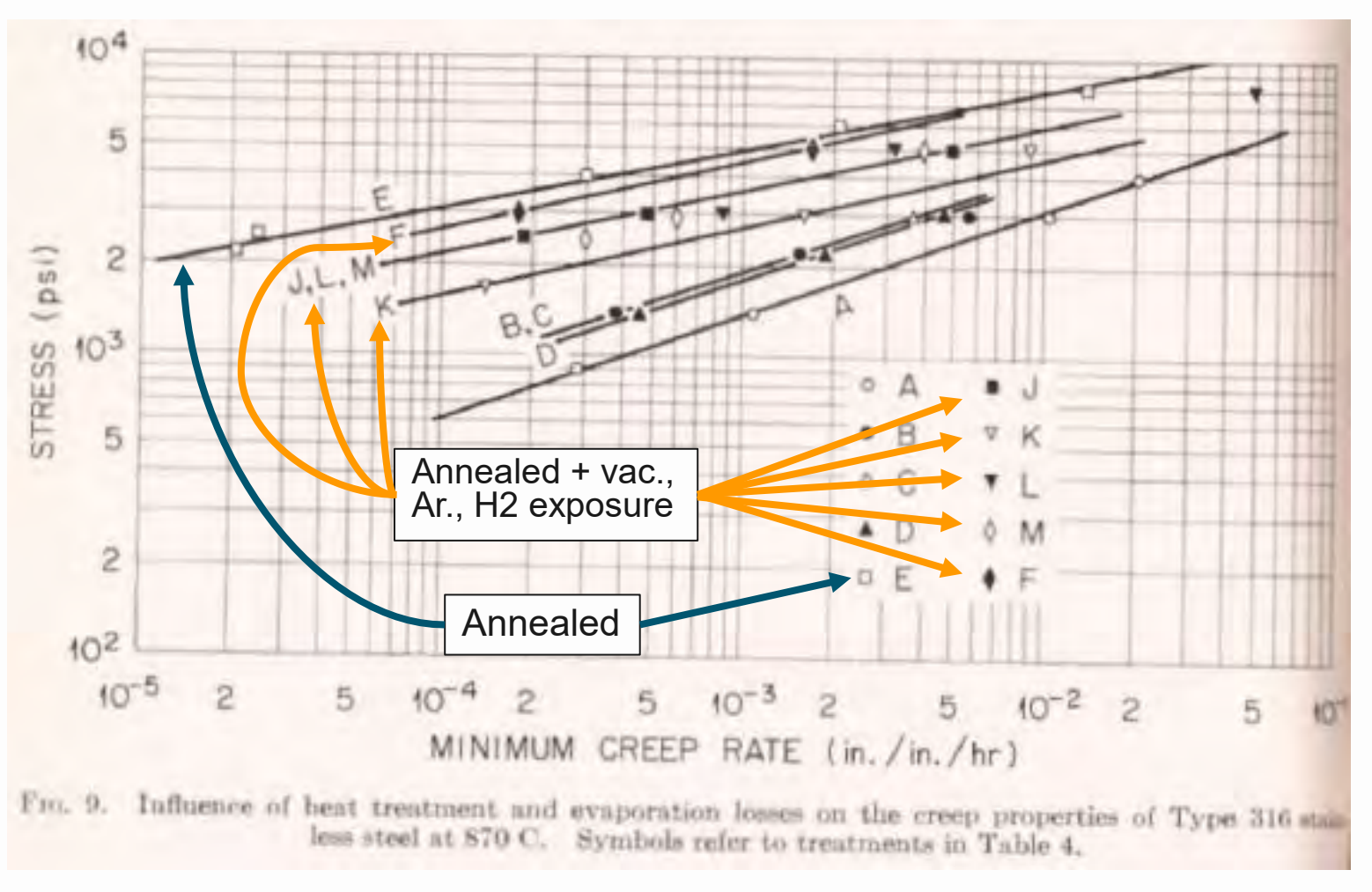
ER SUSTAINED ER CORE

26

Ref 3

Specimens exposed to various conditions then creep tested in Ar gettered with Zr at 870°C.

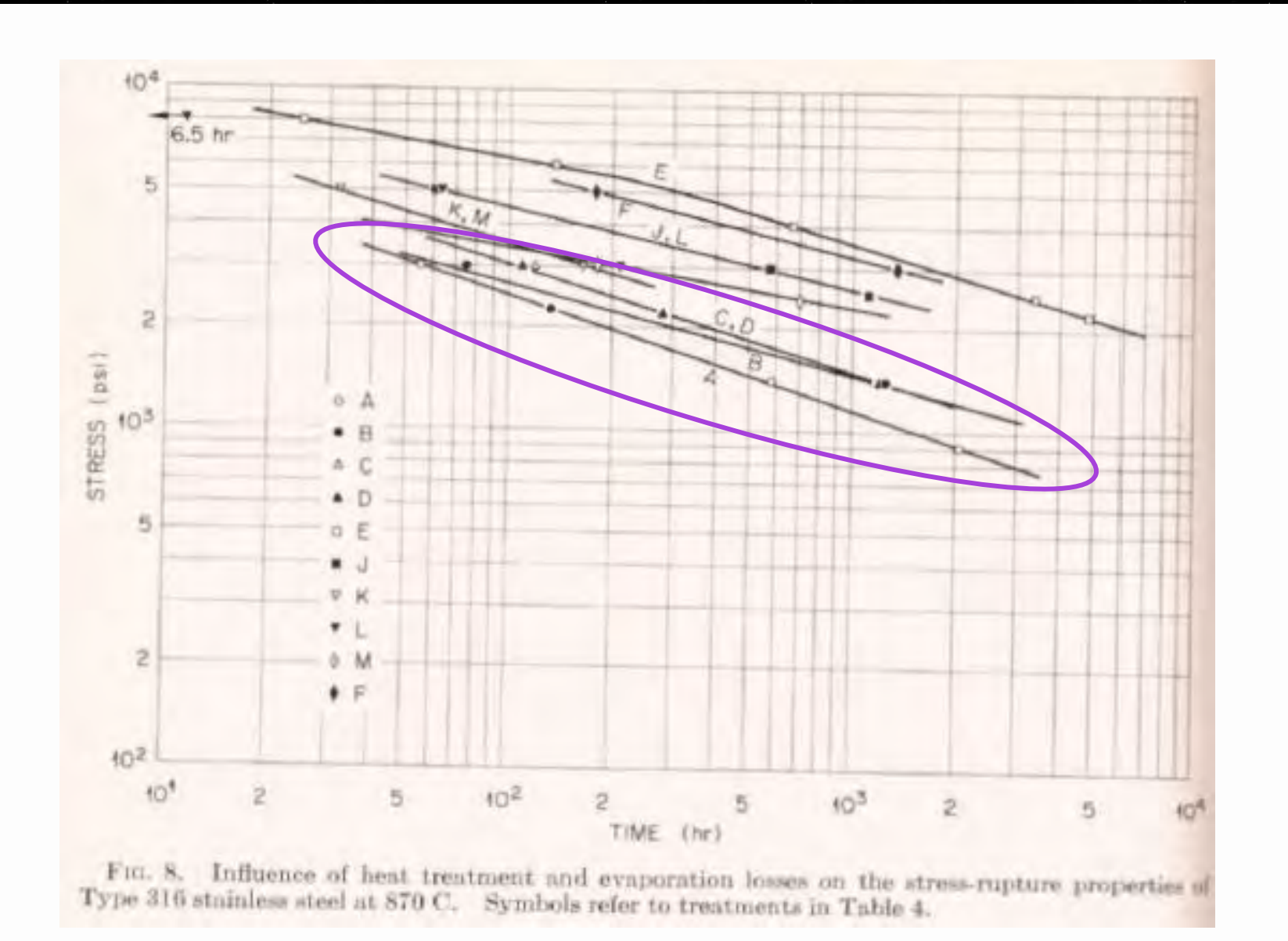
Annealing increased grain size by x6 – 7.





27

Ref 3



A = As-received

B = Vac. 870°C 576 hr

C = Ar. 870°C 550 hr

D = Vac. 870°C 1321 hr

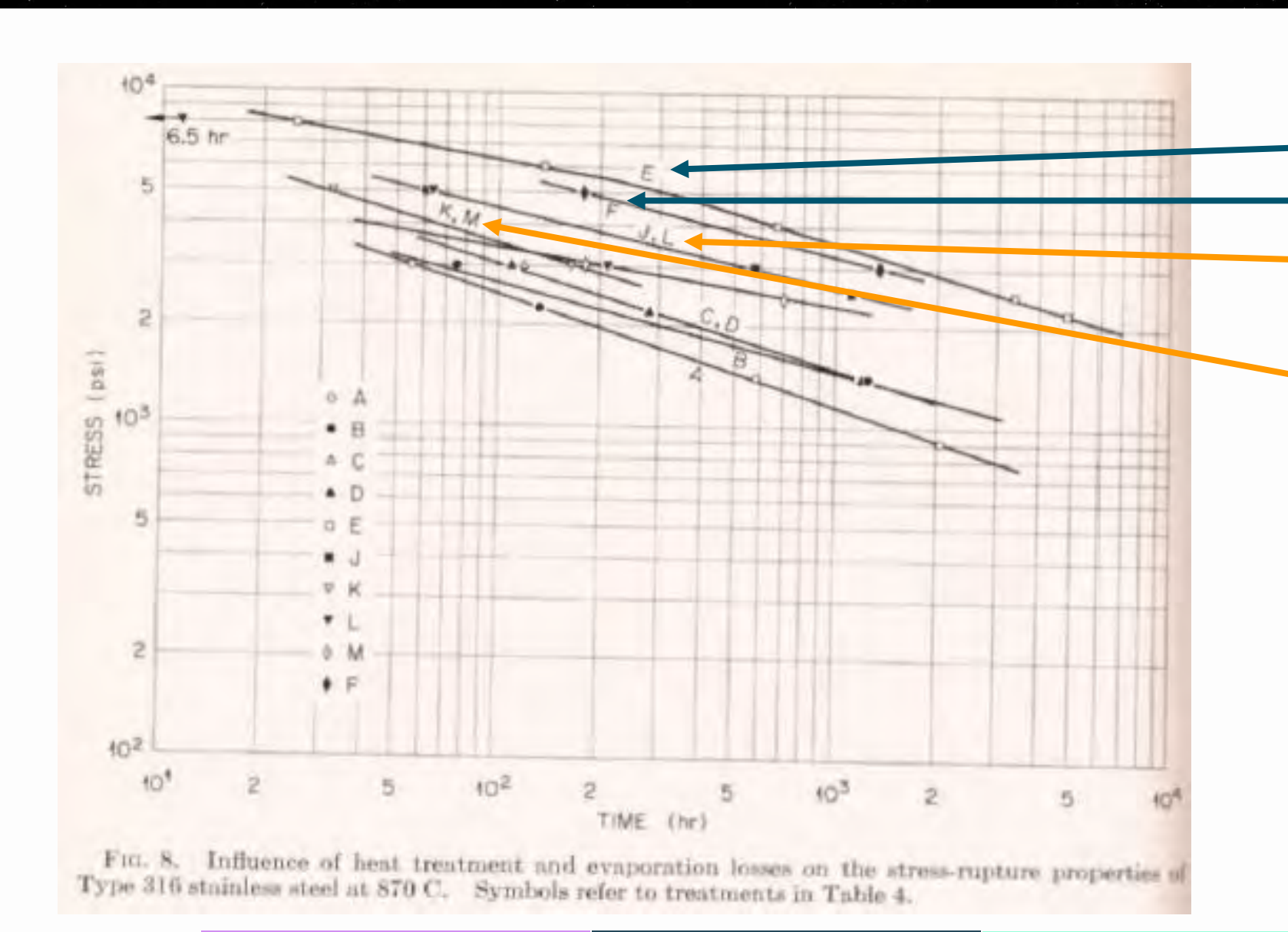
Exposure to long-term vacuum and short-term Argon have similar effects (C, D)...

Data is very sparse, hard to distinguish



28

Ref 3



E = Anneal

F = Anneal + Ar. 550 hr

J = Anneal + vac. 2129 hr

K = Anneal + vac. 3521 hr

M = Anneal + vac. 5028 hr

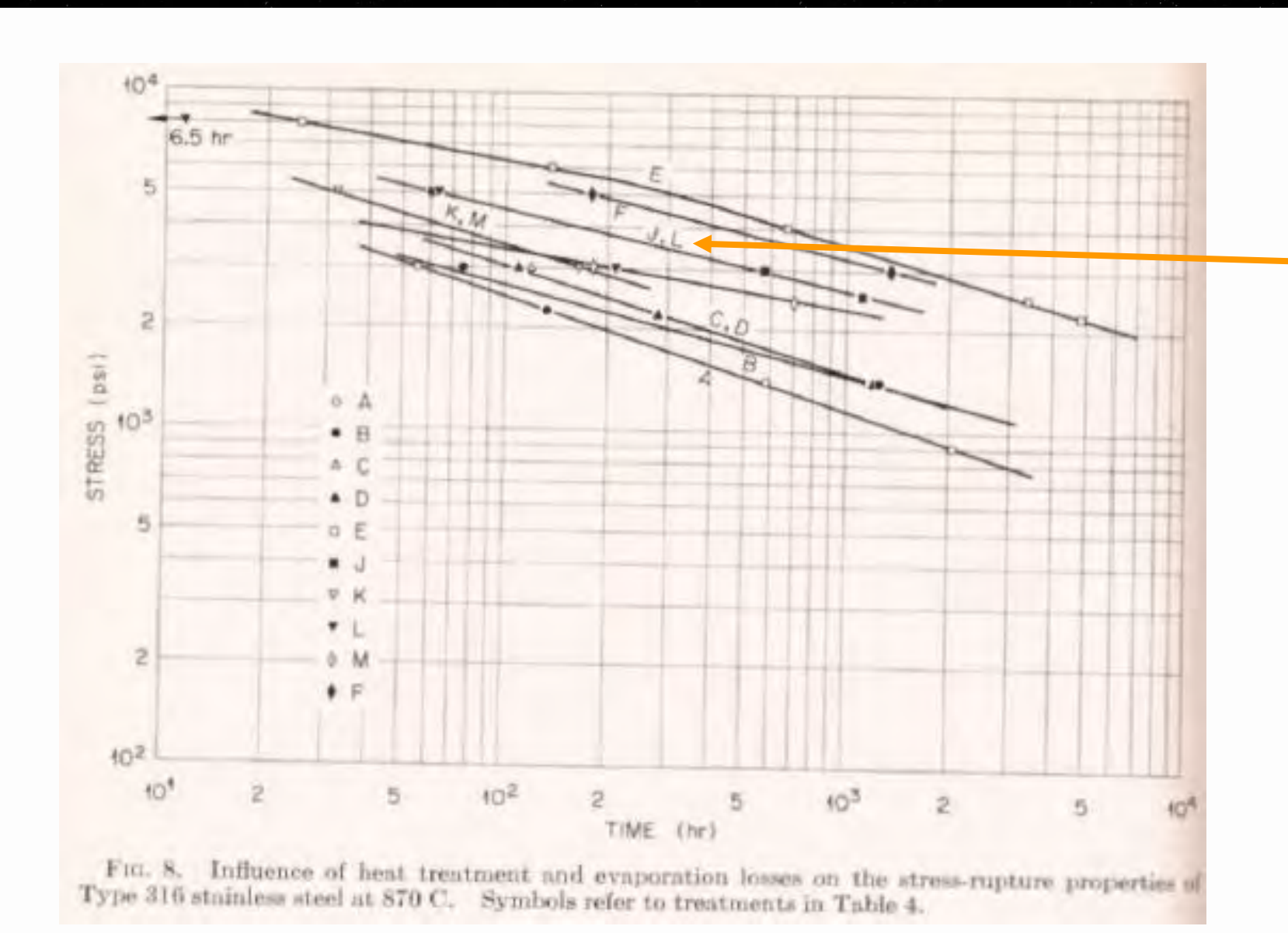
Exposure to vacuum seems to have effect...

Data is sparse, hard to distinguish



29

Ref 3



J = Anneal + vac. 2129 hr

L = Anneal + wet H2 170 hr + vac. 2584 hr

Specimen L was exposed to wet hydrogen to build up oxide, then to vacuum.

J lost 2x the mass that L did, but creep behavior is the same.

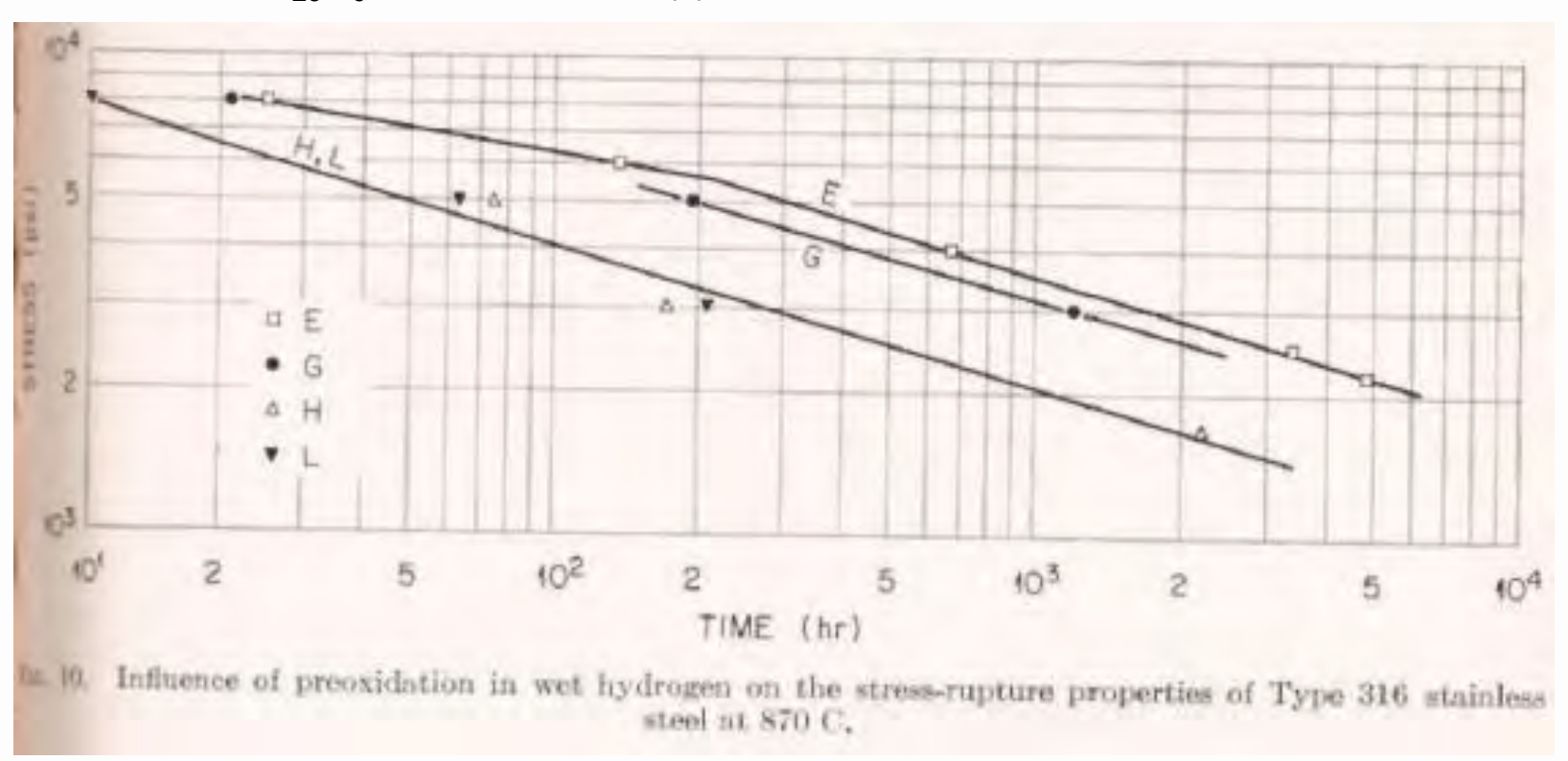


30

Ref 3

#### Observations from creep testing at 870°C

- Data is sparse
- Per authors, vacuum exposure affects creep through microstructure evolution, not mass loss
  - Fine M<sub>23</sub>C<sub>6</sub> and coarse Chi (χ) phases observed



E = Anneal

G = Anneal + wet H<sub>2</sub> 170 hr

H = Anneal + wet H<sub>2</sub> 170 hr + vac. 816 hr

L = Anneal + wet  $H_2$  170 hr + vac. 2584 hr

### Applicability: Microstructural Effects – CRES 316 (ferrite stuff)

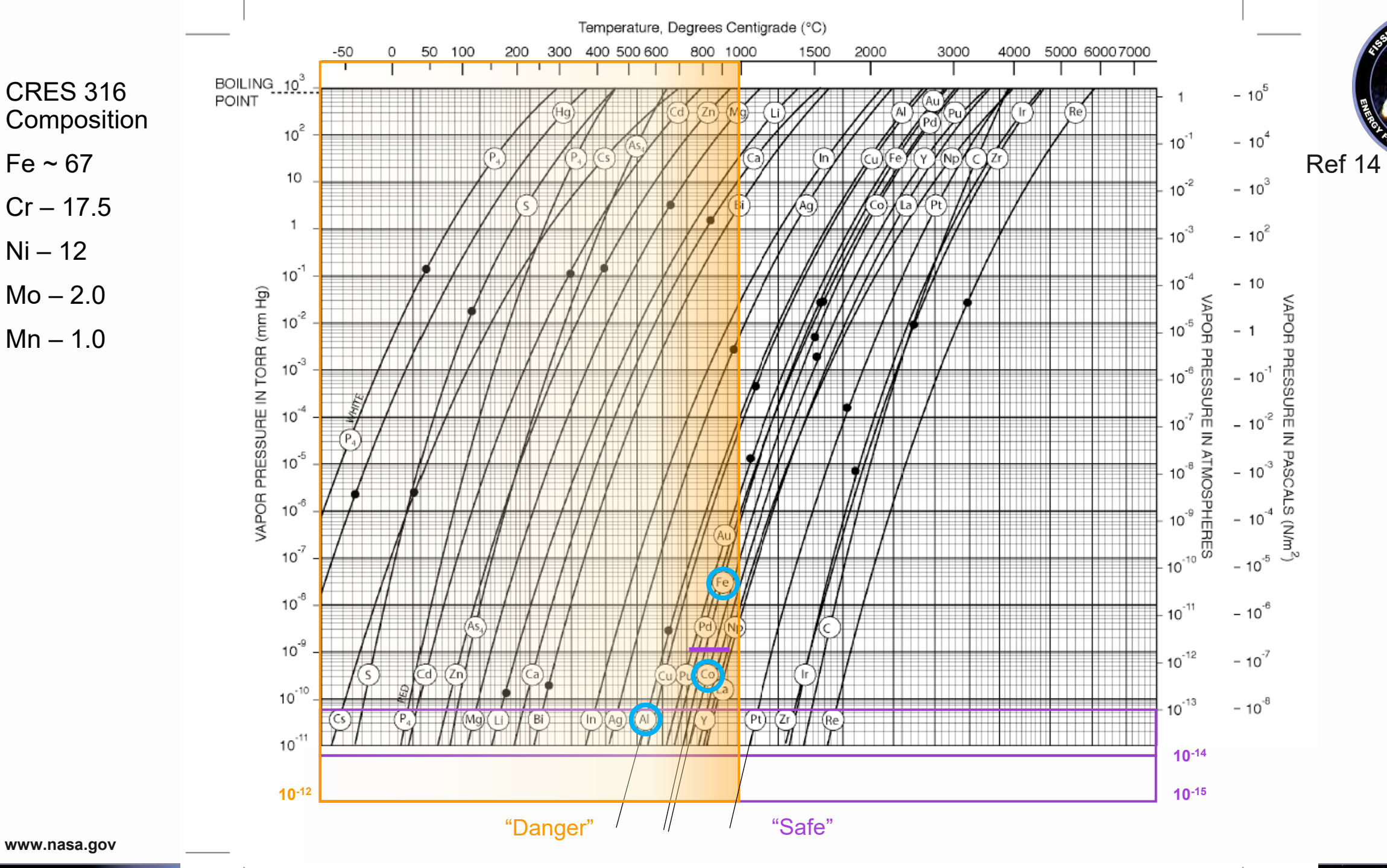


31

Ref 3

Observations from creep testing at 870°C continued

"When the material is very thin or exposed for times sufficient to alter a signification part of the stressed section, the properties will be altered. There is also a possibility that the mechanical behavior under conditions of simultaneous stressing and evaporation would be different from that observed under the present conditions. This is because material is preferentially lost from the grain boundaries and this instability might result in easier grain boundary motion with reduction in creep strength."



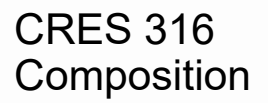
Fe ~ 67

Ni - 12

Mo-2.0

Mn – 1.0

Cr - 17.5



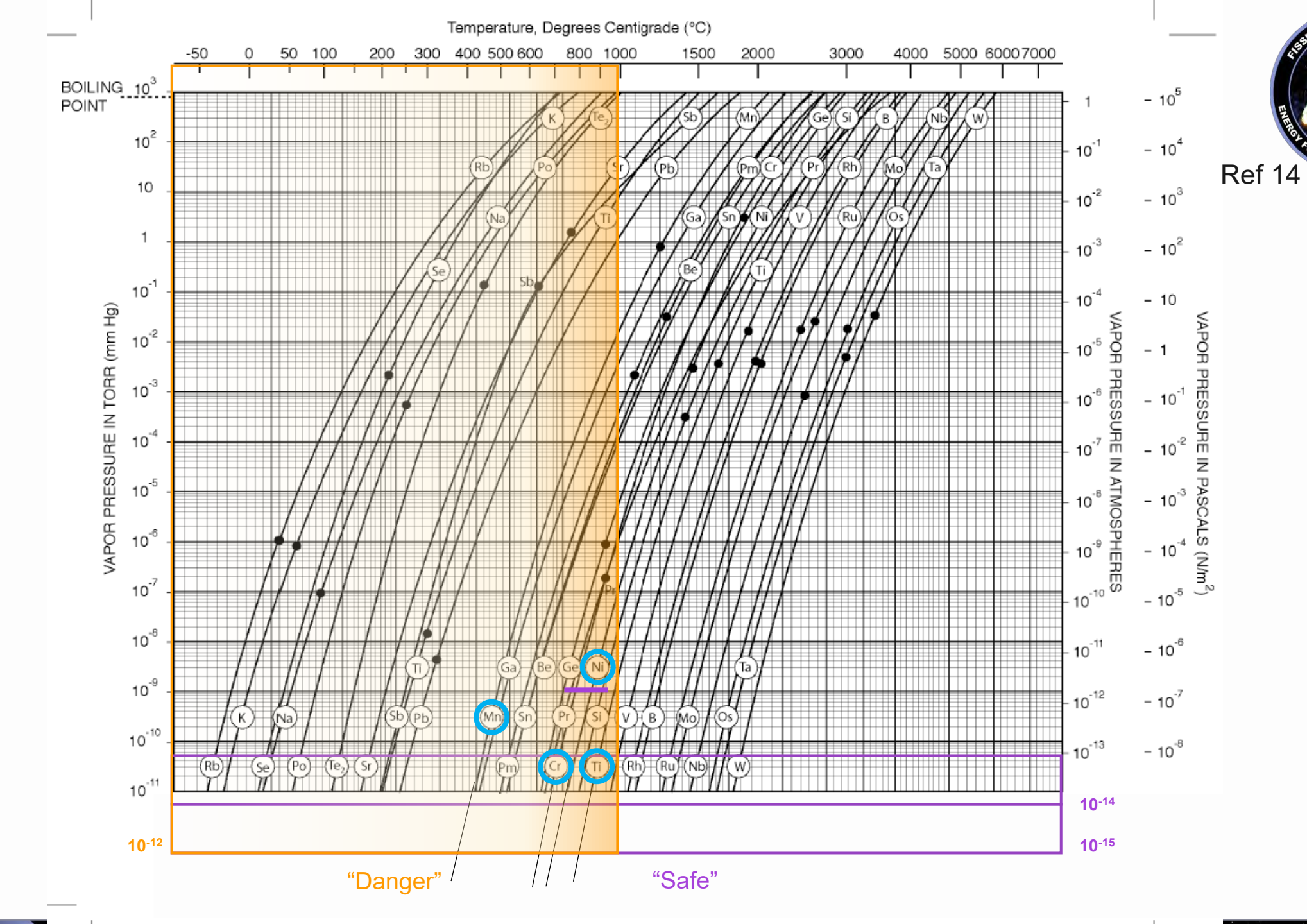
Fe ~ 67

Cr - 17.5

Ni – 12

Mo-2.0

Mn – 1.0





### Applicability Hastelloy N / INOR-8

#### **Applicability: Hastelloy N**



35

Ref 8

- Evaporation rates of Hastelloy N were measured at 800 to 1050°C and 10-9 Torr
- Evaporation rates decreased with time at constant temperature
- Up to 1500 hr, the thicker the specimen, the less decrease in evaporation rate
- Voids formed primarily at grain boundaries
- SEM observations of evaporated surfaces indicate a complete change in surface morphology
- Weight losses in excess of 4 mg/cm<sup>2</sup> resulted in precipitation of intermetallic phases at the surface



# Applicability Hastelloy B2

#### **Applicability: Hastelloy B2**



37

Ref 11

					5k hrs Vacuum Exp. 10k hrs Vacuum Exp. 5k l					5k hrs	S Vacuur	n Exp.	10k hrs Vacuum Exp.			
Alloy	Temp.	Air YS	Air UTS	Air %El		Vac UTS	Vac %El	Vac YS		1						% air %El
Hastelloy B-2	77	549.7	1270.7	56.6	489.9	1085.6	65.4	526.2	1062.1	59.4	89%	85%	116%	96%	84%	105%
UNS N10665	298	423.7	939.6	52.1	356.9	838.2	62.7	399.2	818.8	56.5	84%	89%	120%	94%	87%	108%
Cortest Labs	750	340.0	800.9	45.0	269.5	693.6	52.0	309.7	698.3	51.3	79%	87%	116%	91%	87%	114%
Tests	900	348.6	582.2	16.9	247.7	564.7	29.9	299.6	550.3	24.4	71%	97%	177%	86%	95%	144%
	1050	515.2	563.3	2.1	404.1	428.3	1.8	357.6	400.3	2.3	78%	76%	86%	69%	71%	110%
	1200	269.9	279.4	13.3	201.6	251.0	12.9	192.2	258.3	11.1	75%	90%	97%	71%	92%	83%

Vacuum heat treatment at 1173 K (900°C) in "1.3E-04 Pa or better" (10E-09 atm, 10E-07 Torr). "None of these exposures was continuous; all experienced shutdowns due to the loss of electrical power or cooling water, vacuum furnace leaks, regeneration of the cryopumps, and so forth."



## Applicability Haynes 25

Ref 4



39

#### Table 3. Chemical Analyses of Vapor Deposits Evaporated from Haynes-25

	Actual		Analyses of Vapor Deposits													Total Weight
Test Conditions <sup>a</sup>	Weigh Lossb	d Proces		Mn		Co		Fe		Ni		Si		W		of Vapor Deposit
	(mg)	(mg)	(wt %)	(mg)	(wt %)	(mg)	(wt %)	(mg)	(wt %)	(mg)	(wt %)	(mg)	(wt %)	(mg)	(wt %)	(mg)
872°C for 504 hr	3.40	2.11	66.88	0.56	17.75	0.26	8.27	0.18	5.70	0.03	1.01	0.001	0.03	0.01	0.35	3.155
927°C for 507 hr	4.70	3.08	66.31	0.68	14.64	0.48	10.33	0.17	3.66	0.21	4.52	0.001	0.02	0.024	0.52	4.645
982°C for 509 hr	11.80	7.63	66.58	.1.24	10.82	1.75	15.27	0.38	3.32	0.28	2.41	0.15	1.31	0.03	0.29	11.46
1038°C for 505 hr	23.6	14.90	64.50	2.18	9.44	4.43	19.18	0.79	3.42	0.65	2.81	0.08	0.35	0.07	0.30	23.10
1093°C for 503 hr	303.90	146.50	47.79	17.10	5.58	106.0	34.58	9.00	2.94	26.60	8.68	0.94	0.30	0.41	0.13	306.55

 $<sup>^{\</sup>rm A}$ At 1  $\times$  10 $^{-9}$  torr.

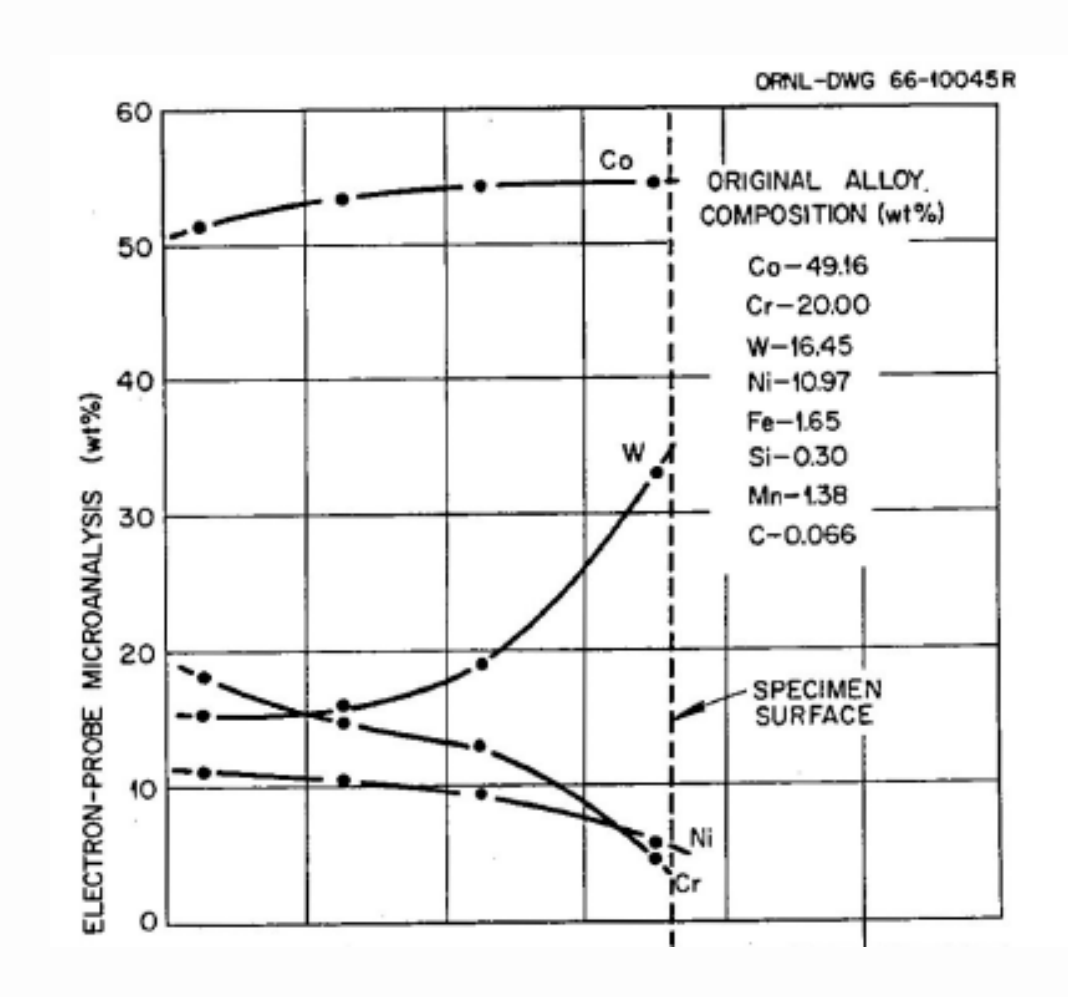
bInitial sample weight minus final sample weight.

cWeight of deposit determined by analytical chemistry methods.



40

Ref 4



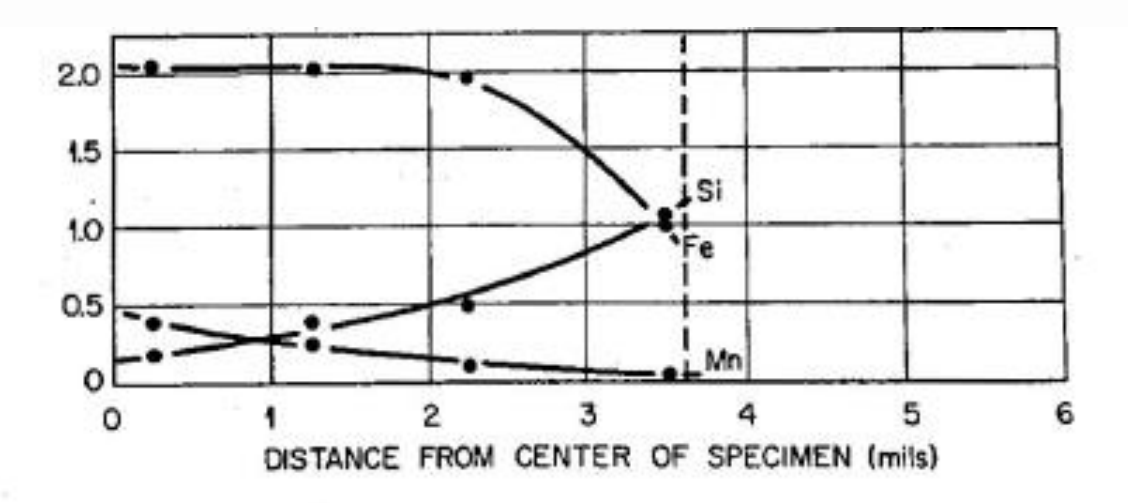


Fig. 2. Composition profile of a Haynes-25 specimen evaporation tested at 1040°C for 2672 hr.

### **Applicability: Haynes 25**



41

Ref 4

Table 5.	Effect of	Stress of	the :	Evaporation	Losses
				r 1000 hr	

Stress	Weight Loss
(psi)	(mg/cm <sup>2</sup> )
0	0.06
2,100	0.1477
4,500	0.1864
6,900	0.2014
9,500	0.2236
14,500	0.048

<sup>&</sup>lt;sup>a</sup>Specimen ruptured in 246 hr.

#### **Applicability: Haynes 25**

E ROLL TOR SUSTAINED EMPLOY

42

Ref 7

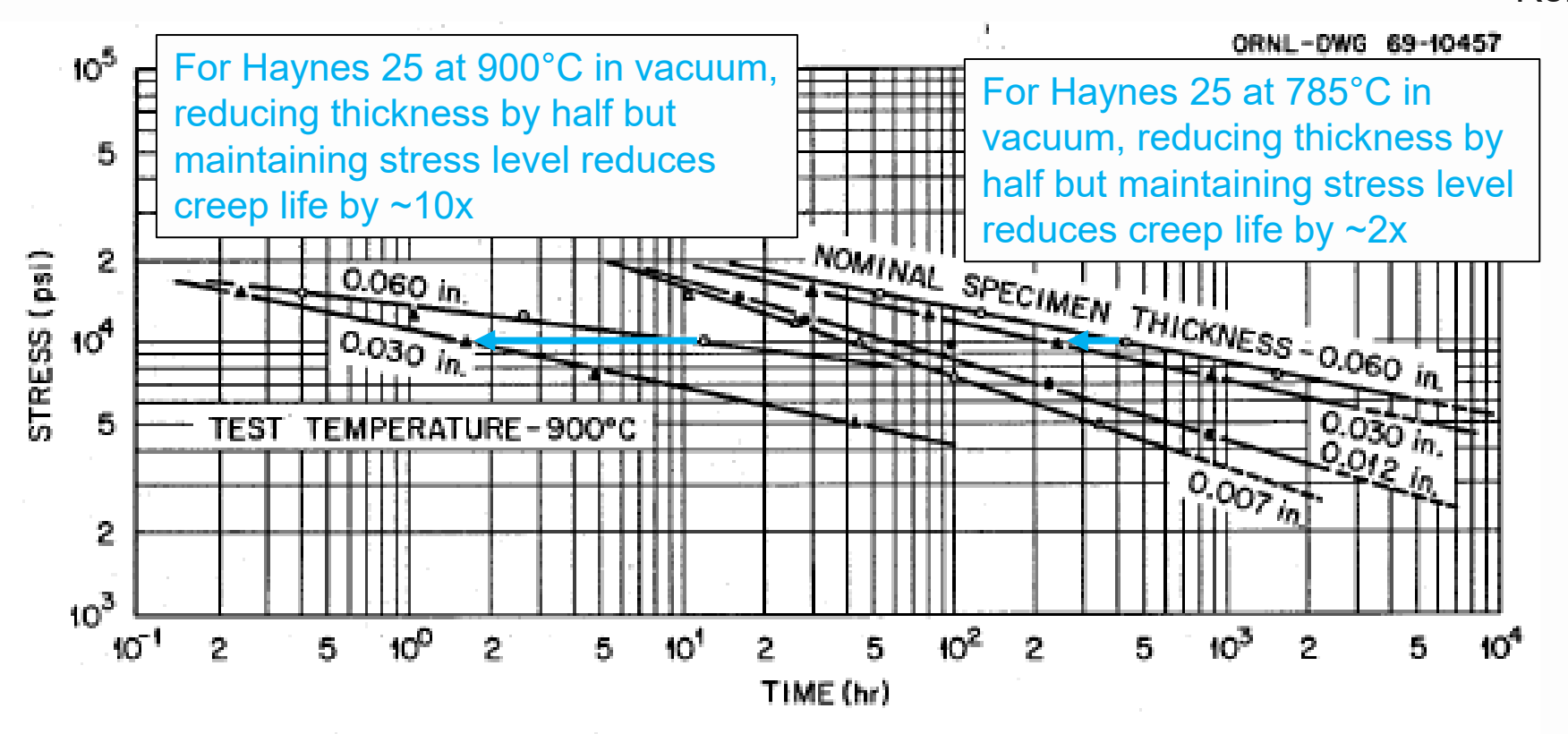


Fig. 13.1. Effect of Thickness and Stress on the Time Necessary to Produce 1.0% Plastic Strain in Haynes Alloy No. 25 in a Vacuum of 10<sup>-7</sup> to 10<sup>-9</sup> torr at Test Temperatures of 785 and 900°C.



43

Ref 7

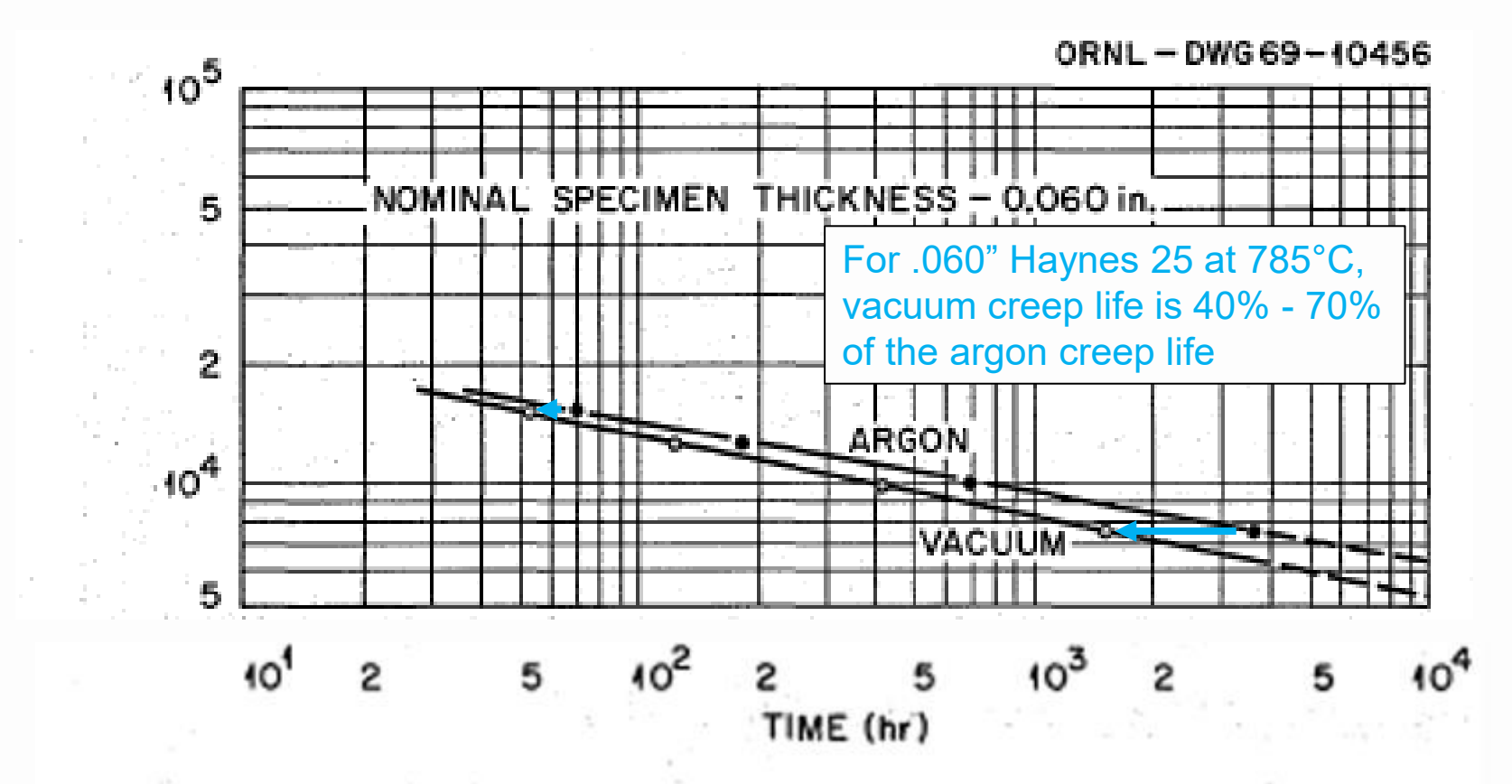


Fig. 13.2. Effect of Thickness and Stress on the Time to Produce 1.0% Plastic Strain in Haynes Alloy No. 25 at 785°C in Vacuum, Argon, and Air.

#### **Applicability: Haynes 25**



Ref 7

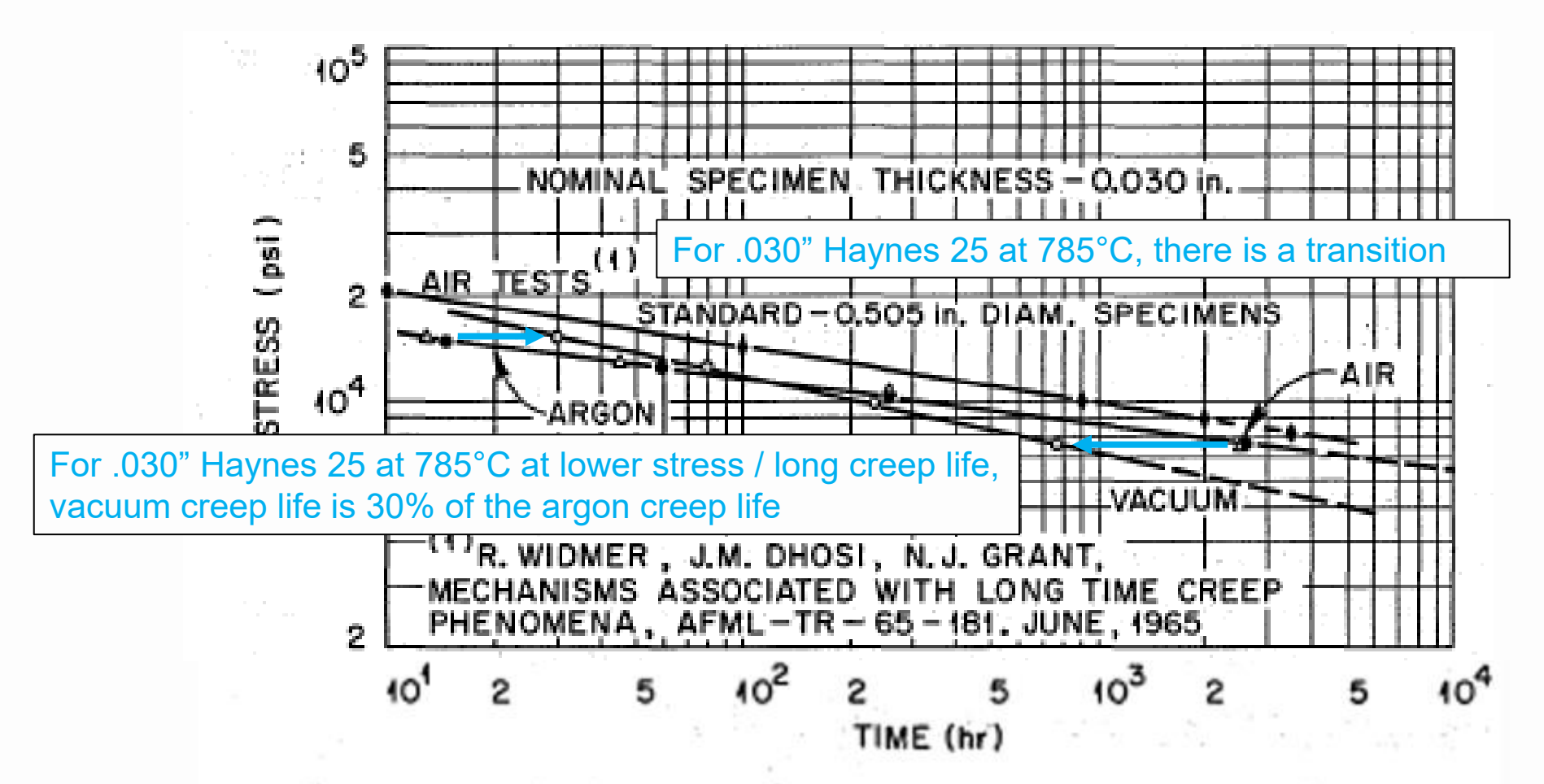


Fig. 13.2. Effect of Thickness and Stress on the Time to Produce 1.0% Plastic Strain in Haynes Alloy No. 25 at 785°C in Vacuum, Argon, and Air.

45

Ref 7

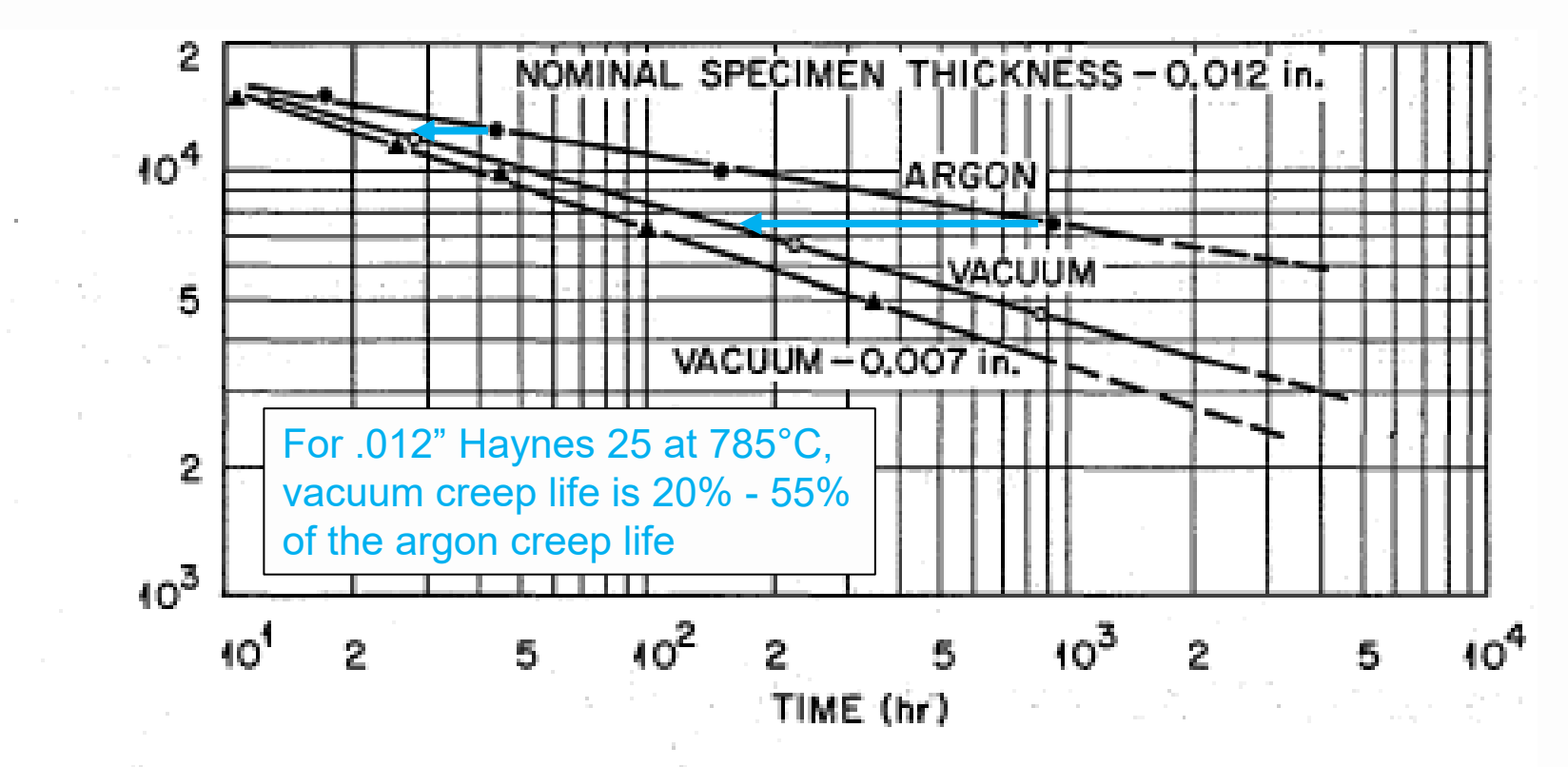
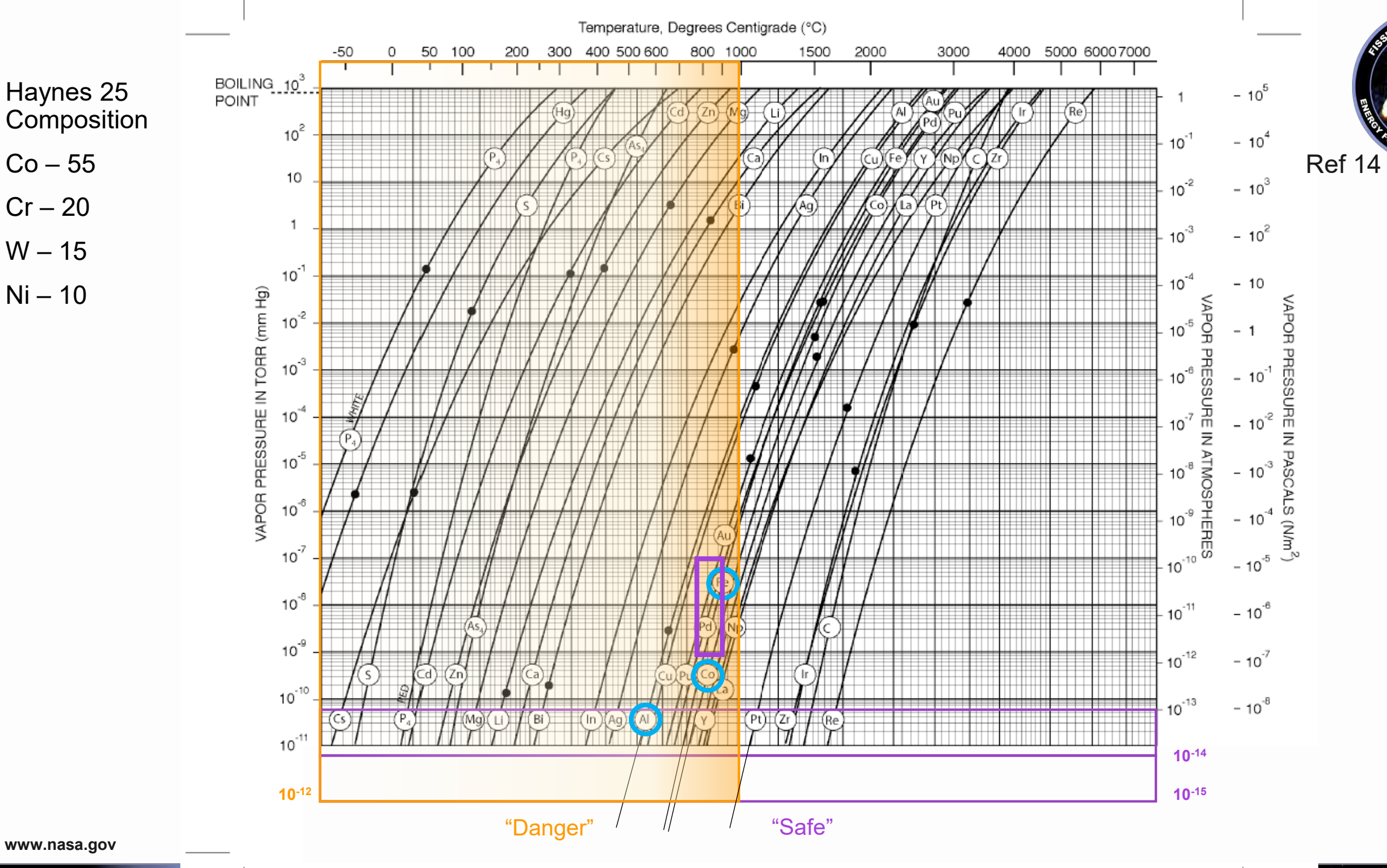


Fig. 13.2. Effect of Thickness and Stress on the Time to Produce 1.0% Plastic Strain in Haynes Alloy No. 25 at 785°C in Vacuum, Argon, and Air.

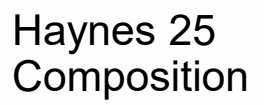


Co - 55

Cr-20

W - 15

Ni – 10

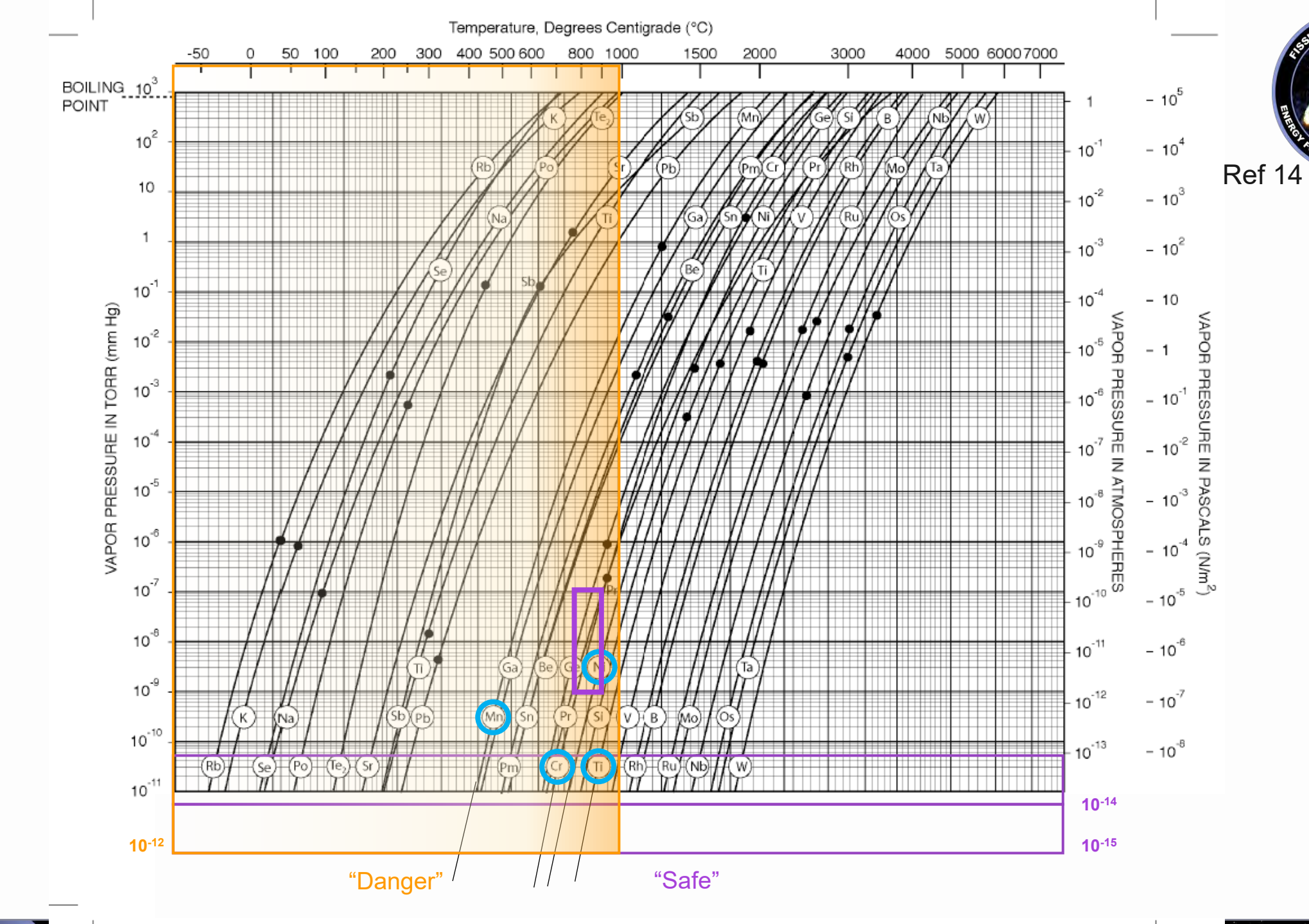


Co - 55

Cr-20

W - 15

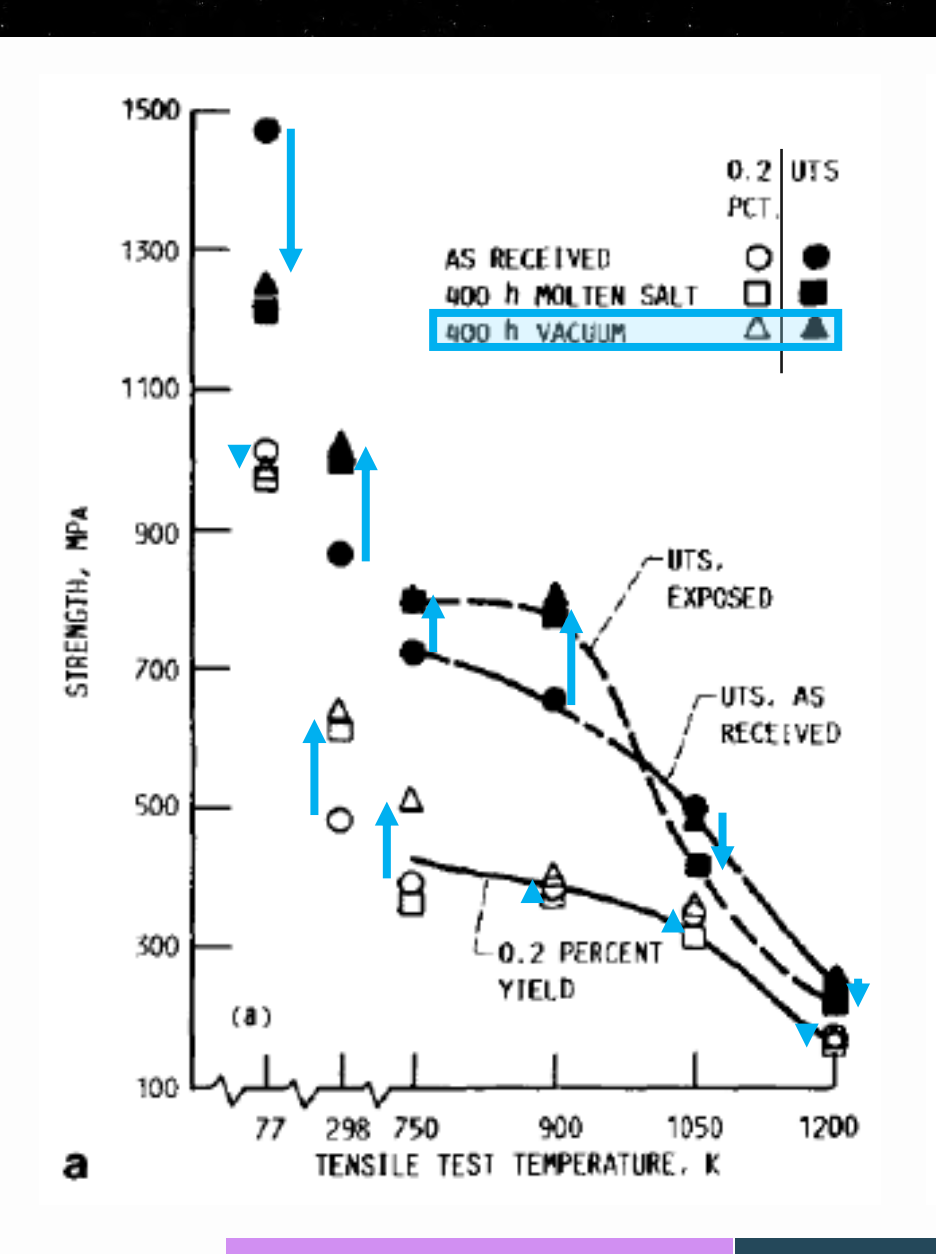
Ni – 10

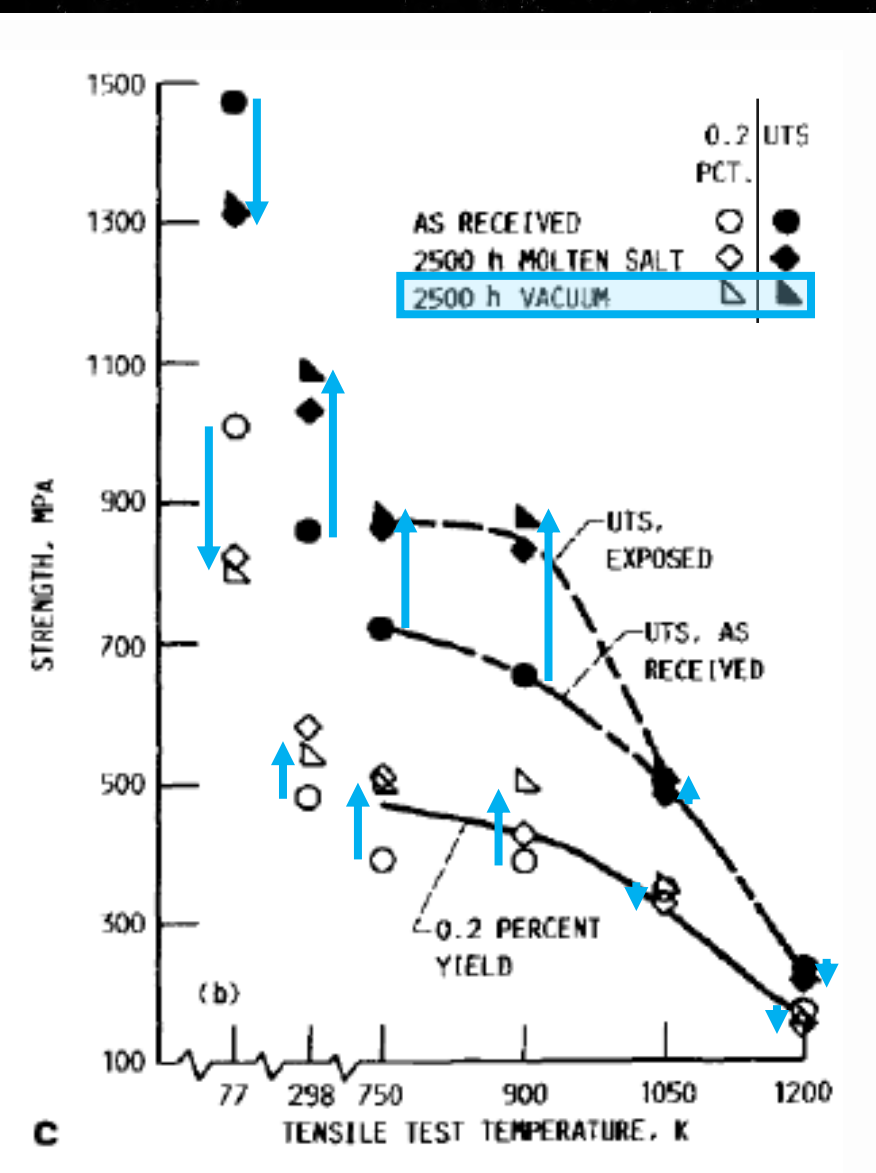




## Applicability Haynes 188

#### **Applicability: Haynes 188**





Ref 9

From Fig. 6.

- (a) UTS and YS after 400 hr exposure to vacuum.
- (c) UTS and US after 2500 hr exposure to vacuum.
- "...heat treatments at 1093K (820°C) in a cryogenically pumped vacuum of ~1.3 × 10<sup>-4</sup> Pa (10<sup>-9</sup> atm, 10<sup>-7</sup> Torr) or better. None of these exposures were continuous; all experienced shutdowns due to loss of electrical power or cooling water, vacuum leaks, regeneration of the cryopumps, etc."

298K tests in air

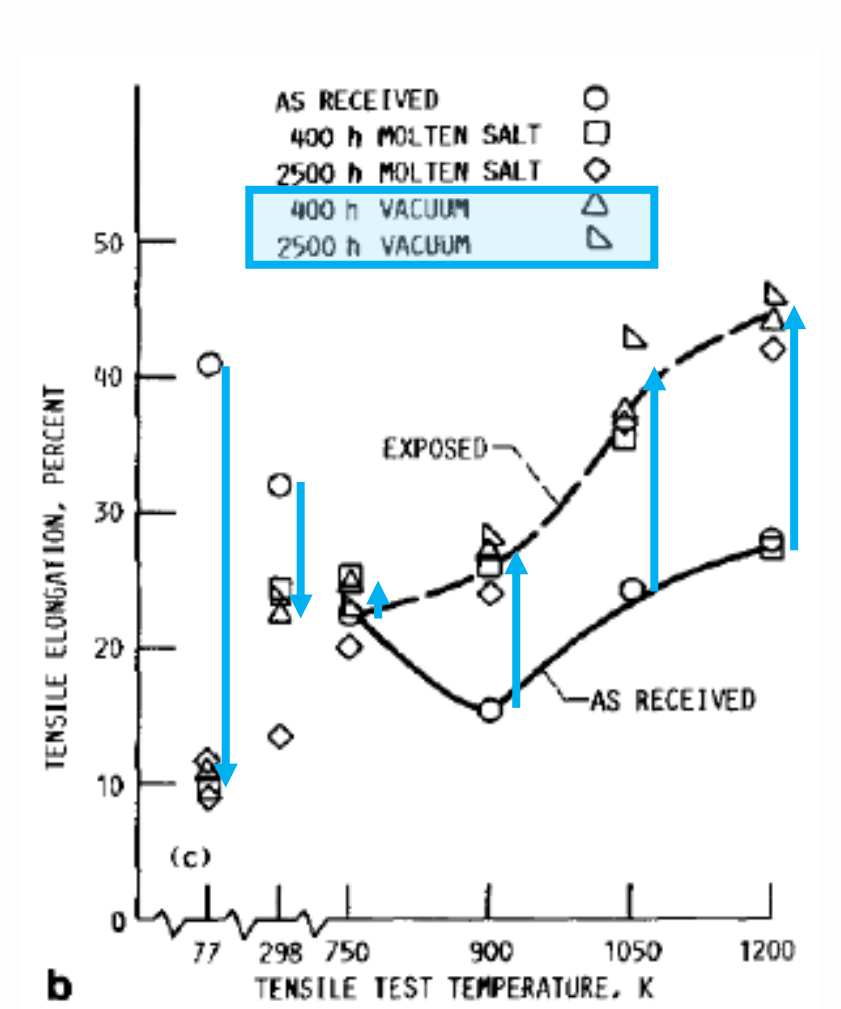
≥750K tests in 10<sup>-3</sup> Pa / 10<sup>-8</sup> atm / 10<sup>-6</sup> Torr or better

49

### **Applicability: Haynes 188**

PRESENT SUSTAINED ENVIOLE

Ref 9



Ref 11

				5k hrs Vacuum Exp.			5k hrs Vacuum Exp.			
Alloy	Temp.	Air YS	Air UTS	Air %El						% air %El
Haynes 188 UNS R30188	77	540.6	1037.8	61.9	415.8	984.8	41.4	77%	95%	67%

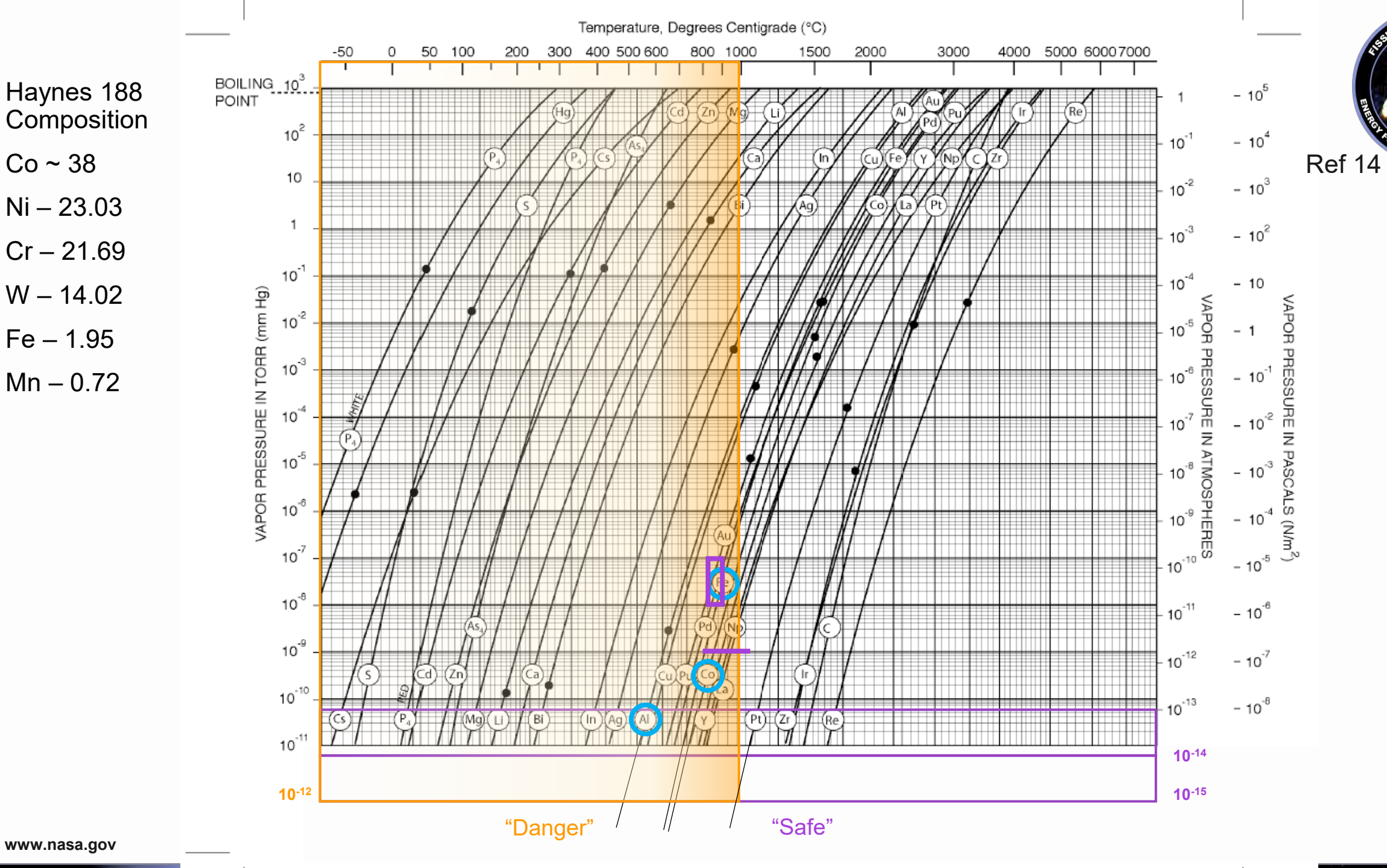
Same heat treatment as in Ref 11, except at 1173K (900°C)

- Evaporation rates of Haynes 188 were measured at 800 to 1050°C and 10-9 Torr
- Evaporation rates decreased with time at constant temperature
- Up to 1500 hr, the thicker the specimen, the less the decrease in evaporation rate

Ref 8

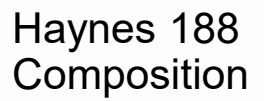
50

- The formation of voids was confined to grain matrices
- SEM observations of evaporated surfaces indicate a complete change in surface morphology
- Weight losses in excess of 4 mg/cm<sup>2</sup> resulted in precipitation of intermetallic phases at the surface



Co ~ 38

Fe – 1.95



Co ~ 38

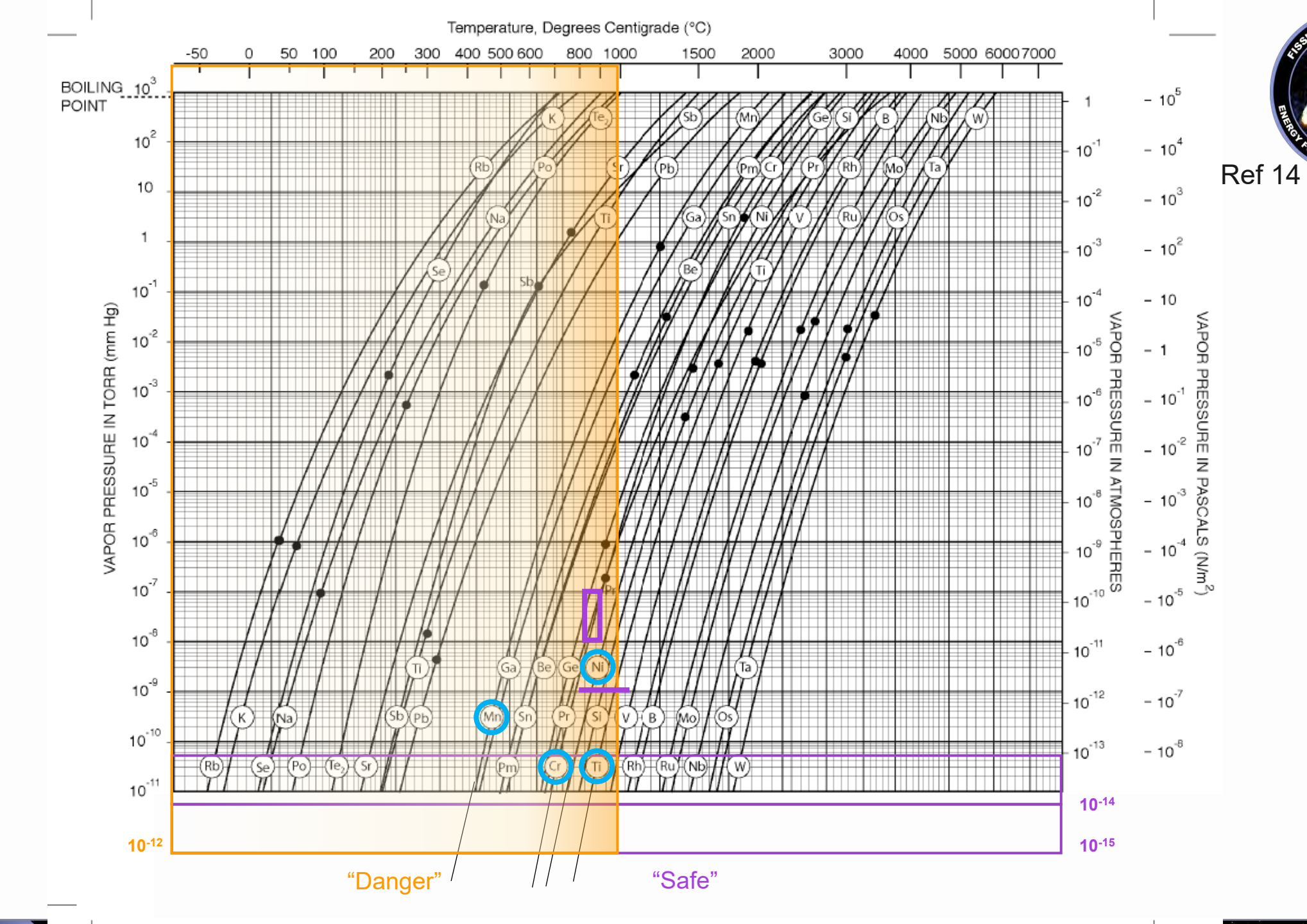
Ni - 23.03

Cr - 21.69

W - 14.02

Fe – 1.95

Mn - 0.72



#### **Possible Solutions: Haynes 188**



Ref 10





Fig. 3 Effect of long-term 1093 K air exposure on near-surface microstructure of HA 188. (a) As received. (b) 4900 h. (c) 10,000 h. (d) 22,500 h. All specimens are unetched.



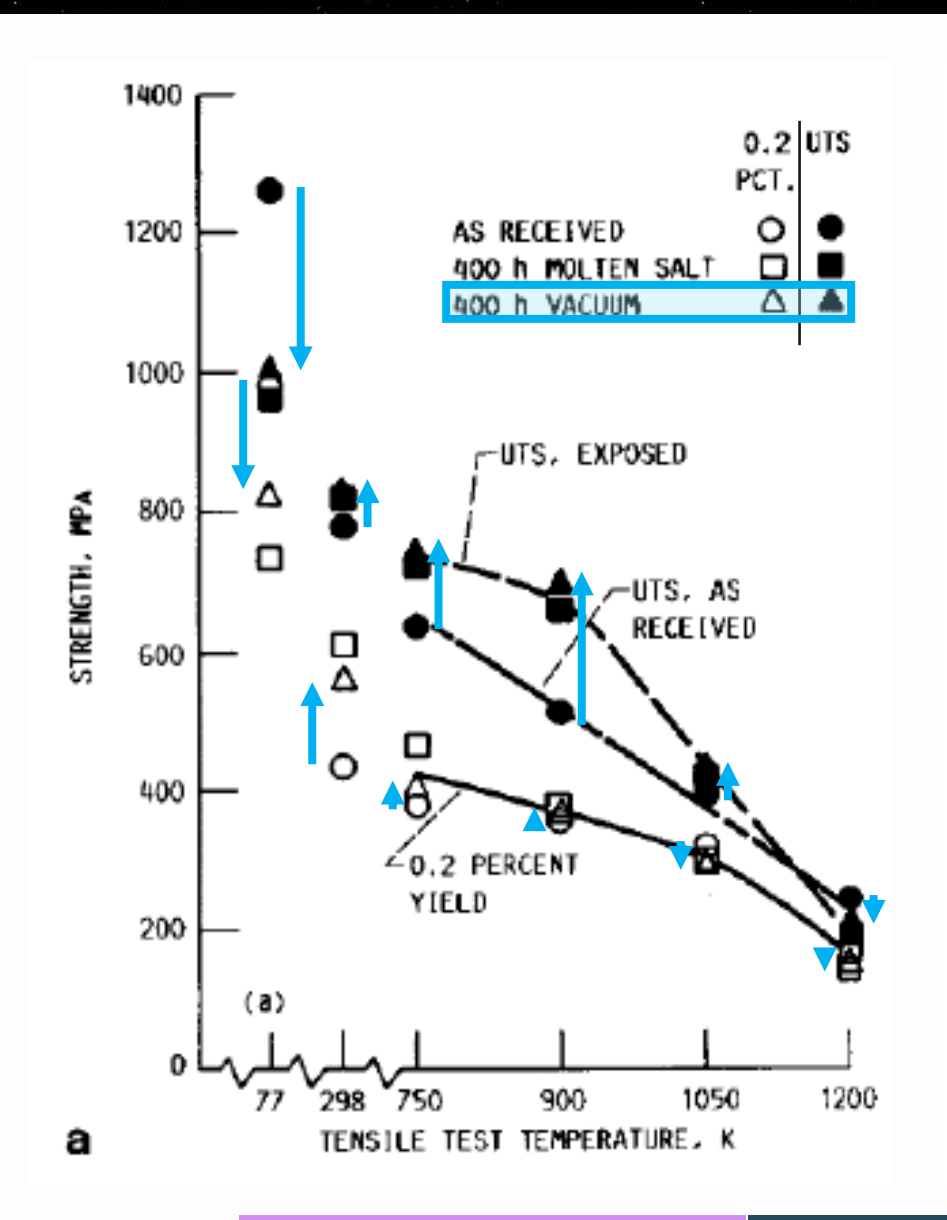


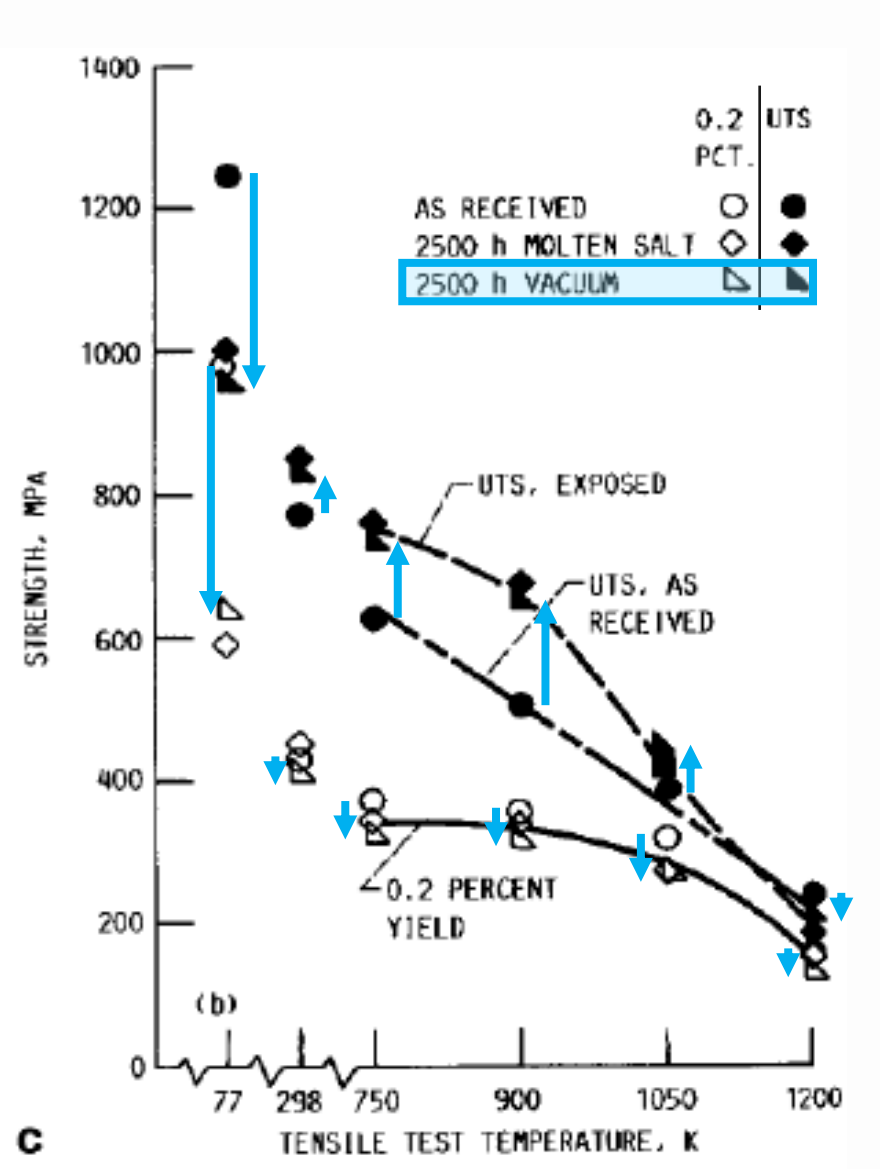
Fig. 5 Effect of long-term 1093 K vacuum exposure on HA 188. Specific weight change as a function of sample position and time (a), near-surface unetched microstructure in the as-received condition (b), and after 22,500 h (c).



# Applicability Haynes 230

# **Applicability: Haynes 230**





Ref 9

From Fig. 7.

- (a) UTS and YS after 400 hr exposure to vacuum.
- (c) UTS and US after 2500 hr exposure to vacuum.
- "...heat treatments at 1093K (820°C) in a cryogenically pumped vacuum of ~1.3 × 10<sup>-4</sup> Pa (10<sup>-9</sup> atm, 10<sup>-7</sup> Torr) or better. None of these exposures were continuous; all experienced shutdowns due to loss of electrical power or cooling water, vacuum leaks, regeneration of the cryopumps, etc."

298K tests in air

≥750K tests in 10<sup>-3</sup> Pa / 10<sup>-8</sup> atm / 10<sup>-6</sup> Torr or better

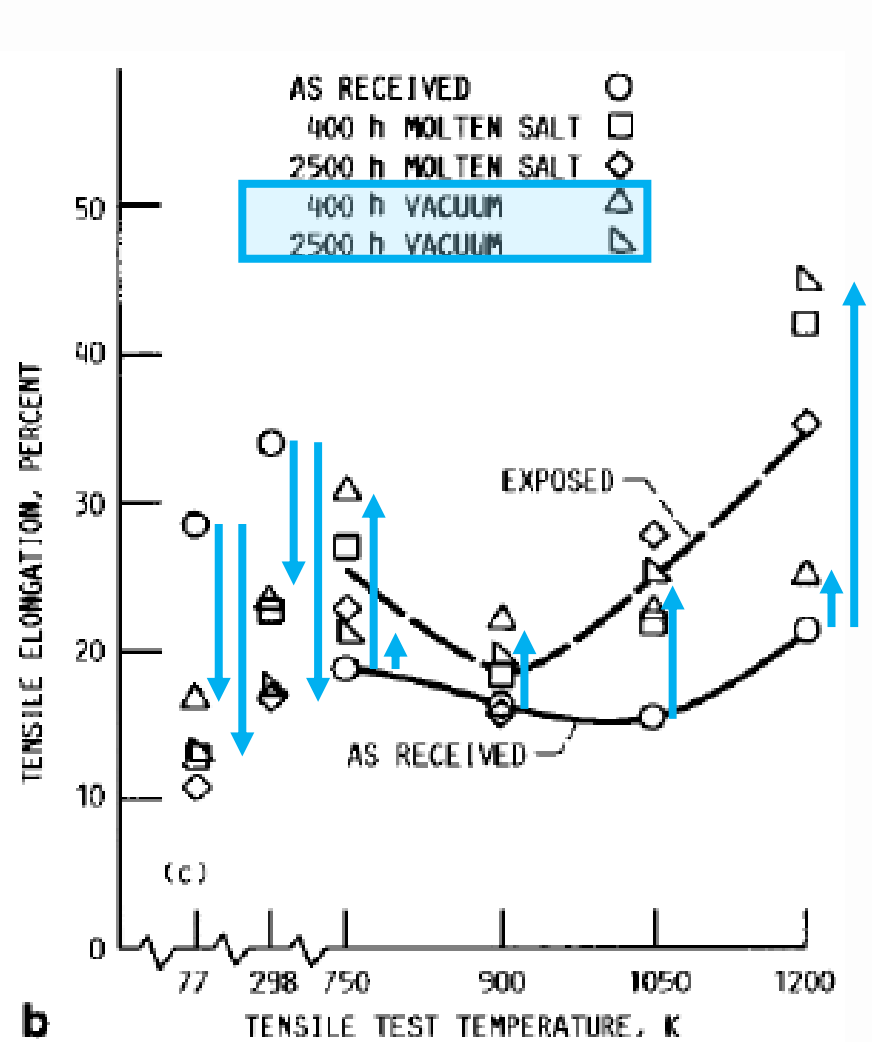
55

# **Applicability: Haynes 230**



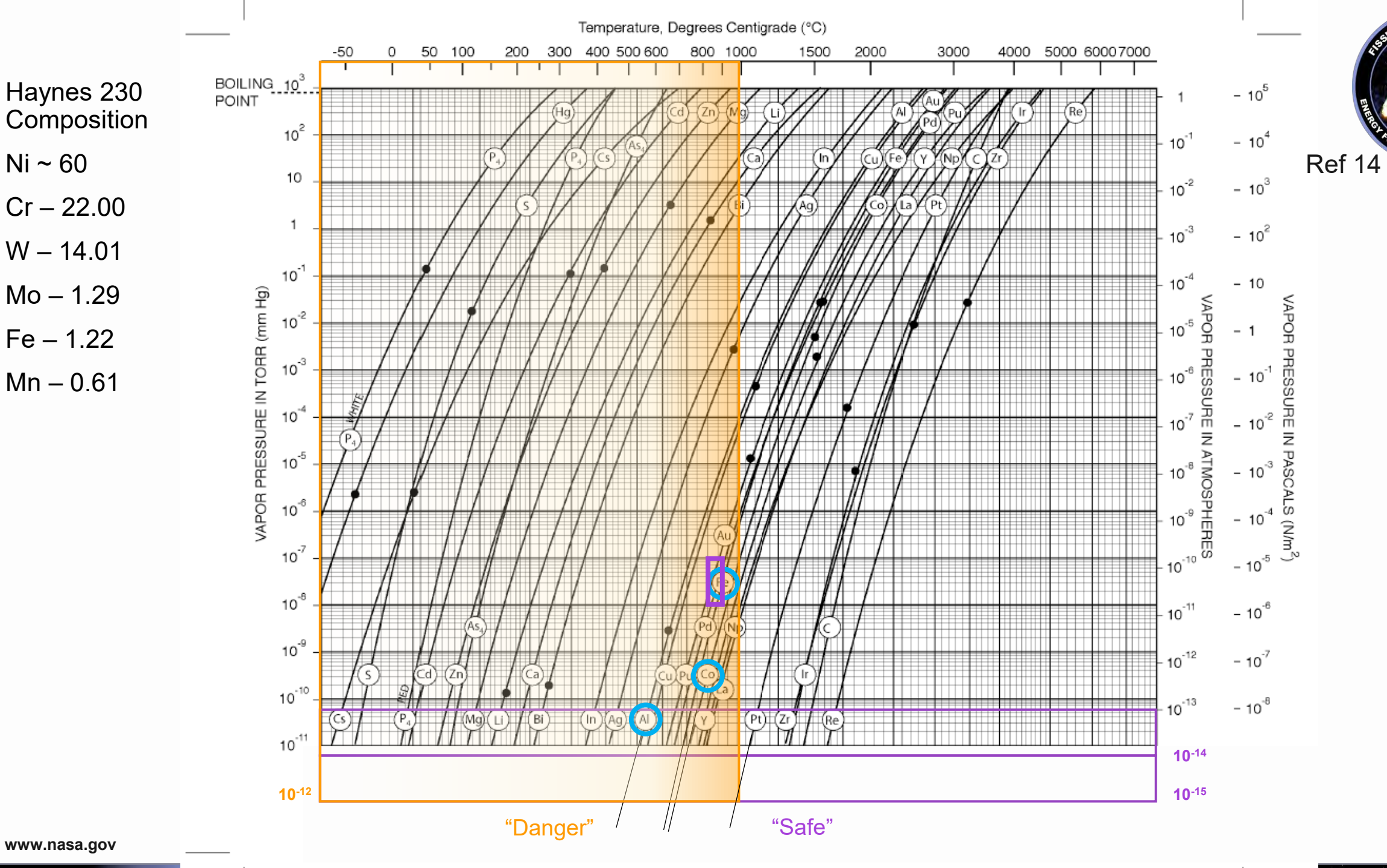
56





				5k hrs	Vacuun	n Exp.	5k hrs Vacuum Exp.			
Alloy	Temp.	Air YS	Air UTS	Air %El						% air %El
Haynes 230 UNS N06230	77	448.3	891.7	55.0	335.9	810.9	63.1	75%	91%	115%

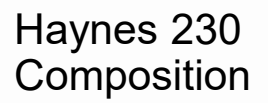
Same heat treatment as in Ref 11, except at 1173K (900°C)



Ni ~ 60

Fe - 1.22

Mn - 0.61



Ni ~ 60

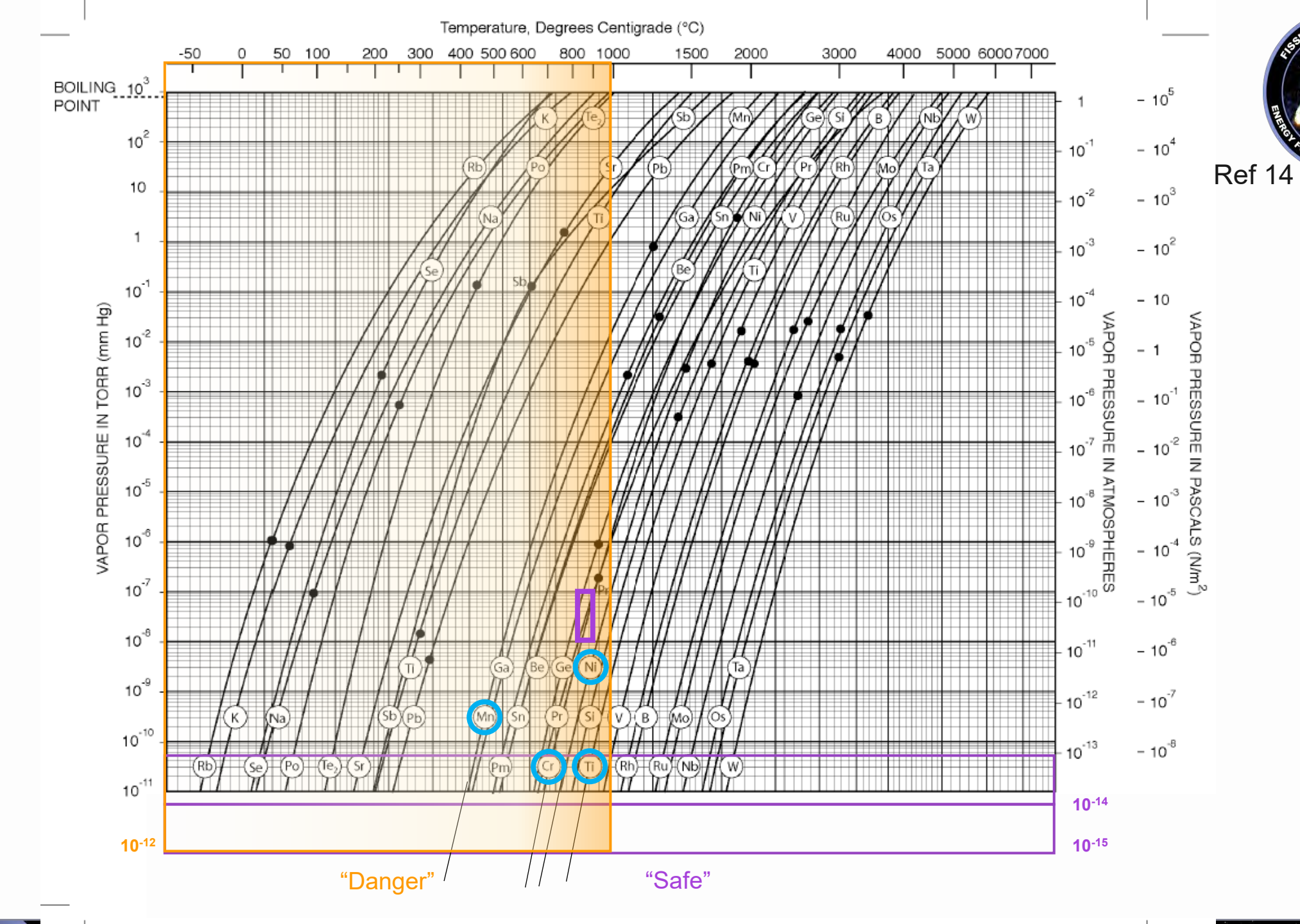
Cr - 22.00

W - 14.01

Mo - 1.29

Fe - 1.22

Mn - 0.61



# **Possible Solutions: Haynes 230**



Ref 10

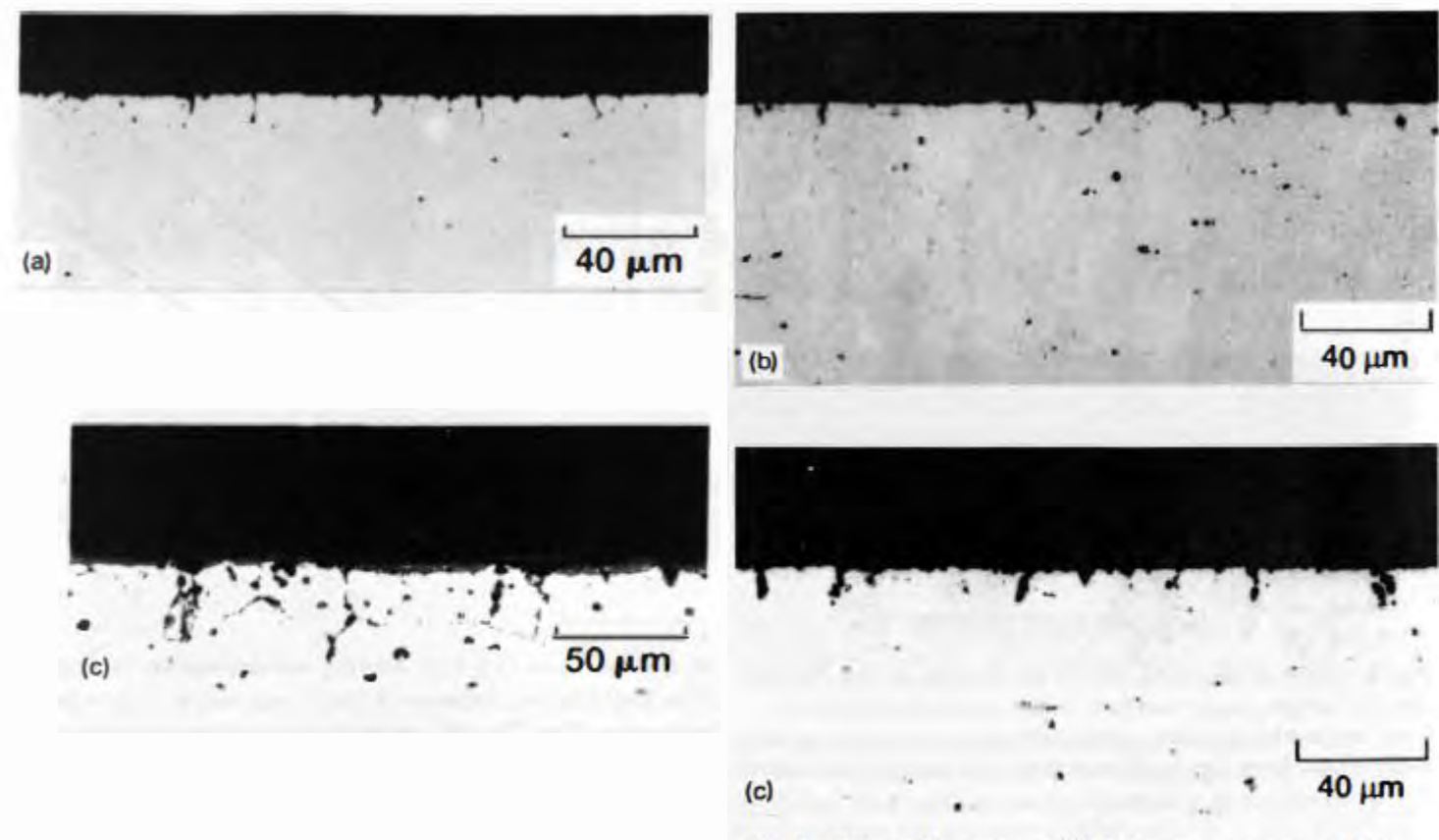


Fig. 7 Effect of long-term 1093 K air exposure on near-surface microstructure of HA 230. (a) As received. (b) 4900 h. (c) 10,000 h. (d) 22,500 h. All specimens are unetched.

Fig. 9 Effect of long-term 1093 K vacuum exposure on HA 230. Specific weight change as a function of sample position and time (a), near-surface unetched microstructure in the asreceived condition (b), and after 10,000 h (c).



# **Potential Solutions**

# **Possible Solutions**



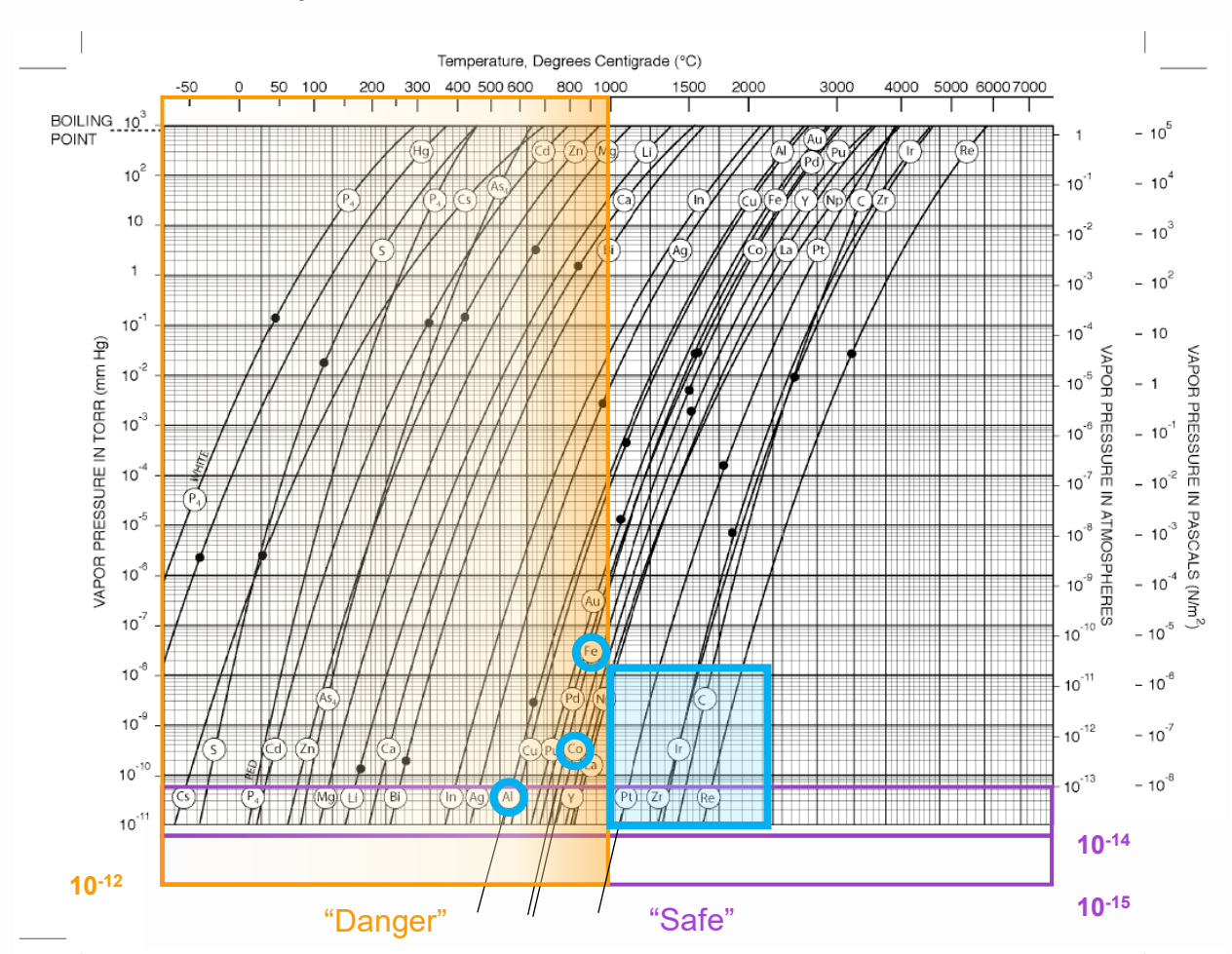
61

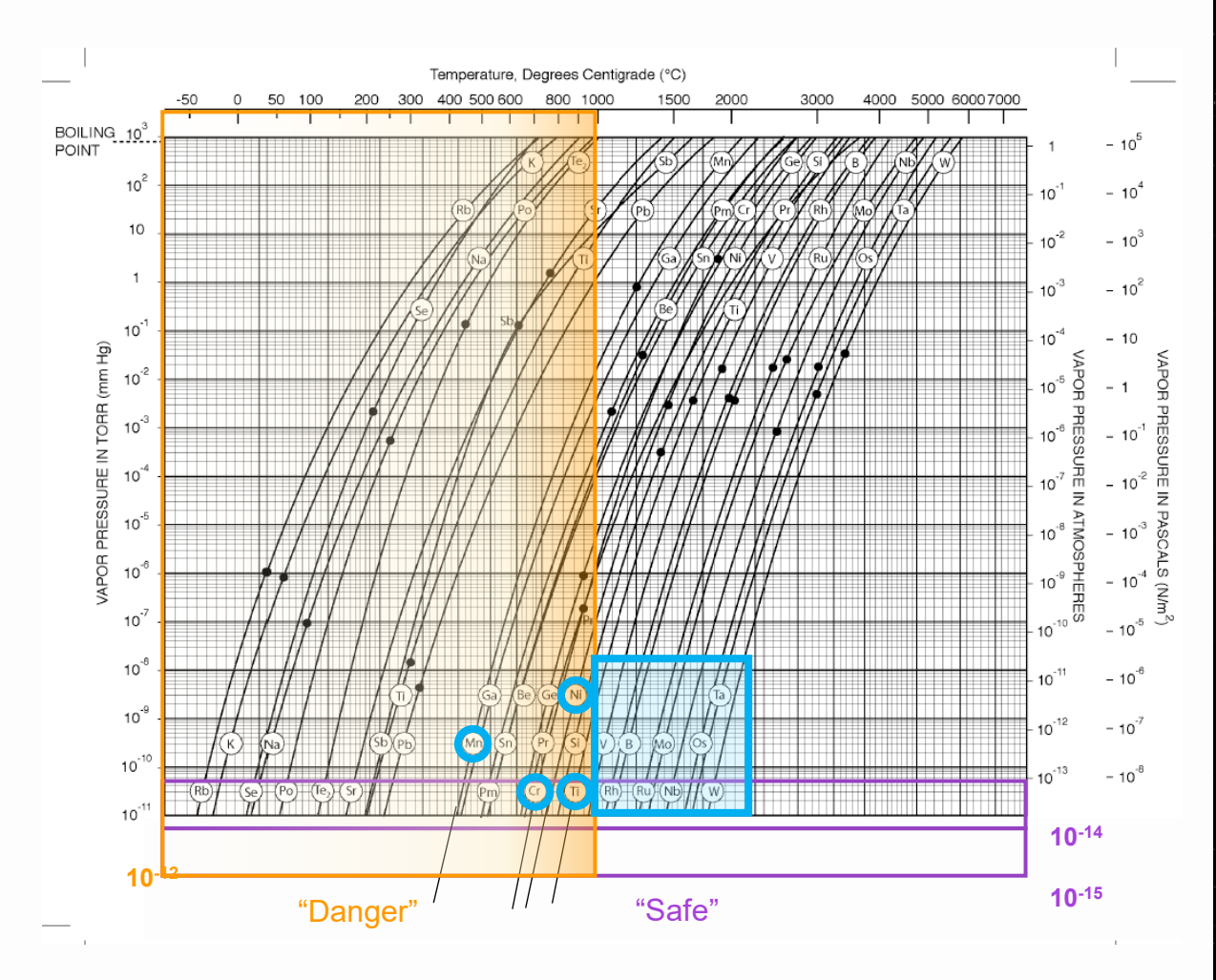
- 1. High Vapor Pressure Elements
- 2. Ordered Alloys
- 3. Multi-Layer Insulation
- 4. Coatings
  - 1. Protective Coatings
  - 2. Sacrificial Coatings



# Potential Solutions High Vapor Pressure Elements

#### Refractory metals and precious metals





63

REACT AON SUSTAINED EXPONENT

Ref 2

Table 1. Alloys of Interest Investigated in This Study

Commercial Designation		Nomir	al C	omposi	ition	(wt	<b>%</b> )				Interent (1	
	Ta.	Nb	W	Hf	Zr	V	Мо	Y	C	0	N	Н
T-111	90		8	` 2					70	57	29	4
FS-80		99			1				100	180	78	10
FS-85	28	60	11		1				40	100	28	2
C-129Y (a)		79.9	10	10				0.1	75	150	60	5
<b>B</b> -66		89			1	<sup>:</sup> 5	5		110	97	250	4
D-43		89	10		1				980	63	89	6

<sup>(</sup>a) Alloy contained 0.4 wt % Zr as an impurity.

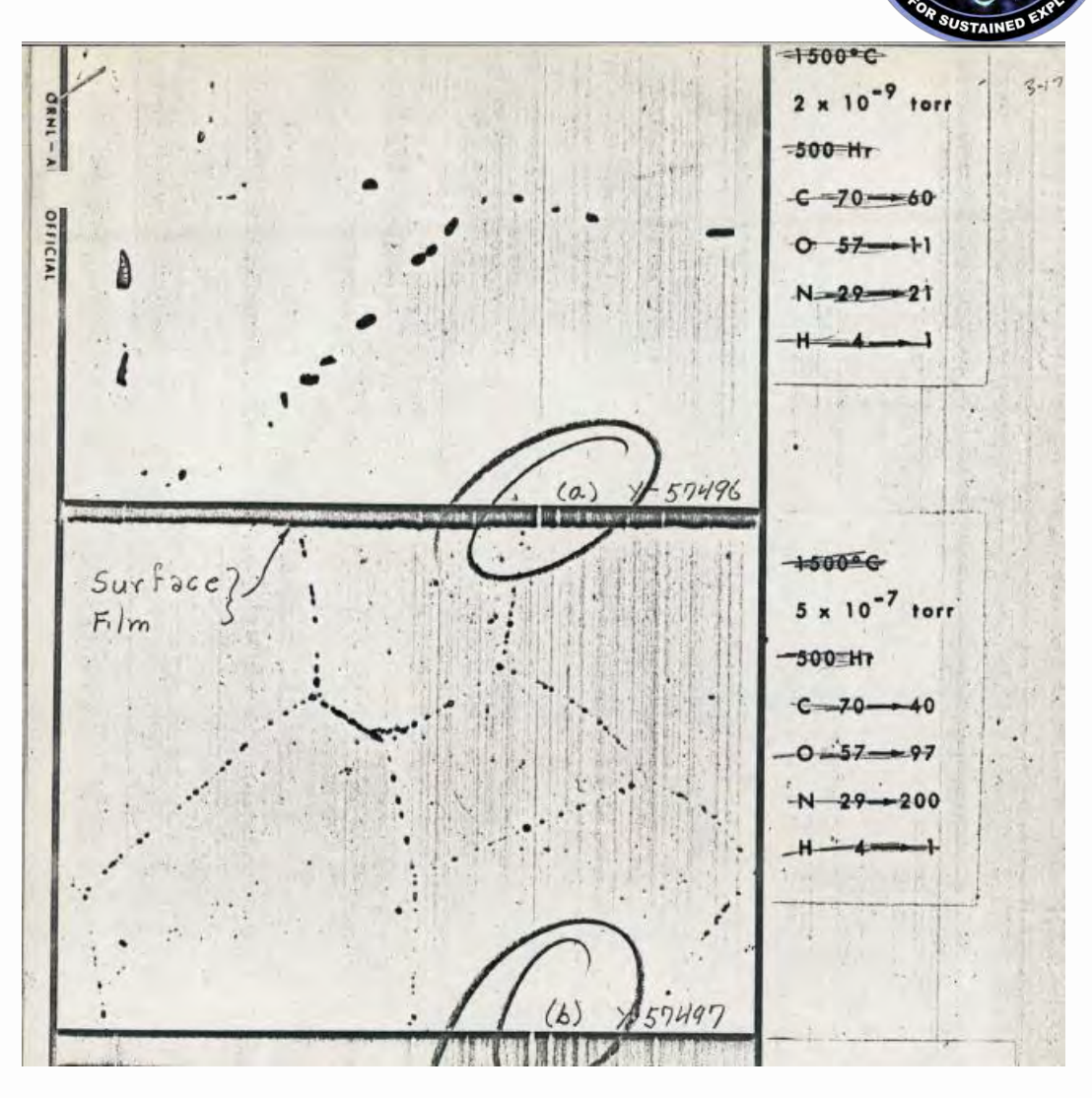
Ref 2

65

"When certain refractory-base alloys undergo a severe change in concentration of interstitial carbon, oxygen, or nitrogen, a corresponding change in the size and quantity of precipitates containing these elements will also occur...

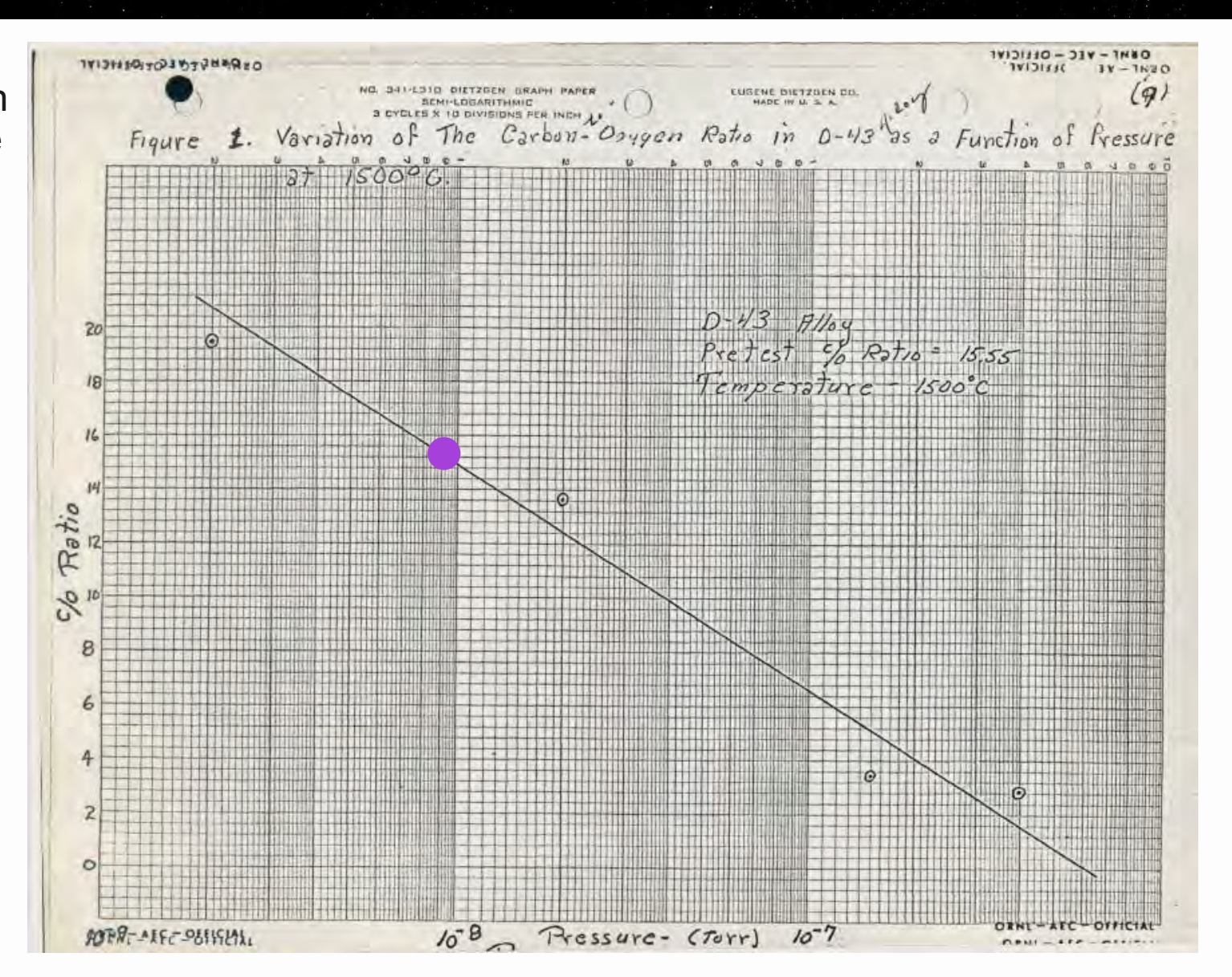
T-111 alloy lost oxygen and nitrogen at 1500°C and [2.6E-12 atm], while the carbon content was not grossly affected... the corresponding microstructure [in] Fig. 3(a) shows a comparatively large grain-boundary precipitates accompanied by clear specimen surfaces.

At [6.6E-10 atm], however, carbon was lost, while the oxygen and nitrogen concentrations increased. Figure 3(b) shows that the resulting microstructure contained a very fine grain-boundary precipitate and that the specimen surfaces were now covered by a thin film. At [2.6E-12 atm], the grain-boundary phase is believed to be carbides, while at [6.6E-10 atm] it is believed that both carbides and nitrides are present in the grain boundaries because of the increase in nitrogen concentration in Table 2."



Microstructural evolution is very sensitive to trace gasses at 1500°C:

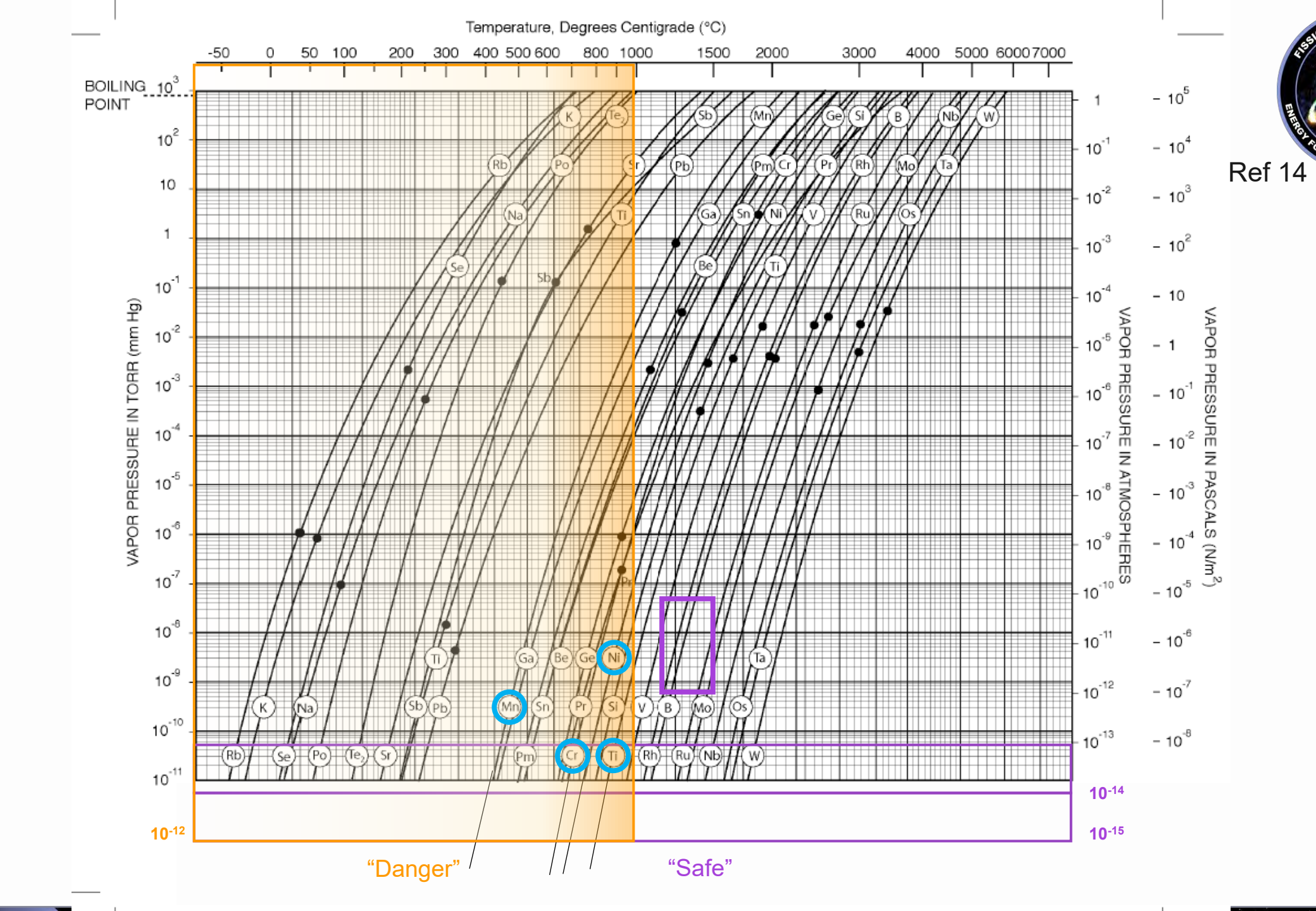
- Initial C/O ratio of 15.5
- For pressures <10-8</li>
   Torr, lose O
- For pressures >10-8
   Torr, gain O



Ref 2



66





# Potential Solutions Ordered Alloys

# **Possible Solutions: Ordered Alloys**

Ref 5,6,7,8

Alloy	Wt% Comp.	At% Comp.	Structure	Temp. (°C)	Mass Loss Rate (mg/cm²/hr)×10-3	Temp. (°C)	Hrs to 1% strain
Fe	Fe	Fe		1000	22		
Со	Со	Со			7.7		
Ni	Ni	Ni			4.6		
H. 25	Co-20Cr-15W- 10Ni		Disordered	1000	23	900	11
S-1	Ni-26Co		Disordered				
S-2	Ni-22Co-4.7V		Disordered				
S-3	Ni-46.4Co-9V		Disordered	1000	4.6	900	1.5
S-4	Ni-32.5Co-24V		Ordered*	1000	2.0	899	5.0
S-5	Pt-45Fe		Disordered*	1000	6.9		
S-6	Pt-23.2Co		Ordered*	1000	0.16		
S-11	Co-27Pt			1000	2.8		
S-12	Ni-27Pt			1000	2.8		
S-13	Fe-28Pt			1000	12		
S-19		Pt-25Cr	Ordered*			897	450
S-22			Disordered				<28

Tests conducted at 10<sup>-7</sup> Torr

\*Order depends on heat treatment and temperature

# **Possible Solutions: Ordered Alloys**

Ref 5,9

70

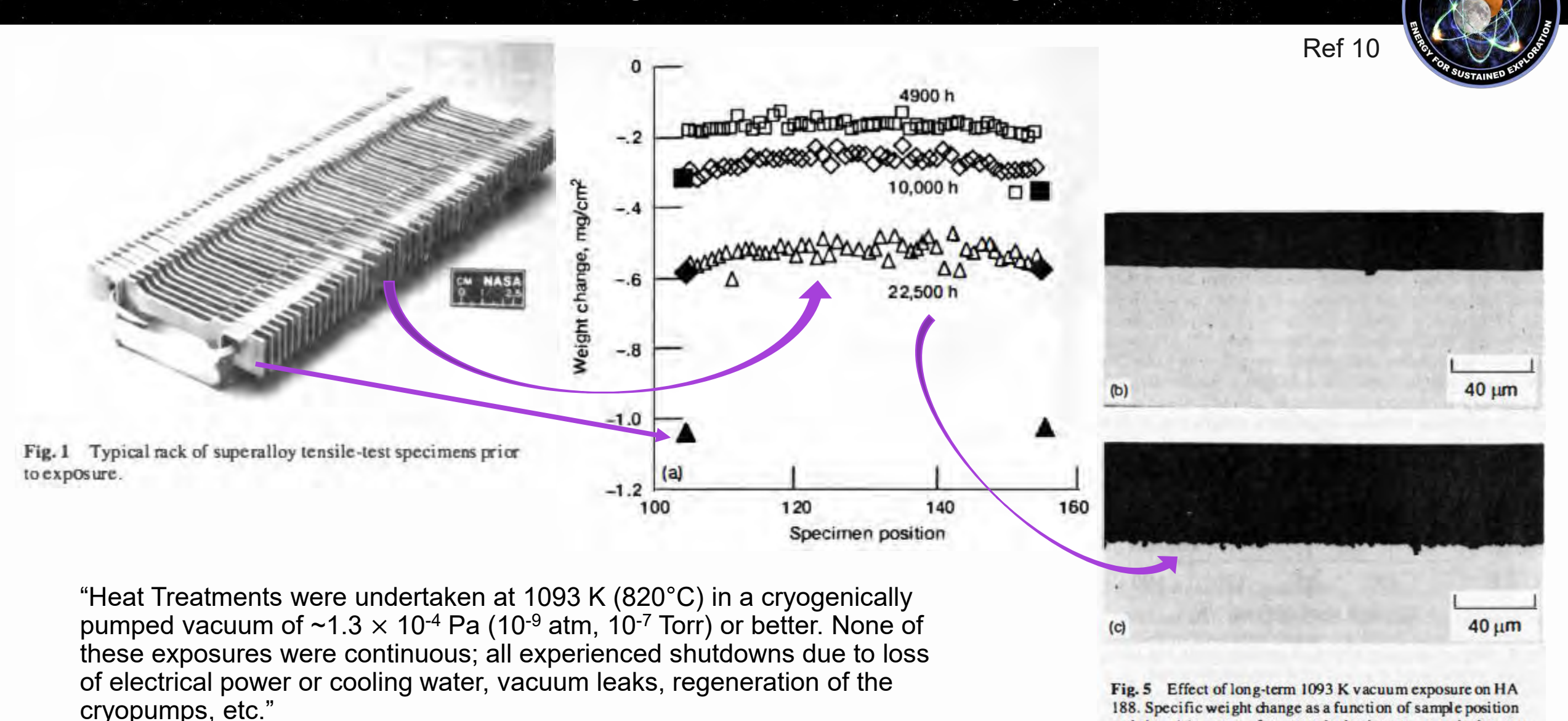
"Alloy S-3 is in the disordered state, and S-4 forms the ordered phase (Co,Ni)<sub>3</sub>V at [1000°C]. Comparison of the evaporation rates of these two alloys indicates that ordered alloys evaporate more slowly than disordered alloys."

"The initial evaporation rate of Haynes Alloy No. 25 in high vacuum is about 480 mg cm<sup>-2</sup> hr<sup>-1</sup> at 982°C, due to the preferential loss of Mn and Cr elements. Our preliminary data show that although alloy S-19 contains 25at% Cr, the evaporation rate cannot be measured even after 200 hr of exposure in vacuum at 984°C."



# Potential Solutions Multi-Layer Insulation

# Possible Solutions: Multi-Layer Insulation – Haynes 188



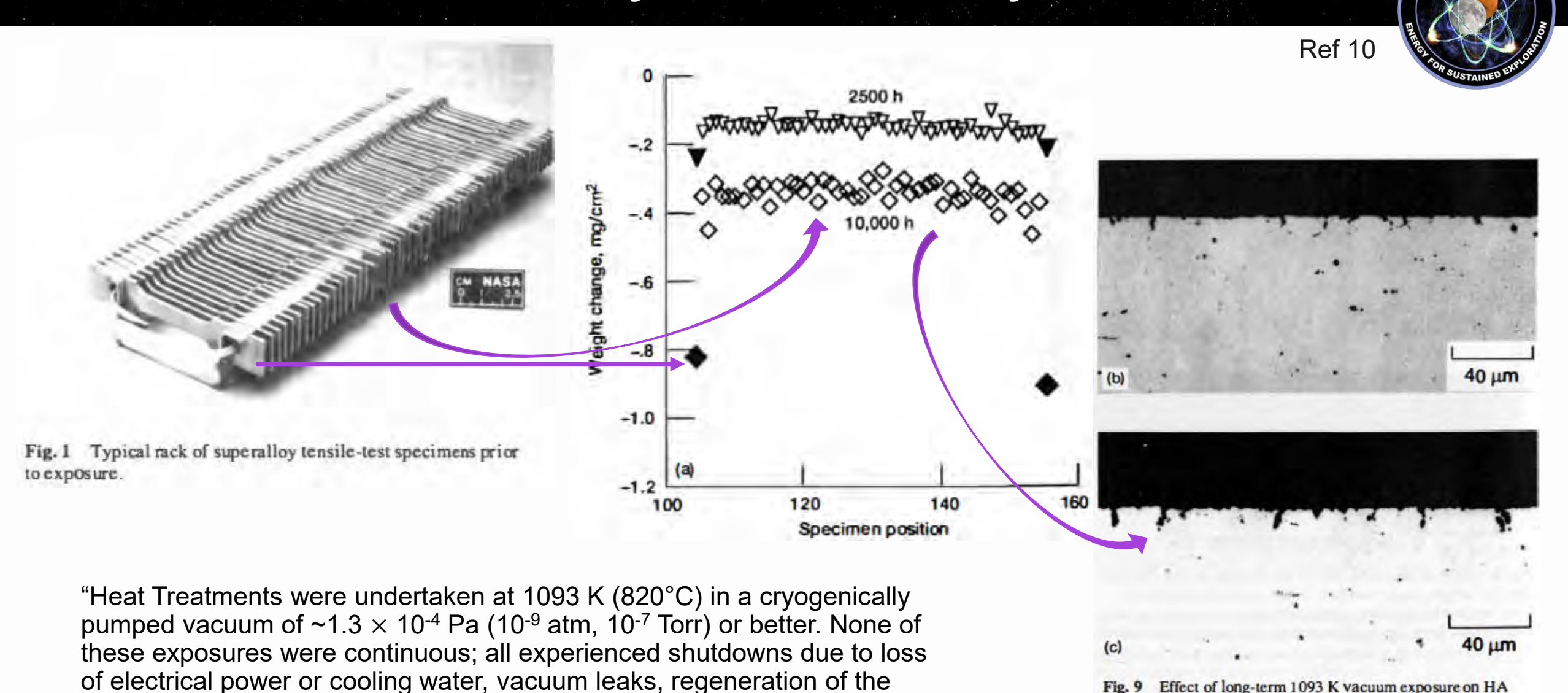
www.nasa.gov Introduction Applicability Solutions GRC

and time (a), near-surface unetched microstructure in the as-re-

ceived condition (b), and after 22,500 h (c).

# Possible Solutions: Multi-Layer Insulation – Haynes 230

cryopumps, etc."



www.nasa.gov Introduction Applicability Solutions GRC

230. Specific weight change as a function of sample position

and time (a), near-surface unetched microstructure in the as-

73

received condition (b), and after 10,000 h (c).



# Potential Solutions Coatings

# **Possible Solutions: Coatings - Oxides**

Ref 1

Thermally grown oxide reduces vaporization rate: initial and final vaporization rates of oxidized metal at 982°C after ~500 hrs is less than oxide-free vaporization at 982°C after 700 hrs.

Table 4. The Effect of Air Oxidation on the Subsequent Evaporation Rates of Various Alloys at 982°C

Oxidation Temper- Oxygen Durat					Duration	Evaporation Rate ation (mg/cm <sup>2</sup> /hr) × 10 <sup>-4</sup>		Oxide Present		aporation (cm <sup>2</sup> /hr)		
Alloy	ature (°C)	Time (hr)		X-Ray Identification of Oxide Film	of Test (hr)	Initial <sup>8</sup>	2-	after vaporation	872 Initial b		983 Initial	2°C Final
INOR-8	870	50	0.0521	NiMoO <sub>4</sub> + NiCr <sub>2</sub> O <sub>4</sub> + Cr <sub>2</sub> O <sub>3</sub> + NiFeO <sub>4</sub>	531	8.5	25.0	none	1.54	1.54	30.8	30.8
Inconel	980	25	0.1735	Cr <sub>2</sub> O <sub>3</sub>	522	36.3	30.5	Cr <sub>2</sub> O <sub>3</sub>	7.57	2.89	59.7	33.5
Type 316 stainless steel	980	100	4.3950	αFe <sub>2</sub> O <sub>3</sub> + NiO·Fe <sub>2</sub> O <sub>3</sub> + 3Fe <sub>2</sub> O <sub>3</sub> ·Cr <sub>2</sub> O <sub>3</sub>	504	1.94	6.65	Cr <sub>2</sub> O <sub>3</sub> + Fe <sub>3</sub> O <sub>4</sub> (trace)	30.0	6.59	114.0	66.4
Haynes alloy No. 25	1038	90	0.0229	Cr <sub>2</sub> O <sub>3</sub> + NiO·Fe <sub>2</sub> O <sub>4</sub> + CoFe <sub>2</sub> O <sub>4</sub> + Co <sub>2</sub> MnO <sub>4</sub>	510	66.5	3.34	Cr <sub>2</sub> O <sub>3</sub> + αFe <sub>3</sub> O <sub>4</sub> (trace)	58.5	5.66	140.0	69.2

<sup>&</sup>lt;sup>a</sup>Maximum rate during initial 50 hr of test.

Bate during last 50 hr of test.

# **Possible Solutions: Coatings - Oxides**



76

Ref 1

CRES 316 exhibits minimal mass loss after 1142 hrs at 760°C if pre-oxidized.

Table 7. Experimental Evaporation Rates of Type 316 Stainless Steel Preoxidized in Wet Hydrogen at 870°C

Evaporation Temperature (°C)	Duration of Test (hr)	Evaporation (mg/cm²/h) Initial		Oxygen Pickup (mg/cm²)	Final Oxide Layer
982	1058	26.9	35.7	0.2804	Cr <sub>2</sub> O <sub>3</sub>
927	1226	7.89	12.5	0.2983	Cr <sub>2</sub> O <sub>3</sub>
872	14 <i>5</i> 6	4.42	4.44	0.3134	Cr <sub>2</sub> O <sub>3</sub> + MnO <sub>2</sub> (trace)
760	1142	No wei.gl	nt loss	0.2525	Cr <sub>2</sub> O <sub>3</sub>

# **Possible Solutions: Coatings - Elements**

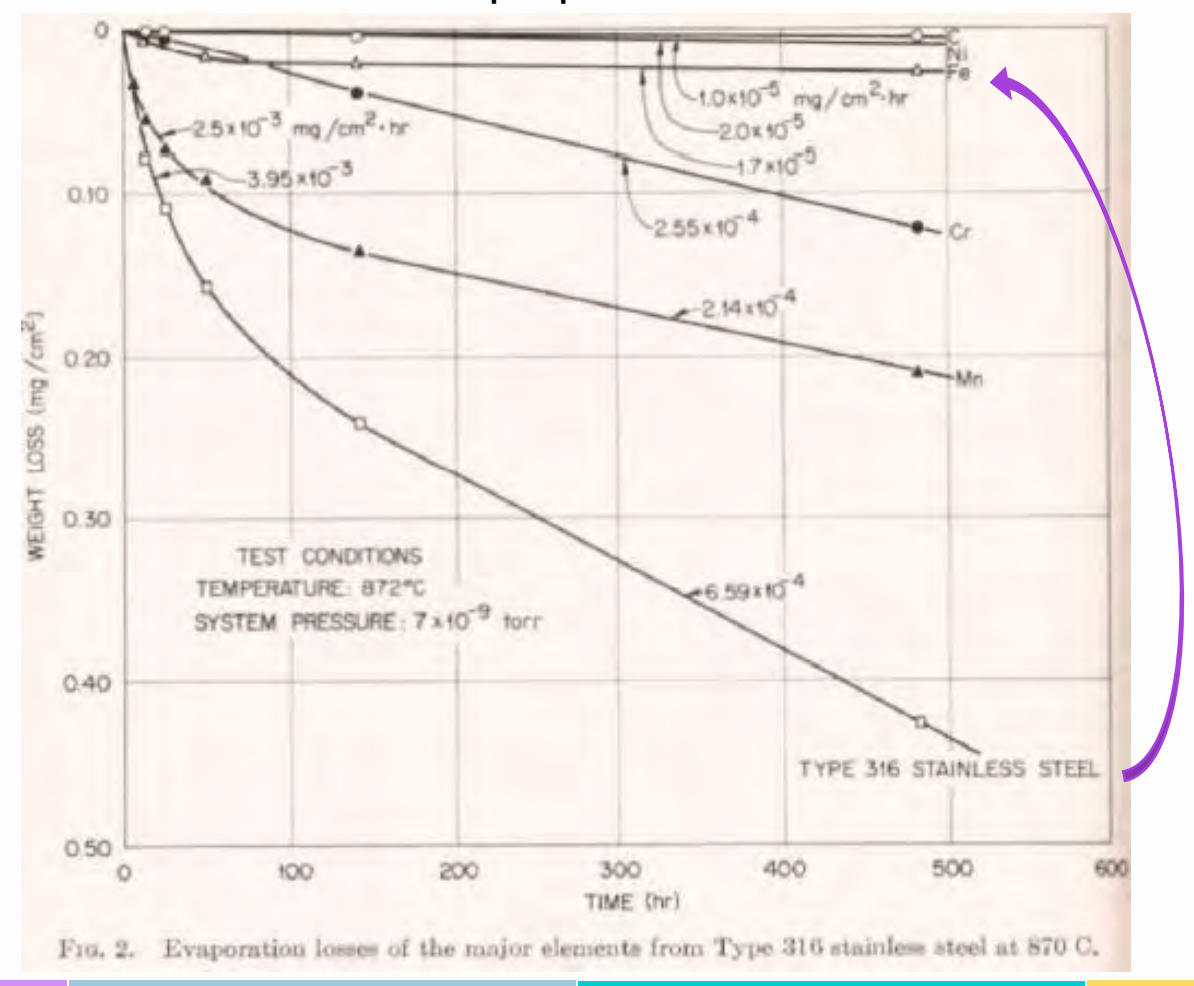
READ SUSTAINED ENTON

77

Ref 1

Can e.g. Ni plating on Ni alloys inhibit vaporization?

How does diffusion and dilution affect mechanical properties?



# **Possible Solutions: Coatings - Other**

SURFACE ROMER

Ref 1

R512E or similar

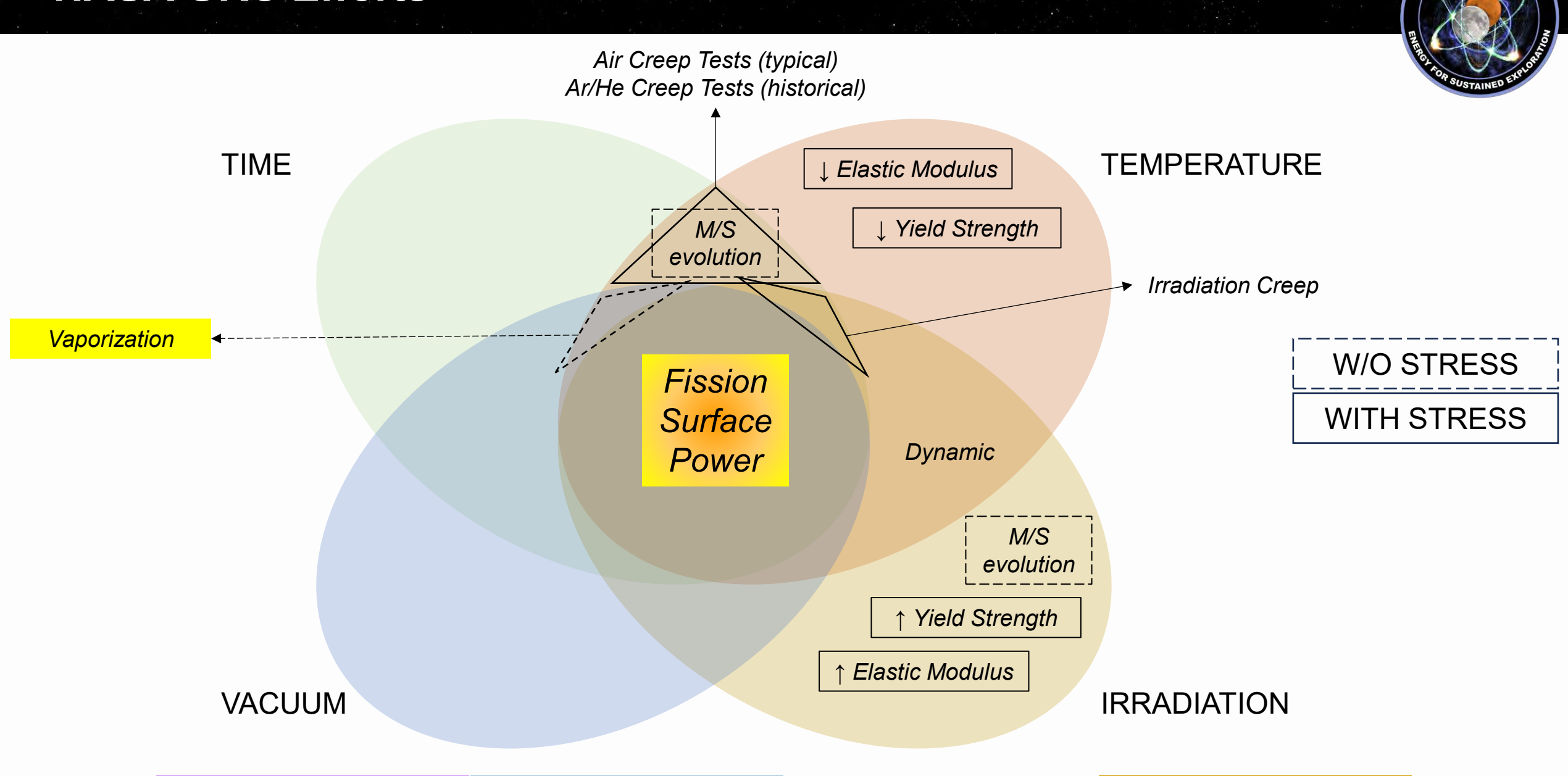
Mullite

Ytterbium Silicate

AZ96 or similar

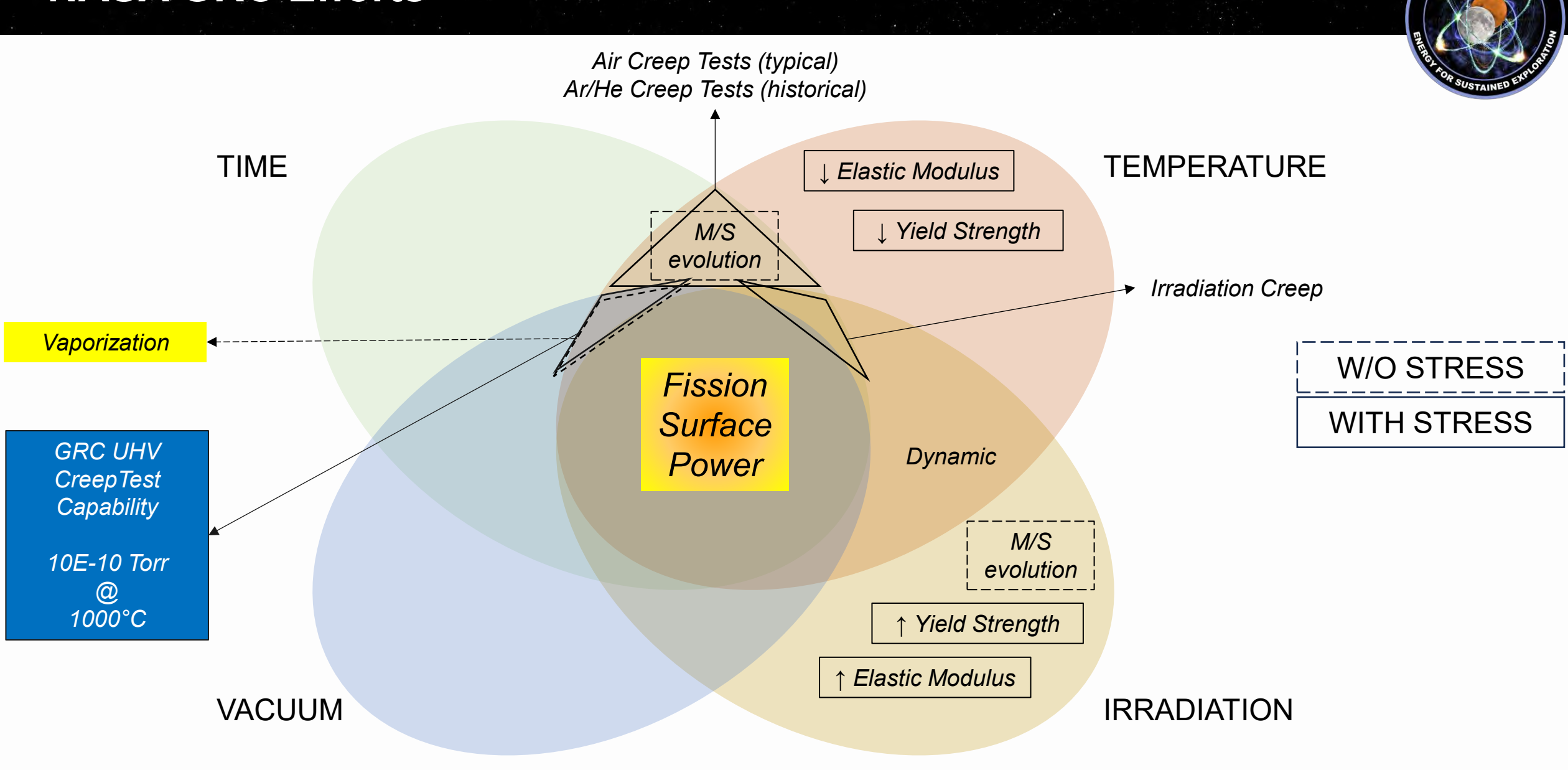


# **GRC Efforts**





80



www.nasa.gov Introduction Applicability Solutions GRC

81



82

- Purchased 36"x36"x.065" sheet of Nitronic 50
- Machining specimens from Haynes 230 sheet stock
- Designing specimens from Nb-1Zr tube stock

#### Test Plan

- 1a) Expose QTY 4 Haynes 230 specimens to 10<sup>-10</sup> Torr at 900°C for 1000 hours
- 1b) Expose QTY 1 Haynes 230 specimen to 10<sup>-10</sup> Torr at 900°C for 1000 hours
- 1c) Expose QTY 1 Haynes 230 specimen to 10<sup>-6</sup> Torr at 900°C for 1000 hours
- 2) Tensile test specimens at room temperature, metallography
- → Verify vacuum at temperature, verify mechanical effects of exposure, compare vacuum quality and "MLI" effects



83

#### Test Plan

- 3) Expose more alloys:
- 3a) CRES 304: 350°C, 400°C  $\rightarrow$  Mn vaporization at  $10^{-10}$  Torr
- 3b) Nitronic 50: 400°C → Mn vaporization at 10<sup>-10</sup> Torr, 800°C → notional FSP temp.
- 3c) Inor-8 / Hastelloy N-Hastelloy C-4: 600°C → Cr vaporization at 10<sup>-10</sup> Torr, 800°C → notional FSP temp.
- 3d) Haynes 230: 600°C → Cr vaporization at 10<sup>-10</sup> Torr, 800°C → notional FSP temp.
- 3e) Nb-1Zr: 400°C, 600°C, 800°C → Comparison
- 4) Tensile test all specimens after testing, add data to "database".



84

#### Test Plan

5) Compile literature and new test data into database.

		INPUTS					
		Alloy	Temperature	Pressure			
	Mass loss rate	Literature presented + Ref 13, 14					
OUTPUTS	M/S Evolution	Literature presented + test data					
OUT	Mech. Prop.	p. Literature presented + test data					

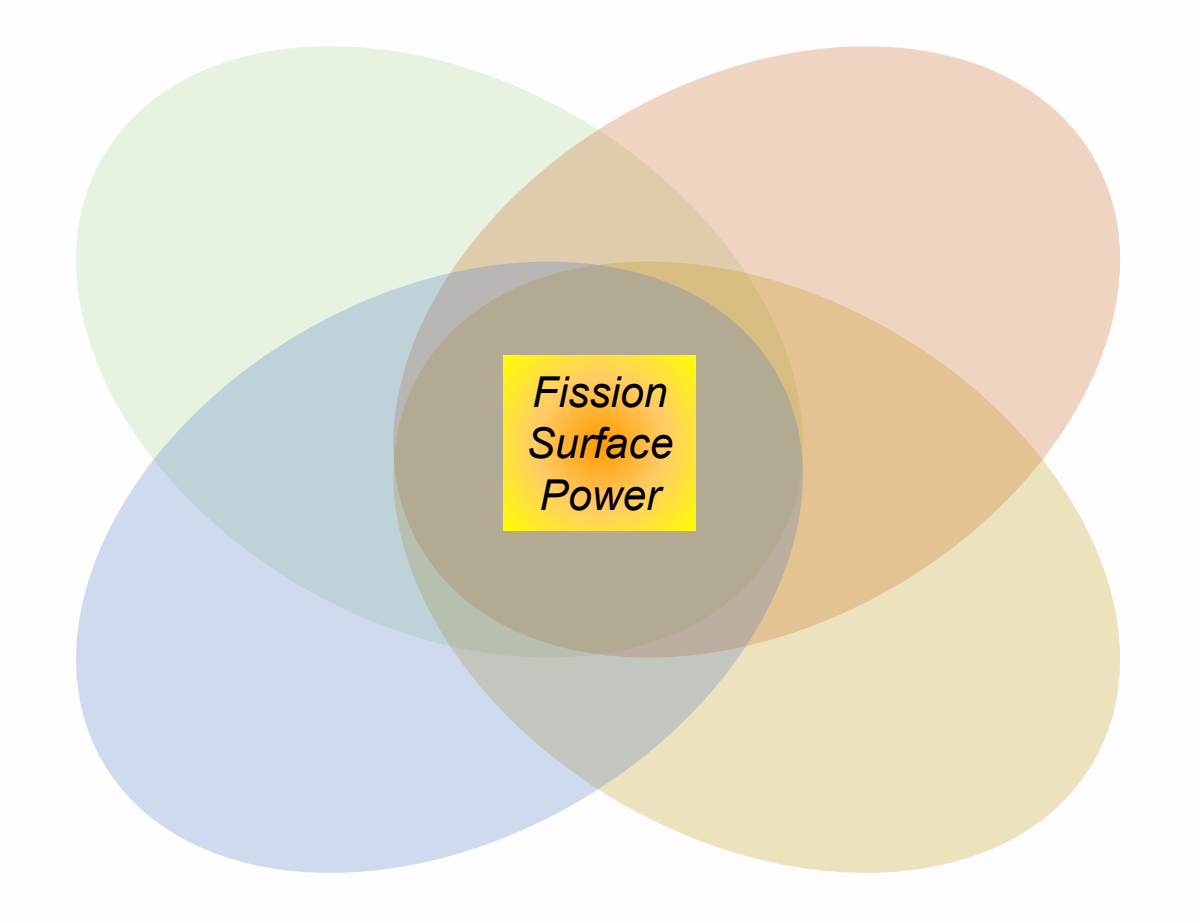
- 12. Mikhailov et al, "Vaporization of the Components of Nickel Alloys in a Vacuum Induction Furnace", 2016
- 13. Mukherjee et al, "Integrated Modeling to Control Vaporization-Induced Composition Change During Additive Manufacturing of Nickel-Based Superalloys", 2024



85

#### Test Plan

6) Down-select alloys to test in creep exposed to vacuum and fission radiation



#### References



86

- 1. Bourgette, "Evaporation of Iron-, Nickel-, and Cobalt-Base Alloys at 760°C to 980°C in High Vacuums" 1964
- 2. Bourgette, "High-Temperature Chemical Stability of Refractory-Base Alloys in High Vacuum", 1965
- 3. Bourgette, "A Study of the Vaporization and Cree-Rupture behavior of Type 316 Stainless Steel", 1966
- 4. Bourgette, "Evaporation of Radioisotope Capsule Materials in Vacuum" 1968
- 5. ORNL-4420 Fuels and Materials Development Program Quarterly Progress Report For Period Ending March 31, 1969
- 6. ORNL-4440 Fuels and Materials Development Program Quarterly Progress Report For Period Ending June 30, 1969
- 7. ORNL-4480 Fuels and Materials Development Program Quarterly Progress Report For Period Ending September 30, 1969
- 8. ORNL-4520 Fuels and Materials Development Program Quarterly Progress Report For Period Ending December 31, 1969
- 9. Whittenberger, "Tensile Properties of HA 230 and HA 188 after 400 and 2500 Hour Exposures to LiF-22CaF2 and Vacuum at 1093K", 1990
- 10. Whittenberger, "Effect of Long-Term 1093 K Exposure to Air or Vacuum on the Structure of Several Wrought Superalloys", 1993
- 11. Whittenberger, "Tensile Properties and Structure of Several Superalloys after Long-Term Exposure to LiF and Vacuum at 1173K", 1995
- 12. Mikhailov et al, "Vaporization of the Components of Nickel Alloys in a Vacuum Induction Furnace", 2016
- 13. Mukherjee et al, "Integrated Modeling to Control Vaporization-Induced Composition Change During Additive Manufacturing of Nickel-Based Superalloys", 2024
- 14. Honig, Radio Corporation of America, 1965. Accessed from https://iuvsta.org/iuvsta-publications/ February 27, 2025 as Chart 4 and Chart 5

## **Other Notable Papers:**



87

Bourgette, "Materials in Vacuum Environments", 1967

ORNL-TM-1786, Bourgette, "Vaporization Phenomena of Haynes Alloy No. 25 to 1150°C", 1967

Gabb et al, "Creep Property Characterization of Potential Brayton Cycle Impeller and Duct Materials" 2007

Deadmore, "Influence of Time on Vacuum Vaporization Rate and Surface Compositional Stability of Tantalum Carbide – Hafnium Carbide Solid Solutions Above 2000°C", 1966

Hall Jr., "Compatibility of Space Nuclear Power Plant Materials in an Inert He/Xe Working Gas Containing Reactive Impurities", 2006

Koyanagi et al, "Thermal Diffusivity and Thermal Conductivity of SiC Composite Tubes: The Effects of Microstructure and Irradiation", 2021

Stanislowski et al, "Chromium Vaporization from Alumina-Forming and Aluminized Alloys", 2008

Kurokawa et al, "Chromium Vaporization of Bare and of Coated Iron-Chromium Alloys at 1073 K", 2007

Wild, "Vacuum Annealing of Stainless Steel at Temperatures Between 770 and 1470 K", 1974

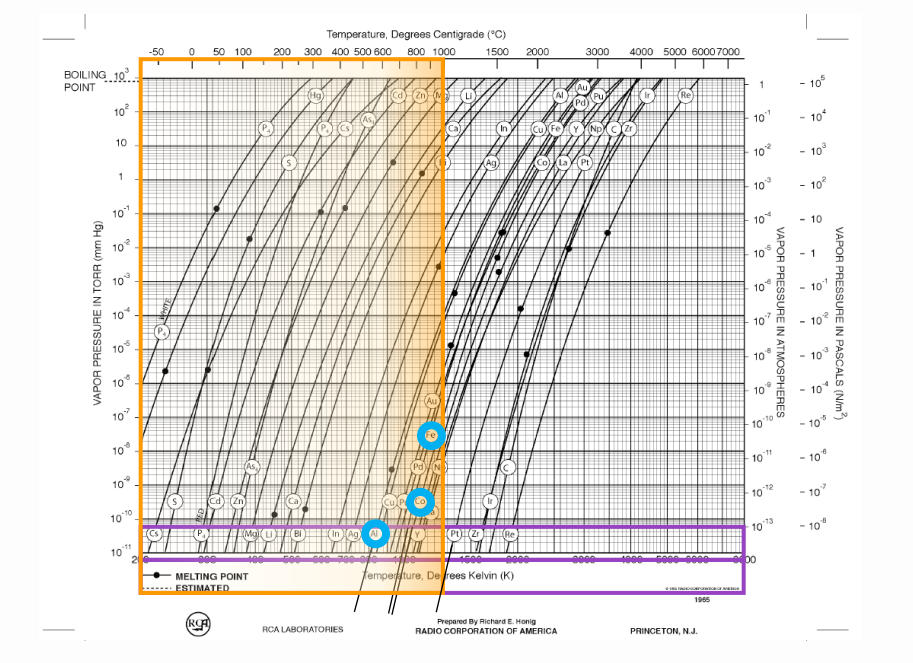
Charlot et al, "High Temperature Corrosion and Evaporation of Haynes 25 and Hastelloy X-280", 1967

Tylczak et al, "Measurement of Cr Evaporation at 760°C for Several Nickel Based Alloys at Moderate Velocities", 2017

Da Fonseca et al, "Evaporation of Chromium at the Surface of Ni-Cr-Fe Heat-Resistant Alloys During Long Exposure Times at 1100°C in Vacuum", 2025

Semiatin et al, "Alloying-Element Loss During High-Temperature Processing of a Nickel-Base Superalloy", 2014

# **Questions?**



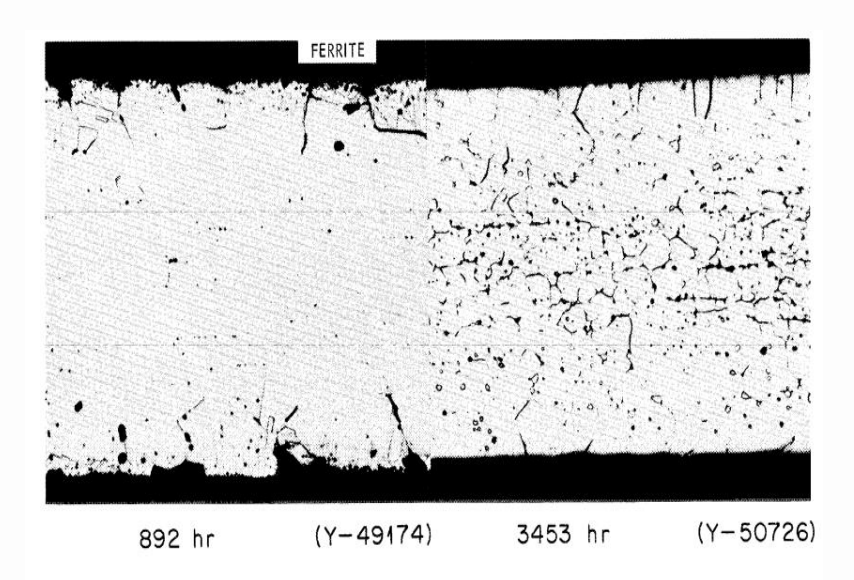
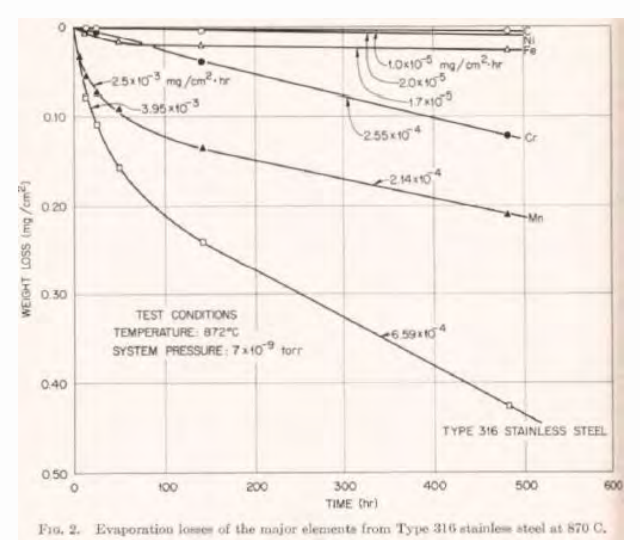


Fig. 12. Cross Section of Type 316 Stainless Steel Evaporation Tested at 872°C and 8  $\times$  10<sup>-9</sup> torr for 892 and 3453 hr, Respectively. Etchant: glyceria regia. 500X



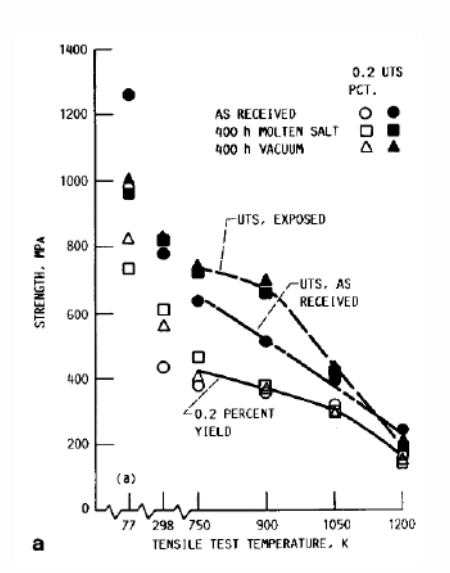
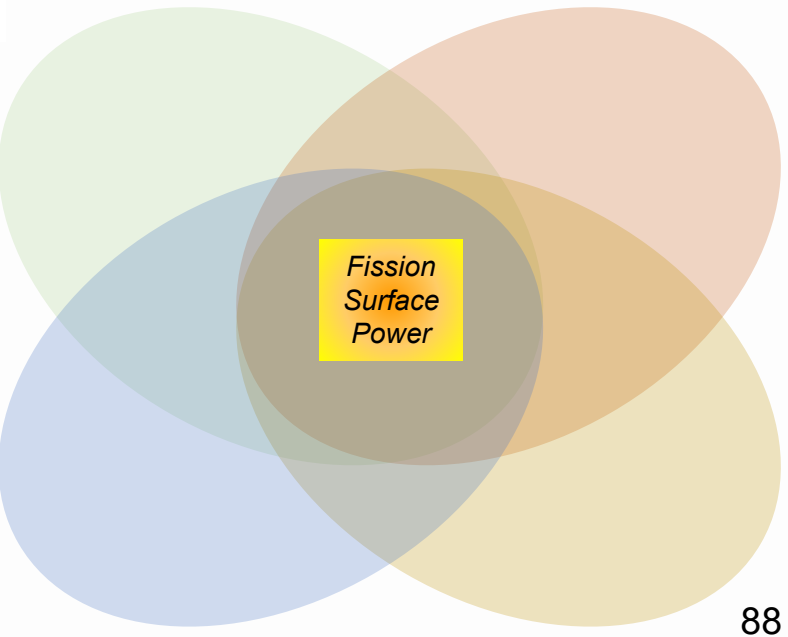
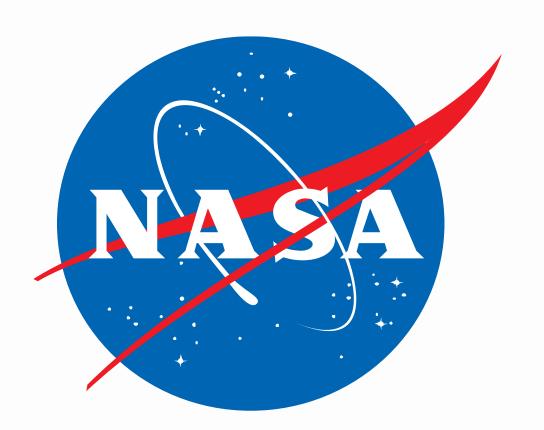




Fig. 1 Typical rack of superalloy tensile-test specimens prior to exposure.





# Advanced Closed Brayton Cycle Modeling for Fission Surface Power

Thomas Lavelle
NASA GRC
September 24, 2025





#### History of Closed Brayton Cycle Analysis

- CCEP Closed Cycle Engine Program
  - Fortran code
  - https://ntrs.nasa.gov/api/citations/20050217204/downloads/20050217204.pdf
    - Paul Johnson
  - Grew out of NNEP (NASA Navy Engine Program)
    - NNEP -> NEPP (NASA Engine Performance Program)
      - NASA's previous analysis code before NPSS
    - Added components
      - Recuperator, Radiator, Waste Heat Exchanger, Altenator
    - Components included sizing and design calculations
      - Efficiencies
      - Sizes and weights
- Conversion to NPSS done in mid 2000's
  - Wrote a code to convert Fortran routines directly into .int files
  - Worked but the components were never broken down and built back up
  - CCEP based elements are still available for use



#### **Brayton Modelling Work**

- JIMO (Jupiter Icy Moon Orbiter)
  - 2000's plan to send a probe to Jovian System
  - Reactor would allow for many high-powered instruments
  - Radars
- Power system for Nuclear Thermal Rocket System
  - Reactor would be set at a low level to provide power for spacecraft
  - PhD on this work done by Josh Clough

https://www.semanticscholar.org/paper/Integrated-propulsion-and-power-modeling-

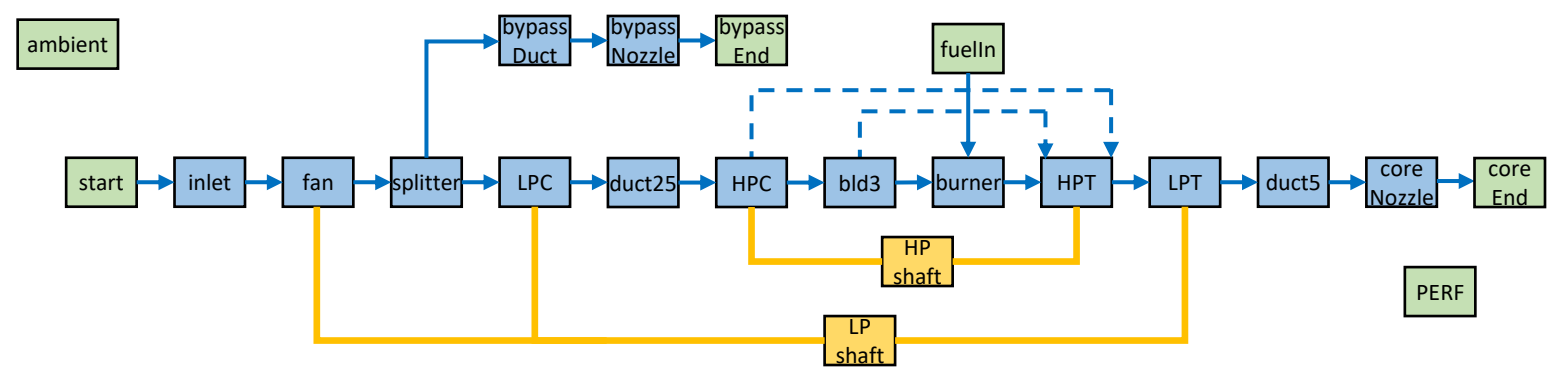
for-Clough/78aa72fe43bd3316ec80d4e991c6ad857ad49c7d







#### NPSS: Cycle Design and Performance Analysis



- NPSS allows the engine performance to be accurately predicted by considering the engine as a system of inter-connected components and thermodynamic processes
- NPSS is used to support aerospace products in all phases of development
  - Conceptual design
  - Detailed design
  - Transient analysis
  - Test data reduction
  - In service digital twins
  - Mature Capability



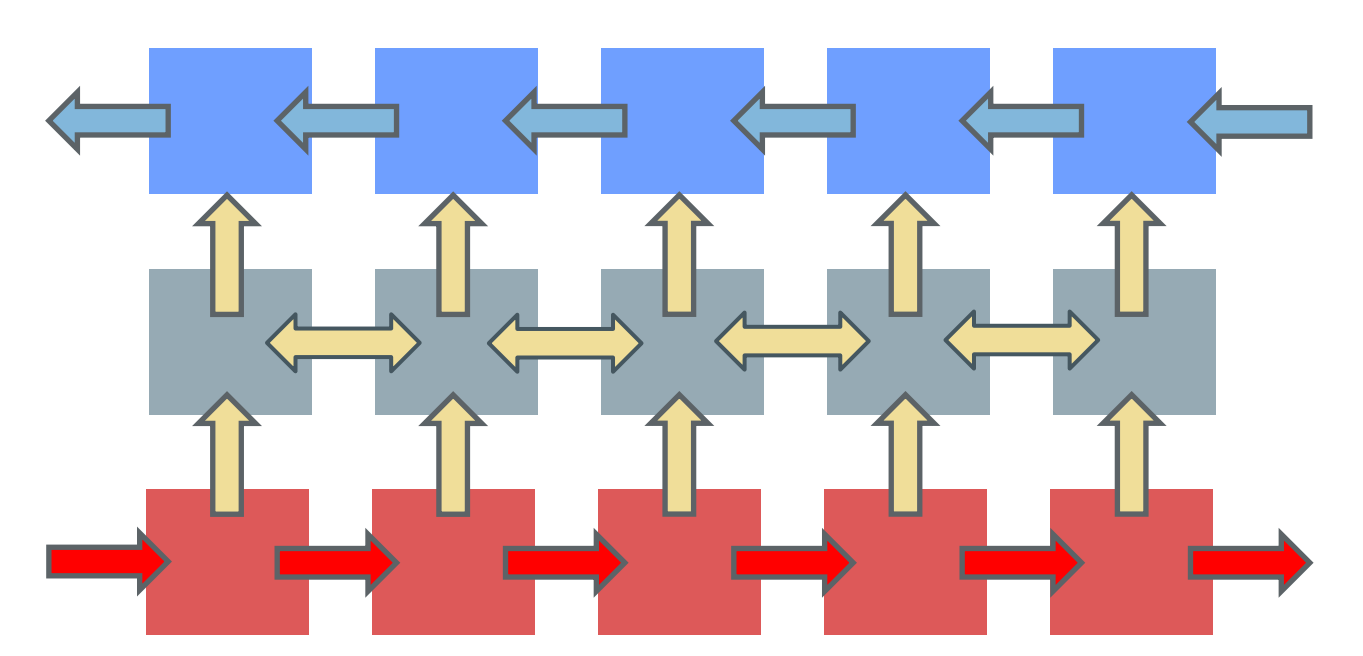
#### Current Task and Basic Element Methodologies

- Create closed Brayton cycle modeling capability with intermediate fidelity components
- Modernize the design and sizing calculations
- Heat transfer elements use 1D or 2D finite volume method
  - Step through both sides of the model calculation dP and temperature change
  - Heat exchangers, radiator trunk line and panels, reactor heat pipes and cooling channels
- Turbomachinery
  - OTAC to calculate efficiency
  - Optimal torque and angular frequency design point for alternator sizing and interface
- Reactor
  - Start off as point heat source and transition to diffusion and MCNP curve fit based sizing and feedback coefficient calculation
  - 6 equation point kinetics for transient
- All components will have preliminary design-level geometric descriptions, e.g. a turbomachine post-meanline design
  - Enables accurate mass calculations



#### Element Example: Heat Exchanger

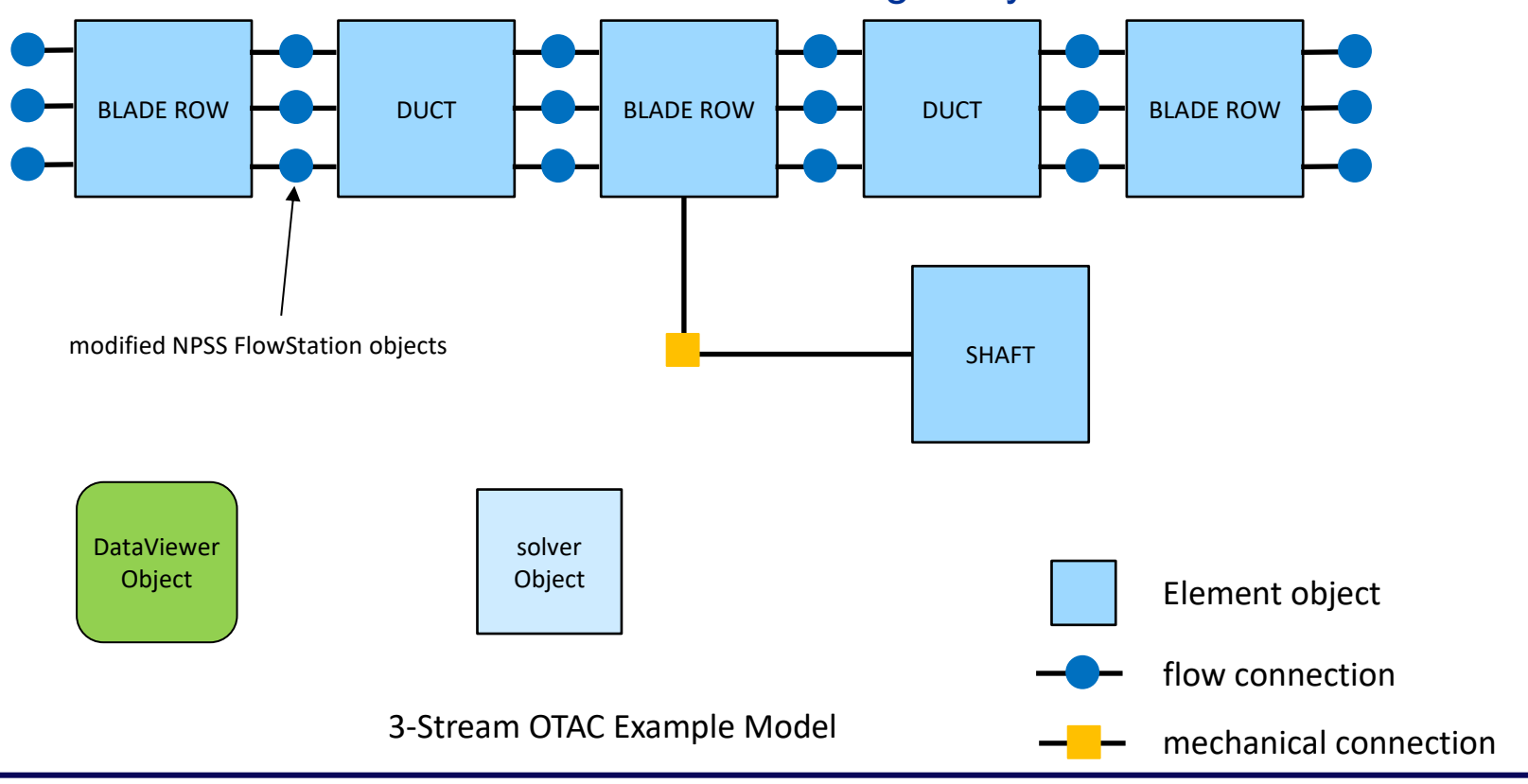
- HX component is a python-based 1D finite-volume model
  - Direct solution to the energy equation
  - Includes longitudinal wall conduction
- Nusselt number and friction factor correlations will be taken from literature: Kays and London, Gnielinski, Shah, etc.
- This element is used for hot and cold side heat exchangers
- Precise mass calculations possible because of complete geometric description





#### Element Example: Turbomachinery

- Uses the Object-Oriented Turbomachinery Analysis Code (OTAC)
  - Written within NPSS
- Allows re-use of Numerical Propulsion System Simulation objects
- Model structure that is similar to NPSS engine cycle model



#### **NPSS Model Validation**

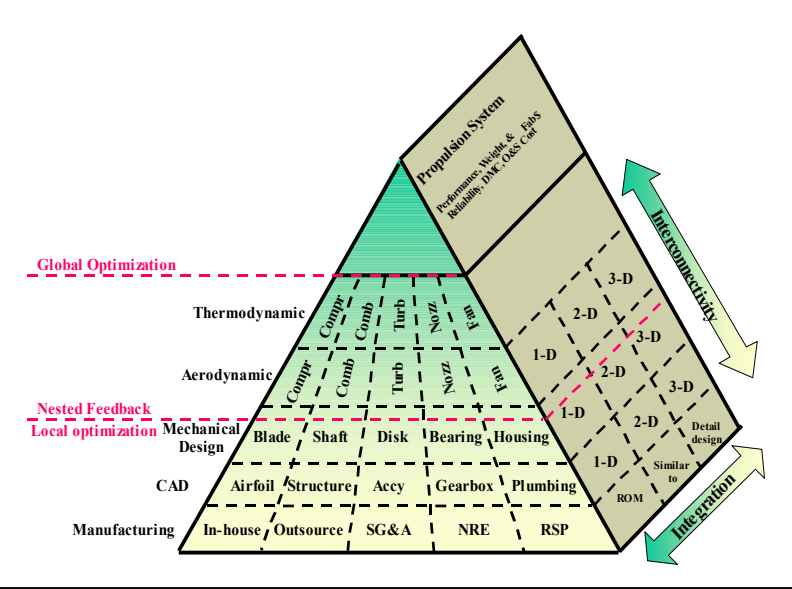


- Model validation based on previous hardware, Brayton Rotating Unit (BRU) and Mini-BRU
- IDE model of BRU below
- Currently assembling Mini-BRU Model
- Adding more fidelity to engineering elements



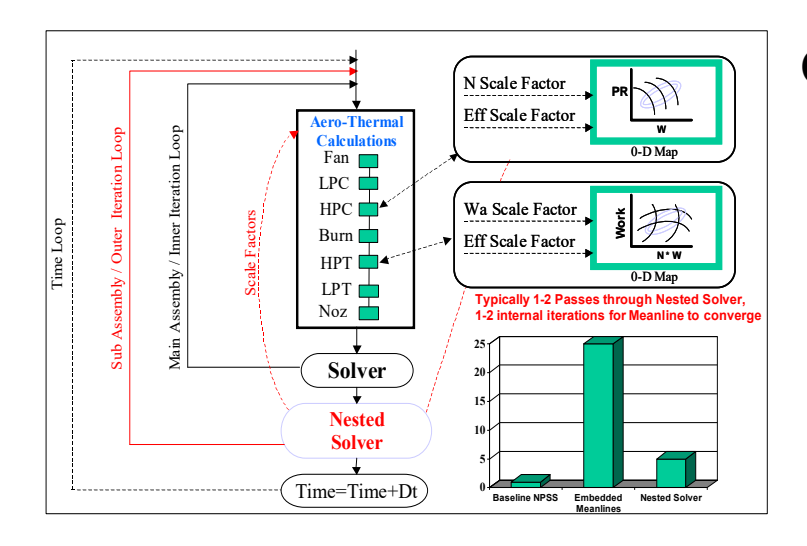
#### Integrating High Fidelity Tools





#### **High Fidelity Simulation and Analysis**

- Use High Fidelity as Appropriate
- Integrate Between Levels of Fidelity
- Implicit Hierarchy in Coupling
  - Minimizes Iterations
  - Global and Local Constraints
- Supports Tie-In to Vehicle Analysis Models



#### **Generic Approach To "Zooming"**

- Use 0-D Modeling System as Focal Point
  - Scale Components to Match High Fidelity
  - Ensure Boundary Conditions Satisfied
- Nested Solver Approach
  - Minimize Internal Iterations
  - Keep High Fidelity Tools in Design Space

<del>)</del>



#### Team Familiar With Multiple Development Environments

- NPSS Modeling
- Python
  - Thermal element being done in Python
- MATLAB
  - Lead developers for T-MATS
  - The Toolbox for the Modeling and Analysis of Thermodynamic Systems (T-MATS) for MATLAB/Simulink toolbox